DOCTOR OF PHILOSOPHY

Development of a global empirical-statistical framework for the probabilistic assessment of wildfire risk under climate change

Liu, Zhongwei

Award date:
2024

Awarding institution:
Coventry University

Development of a global empirical-statistical framework for the probabilistic assessment of wildfire risk under climate change

by

Zhongwei Liu

Supervisor: Dr Jonathan Eden
Dr Bastien Dieppois
Dr Matthew Blackett

December 2023

Centre for Agroecology, Water and Resilience

A thesis submitted in partial fulfilment of the University's requirements for the Degree of Doctor of Philosophy

Acknowledgements

I wish to thank my supervisory team for their guidance on my PhD journey: **Jonathan Eden**, my director of studies, for his vision and tireless input into my research. His overall management of the project and full support in applying fundings and participating academic events facilitated my progress, and his encouragement has kept me motivated to move forward time and time again. I am grateful for the initial and ongoing trust placed in me and the advice provided over the past 3 and a half years. **Bastien Dieppois**, my second supervisor for his experience and advice during the undertaking of this project. I am impressed for his kindness and thoughtfulness, particularly in helping to attend academic conferences and organise development activities. **Matthew Blackett**, my third supervisor for his thoroughness and help with understanding and offering the key concepts in my PhD study. I am grateful to have such a wonderful supervisory team, and I very much hope to continue what has become fine working relationship during the coming years.

I also thank my internal examiner, **Craig Lashford**, for the first three years of my PhD, without his support to reviewing my outcomes each year, expressing his recognition and providing advice on my research, I would not be where I am today.

I am indebted to my colleagues at **Center for Agroecology, Water and Resilience (CAWR)**, many of whom have become lifelong friends, providing support for me through the difficulties as a PhD student. I am also very grateful to the colleagues at **Doctoral College**, many of whom are friendly and helpful to assist me throughout my study and life within **Coventry University**.

I thank **Igor Drobyshev** (Swedish University of Agricultural Sciences), **Carolina Gallo**, **W. Stefaan Conradie** (University of Cape Town), **Folmer Krikken** (Royal Netherlands Meteorological Institute; KNMI) for their contributions of subsequent valued comments and suggested amendments by reviewing the published papers included in my thesis.

Finally, I would also like formally thank **Coventry University** for funding this PhD project. I am also very grateful to the **Royal Meteorological Society (RMetS)** and **CAWR** for funding my research development activities (*i.e.*, conferences, summer school), and

CAWR, again, for funding my publication costs throughout almost the past 3 and a half years.

Dedication

I would like to dedicate this thesis to my parents, Yuxia Liu and Linsen Liu, for their love and support in my life. Without them, this day would not have been possible.

This work is also dedicated to my dear best friend, Mengru Zhao, for the mental support and care she has given me over the past fifteen years, and to my partner, Tongjin Yan, for his unfailing source of help in my daily life throughout the 3 and a half years of studying for my PhD.

List of Publications

This thesis by artefact consists of the following research articles:

Peer-reviewed publications

Liu, Z., Eden, J.M., Dieppois, B. & Blackett, M. (2022). A global view of observed changes in fire weather extremes: uncertainties and attribution to climate change. *Climatic Change*, *173*, 14. **(Chapter 3)**

Liu, Z., Eden, J.M., Dieppois, B., Drobyshev, I., Gallo, C., & Blackett, M. (2022). Were Meteorological Conditions Related to the 2020 Siberia Wildfires Made More Likely by Anthropogenic Climate Change?. *Bulletin of the American Meteorological Society*, *103*(3), S44-S49. **(Chapter 5.1)**

Liu, Z., Eden, J. M., Dieppois, B., Conradie, W. S., & Blackett, M. (2023). The April 2021 Cape Town Wildfire: Has Anthropogenic Climate Change Altered the Likelihood of Extreme Fire Weather?. *Bulletin of the American Meteorological Society*, *104*(1), E298-E304. **(Chapter 5.2)**

Manuscript submitted or prepared for peer-review

Liu, Z., Eden, J. M., Dieppois, B., Drobyshev, I., Krikken, F., & Blackett, M. (2023). Multi-Model Attribution of Extremes in Fire Weather Intensity and Duration to Externally Forced Changes in Global Temperature Anomalies. *Weather and Climate Extremes*. (*In review*). **(Chapter 4)**

Liu, Z., Eden, J. M., Dieppois, B., & Blackett, M. (2023). How does climate change influence the past, present and future likelihood of the extreme meteorological conditions associated with the 2022 Euro-Mediterranean wildfires?. (*In preparation*). **(Chapter 5.3)**

Abstract

As major natural hazards, wildfires pose a significant risk to many parts of the world. The occurrence of extensive fires in both hemispheres in recent years has raised important questions about the extent to which the changing nature of such incidents can be attributed to human-induced climate change. Offering reliable answers to these questions is essential for communicating risk and increasing resilience to major wildfires. While attribution of extreme events to anthropogenic climate change has developed into an important subfield of climate science, wildfires have received less attention compared to other heat-related extremes such as heatwaves and drought. This is primarily due to the scarcity of the observational datasets and the absence of a widely agreed-upon and effective methodological framework for wildfire attribution.

Here, a globally applicable framework is developed to better understand and quantify how wildfire risk is responding to a changing climate. The framework is based on an empirical-statistical methodology, facilitating its application to 'fire weather' extremes from both observational records and the latest generation of global climate model ensembles. Particular attention is given to the sensitivity of the eventual findings to the spatial scale of the event, the chosen event definition and the climate model(s) used in the analysis.

As part of a global analysis, a series of maps are constructed detailing the change in likelihood of fire weather extremes, defined by both intensity and duration, throughout the world's fire-prone regions as a result of rising global temperatures. Both observation- and model-based analyses reveal an increase in likelihood of at least twofold across many parts of the world, with considerable regional and inter-model variation. The value of the framework is demonstrated by combining results from a series of case studies of recent high-impact wildfires that differ by scale, duration and location. The conclusions drawn from this work provide a platform to guide future attribution analysis of fire weather events, and facilitate reliable recommendations for responding to the hazards associated with wildfires and enhancing resilience in the face of climate change.

Table of contents

List of figures

List of tables

Chapter 1

Introduction

1.1 Background

Wildfires constitute a major natural hazard and pose huge risk to many regions of the world, including serious damages to the environment, wildlife, human health and infrastructure (National Geographic Society, 2022; Sullivan et al., 2022; World Health Organization, 2023). The series of large fires across the globe in recent decades led to inevitable questions about how human-induced climate change may be altering the character of such events (National Academies of Sciences, Engineering, and Medicine, 2016). Providing answers to these questions is a crucial step in improving resilience to major wildfires.

Long-term projections produced by state-of-the-art climate models, even reliable, are not always a suitable means of communicating risk. The link between a warming world and heat-related extremes (*e.g.*, heatwaves and droughts) is reasonably well-understood. However, wildfires have been largely ignored by attribution studies to date. To assess past, present, and future risks in wildfire activities associated with climate change, the development of a seamless, globally applicable framework for wildfires becomes essential.

1.2 Climate change and extreme events

Climate change refers to a global shift in climate, persisting for an undetermined period and driving regional impacts on land and oceans, as a result of human-induced changes in atmospheric concentration of greenhouse gases (Field et al., 2012). From the 1970s, climate change has become one of the most critical topics in global environmental debate (Jackson, 2007). Recent publications from the Intergovernmental Panel on Climate Change

(IPCC) emphasise the continuous significant impacts of climate change, including rising global temperatures and sea levels, the loss of ice volume and changes in global precipitation patterns (IPCC, 2021, 2022a,b, 2023). Similarly, there is a growing interest in quantifying how climate change affects regional climate and extremes (Figure 1.1; Ara Begum et al., 2022). Therefore, there is an urgent need to equitably explore the potential role of climate changes and its regional impacts throughout the world.

Figure 1.1: Global density map of the climate impacts evidence from 77,785 studies (Ara Begum et al., 2022).

Extreme weather events constitute one of the most significant impacts of climate change. From the early 1990s, the IPCC suggested that human activities contributed to climate change in the form of a significant global temperature increase and, consequently, to the nature of high-impact events, such as heat waves, heavy rainfall, and drought (IPCC, 2014; National Academies of Sciences, Engineering, and Medicine, 2016; IPCC, 2023). Such changes affecting climate-related extremes have aggravated the vulnerability of natural and human systems around the world (Ara Begum et al., 2022). Understanding how climate change has affected the nature of such events, is therefore of crucial importance due to their significant impacts on human society and ecosystems across the world (Stott et al., 2016; National Academies of Sciences, Engineering, and Medicine, 2016).

Given the unprecedented increase in both the frequency and magnitude of extreme events, and their devasting impacts on natural and human systems, seeking to understand the contribution of anthropogenic climate change to extreme events has become a keen focus within climate science (Seneviratne et al., 2012; Field et al., 2012; National Academies of Sciences, Engineering, and Medicine, 2016; Otto et al., 2016; Philip et al., 2020; van

Oldenborgh et al., 2021a). In 2012, the IPCC issued a Special Report titled "Managing the risks of extreme events and disasters to advance climate change adaptation" (Field et al., 2012). As shown in Figure 1.2, the Report illustrated three broad cases, in which a changing climate is linked to corresponding changes in extremes (Lavell et al., 2012). In case 1 (Figure 1.2a), the distribution of day-to-day weather shifts toward a warming climate, resulting in less cold weather, more hot weather and, crucially, an increase in the likelihood of extreme heat events. In case 2 (Figure 1.2b), the change in temperature variability leads to an increased likelihood of both hot and cold extremes alongside a decrease in the likelihood of mid-range temperatures. Case 3 (Figure 1.2c) shows an altered shape of the distribution resulting in the same probability in the mean, but with asymmetric change in the likelihood of each extreme. These simple cases demonstrate the close connection between various manifestations of climate change and the corresponding alterations of probabilities in extremes, drawing out the potential challenges in terms of the complexity and variability of the research.

While long-term climate change is often presented in an abstract, gradual, and complex way, extreme weather events tend to happen abruptly, and their impacts are immediately felt. In this sense, extremes are a tangible way in which people experience climate change (Howe et al., 2014; National Academies of Sciences, Engineering, and Medicine, 2016). As the most easily perceived extremes of climate change, extreme heat or precipitation often bring tremendous impacts on human society, economy, and ecosystems (National Academies of Sciences, Engineering, and Medicine, 2016; Zhai et al., 2018). Xu et al. (2020) recently suggested that one-third of the global population will face extreme heat (over 29 °C of a mean annual temperature compared with $\sim$11 to 15 °C, currently) by 2070. Therefore, with the increasing challenges posed by the anomalous growth of such extreme phenomena, the scientific community emphasises the need to identify changes in extreme phenomena in terms of understanding their relationship with human activities in order to facilitate further research in this field (Herring et al., 2022).

During the last decade, the scientific community has taken action to explore the extent to which the nature of extreme weather has been altered by anthropogenic climate change. So-called attribution studies seek to quantify the role played by anthropogenic activities, or simply by a warming world, on the characteristics of extremes, including their frequency, magnitude, spatial extent, and seasonal timing. Attribution studies have provided an unprecedented pathway for scientists to draw clear linkages between climate change and specific extreme events in a manner that is accessible to public and media interest (Trenberth et al., 2015; National Academies of Sciences, Engineering, and Medicine, 2016).

Figure 1.2: The probability of specified events by a giving temperature distribution and its changes under three cases (Lavell et al., 2012). The probability density function with solid lines denotes the original distribution while the dashed lines represent the alterations under climate change conditions.

1.3 Wildfires around the world

Wildfires are uncontrolled and often spread rapidly causing destructive damages over woodland or bush (National Geographic Society, 2022). The United Nations Environment Programme (UNEP) recently reported on global fire distribution and increasing prevalence in many parts of the world (Sullivan et al., 2022). Figure 1.3 shows the geographical distribution of the annual average number of fires per square kilometer, highlighting that fires occur in almost every regional of the world that features burnable vegetation (Sullivan et al., 2022). Figure 1.4 details the prevalence of fire activity during a recent five-year period (2014-2019) with respect to a longer period (2001-2019) (Sullivan et al., 2022). Over the past decade, there have been exceptionally more wildfires from Australia to Canada, the United States to China, across Europe and the Amazon (Sullivan et al., 2022). Even in high latitudes, including beyond the Arctic Circle in areas that are not normally prone to large wildfires, record fires have been experienced in recent years (Sullivan et al., 2022). In the United States alone, wildfires accounted for around $14.7 billion in damage between 2021 and 2022, with four of the top 20 largest California wildfire events occurring in 2021 with the reference period of 1932 to 2022 (CAL Fire, 2022; NOAA National Centers for Environmental Information, 2023). In addition to ecosystem degradation, the direct environmental impacts of wildfires include air and water pollution, which are associated with significant societal consequences. For instance, a recent study from the US evidenced that more than 19,700 cases of COVID-19 and 748 deaths were attributable to the increased $PM_{2.5}$ burning from wildfires (Zhou et al., 2021).

Figure 1.3: The annual concentration of all vegetation fires (landscape fires and wildfires) observed per square kilometre (km^2) for the period 2000–2020 (Sullivan et al., 2022).

Figure 1.4: The prevalence of global wildfire activity in 2014-2019, calculated as a normalised difference in annual average burnt area (with respect to 2001-2019) (Sullivan et al., 2022).

The occurrence of large fire events across both hemispheres has led to inevitable questions about the extent to which climate change may be altering the frequency of such extreme events. Although wildfires cannot be explicitly defined as meteorological events, their generating and developing mechanisms are influenced significantly by climate, in particular temperature, wind speed and humidity for fire spread, and rainfall for fire suppression (National Academies of Sciences, Engineering, and Medicine, 2016). Wildfires constitute a major pervasive natural hazard and pose huge risks to many regions of the world not only in the past and current climate but also in the future. Using a global climate and fire model (Frieler et al., 2017), global change in wildfire events were projected to increase by 31% to 57% by the end of the 21st century (Figure 1.5; Sullivan et al., 2022). Such a dramatic increase in global wildfire activity is likely to put enormous pressure on the balance between biodiversity and the climate system in the following several decades (Krawchuk et al., 2009; Flannigan et al., 2009; Jolly et al., 2015; Sullivan et al., 2022).

1.4 Detection and attribution of climate change

Even when reliable, long-term projections produced by state-of-the-art climate models are not always a suitable means of communicating risk (Schewe et al., 2019). Methodologies to attribute trends in meteorological phenomena associated with high-impact events to anthropogenic climate change have the potential to better communicate risk and guide adaptation strategies (Clarke et al., 2022).

Figure 1.5: The likelihoods of catastrophic wildfire events all over the world shown significant increases by the end of the century (Sullivan et al., 2022).

During the early definition of climate change from the United Nations Framework Convention on Climate Change (United Nations, 1992), climate change was first defined as a change of climate that is attributed directly or indirectly to human activity, altering the biogeochemical composition of the atmosphere at the global scale and cumulating its impact to natural climate variability on comparable time periods. The field of detection and attribution is, therefore, universally acknowledged as the main approach to assess whether climate risks have become more or less likely in the face of anthropogenic climate change or not (Knutson et al., 2017).

The report "Attribution of Extreme Weather Events in the Context of Climate Change" published by National Academies of Sciences, Engineering, and Medicine (2016) gave a general overview, aided by a widely-cited schematic depiction (Figure 1.6), of a wide range of extreme events, comparing the knowledge of the effect of climate change with the confidence in attributing each event type to anthropogenic climate change. This comparison illustrates a particularly high degree of confidence in both understanding and attributing temperature-related extreme events, such as heat waves and cold waves. There is medium confidence in attributing drought, extreme rainfall and extreme snow and ice due, in part to the uncertainties in regional variability of the response of precipitation to climate change. However, there are several types of events, including severe convective storms, cyclones and, crucially for this thesis, wildfires, that are hitherto poorly understood. These event types are rarely studied given the restrictions of records, resolution of simulations, and the complex combination of dynamic mechanisms involved in their formation.

Event attribution remains an evolving subfield of climate science, and continues to develop in the face of methodological, philosophical and practical challenges. Most recently, World Weather Attribution (World Weather Attribution, 2023), has sought to provide rapid attribution responses to extreme events, not only to provide answers to growing questions about the role of climate change (*e.g.*, Sippel et al., 2015), but also to publicise the "immediacy" of climate risk while such answers are most in demand in the aftermath of a high-impact event. Responding in such a timely manner has the potential to support mitigation strategies (*e.g.*, Wallace, 2012) and increase resilience to high-impact events.

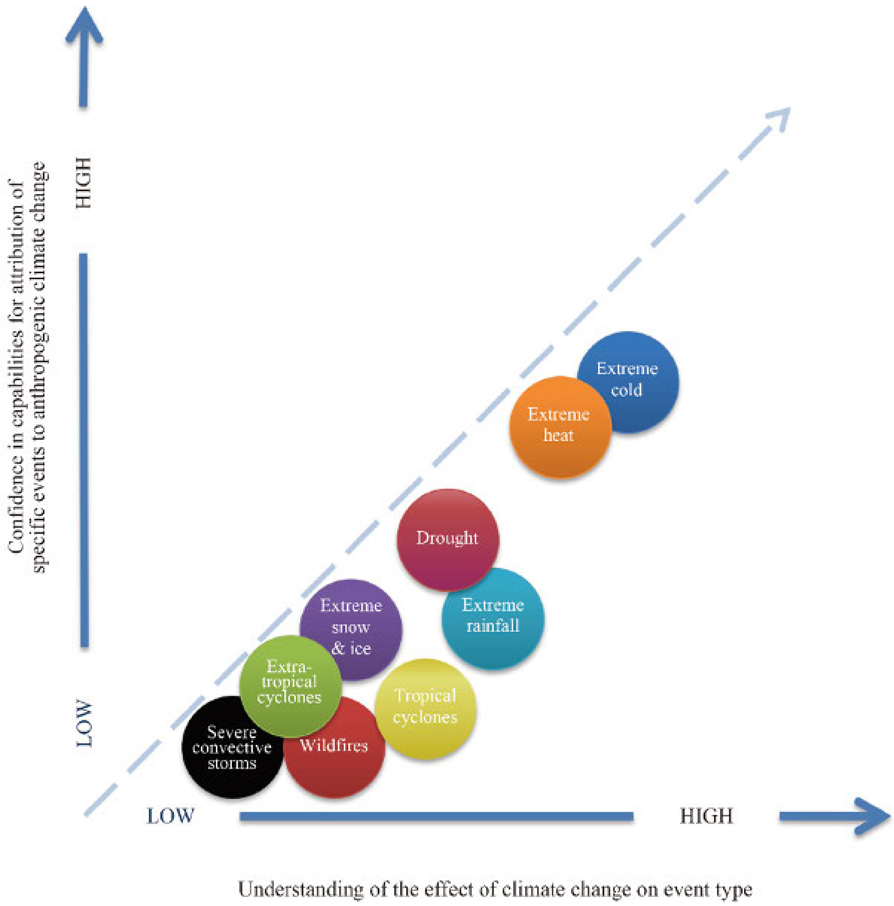

Figure 1.6: The depiction from National Academies of Sciences, Engineering, and Medicine (2016) to assess the state of attributing types of extreme events. The horizontal axis represents the understanding level of the effect of climate change on the event type from low to high. The vertical axis reflects the scientific confidence in capabilities for attribution specific events to human-induced climate change. Positions below the diagonal dashed line show the potential improvements in attribution capability via technical aspects (*e.g.*, for instance, modelling and data).

1.5 Attribution study of extreme fire weather events

While the link between a warming world and heat-related extremes (*e.g.*, heatwaves and droughts) is reasonably well-understood, there have been relatively few event attribution studies that have dealt specifically with wildfires (National Academies of Sciences, Engineering, and Medicine, 2016). In a summary compiled by Carbon Brief (2023), only 14 of 421 attribution studies published between 2004 and 2022 focused on wildfires (Figure 1.7). It is also notable that the figure is not completed, for instance, Li et al. (2021) is not included though it refers to the attribution study of wildfire-prone weather conditions in the Cerrado and Arc of deforestation. Wildfires are not, strictly-speaking, a meteorological event and while their prevalence is heavily linked to climate, it is troublesome to disentangle human and natural roles in fire ignition and spread. The relative paucity of wildfire attribution studies, coupled with limited observational records, makes it difficult to draw solid and collective conclusions to better inform forest and wildland management strategies (National Academies of Sciences, Engineering, and Medicine, 2016).

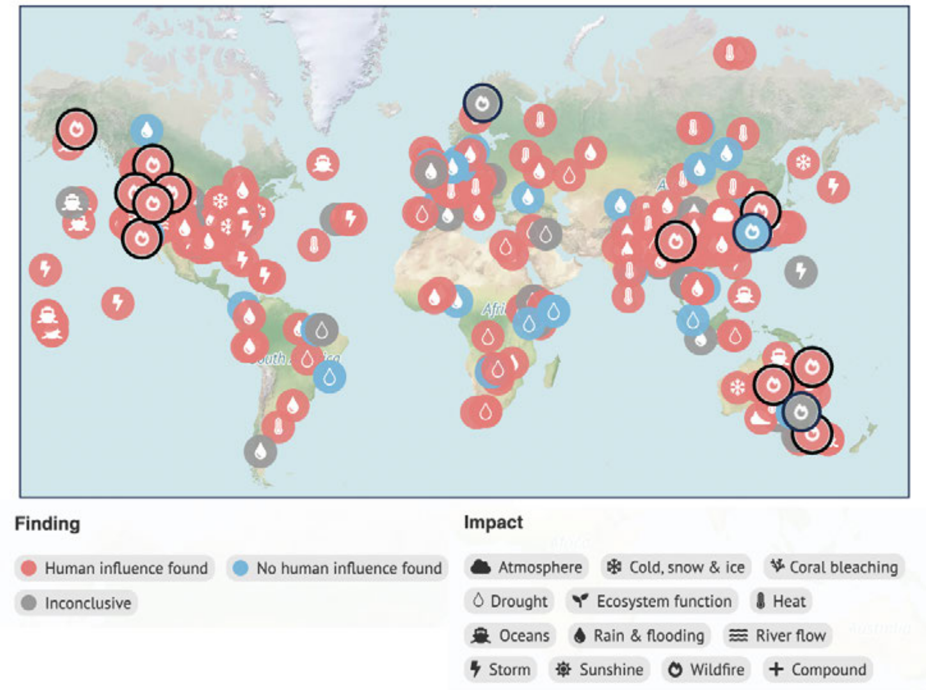

Figure 1.7: Worldwide distribution of 421 attribution studies of different types of extreme weather and climate events published between 2004 and 2022. The 14 attribution studies focused on wildfires are outlined in black (adapted from Carbon Brief, 2023).

From a meteorological perspective, it is often preferable to define an event with respect to 'fire weather', the warm, dry and windy conditions that are conducive to fire ignition and spread. Such a definition has been the subject of several attribution stuides in recent years (Kirchmeier-Young et al., 2019b; Krikken et al., 2021; Barbero et al., 2020; Lewis et al., 2020; van Oldenborgh et al., 2021a). Fire weather is generally represented by a series of fire danger indicators calculated on the basis of several meteorological variables, mainly temperature, precipitation, relative humidity and wind speed. Even though the mechanisms of wildfire ignition (particularly the contribution from lightning; Dowdy and Mills, 2012) and spread remain unclear (National Academies of Sciences, Engineering, and Medicine, 2016), an alternative focus on demonstrating changes in fire weather risk is universally acknowledged in wildfire attribution studies.

Outside of a handful of studies, attribution of wildfires, or alternatively extreme fire weather, has yet to match the pace of other studies focusing on other thermodynamic extremes. Outside western North America and Australia, few fire-prone regions of the world have received much attention from the attribution community (Figure 1.7). In the case of southern Europe, eastern North America and northern Eurasia, this is particularly surprising given the prominence of wildfire outbreaks in recent years in these regions and the limited number of studies to date addressing global wildfires (or say fire weather extremes) to date (Jain et al., 2022). Notably, very few systematic global attribution analyses have been conducted for wildfires (or otherwise fire weather extremes) to date (Jain et al., 2022).

The pursuit of robust, reliable wildfire attribution thus faces many challenges. Some of these, such as inter-study differences that emerge due to the choice of methodology and event definition, are common to many attribution studies (Philip et al., 2020; van Oldenborgh et al., 2021b). For fire weather attribution in particular, the lack of consensus on how fire danger should be defined in a meteorological context presents a crucial challenge. The lack of continuous observational records for wildfires is also a key limitation, while uncertainties about the most appropriate climate model(s) to use also limits the development of such studies, in addition to the accuracy and resolution of their results (National Academies of Sciences, Engineering, and Medicine, 2016). Empirical-statistical probabilistic methodologies have been widely applied to attribute other meteorological extremes by quantifying the changes in frequency and/or magnitude as a result of anthropogenic climate change or, otherwise, long-term changes in global mean temperature (Field et al., 2012; cf. Chapter 2, section 2.4). There is great potential for fire weather, as a construct of several meteorological variables, to be the target of a probabilistic framework for event attribution.

1.6 Aim and objectives

To summarise the introduction and background provided earlier in Chapter 1, this PhD project is motivated by three themes: (a) the increasing prevalence and impact of severe wildfires in many parts of the world; (b) the relative paucity of wildfire, or otherwise fire weather, attribution studies and, consequently, the uncertainties associated with conducting such studies; (c) the potential of empirical-statistical methods to provide robust conclusions when applied to data from both observations and the latest generation of climate models. The overarching aim of this work is thus to develop a globally applicable empirical-statistical framework to better understand and quantify the changing nature of wildfire risk in the face of a changing climate. To achieve this aim, three Research Questions are posed followed by a series of related objectives, with the corresponding approach applied for achieving each task outlined below.

Research Question 1: *To what extent can observed worldwide changes in extreme fire weather during recent decades be linked to warming global temperatures?*

Objective 1.1: To develop and apply a global approach for extreme fire weather attribution upon which future studies can build. Despite the rapid development of attribution methodologies for extreme events in the last decade, studies dedicated explicitly to wildfire, or otherwise extreme 'fire weather', are still relatively few and generally limited to a handful of regions around the word. There is a lack of consensus on how to define and attribute fire risk in a meteorological context. Here, a probabilistic framework is proposed that draws on existing protocols applied to attribution analyses of other extreme event types. This involves the simultaneous attribution of multiple extreme fire weather episodes using an empirical-statistical methodology.

Objective 1.2: To evaluate the uncertainty concerning the choice of fire weather indicators and metrics in linking regional trends in observed fire weather extremes to globally warming temperatures. Using observational data, the influence of recent global warming on the frequency and magnitude of fire weather extremes is quantified according to a common spatiotemporal definition, which also benefits the further application to climate model ensembles. Using a series of fire weather indices, the applicability, sensibility and uncertainties associated with the selection of indices and metrics are evaluated to better understand the capacity to represent fire weather risks all over the world's fire-prone regions.

Research Question 2: *What do state-of-the-art global climate models reveal about the extent to which extreme fire weather across the world has been altered as a result of anthropogenic climate change?*

Objective 2.1: To evaluate the performance of the latest generation of global climate models in representing extreme fire weather. It is important to evaluate the applicability of each model since significant differences exist between climate models, especially for different variables where the output results can be considerably varied. Therefore, in attribution studies, model-to-real-world comparison of parameters estimated from the extreme value distribution can be applied to assess the capacity of climate model simulations. However, often restricted by the limited number of years available for observational data, the assessment of differences based on the parameters between models and real-world data is also subject to large uncertainties and is generally considered challenging (Philip et al., 2020; van Oldenborgh et al., 2021b).

Objective 2.2: To estimate the changes in extreme fire weather using multiple large ensembles from the latest generation of climate models. Using historical scenarios from the latest generation of climate models that provide longer-term time series, we use multiple large ensembles to produce maps representing changes in the probability ratio of the intensity and duration of extreme fire weather intensity and duration in response to externally forced rising global temperatures. Climate model large ensembles (>10 realisations, or ensemble members, of climate) indeed enable a more robust estimation of externally forced signal (*e.g.*, global warming temperature), via extracting the ensemble means, and reduce the influence of internal/natural climate variations in the climate system, and in the probabilistic attribution studies.

Objective 2.3: To facilitate and simplify communications from climate change modelling studies, while dealing with large uncertainties. Evaluations and selections of models in strong performance based on Objective 2.2 is beneficial to account for the impact of internal (natural) climate variations affecting climatic mean-state on regional and decadal scales, therefore generating the global synthesis plots with a holistic summary, supporting and informing decision-makers and practitioners in an intuitive way, while also reducing the internal uncertainties of the climate models.

Research Question 3: *How is climate change altering the risk associated with recent episodes of high-impact fire weather?*

Objective 3.1: To conduct attribution analysis on a series of extreme fire weather case studies in different parts of the world. A series of attribution case studies target recent high-impact wildfires driven by one or more episodes of extreme fire weather. The case studies follow the approach initially set out in Objective 1.1, along with the conclusions and recommendations drawn from Objectives 1.2, 2.1 and 2.2, in order to demonstrate the applicability of the empirical-statistical framework to real world events.

Objective 3.2: To explore the potential for collective attribution of multiple extreme fire weather events. To date, the relative paucity of wildfire attribution studies, coupled with limited observational records, makes it difficult to draw solid and collective conclusions to better inform risk assessment and adaptation strategies. The inter-study differences that emerge due to the choice of methodology and event definition are common to many attribution studies; for wildfire attribution in particular, the lack of consensus on how fire danger should be defined in a meteorological context presents an additional challenge.

1.7 Structure of thesis

Following the introduction given in **Chapter 1**, this thesis contains five further chapters. In **Chapter 2**, wildfire events associated with human-induced climate change will be reviewed from perspectives of the driving mechanism, historical trends and current occurrence, approaches of framing and assessing in a climatic aspect and the potential attempts in the future. This part of the literature review encompasses the development of attribution studies on extreme weather events in the context of climate change over the last two decades, most importantly detailing the probabilistic framework and advanced statistical methods in attribution studies and illustrating the potential applicability of this approach to fire weather extremes. The following three chapters (Chapters 3-5) constitute the empirical component of the thesis and contains materal that has either been published in (Chapter 3 and sections 5.1 and 5.2 of Chapter 5), submitted to (Chapter 4), or in preparation for submission to (section 5.3 of Chapter 5) peer-reviewed journals. **Chapter 3** demonstrates the observed global trends in fire weather risks using reanalysis data, with the exploration of uncertainties on the choice of fire weather indicators and the attribution of recent exceptional fire weather events, based on the probabilistic framework conducted at the beginning. In **Chapter 4**, a series of large-ensemble climate models with long-term time series are evaluated and selected to attribute the current fire weather risks associated with the external forced warming temperature anomalies in both intensity and duration, with an additional step to generate a global synthesis plot. **Chapter 5** draws together analyses of three independent case studies of wildfires associated with

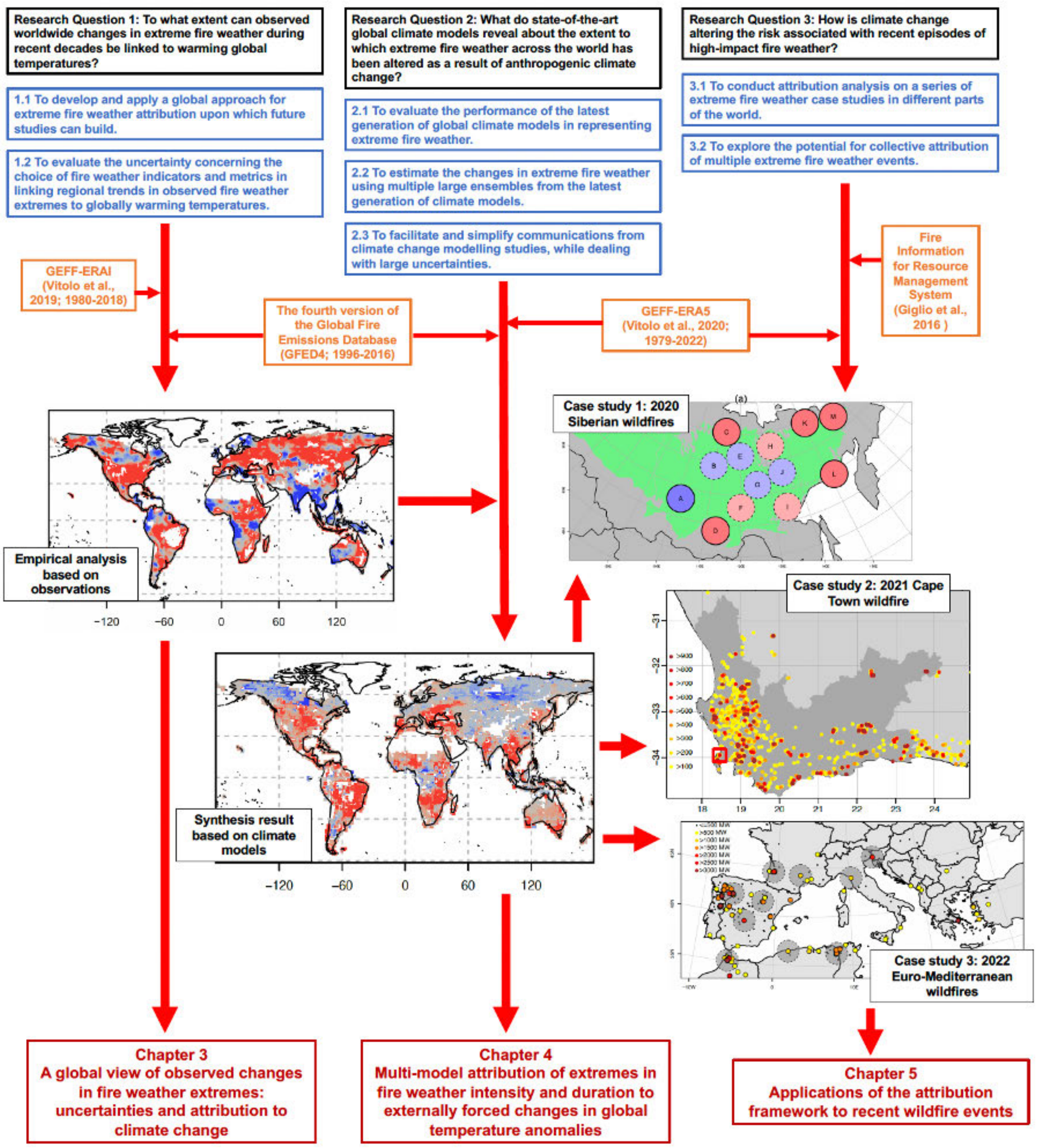

Figure 1.8: Schematic diagram of the research questions and objectives, including datasets and result chapters.

extreme fire weather to understand and quantify the past, present and future risk associated with a changing climate. In **Chapter 6**, all the findings are summarised in relation to the questions and objectives stated in section 1.6. Further discussions and recommendations with potential limitations and improvements are concluded for future developments.

Chapter 2

Literature Review

2.1 Linking fire weather and fire risks in the context of climate change

Early studies of wildfires often concentrated on assessing burning areas and severities of burning as basic statistical analyses. With recent progress in research, the issue of identifying and analysing the risk of wildfires quantitatively became the focus. The intuitive reasoning that the combination of low humidity and high temperature can increase the ignition of fuels, and lead to the risk of wildfire has gradually led to ideas about the association between fire danger and weather (Vitolo et al., 2019).

In one of the earliest attempts to link climate-fire relationships, Cohen and Deeming (1985) introduced a system called National Fire Danger Rating System (NFDRS) to establish the degree of fire hazard and the risk of fire spread by utilizing various models with the constitution of daily meteorological fields. Subsequently, Van Wagner (1987) introduced a similar approach to assess relative risks termed the Canadian Fire Weather Index System (CFWIS), which generates a set of fire behaviour indices using observational weather data. CFWIS was first introduced and developed for the Canadian forests, and has been widely used across the world's forested regions (*e.g.*, France, Italy and Portugal [Viegas et al., 1999], New Zealand [Dudfield, 2004], southeast Australia [de Groot et al., 2006], southeast Asia [de Groot et al., 2007], Greece [Dimitrakopoulos et al., 2011], Brazil [Li et al., 2021] and south-eastern Australia [van Oldenborgh et al., 2021a]). Notably, in Australia, the CFWIS has successfully been used to study the past occurrence and future likeliness of an event to occur (Dowdy et al., 2009; Abatzoglou et al., 2019).

CFWIS uses fundamental weather variables to assess the risks of fire ignition and spread (Van Wagner, 1987). As shown in Figure 2.1, the system contains three unitless indices, or codes of the Fine Fuel Moisture Code (FFMC), the Duff Moisture Code (DMC) and the Drought Code (DC) (National Wildfire Coordinating Group, 2023). These different indices represent slightly different characteristics of fires (Van Wagner, 1987):

Figure 2.1: Basic structure of the FWI system (National Wildfire Coordinating Group, 2023).

The first level of 'Fire weather observations' is composed of all the necessary weather variables (*e.g.*, temperature, relative humidity, wind and rain), which are classified and available at daily or hourly time step (Figure 2.1; National Wildfire Coordinating Group, 2022). These variables are firstly used to construct a set of 'fuel moisture codes' (Vitolo et al., 2019): Fine Fuel Moisture Code (FFMC) is an indicator of the moisture content, and therefore relative flammability and combustibility, of fine fuels (*i.e.* surface organic materials, such as needles, grasses and small twigs), and is characterized by their rapid response to weather changes; Duff Moisture Code (DMC) represents a numerical rating of the averaged moisture content of decomposed organic material, and is characterized by a medium-term response to weather changes; Drought Code (DC) represents the averaged moisture content of the soil at depth, and is characterized by the long-term response to weather changes. Subsequently, a set of 'fire behaviour indices', is calculated (Vitolo et al., 2019): Initial Spread Index (ISI) represents a numerical rating of the spread potential of a fire in the early stages shortly after ignition; Buildup Index (BUI) combines current DMC and DC to represent a numerical rating of the total amount of fuel available for combustion and is an estimate of potential heat release in heavier fuels. The final calculation is the Fire Weather Index (FWI), which represents a numerical rating of the general fire intensity and, therefore, a general index of fire danger (Vitolo et al., 2019). While the CFWIS parameters pertaining to, for instance, vegetation type, fuel availability and thresholds for ignition could in principle be subjected to a spatiotemporal adjustment, it is commonplace for the existing setup to be applied across all parts of the world.

In summary, through the simple input of sole weather patterns and procedures of calculating relative indices, the risks of potential fires can be estimated. According to previous studies, CFWIS often shows the best performance among indices (including NFDRS) almost all over the world and its replicability and adaptability are universally acknowledged (Krikken et al., 2021). Hence, the focus will be mainly given to the CFWIS.

Studies using the global fire danger reanalysis dataset by Vitolo et al. (2019) enabled to provide a worldwide map for FWI calculated cell by cell from 1980 to 2017 (Figure 2.2). Areas with red-covered, particularly in northern Africa and the Middle East region, manifest the severe conditions prescribed by FWI (Figure 2.2). It is important to note that the most extreme FWI conditions (*i.e.* hot, dry and windy prevailing meteorology) are not necessarily associated with fire activity; many such conditions are prevalent in desert regions with minimal burnable vegetation. Rather than acting as precise proxy for fire occurrence, the FWI (and other indices based on meteorological parameters) should be considered an indicator of fire risk given particular land cover conditions.

2.2 "Detection" and "attribution" study

The concept of "detection of change" was first introduced in the 1990s by IPCC (1995), illustrating the progress in better defining the background natural variability of the climate system. "Detection" studies aim to identify long-term changes in meteorological variables or climate phenomena irrespective of their causes. Attempts to detect observed changes in climate variables, such as global mean surface temperature (GMST), were also shown by using various approaches and observational datasets across different regions (Figure 2.3; Le Treut et al., 2007).

Estimates of naturally and non-naturally driven climate fluctuations on a century scale remain difficult to obtain directly from observations, especially due to the lack of multi-centennial datasets, and the complexity of accurately disentangling natural and non-natural

Figure 2.2: 90^{th} percentile of FWI calculated cell by cell for the period 1980 – 2017 (Vitolo et al., 2019).

forcings from one realisation of climate (the observed one). This is why "attribution" studies were developed to quantify the relative contribution of one or more drivers of detected changes (Le Treut et al., 2007; Hegerl et al., 2010). "Detection" and "attribution" are individual concepts, but are also closely interrelated at a technical level, as defined by the Second and Third Assessment Report of the IPCC at the early stage (IPCC, 1995, 2001). For instance, Figure 2.4 illustrates how two scenarios from one climate model can be used to estimate the relative contribution of all forcings (anthropogenic and natural forcings) and natural forcings to the observed trend in GMST anomalies (Meehl et al., 2004).

Detection and attribution analyses of climate change were originally designed for observed changes and trends in any climate-related phenomena at both short-term and long-term time scales, for instance, the extreme heat events from as little as one day to at least one year (Hegerl et al., 2010; National Academies of Sciences, Engineering, and Medicine, 2016). With the increasing frequency and intensity of extremes, attribution science has shifted towards quantifying changes in the likelihood, and/or magnitude of such events, as a result of rising global temperatures (Stott et al., 2016; Knutson et al., 2017). Consequently, detection and attribution methods had been applied in a series of studies, including studying trends or long-term changes in climate mean states (*e.g.*, mean temperatures, mean intensity and frequency of extreme events and their impacts).

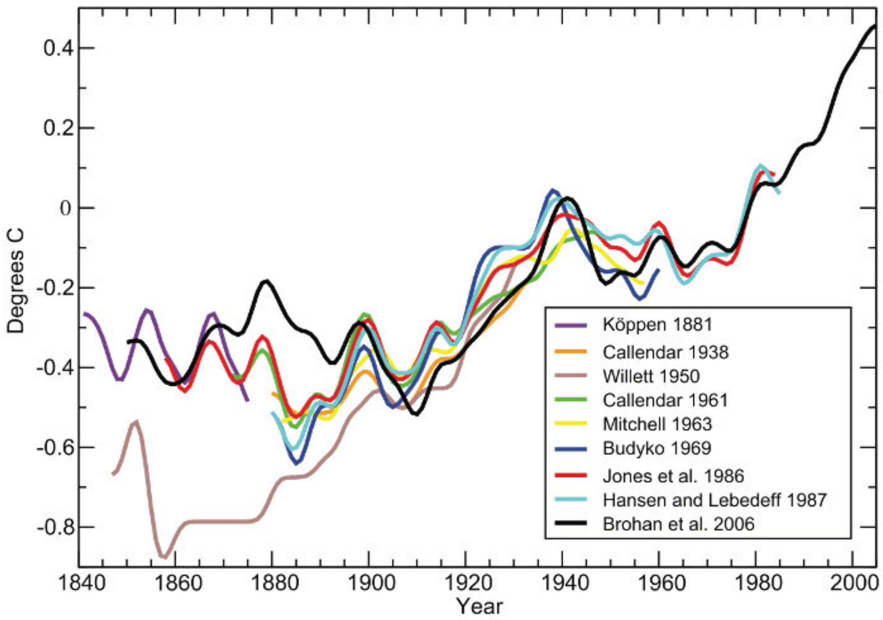

Figure 2.3: Changes in surface temperature over large regions derived from publications since 1881 (Le Treut et al., 2007). Köppen (1881) represented the land air temperature over tropics and temperate latitudes. Callendar (1938), Willett (1950), Mitchell (1963), Jones et al. (1986a, b) and Hansen and Lebedeff (1987) showed the observational records from global land stations. Callendar (1961) represents the observed temperature from 60°N to 60°S using land stations. Budyko (1969) displayed the temperature in the northern hemisphere using land stations and ship reports. Brohan et al. (2006) used land air temperature and sea surface temperature data to present the longest global temperature time series as of 2007.

Detecting and attributing long-term trends and changes in climate, therefore, requires observational data sets, whose network density as well as temporal resolution have substantially increased over the past two decades (National Academies of Sciences, Engineering, and Medicine, 2016). Meanwhile, the capability of computing power continues to grow rapidly, offering the necessary support for large climate model ensembles and probabilistic statistical modelling (National Academies of Sciences, Engineering, and Medicine, 2016). The fifth assessment report then further acknowledges the achievement by quantifying these contributions of anthropogenic climate change (IPCC, 2014). Other examples of attribution studies also include quantification of the contribution of specific modes of climate variability, such as the impact of tropical cyclones (Knutson et al., 2010).

An overview of the evolution of detection and attribution science is illustrated in Figure 2.5. Early work in the detection and attribution of warming and increased rainfall concentrated

Figure 2.4: GMST anomalies (°C; as the reference period of 1890–1919) from the ensemble mean (red line) and corresponding ensemble member range (pink shading) for each run from its time series of annual values (Meehl et al., 2004).

on defining the "unusual" changes in statistical aspects and identifying the signal from anthropogenic aspects compared with disparate scenarios in models (IPCC, 1995).

Subsequently, the science community combined the approaches to the probabilistic theory of extremes, quantifying changes in the likelihood of extremes (IPCC, 2007, 2014). Among these studies, Allen (2003) introduced the metric known as the fraction of attributable risk (FAR) from the legal instead of physical perspective, and this method was widely acknowledged in the attribution studies to show the estimate of the probability of an adverse event risk attributable to human influence on climate. Stott et al. (2004) illustrated the human contribution to the European heatwave in 2003 was the first paper in attributing extremes in a relatively comprehensive probabilistic way. The review paper by Zhai et al. (2018), however, highlighted early work in attributing climate change impacts to humans and natural systems, for instance, the IPCC report in 2001, as well as Smith et al. (2001). Likewise, the initial investigations into damaging events, such as the heatwaves observed in the period from 1900 to 1950 during a phase of rapid global warming (Hegerl et al., 2007) and the floods in England in 2000 (Pall et al., 2011), have significantly advanced our understanding of extreme events. More recently, Stott et al. (2016) refined the definition of attribution to anthropogenic climate change, proposing to use globally warming temperature anomalies as a proxy of anthropogenic climate change. Using this method, the authors highlighted that changes in the likelihood of extreme could be linked to changes in global or regional temperature, and therefore could be attributed to anthropogenic climate change. Subsequently,

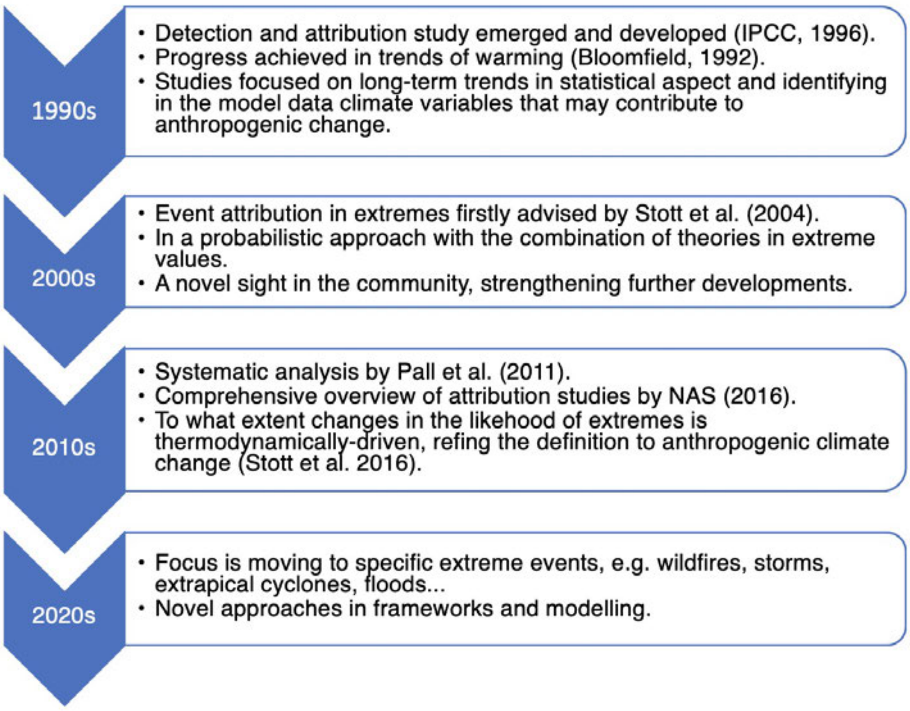

Figure 2.5: Evolution of detection and attribution study since 20$^{\text{th}}$ century.

a series of studies advised by the *Bulletin of the American Meteorological Society* and IPCC concentrated on attribution studies of extremes, brought substantial outcomes, *e.g.*, to what extent changes in the likelihood of extremes are thermodynamically-driven (*i.e.*, purely driven by changes in temperature; Stott et al. 2016).

2.3 Conditional vs. non-conditional attribution approaches

The notions of conditional and non-conditional aspects of event attribution divided the community (Stott et al., 2016). Conditional attribution aims at answering the questions about the changes in likelihood or intensity under the limitation of one or more slowly varying parts of the climate system (for instance, selections of specific years under the condition of El Nino as observed for conditional attribution studies; National Academies of Sciences, Engineering, and Medicine, 2016). By contrast, non-conditional attribution aims to provide probabilistic estimates of changes in likelihood and intensity of a given risk irrespective of the cause (National Academies of Sciences, Engineering, and Medicine, 2016).

The so-called "conventional" (conditional) approach to attribution described by (Stott et al., 2013) uses physical-based assessments of observed weather or climate-related events to identify the changes of risks to specific factors and estimate the contributions of factors in event attribution. This conventional method of probabilistic analysis can directly assess the risk for the extreme event in response to a particular weather situation or weather pattern, having considerable success with extremes involved with the thermodynamic aspect of climate change (Trenberth et al., 2015). For thermodynamic-related events, higher performances both in the confidence of attributing extremes and understanding of the effect of climate change confirmed the influence of anthropogenic climate change on the increasing frequency and intensity of extremes.

Due to the intricacy and incomplete comprehension of the physical mechanisms involved, various attribution studies on tropical cyclones, wildfires, and storms remain constrained by the availability of observations, modeling approaches, and specific topographical considerations (National Academies of Sciences, Engineering, and Medicine, 2016). This challenge is, therefore, promoting other approaches to make efforts in estimating the change in probability of the climatic or weather state (Otto et al., 2016). However, this method, focusing on thermodynamically-driven extremes and changes, struggled with dynamically-driven extremes due to the small changes in the context of climate (*e.g.*, internal atmospheric circulations) and its associated modulations of forced changes (Trenberth et al., 2015). Although natural climate variability happens all the time with tiny differences in large-scale circulations, the chaos in ensemble simulation models might be significant (Deser et al., 2012a,b, 2014; Kay et al., 2015).

In a specific individual circumstance, to what extent the anthropogenic climate change influences the relationship between large-scale circulations and regional events is helping understand isolating drivers in extremes (Otto et al., 2016). The framing of the attribution question has a considerable influence on the results and their interpretation. This issue can be illustrated using the example of the Colorado Boulder flood in September 2013, which was first analysed by Hoerling et al. (2014) and then by Trenberth et al. (2015). This pair of studies produced contradictory results with respect to the role of anthropogenic climate change. The non-conditional approach of Hoerling et al. (2014) concluded that there is no trend in the likelihood of the climate change effect on this extreme event by exploring the relationship between the probability of extreme rainfall and atmospheric water vapour using the ensemble-averaged GEOS-5 simulation outputs. However, Trenberth et al. (2015) were critical of the non-conditional approach taken by Hoerling et al. (2014), as the methodology from the latter focused solely on the regional scale and did not consider where the moisture, leading the heavy rain event, was coming from. As mentioned in Trenberth et al. (2015), the moisture was transported from a region of anomalously high sea surface temperature (*i.e.*, the eastern Pacific Ocean) to the west of Mexico and one of the reasons for the anomalously warm sea surface temperature in this region is anthropogenic climate change itself (Trenberth et al., 2015). This case stressed the importance of different framing of the attribution studies, so that only comprehensive and systematic evaluations of all possible sources and internal relationships between the variables can be provided in the most consistent and accurate way. However, investigating the cause of the same event, Eden et al. (2016) found that most of the moisture originated in the Gulf of Mexico and the western Atlantic rather than the previous suggestion from the Pacific Ocean. Thus, as the anthropogenic influence on sea surface temperature is weaker in the Gulf of Mexico than in the Pacific Ocean, the generating mechanism of an event presents possible contradictory results (Eden et al., 2016). This example challenges the corresponding work of attribution questions and highlights the complexity of the choice of conditional vs non-conditional approaches. Additionally, using both observations and simulations, Hoerling et al. (2014) also demonstrated that the trend in higher pressure over Boulder (Colorado) during September could potentially reduce the likelihood of extreme precipitation events. According to this extreme event and the contradictions above, Stott et al. (2016) illustrated that the attribution from the anthropogenic aspect could be considered under the condition of climatic variability in a certain state. This idea addresses the difference between the overall and the conditional probabilities of the event, offering a broader view of the attribution assessment. Therefore, conditional attribution studies have the potential to invoke controversy in the linkage between large- and local-scale systems (Eden et al., 2016).

The conditional vs non-conditional comparison has slowly grown into a refined debate about storyline vs probabilistic (or, alternatively, risk-based) approaches to attribution, their relative merits and limitations, and how they can be used to complement one another. The storyline vs probabilistic debate is discussed in further detail in Chapter 3 (section 3.2.1). Philip et al. (2020) note that, while the storyline approach is very important in understanding the meteorological origin and anatomy of a particular event, and in highlighting the role of climate change in influencing both dynamic and thermodynamic processes, it does not reveal any information about the changing probability of the event itself. By contrast, a probabilistic approach to attribution (that focused on the risk itself and is not conditional on the processes that led to the risk) provides immediately numerical results that can directly assist stakeholders and decision-makers. The greater potential of the probabilistic approach for standardising attribution analyses as part of a global framework makes it the most suitable framing for the objectives of this thesis.

2.4 Framing of the attribution question

A scientific answer is always based on the question to be addressed. In the context of attribution studies, this refers to framing the work to be undertaken according to the context, for instance, different variables and/or regions (National Academies of Sciences, Engineering, and Medicine, 2016). When the relative impact of anthropogenic forcing versus natural variability comes into play, further framing issues are advised (National Academies of Sciences, Engineering, and Medicine, 2016).

2.4.1 Review of advances in attribution studies

During the 1990s, most efforts addressing the attribution question focused on observed long-term trends, meteorological variables, climate phenomena and the relationship with anthropogenic activities (Zhai et al., 2018). Given the limitation of computing power and data resolutions, using a global atmospheric model in extreme attribution studies was limited for years (National Academies of Sciences, Engineering, and Medicine, 2016). In 2003, a widely acknowledged method, known as the fraction of attributable risk (FAR), was first introduced by Allen (2003), to calculate the liability for climate change (Figure 2.6), here namely to show the estimate of the probability of an event in the attribution studies. Throughout comparing the differences between 'mean likelihood-weight liability' of a specific event, results can be calculated to show to what extent the 'external cause A' (*i.e.*, climate change) altered the occurring probability of this event (Figure 2.6).

Figure 2.6: Fraction of attributable risk of undesirable events (Allen, 2003). A 'mean likelihood-weighted liability' by averaging over all possibilities consistent with currently available information is estimated to show the changes.

The first attempt at attributing an individual extreme event was the analysis of the European heatwave in 2003 conducted by Stott et al. (2004). As Stott et al. (2004) discussed, it is difficult to answer whether the external forcing (such as the increase of greenhouse gas emissions) is blamed to cause such kinds of heatwaves, because internal climate variability could also lead to the occurrence of this event by chance. However, the estimation of the changing likelihoods can be attributable to how much human activities may be altering the risks (Stott et al., 2004). Generally, the likelihood of an event is associated to some extent with the observed event, but this requires using model simulations and long-term observational data. Through the comparison between the factual world under climate change (refers to the current climate) and the counterfactual world without climate change (refers to a past climate), the probability is taken to reflect the effect of climate change. In such model-based attribution studies, ensembles of model simulations were used to help disentangle the contribution of anthropogenic and natural variability (Stott et al., 2004; National Academies of Sciences, Engineering, and Medicine, 2016). Since then, rapid developments and improvements have been made to the subfield of extreme event attribution.

According to Allen (2003), Hannart et al. (2016), National Academies of Sciences, Engineering, and Medicine (2016), the concept of 'Risk Ratio (RR)' or 'Fraction of Attributable Risk (FAR)' or 'Probability Ratio (PR)' became the dominant metric to define the change in the probability of occurrence of an extreme event, which can be calculated as in Eq. (2.1-2.2):

$$RR = \frac{p_f}{p_c} \; or \; FAR = \frac{p_f - p_c}{p_f} \tag{2.1}$$

$$PR = \frac{p_{past}}{p_{present}} \; or \; \frac{p_{present}}{p_{future}} \tag{2.2}$$

where p_f represents the likelihood of an extreme event in the factual climate containing the anthropogenic contribution to climate change and p_c is the counterfactual climate without the impact of human-induced climate change; p_{past} represents the likelihood of an extreme event occurred under the past climate, $p_{present}$ is the likelihood of such event occurred under the present climate and p_{future} shows that under the future scenarios.

Using this concept, Stott et al. (2004) provided a comparison between the occurring probabilities of a recorded heatwave event and its likelihood without anthropogenic effects on climate using an ensemble of climate model simulations. The study showed that a heatwave like the 2003 event has an increased likelihood as a response to anthropogenic climate change. After that, new operational systems, applying the FAR for assessing the attribution of extremes emerged and developed. Hannart et al. (2016) proposed a causal framework for event attribution, providing likelihoods of necessary and sufficient causation of an event. As the easiest way to interpret the probability of a class of events rather than an individual event, the FAR offers a very useful insight through comparisons between factual and counterfactual worlds (National Academies of Sciences, Engineering, and Medicine, 2016).

2.4.2 Methodology of event attributions

For any extreme event, multiple factors from natural or anthropogenic sources always interact with each other, thus, event attribution should not be framed as human-induced or natural given that it will always be a combination of both (National Academies of Sciences, Engineering, and Medicine, 2016). An essential part of the event attribution is the way of framing, while the result is sensitive to the question and its context. Therefore, it is useful and vital to state an explicit framework and explain the relative reasons for choosing.

The choices of the framework can contain the interpretation of a single event, the condition that is involved, the assessment of the frequency and intensity of an event, and the definition of the event, among other factors (National Academies of Sciences, Engineering, and Medicine, 2016). The last decade has seen the development of different approaches for event attribution analysis, which in turn has led to a significant discussion of their merits, offering results in more than one way and providing disparate sights of looking at the event (National Academies of Sciences, Engineering, and Medicine, 2016; Kirchmeier-Young et al., 2019a). For instance, using a one-dimensional definition to describe the extremeness of the event, the monthly mean maximum temperature (1951-2021) for the warm 2021 February over East Asia (Xie, 2022), and daily the mean temperature from the first half of the October temperature (2001-2020) for the heatwave in South Korea (Kim et al., 2022) are defined in different spatial and temporal contexts of events.

Considering the setup of a spatiotemporal event definition, the natural first step of event attribution is always the study of observations to determine the extremeness and rarity of the events in historical records, *e.g.*, using statistical analysis to estimate the return period for types of events. Subsequently, climate models may be utilised to link the knowledge of the whole climate system to typical events by suitable observations, quantifying the contributions from human activities (National Academies of Sciences, Engineering, and Medicine, 2016). In addition, to obtain better assessments for event attribution, large ensembles and the use of multiple models can offer more robust detections and analysis of extremes, and a better representation of the real diversity of events with or without the effect of anthropogenic climate change (Stott et al., 2016, Zhai et al., 2018; further explanations are available in section 2.4.4).

Observations are broadly employed in all attribution studies. However, real-world trends always have large uncertainties, particularly for the wildfire extremes, due to the limited years of observational records. Thus, when available, the employment of long-term historical records and statistical analysis is an excellent way to quantify the likelihood of extreme events and their corresponding circulation periods. For instance, Pall et al. (2011) used the data of daily river runoff for England and Wales in the autumn of 2000, estimating the FAR and return periods for potential circulations of floods in England as a milestone for event attributions. Additionally, many studies applied observations for further standards or thresholds for simulations of typical types of events (Jain et al., 2022).

Climate models with longer-term simulations (>100 years) are widely applied to present the proper signals for the event (National Academies of Sciences, Engineering, and Medicine, 2016). Different types of climate model simulations can be used, but coupled ocean-atmosphere general circulation models (AOGCMs or CGCMs) are commonly used to provide the most comprehensive and systematic simulation of the climate systems. CGCMs are also the primary choice for analysing the historical and future trends in extreme events across the world. In particular, CGCMs provided by the sixth phase of the Coupled Model Intercomparison Project (CMIP6) are the latest version to be used in the field (Eyring et al., 2016). Compared to the previous fifth version, *i.e.* CMIP5, CMIP6 offered a wider range of forcings in future scenarios to account for the mitigation and adaptation strategies to the challenges in the future (Eyring et al., 2016; Stouffer et al., 2017; Bourdeau-Goulet and Hassanzadeh, 2021). In addition, a higher number of simulations for the same forcing is developed in CMIP6 to better represent the internal variabilities (see Figure 2.7) as well as the improvement of the historical representation in climate extremes indices on a global scale compared to the CMIP5 model (Eyring et al., 2016; Chen et al., 2020; Di Luca et al., 2020). Owing to the model outputs employed by CMIP6 (Eyring et al., 2016), comparisons between different forcing (with or without anthropogenic effects) can be helpful to directly quantify changes presenting potential impacts from specific aspects (*e.g.*, anthropogenic vs. natural; Stott et al., 2004; National Academies of Sciences, Engineering, and Medicine, 2016).

Additionally, atmospheric-only GCMs (AGCMs), with forced changes in the atmosphere induced by observed sea-surface temperature, are also recommended in recent years. According to Walters et al. (2017), the Hadley Centre system (HadGEM3-A-N216) developed by the UK Met Office is to attribute extreme events, the role of human-induced climate change can be more clearly discerned, as uncertainties associated with AGCMs are lower

Figure 2.7: Comparisons in model resolutions, number of simulations for the historical and future periods between CMIP5 (the top CMIP belonging to each climate modelling center) and CMIP6 (the bottom CMIP belonging to each climate modelling center) (Bourdeau-Goulet and Hassanzadeh, 2021).

than in CGCMs. The conditioning result is frequently employed to prescribe observed sea surface temperature anomalies by considering a counterfactual world rather than an unforced nature without anthropogenic effects (Stott et al., 2016). It is desirable to include multiple counterfactual conditions (mentioned in Eq. 2.2) to compare with human-induced impacts. Besides, new ideas about applying the Weather Research and Forecasting (WRF) model to extreme event attribution introduced by Tradowsky et al. (2020) also drew scientists' interest in the recent European Geosciences Union General Assembly 2020. Such an attempt could have an accurate estimate of extreme events by employing an explicit convection algorithm with high-resolutions instead of a parameterized convection scheme.

2.4.3 Quantifying changes in the likelihood of extreme fire-weather in response to warming temperature

Generally, the study of changes in extreme events primarily focuses on frequency and intensity (Stott et al., 2016). With the available datasets for event attributions, the approach of plot fitting became a good point to see the corresponding distributions for the outputs (King et al., 2015; van Oldenborgh et al., 2015). In event attribution study, two main statistical distributions, namely Generalized Extreme Value (GEV) distribution ($P(x)$) and Generalized Pareto Distribution (GPD; $H(x-u)$) are often utilized as Eq. (2.3) and (2.4), respectively.

$$P(x) = exp[-(1+\xi\frac{x-\mu}{\sigma})^{-\frac{1}{\xi}}] \tag{2.3}$$

where x is the variable for the research objective (for instance, here x represents FWI for wildfires), $-\infty < \mu < \infty, -\infty < \xi < \infty$. μ and σ here are location and scale parameters, respectively, and ξ is the shape parameter.

$$H(u-x) = 1-(1-\frac{\xi x}{\sigma})^{-\frac{1}{\xi}} \tag{2.4}$$

where x is still the variable for the research objective, u is the threshold, σ and ξ are the scale and shape parameter, respectively (Coles, 2001).

The parameterization scheme for the parameters in GEV and GPD is also commonly used to estimate the trend in transient data. The 4-yr smoothed global mean surface temperature (GMST) anomaly $T^{'}$ is employed to present parameters, combined with the bootstrapping steps and the 95% uncertainty range shown below (Figure 2.8) according to van Oldenborgh et al. (2021a). The 4-yr smoothing is chosen to reduce the ENSO component of GMST, which is not external forcing and therefore not related to the trend, and this shortest smoothing timescale allows as much of the forced variability as possible at the same time (Haustein et al., 2019). Therefore, the function in Eq. (2.3) and (2.4) can be assumed to be covariate with GMST by $\mu = \mu_0 + \alpha T^{'}$ and $\sigma = \sigma_0 + \alpha T^{'}$ where α represents the trend in fire indicator maxima as a function of smoothed GMST anomaly $T^{'}$, then the parameters in Eq. (2.3) for a GEV fit and that in Eq. (2.4) for a GPD fit are converted as

$$\mu = \mu_0 \cdot exp\frac{\alpha T^{'}}{\mu_0} \tag{2.5}$$

$$\sigma = \sigma_0 \cdot exp\frac{\alpha T^{'}}{\sigma_0} \tag{2.6}$$

with the shape parameter ξ assumed constant. Significant increases in temperatures are strong evidence for the applicability of the methods.

Almost all the statistical analyses for wildfires applied these two fits (especially GEV fit). For instance, Krikken et al. (2021) applied a GEV fit only, while others applied both

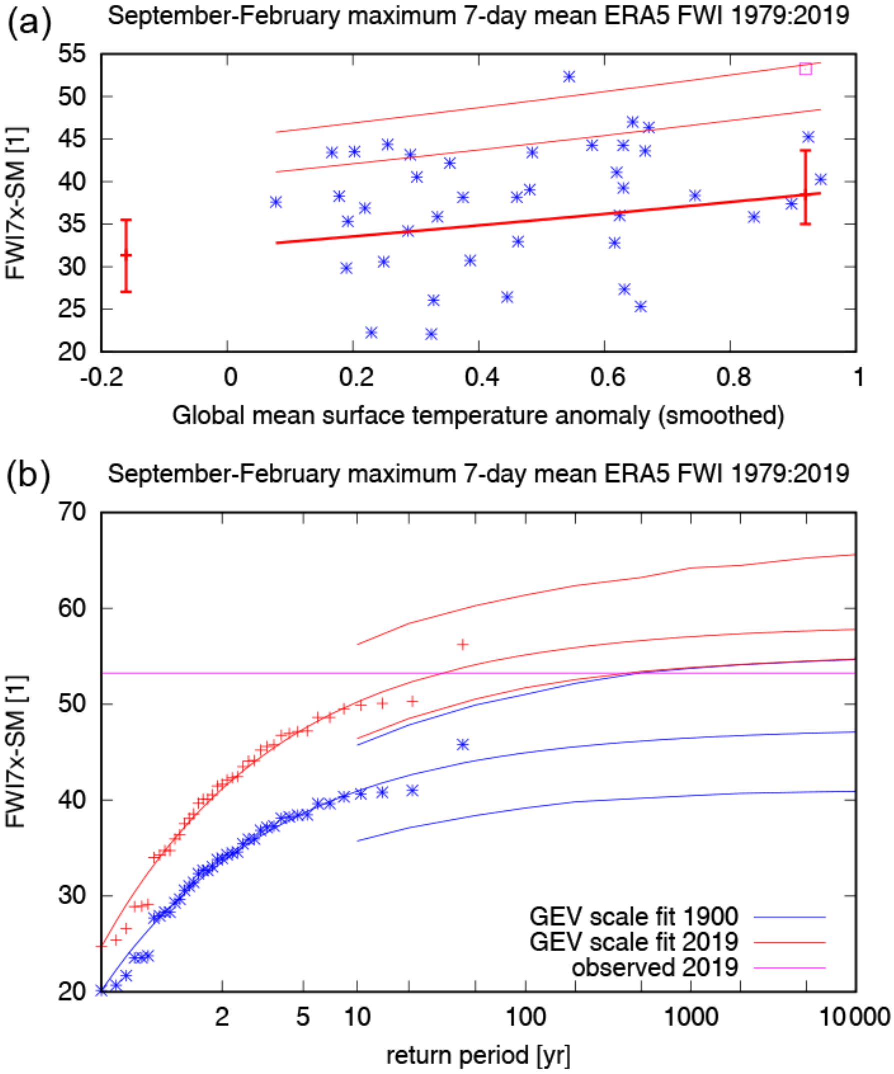

Figure 2.8: GEV fit to the bushfire regions of a new parametrization method by van Oldenborgh et al. (2021a). The position parameter is linearized by GMST while the scale and shape parameters are constant.

a GEV fit and a GPD fit (Barbero et al., 2020; van Oldenborgh et al., 2021a). By applying the spatial and temporal extents of the risks that relate to fire suppressions, a decision for the threshold of the minimal occurring condition can be obtained afterwards. Throughout the fitting plots supported by the observational dataset and model simulations, appropriate statistical distributions including probability density function scaled to the past (blue), present (dark grey) and future climates (orange and red) with ranges of return periods can be shown ultimately (c.f., Figure 2.9 for GEV fit). Then probabilities estimated for a specific magnitude of the event are used to show the changes in the likelihood of such extremes based on Eq. (2.2). As an example, in Figure 2.9, the central return period is around 60 years in the past (blue) while that shows about 15 years to occur once under present climate (dark grey), then the corresponding probability ratio is approximately a factor of four between the past and present climates, namely such kind of extreme event is currently four times more likely to occur compared to the past days. This offers the first step of reasonable understanding to the records (National Academies of Sciences, Engineering, and Medicine, 2016; Barbero et al., 2020).

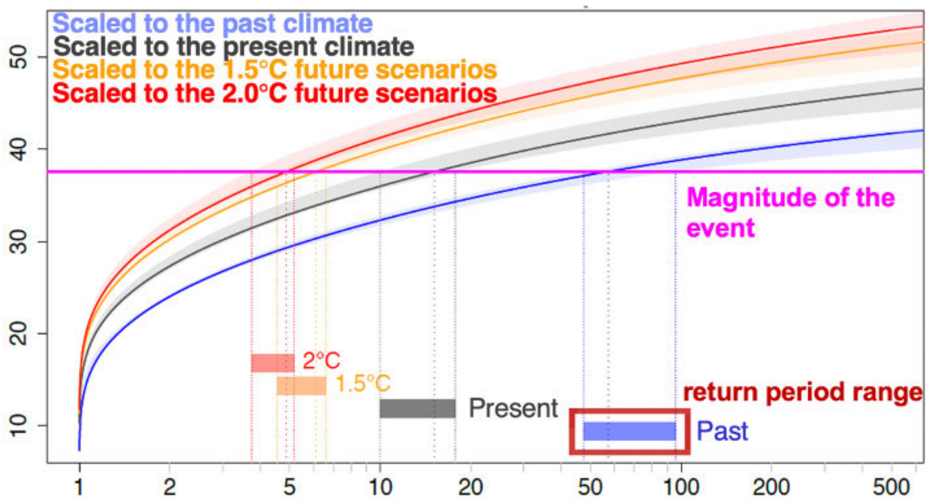

Figure 2.9: An example of annual Fire Weather Index (FWI) maxima fitted to GEV scaled to the global mean surface temperature under the past, present and future climates.

The demonstrated statistical approach above offers substantial outcomes for the attributions of not only wildfires, but most extreme events (*i.e.*, heavy precipitations, heat waves, tropical cyclones; National Academies of Sciences, Engineering, and Medicine, 2016).

Note, however, that this statistical approach is desirable only if there is a strong causal link between the covariate and anthropogenic climate change (National Academies of Sciences, Engineering, and Medicine, 2016). Otherwise, an underestimation or overestimation of trends would be produced eventually due to other factors from natural variability (National Academies of Sciences, Engineering, and Medicine, 2016). Based on the latest research by van Oldenborgh et al. (2021a), two types of uncertainties can be witnessed: i) internal/natural climate variability can strongly influence regional and decadal climate trends; ii) different computing tools and inputs could lead to slightly different results (*e.g.*, datasets [different observational datasets or models], fire weather indices, statistical framework). Therefore, strategies for reducing the impact of internal/natural climate variability presented by model spread and a weighted mean by climate models are beneficial for providing more robust information in the study.

2.4.4 Sensitivities and uncertainties of climate models

Estimating climate sensitivity is becoming a crucial aspect to understand climate change (Stott et al., 2016; Knutson et al., 2017). Model-to-model differences largely exist given the internal variability and the forced response to external forcing in the models (Maher et al., 2021), while multi-model averaging is an efficient approach to reducing the uncertainties related to climate models (Georgakakos et al., 2004; Exbrayat et al., 2010; Taylor et al., 2012; Sansom et al., 2013; Her et al., 2016; Eyring et al., 2016; Milinski et al., 2020).

The main sources of uncertainty in CGCMs come from two aspects, namely model and scenario uncertainty, internal/natural climate variability (Hawkins and Sutton, 2011). For model uncertainty, model simulations, either over the historical period or the future, might be disparate between different models, which were built using different atmospheric, ocean, sea-ice and land-surface models (Knutti, 2010; Masson and Knutti, 2011; Dieppois et al., 2019); even under the same radiative forcing, some models may be more sensitive than others (Andrews et al., 2018; Zelinka et al., 2020). Regarding the role of internal/natural climate variability, recent studies highlighted its importance in modulating climatic trends at regional and decadal scales (Deser et al., 2012a, 2020; Deser and Phillips, 2023). In the context of event attribution studies, it is worth noting that internal climate variability may wrongly be included in the effect of anthropogenic forcing, for instance. Separating internal climate variability from externally forced changes (ca. anthropogenic climate change) from the GMST is crucial. In that sense, in any regional studies, the use of large-ensembles (> 10 simulations of the same model) of CGCMs is recommended, as it allows to smooth the impact of internal variations at the global scale, and more accurately extracts externally forced signals (Milinski et al., 2020; Maher et al., 2021). This is illustrated in Figure 2.10, where the shading area in light grey shows a large range of uncertainty in GMST when using individual realizations, while that uncertainty range is progressively reduced when using larger ensemble sizes (*i.e.*, 10, 20, 50, 200). Therefore, using climate models with a larger ensemble size can be more effective to separate the forced response from internal variability, and to reduce associated uncertainties (Milinski et al., 2020; Maher et al., 2021).

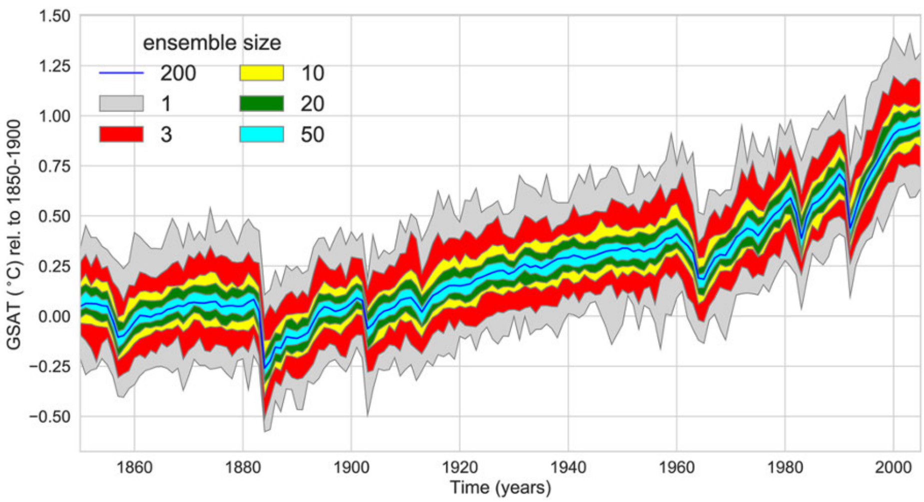

Figure 2.10: Global annual mean near-surface air temperature from the MPI-GE 200-member historical ensemble from 1850 to 2005 (Milinski et al., 2020). The dark blue line represents the time series of 200-member ensemble mean. Shaded regions show the range of forced responses estimated by resampling 1000 times for 3, 10, 20 and 50 ensemble sizes. The light grey shading shows the range of the full ensemble, *i.e.*, the minimum to maximum of all the 200 realisations for every single year.

In addition, reliabilities from climate model simulations, either at the global or regional scale, determine the attribution outputs substantially (Stott et al., 2016). Model errors occur not only in the dynamic aspect of climate change but are also affected by climate sensitivity (Shepherd et al., 2018). The observations are vital for the whole study, as the model evaluation and selection step are based on the fidelity to observed, realistic data (National Academies of Sciences, Engineering, and Medicine, 2016).

Given the discrepancies between the observations and simulations, bias correction methods are universally utilized in event attributions (Philip et al., 2020; van Oldenborgh et al., 2021b). For instance, simple additive and multiplicative bias corrections are applied in the three case studies (cf. Chapter 5, section 5.1, 5.2 & 5.3). Notably, biases also arise from the motivation of choices, such as the choice of a specific event and the metric used to communicate the changes in risks, and this has potential influences on summaries across the studies to some extent (National Academies of Sciences, Engineering, and Medicine, 2016). The differences in event selections and spatiotemporal definitions can affect the rarity of the meteorological event, and therefore the return period of the event can be very sensitive to this choice (Philip et al., 2020). However, if the primary focus is addressed on a climatological understanding of events, or to inform adaption and strategies, these biases caused by selections will be not relevant (National Academies of Sciences, Engineering, and Medicine, 2016).

2.5 Summary of the datasets used in recent wildfire attribution studies

Often, even under the common spatiotemporal definition of the extreme event, attribution results can vary considerably due to the choice of the indicator used and climate models chosen to represent the fire weather risks. Hence, this thesis is seeking and exploring the sensitivities and uncertainties of disparate possibilities, including the choice of fire weather indicators, state-of-art models with long-term simulations and corresponding model evaluation and selection steps. In addition, a bias-correction algorithm is involved in specific case studies on recent or historical individual or collective fire weather extremes, contributing to the reduction of systematic bias arising from climate simulations and obtaining a close fit to the reality. Because of such limitations, the only few attribution studies about wildfires were examining changes in the likelihood of extreme heat and drought, and their potential relationship between anthropogenic summer warming and the increasing burned areas, for example in Canada (Gillett et al., 2004; National Academies of Sciences, Engineering, and Medicine, 2016).

Table 2.1 presents the latest attribution study of wildfires in regions worldwide. Throughout the exploration, the influence of human-induced components can be compared with counterfactual situations intuitively, evidenced by the real impacts from humans (Otto et al., 2016; National Academies of Sciences, Engineering, and Medicine, 2016). Although results differ from time to regions, apparent growth in risk ratios still strengthens the study of framing and attributing wildfire events.

The Global Fire Emissions Database (GFED) for the observational datasets always became the choice for researchers to analyze the burning areas worldwide (for instance, biomass burning emissions from small fires by Randerson et al. (2012) and global fire emissions by van der Werf et al. (2017). This dataset can provide the global monthly burned area with a resolution of 0.25° (∼27-28 km). Based on these observations, combinations with the satellite-derived data from the Moderate Resolution Imaging. Spectroradiometer

Table 2.1: Latest attribution studies in wildfires.

Country/ Region	**Observational/ Reanalysis Data (applying period)**	**Fire Indices**	**Models (with bias correction in bold)**	**RR or PR**
British Columbia, Canada (Kirchmeier-Young et al., 2017b)	MERRA2(1980-2018), GFWED	CFFDRS (FWI)	**CanESM2 (CanRCM4)**	$\sim$6
Sweden (Krikken et al., 2021)	ERA-I, ERA5, MERRA2 (1980-2018); JRA-55 (1955-2018)	FWI	CMIP5 (EC-Earth v2.3 [1.1°], CESM1 [1°], etc.), Weather@Home [0.25°]	$\sim$1-3
France (Barbero et al., 2020)	SAFRAN (1958-2017)	FWI, KBDI	CMIP5	> 50
Southeastern Australia (van Oldenborgh et al., 2021a)	Berkeley Earth climate analysis, AWAP, GISTEMP, ACORN-SAT, CERA-20C (1900-2010)	FWI	CMIP5 (EC-Earth v2.3 [1.1°], CESM1 [1°], CanESM2 [2.8°], etc,) HadGem3-A [0.6°], ASF20C [0.71°], CMIP6 (low resolution), Weather@Home [1.8°]	$\sim$0.8-8
Brazil (Li et al., 2021)	ERA5 (1987-2019)	FWI, BUI, ISI, FFMC, DMC, DC	Weather@home [1.8°], HadGEM3-A [0.6°]	$\sim$0.95-1.64

(MODIS), active fire data offered by the Tropical Rainfall Measuring Mission (TRMM) Visible and Infrared Scanner (VIRS), the full dataset of fires can be acquired, and is regularly automatically updated (Giglio et al., 2016; Randerson et al., 2018).

Apart from the directly observed data, reanalysis data also make indispensable contributions to wildfire risk modelling. The second version of Modern-Era Retrospective analysis for Research and Applications (MERRA2; Gelaro et al., 2017), the global atmospheric reanalysis, from ECMWF Re-Analysis (ERA) Interim (ERA-Interim; Dee et al., 2011) and its improved version, ERA5 (Hersbach et al., 2020) and the French reanalysis Système d'Analyse Fournissant des Renseignements Atmosphèriques à la Neige (SAFRAN; Vidal et al., 2010 play important roles in recent attribution studies (Table 2.1; Kirchmeier-Young et al., 2017b, Krikken et al., 2021, Barbero et al., 2020, van Oldenborgh et al., 2021a). Reanalysis based on the Canadian Forest Fire Weather Danger Rating system and weather forcing from ECMWF Re-Analysis (ERA) Interim and ERA5 produced by the European Centre for Medium-range Weather Forecasts have been developed as GEFF-ERAI and GEFF-ERA5 (Vitolo et al., 2019, 2020). These reanalysis datasets will be part of the essential attempts for this project to quantify worldwide fire danger.

Most attribution studies of extreme events also rely to some extent on climate models (National Academies of Sciences, Engineering, and Medicine, 2016). CMIP models with different forcing, natural-only, anthropogenic-only or all-forcing, offer a comprehensive view of the system complexity, and become one of the most popular and sophisticated tools for the cause or the dominant forcing of an extreme event (Stott et al., 2016). Thus, while relying on large ensembles of simulations, with or without anthropogenic influences, the likelihood of extreme events can be finally estimated (Stott et al., 2016; Zhai et al., 2018). Because of the specific type and configuration of climate models, results are highly dependent on the types of extremes being attempted, a large ensemble of ocean-atmosphere coupled climate models is always utilized for simulating the fire weather conditions with or without anthropogenic influence (National Academies of Sciences, Engineering, and Medicine, 2016). By defining applicable models with disparate scenarios and relative thresholds, systematic models can be obtained, and corresponding outputs are reasonably reliable. The model outputs can finally show clear risks with different forcings.

In terms of wildfires, the use of a large ensemble in climate models seems to perform better in circumventing the problems of undersampled internal/natural climate variability (Krikken et al., 2021). All the simulations present increasing temperature trends in typical wildfire events, as shown in Table 2.1. Even though they found clear changes in precipitation under a warmer climate, no robust evidence can link the dry periods during summer with increased fire risk. Further studies will be about continuing the novel bias correction method designed by Cannon (2018), which is not applied in any latest simulations yet. It is expected to solve the issues related to the scale mismatched between regional/global climate models and the scale of a fire occurrence, as well as systematic bias (not necessarily related to the resolution, with unclear or uncontrolled sources), improving modelling accuracy.

Chapter 3

A global view of observed changes in fire weather extremes: uncertainties and attribution to climate change

Abstract - In many parts of the world, wildfires have become more frequent and intense in recent decades, raising concerns about the extent to which climate change contributes to the nature of extreme fire weather occurrences. However, studies seeking to attribute fire weather extremes to climate change are hitherto relatively rare and show large disparities depending on the employed methodology. Here, an empirical-statistical method is implemented as part of a global probabilistic framework to attribute recent changes in the likelihood and magnitude of extreme fire weather. The results show that the likelihood of climate-related fire risk has increased by at least a factor of four in approximately 40% of the world's fire-prone regions as a result of rising global temperature. In addition, a set of extreme fire weather events, occurring during a recent 5-year period (2014-2018) and identified as exceptional due to the extent to which they exceed previous maxima, are, in most cases, associated with an increased likelihood resulting from rising global temperature. The study's conclusions highlight important uncertainties and sensitivities associated with the selection of indices and metrics to represent extreme fire weather and their implications for the findings of attribution studies. Among the recommendations made for future efforts to attribute extreme fire weather events is the consideration of multiple fire weather indicators and communication of their sensitivities.

This chapter appears as the following published paper in *Climatic Change*: **Liu, Z.**, Eden, J. M., Dieppois, B., & Blackett, M. (2022). A global view of observed changes in fire

weather extremes: uncertainties and attribution to climate change. *Climatic Change 173*, 14. https://doi.org/10.1007/s10584-022-03409-9.

3.1 Introduction

Understanding the climatological drivers of wildfires has become an increasingly important area of research with relevance for many parts of the world. In addition to the threats posed to human lives, wildfires are associated with several socioeconomic and environmental impacts (Gill et al., 2013; Tedim et al., 2018; Wang et al., 2021). The recent World Meteorological Organization (WMO) Atlas of Mortality and Economic Losses from Weather, Climate and Water Extremes outlined the significant contribution of wildfire events to disaster-incurred economic losses (World Meteorological Organization, 2021). For instance, across North America, Central America and Caribbean regions, only tropical storms result in a higher number of reported economic losses than wildfires (World Meteorological Organization, 2021). Notably, the 2019 wildfires in California and Alaska have incurred costs of more than $24bn (World Meteorological Organization, 2021). Environmental impacts include ecosystem degradation and both air and water pollution. Furthermore, the substantial increase in global wildfire activity predicted by the end of the 21st century will place enormous stress on the balance between biodiversity and the climate system (Krawchuk et al., 2009; Flannigan et al., 2009; Jolly et al., 2015). To mitigate future risks associated with wildfires, understanding the nature of, and trends in, such events has become an emerging priority, resulting in the necessity to quantify the influence of anthropogenic climate change on wildfire events (Kirchmeier-Young et al., 2017b; Abatzoglou et al., 2019; van Oldenborgh et al., 2021a).

Analysis of wildfires as extreme events tends to be approached similarly to the analysis of extreme heat and cold, drought, extreme rainfall or other meteorological phenomena. The World Meteorological Organization Atlas, for instance, defines wildfire as "climatological”, alongside drought and glacial lake outburst, in its classification of disaster subgroups (World Meteorological Organization, 2021). Strictly speaking, wildfires are not meteorological events – there are other factors at play in their development and the precise link to climate is difficult to quantify (National Academies of Sciences, Engineering, and Medicine, 2016). However, the mechanisms favouring wildfire generation are clearly influenced by climate. Periods of below-average precipitation coupled with high-temperature anomalies are obvious drivers of drought conditions which many of the largest fires are associated with (*e.g.*, van Oldenborgh et al., 2021a). Additionally, temperature, wind speed and humidity play a crucial role in dictating fire spread (Jain et al., 2022), and rainfall has an equally important effect on fire suppression. Climate-related wildfire studies have generally focused on one of three aspects (Hardy, 2005): (i) fire activity itself, which is usually quantified by the number of fires or the extent and intensity of burned area (Campos-Ruiz et al., 2018); (ii) fire risk, which is usually understood to be the climate-related probability of ignition, a function of both hazard and vulnerability (Seneviratne et al., 2021); (iii) fire danger, which typically takes the form of a rating system combining meteorological information, to describe the severity of fires (Deeming et al., 1978; Sharples et al., 2009). However, despite this distinction, advances in the analysis of wildfire extremes in the context of climate change have been limited, partly by the absence of a common framework for best practice.

During the last decade, a growing emphasis has been placed on drawing attention to and understanding changes in the nature of extreme weather and climate events (*e.g.*, Otto et al., 2016; National Academies of Sciences, Engineering, and Medicine, 2016; Philip et al., 2020). There is now a wealth of literature dedicated to the attribution of individual extreme events to climate change, the majority of which have focused on extreme temperature (*e.g.*, Kim et al., 2016) and precipitation events (*e.g.*, Kunkel et al., 2013), in addition to episodes of drought (*e.g.*, Funk et al., 2015), flooding (*e.g.*, van Oldenborgh et al., 2012) and other impacts (*e.g.*, Kirchmeier-Young et al., 2017a; Knutson et al., 2019) that pose substantial societal challenges. A number of these studies have been published during the last decade in the annual special report, 'Explaining Extreme Events from a Climate Perspective' from the Bulletin of the American Meteorological Society (BAMS), summarizing substantial outcomes for types of extremes (*e.g.*, Herring et al., 2021). Additionally, the evolution of philosophical and methodological approaches in event attribution has been documented in numerous publications (National Academies of Sciences, Engineering, and Medicine, 2016; Stott et al., 2016; Philip et al., 2020; van Oldenborgh et al., 2021b).

Event attribution studies allow us to assess and quantify how the nature of individual climate risks has been altered by climate change (*e.g.*, Trenberth et al., 2015; Otto et al., 2016; Knutson et al., 2017). By quantifying the relative contribution of one or more drivers of the observed changes, the classical event attribution approach seeks to determine to what extent the frequency and/or magnitude of extreme events has changed as a result of anthropogenic climate change or, otherwise, long-term changes in global mean temperature (Field et al., 2012). However, while attribution study of extreme heat-related and precipitation events is commonplace, analysis of wildfire or, alternatively, extreme fire weather events are comparatively rare. To date, of the 200 studies published in the BAMS 'Explaining Extreme Events from a Climate Perspective' special reports, only eight have been developed for wildfire events (Yoon et al., 2015; Partain et al., 2016; Tett et al., 2018; Hope et al.; 2019; Brown et al., 2020; Lewis et al., 2020; Yu et al., 2021; Du et al., 2021). A comprehensive report published by the National Academies of Sciences, Engineering, and Medicine (2016), outlined four components that complicate attribution questions for wildfires (Abatzoglou and Kolden, 2011; Lin et al., 2014; Gauthier et al., 2015): (i) the motivating role of human activities in fire ignitions and suppression, management of forests; (ii) the chaotic nature of small-scale weather systems, such as lightning in igniting large fire outbreaks; (iii) the importance of larger-scale weather in the wildfire spread and growth of fires into major events (*e.g.*, wind and humidity for fire spread, and precipitation for extinguishing fire outbreaks); (iv) the health of the forest or the condition of the burnable vegetation. While some components can be affected by prevailing weather and climate conditions (*e.g.*, likelihood of thunderstorms, long-term droughts), a lack of understanding of the suitability of fire weather indicators limits detailed exploration. Shedding light on these sensitivities and progressing toward a more robust approach for wildfire attribution is, therefore, an important challenge.

Aside from the lack of application to wildfire studies, event attribution faces several broader challenges. Arguably the most important is reaching a consensus on the way that different types of extreme events should be defined, given that the differences can result in disparate conclusions (Philip et al., 2020). Such definitions should include the goal of the event attribution, the choice of variables, the spatial and temporal extent of the event in question, the specific motivations according to the event types and researchers or partnerships leading the studies (Philip et al., 2020). Other challenges are relevant to the difficulty in drawing comparisons between studies of similar events using different methods and event definitions (National Academies of Sciences, Engineering, and Medicine, 2016). The application of established attribution methodologies to different event types has the potential to address some of these challenges directly and, in turn, to provide guidance that will support the continued development of robust attribution science.

Here, we assess worldwide observed trends in annual maxima in a range of fire weather indicators and quantify to what extent recent climate change has altered the nature of fire weather extremes. We use an established empirical-statistical methodology as part of a global framework designed to enable the simultaneous attribution of multiple extreme fire weather episodes. Key to this framework is the use of a standardised spatiotemporal event definition, and the quantification of uncertainties associated with the choice of various fire-weather indices. The chapter is organized as follows. In section 3.2, the methods and data are described. In section 3.3, we present three sets of results: (i) recent trends in seasonal fire weather statistics and the relationship between different fire weather indices and burned area; (ii) empirical attribution of worldwide changes in the likelihood of extreme fire danger indices; and (iii) empirical attribution of a collective of recent "exceptional" fire weather events. In section 3.4, we present our conclusions and recommendations for the framework's application to climate model ensembles as part of comprehensive attribution methodologies.

3.2 Methods and Data

3.2.1 Probabilistic vs. Storyline approaches to event attribution

The way an attribution question is framed is an important consideration that can substantially influence a study's overall results (Philip et al., 2020). Recently, the event attribution literature has settled on a distinction between two overarching approaches. The 'probabilistic' approach, is used to estimate the probability of a class of events for a given magnitude occurring in the past and present climate, regardless of their meteorological cause (Allen, 2003; Stott et al., 2004). An alternative is the so-called 'storyline' approach, which places an emphasis on the meteorological roots of a given event and aims to deliver qualitative analyses instead of quantitative estimations (Clark et al., 2016; Shepherd, 2016). A major caveat of storyline-based studies is the general requirement for specialist knowledge to interpret results, which impedes the ease with which this approach can be applied to multiple events (Philip et al., 2020). Given our desire for a framework that can be applied routinely to any event, or indeed multiple events, our study implements a probabilistic approach. In making this choice, we acknowledge that both the probabilistic and storyline approach is not without fault, and its application should be evaluated accordingly.

Probabilistic application to attribution study typically involves the use of empirical-statistical methods applied to observations and climate model outputs. Examples include the rainfall-related extremes in America (Eden et al., 2016; van Oldenborgh et al., 2017) and Netherlands (Eden et al., 2018), heat-related extremes in America (Mera et al., 2015), and Australia (Hope et al., 2016), and fire-related extremes in Canada (Kirchmeier-Young et al., 2019b), Sweden (Krikken et al., 2021) and Australia (van Oldenborgh et al., 2021a). Here, we focus on the direct application of an established statistical technique to reanalysis-derived historical data to estimate how climate change has affected the likelihood or magnitude of particular types of fire weather events (Stott et al., 2016).

3.2.2 Sensitivity to the representation of fire weather

The index chosen to represent fire weather is often circumstance, and location, dependent. There remains considerable uncertainty surrounding the potential sensitivity of trends and attribution metrics to the definition of fire weather. As discussed in the introduction, quantifying the relationship between fire and climate is not trivial. The development of specific indices for 'fire weather', particularly the widely used approach of the Canadian Fire Weather Index System (CFWIS) (Van Wagner, 1987), has set a benchmark for drawing quantifiable links between climate and fire. The CFWIS uses meteorological variables, specifically temperature, relative humidity, surface wind speed and precipitation, that collectively constitute fire-prone conditions, or so-called 'fire weather'. These variables are firstly used to construct a set of 'fuel moisture codes' depending on the fuel consistency (Vitolo et al., 2019): Fine Fuel Moisture Code (FFMC) is an indicator of the moisture content, and therefore relative flammability and combustibility of fine fuels and is characterised by their rapid response to weather changes; Duff Moisture Code (DMC) represents a numerical rating of the averaged moisture content of decomposed organic material, and is characterised by a medium-term response to weather changes; Drought Code (DC) represents the averaged moisture content of the soil at depth; and is characterised by long-term response to weather changes. Subsequently, a set of 'fire behaviour indices' is calculated (Vitolo et al., 2019): Initial Spread Index (ISI) represents a numerical rating of the spread potential of a fire in the early stages shortly after ignition; Buildup Index (BUI) represents a numerical rating of the total amount of fuel available for combustion and is an estimate of potential heat release in heavier fuels and a weighted combination of current DMC and DC. The final calculation is the Fire Weather Index (FWI), which represents a numerical rating of the general fire intensity and therefore a general index of fire danger (Vitolo et al., 2019).

Although initially developed for application in Canada, FWI has been used to describe fire-climate relationships in other parts of the world, such as France, Italy and Portugal (Viegas et al., 1999), New Zealand (Dudfield, 2004), southeast Australia (de Groot et al., 2006), southeast Asia (de Groot et al., 2007) and Greece (Dimitrakopoulos et al., 2011). These studies assume that FWI is an appropriate metric for fire weather, but a systematic worldwide comparison of multiple indices is lacking in the literature. Further discussion of the merits of FWI is given in Section 2.1. While FWI has been the most widely used metric to describe fire-climate relationships (Cortez and Morais, 2007; Ager et al., 2014; Pinto et al., 2020), and as the basis of some attribution studies (Abatzoglou and Williams, 2016; Krikken et al., 2021; van Oldenborgh et al., 2021a), other works have justified the use of alternative CFWIS indices. For example, in the western United States, the six ecoregions use

DC, FFMC, FWI, BUI and the Daily Severity Rating (an additional component of CFWIS; Van Wagner, 1987) to present individual fire danger risks separately (Spracklen et al., 2009). Similarly, the derived monthly DC has been employed in northern Europe, northern Asia and Canada (de Groot et al., 2007), while the daily BUI has been utilised in Alaska (Bhatt et al., 2021). Furthermore, Jain et al. (2022) used ISI alongside FWI and vapour pressure deficit as the basis to assess global trends in extreme fire weather. Though these studies widely applied different indices, robust justifications for the choice of an index for each region are not critically developed, and a systematic worldwide comparison of multiple indices is lacking in the literature, which motivates our desire to quantify the sensitivity of different indices.

We make an initial assessment of the sensitivity of fire weather analysis to the choice of CFWIS index, firstly by comparing trends in annual mean fire weather and secondly by comparing interannual fire weather variability with area burned (section 3.3.1). Historical fire weather data is derived from the Global Fire Danger Reanalysis (0.25° resolution; Vitolo et al., 2019), produced by the Copernicus Emergency Management Service for the European Forest Fire Information System, for the period 1980-2018. While the calculation of all indices closely follows the CFWIS methodology outlined by Van Wagner (1987) and Lawson and Armitage (2008), a worldwide application across different climates and fire regimes means it is necessary to note some caveats. There is some debate on whether the fuel moisture codes, particularly DC, should be reset to a start-up value ahead of the fire season or 'overwintered' to account for the effects of inter-seasonal drought (McElhinny et al., 2020). The calculations of ISI, BUI and FWI in the Global Fire Danger Reanalysis are reset to zero at locations with greater than 20% snow cover but the calculation of the FFMC, DC and DMC is not suspended (Vitolo et al., 2019). By default, the Global Fire Danger Reanalysis thus does not implement overwintering. Instead, the start and duration of the fire season is determined by the user (Vitolo et al., 2019).

Our analysis used the following CFWIS indices: DMC, DC, ISI, BUI and FWI. FFMC is omitted as the constrained upper limit of its range (maximum value: 101), which is frequently reached in many parts of the subtropics, makes this index unsuitable for extreme value analysis. DC has a probable maximum value of around 800 but even the most extreme drought conditions do not reach this upper limit (de Groot, 1987; National Wildfire Coordinating Group, 2022). To limit the analysis to parts of the world that are prone to fire, monthly burned area dataset is taken from the fourth version of the Global Fire Emissions Database (GFED4; Global Fire Emissions Database, 2022) for which data is available between 1996 and 2016 (0.25° resolution; van der Werf et al., 2017).

3.2.3 Event Definition

The next step is to define the extreme fire weather event quantitatively. The event definition is crucial within the event attribution process; overall results can be dramatically influenced by the definition itself (van Oldenborgh et al., 2021b). As stated earlier, we take a class-based approach to estimate the likelihoods of the occurrence of a given event in the real world and present climate. The event class would typically be defined in spatiotemporal terms according to the meteorological anatomy of the target event. The framework used here necessitates a definition that can be applied globally. Previous efforts to attribute fire weather extremes have focused on 5-day (*e.g.*, Lewis et al., 2020) or 7-day (*e.g.*, Krikken et al., 2021) averages, while analysis of soil moisture as a fire risk indicator found little difference between 3-day, 5-day and 7-day anomalies preceding fire occurrences (Thomas Ambadan et al., 2020). Here, in order to best account for extreme events occurring on shorter timescales and ensure inter-index comparability, we focus on annual maxima in 5-day averages in each CFWIS index. The definition must also declare the spatial extent of the extreme event; at each target grid cell, we consider all information within a pre-defined 5×5 (1.25° × 1.25°) surrounding grid box. This was done (i) because an event may be larger than one grid point, and (ii) to negate the influence of atmospheric noise, or spurious observational errors. Finally, to limit our analysis to areas of the world that can be considered fire-prone on the basis of historic fire activity, we smoothed the GFED4 data with a quadrilateral curvilinear grid and masked all grid points at which burned area was recorded between 1996 and 2016.

3.2.4 Attributing changes in event likelihood

The generalized extreme value (GEV) distribution (Coles, 2001) fitted to block maxima has been widely applied to estimate the return period of extreme events (van Oldenborgh et al., 2015; Eden et al., 2016, 2018; Krikken et al., 2021; van Oldenborgh et al., 2021a):

$$P(x) = exp[-(1+\xi\frac{x-\mu}{\sigma})^{\frac{1}{\xi}}] \tag{3.1}$$

where location, scale and shape parameters of the distribution are μ, σ, and ξ, respectively. Here, we fit the annual maxima of 5-day running means for each CFWIS index to a GEV distribution across all fire-prone parts of the world to quantify the change in likelihood and magnitude in fire weather extremes. While it may be more appropriate for regional analysis to consider maxima during a period representative of the regional fire season, we choose to focus on the calendar year (January-December) in line with a consistent approach designed for global applicability. To account for possible changes due to climate change over time, we assume the GEV fit is scaled linearly to annual global mean surface temperature (GMST), taken from the Goddard Institute for Space Studies Surface Temperature Analysis (GISTEMP Team, 2022) and smoothed with a 48-month running mean, as a representation of global warming. This is the shortest that not only effectively diminishes the ENSO component of GMST (van Oldenborgh et al., 2021a), which is not externally forced and therefore doesn't contribute to the overall trend, and also retains as much of the forced variability as possible (Haustein et al., 2019). In addition, a longer smoothing timescale would pose challenges in extrapolating data, especially in the highly relevant last few years of the instrumental record (van Oldenborgh et al., 2021a). This approach is consistent with similar application in previous work (van Oldenborgh et al., 2018; Otto et al., 2018b; Eden et al., 2018). Observations are fitted to a non-stationary distribution under the assumption that the $\frac{\sigma}{\mu}$ 'dispersion' ratio and the shape parameter ξ remain constant (Philip et al., 2020). The location and scale parameters μ and σ are assumed to vary with an exponential dependency on GMST (van der Wiel et al., 2017):

$$\mu = \mu_0 \cdot exp\frac{\alpha T}{\mu_0} \tag{3.2}$$

$$\sigma = \sigma_0 \cdot exp\frac{\alpha T}{\sigma_0} \tag{3.3}$$

where μ_0 and σ_0 are the fit parameters of the distribution and α is the trend in fire indicator maxima as a function of smoothed GMST anomaly T. To estimate the uncertainty, a 1000-sample non-parametric bootstrapping method with a moving-block approach is applied (Efron and Tibshirani, 1998; van der Wiel et al., 2017). At each grid point, we evaluate return time, and hence the probability, of an extreme fire weather event defined by the 95th percentile occurring in the climate of 2018 (p1) and that is occurring in an 'alternative climate' associated with a reduced anthropogenic forcing (p0). Here, the year 1961 is chosen to represent an 'alternative climate' to capture the full extent of global warming witnessed since the 1970s (IPCC, 2021). Several previous attribution studies have used 1961 as a reference year for 'alternative climate' (*e.g.*, Zhou et al., 2018; Eden et al., 2018); Kirchmeier-Young et al. (2019b) used a similar period, noting that the extent of global temperature change between the 1960s and the 2010s is similar to the difference between fully- and natural-forced simulations of the second-generation Canadian Earth System Model (CanESM2). Change in the likelihood of fire weather extremes is expressed using the 'probability ratio' (PR) p1/p0 (also known as the ‘risk ratio’). We also quantify the percentage change of a recent fire weather event and an event of equivalent likelihood occurring in a past climate (%MAG). This empirical-statistical method is applied to attribute extreme fire weather worldwide (section 3.3.2) and, more specifically, to collectively attribute a set of exceptional fire weather events observed during recent years (section 3.3.3; IPCC, 2021).

3.3 Results

3.3.1 Recent trends in seasonal mean fire weather and links to fire activity

To identify the potential differences between the CFWIS indices, we first seek to quantify recent trends in fire weather and its relationship with fire activity. It is important for a global analysis to consider regional variability in the timing of the period of greatest fire risk. As stated in section 3.2.2, the Global Fire Danger Reanalysis encourages a user-driven definition of the start and duration of the fire season (Vitolo et al., 2019). Here, given our emphasis on extreme fire weather, and specifically on annual fire weather maxima, the fire season is defined at each grid point by the set of months that experienced the highest 5-day CFWIS average in each year between 1980 and 2018.

The tendency and significance (95% confidence level) of trends in CFWIS seasonal means from 1980 to 2018 are shown in Figure 3.1a. Spatial patterns in regions of significant positive and negative change exhibit differences between indices. For all five indices, most of the globe is associated with an increase in mean fire weather. For all indices, a significant positive trend is found at more than 25% of fire-prone grid points, and at more than 30% of grid points for ISI and FWI, including large parts of the Americas, Australia, Europe, central Asia and central and southern Africa. Negative trends are limited to parts of sub-Saharan Africa, southern Asia and southwestern Australia. The results indicate a certain degree of discrepancy in the recent trends detected in the five CFWIS indices. Additionally, trends are generally weaker in the high latitudes of the Northern Hemisphere, most notably in central Canada where negative trends are found, despite the occurrence of extreme wildfires in these regions in recent years (Kirchmeier-Young et al., 2017b; Witze, 2020).

Point-wise Pearson’s product-moment correlation between seasonal means in each CFWIS index and corresponding GFED4 burned area (for which data is available between 1996 and 2016) is shown in Figure 3.1b. Positive correlation between seasonal CFWIS and burned area is found across North and South America, eastern Europe, equatorial Africa, southeast Asia and southern Australia. Significant positive correlations ($p<0.05$; $r>0$) are found at between 19.8% (for DC) and 26% (for FWI) of all grid points. Interestingly, areas of relatively strong positive correlation ($r>0.4$) between FWI and burned area are somewhat limited across northern and western Europe, where FWI has been frequently used as an indicator for fire risk (Viegas et al., 1999; Tanskanen and Venäläinen, 2008; Krikken et al., 2021). Negative correlations tend to be detected over dry and/or data-scarce regions (Menne et al., 2012), including parts of Australia and sub-Saharan Africa, in addition to the isolated points in central Asia. Overall, positive correlations between fire weather conditions and burned area are witnessed in most regions of the world, while there are few inter-index differences in the relationship between each CFWIS index and fire-prone areas. In terms of choosing an index as the most appropriate fire weather indicator as part of attribution analysis, there is little to suggest that any particular index would prove more suitable than any other, at least on a global scale.

3.3.2 Empirical Attribution of extreme fire weather

As previously mentioned, an empirical-statistical method is utilized to attribute the changes in likelihoods of extreme fire weather, namely the annual maximum of 5-day running mean to each CFWIS index. Here, the GEV-scaling method is applied to the annual maxima in each CFWIS index. Global maps showing the goodness of the GEV fit by using Kolmogorov Smirnov test, probability ratio (PR) and change in magnitude (%MAG) at each grid point are presented in Figure 3.2. The assumption that the distribution of annual maxima can be approximated well by the GEV can be made throughout most of the world's fire-prone regions; for FWI for instance, the Kolmogorov-Smirnov test statistic falls within the critical value of 95% significance at 70% of fire-prone grid points. There are some exceptions (in grey), including parts of Mediterranean Europe, and we recommend exercising a degree of caution in the interpretation of the attribution results in such regions.

Overall, there are several similarities in spatial patterns of both PR and %MAG across the five CFWIS indices (Figure 3.2). A 4-fold increase in likelihood ($PR>4$) in response to globally warming temperature is found in approximately 40% of the world's fire-prone grid points. This corresponds to an increase in the magnitude of around 20%, ranging from 15.5% in DC to 25.5% in DMC. Regions with increasing likelihoods in %MAG are mainly similar to that in PR. Such increases in the likelihood of extreme fire danger are particularly strong in temperate North America, Europe, Africa, Boreal and Central Asia. On the contrary, extreme fire weather appears to be less likely across all CFWIS indices in South Asia, Southeast Asia,

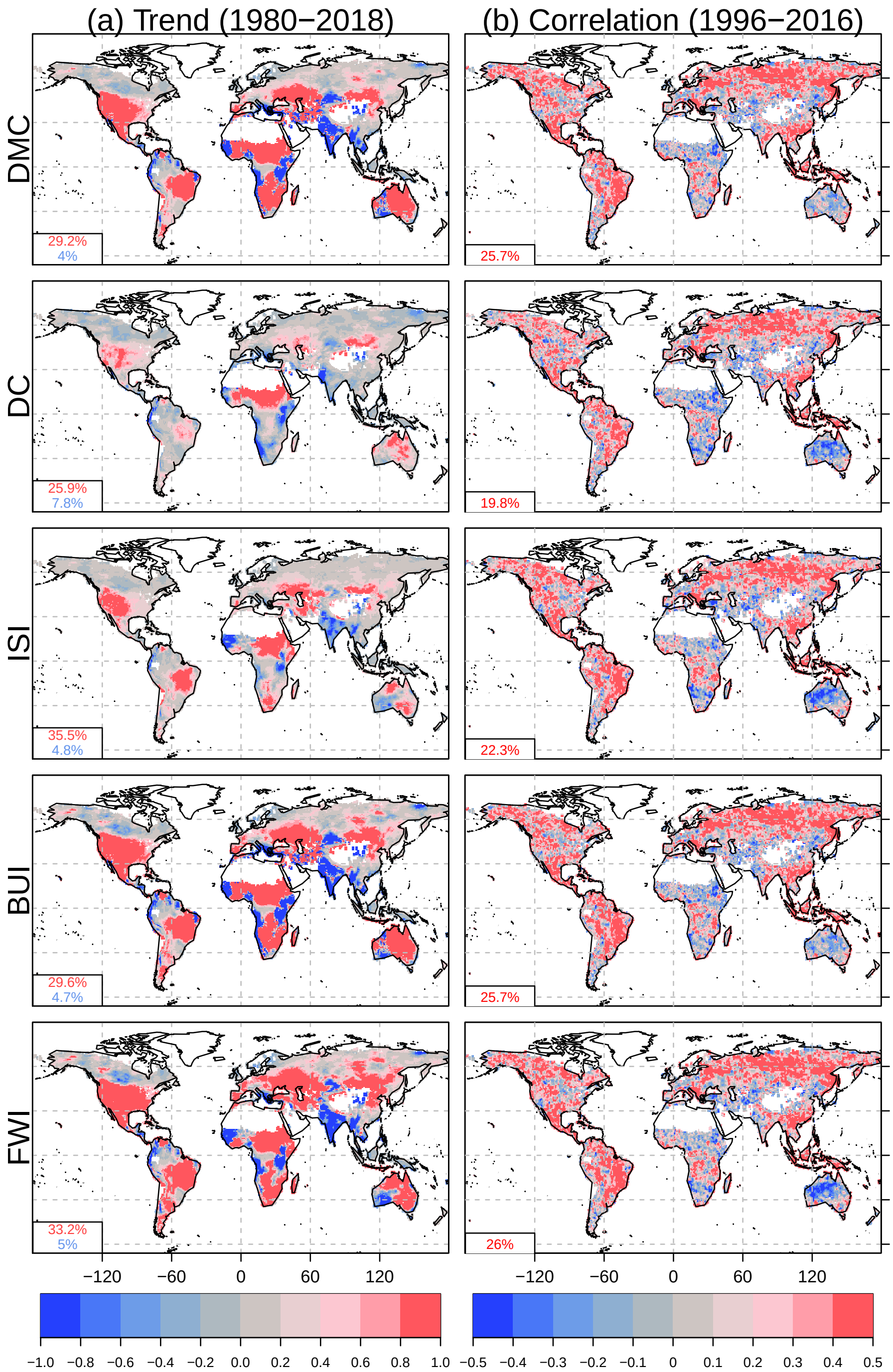

Figure 3.1: (a) Trends in five CFWIS indices from the Global Fire Danger Reanalysis (Vitolo et al., 2019) during the regionally-varying fire risk season for the period 1980-2018. Fire-prone regions where a positive trend is detected are shown in red; regions of negative trends are shown in blue. Values in the bottom-left corner of each panel show the percentage of grid points that represent a significant increase (red) and decrease (blue), respectively. (b) Correlation between the seasonal means of each CFWIS index and GFED burned area at all fire-prone grid points from 1996 to 2016. Values in the bottom-left corner of each panel show the percentage of grid points that represent significant positive (red) correlations. The white areas represent the mask of non-burnt areas.

Northern Hemisphere South America, Western West Africa, Southern and Eastern Africa, as suggested by a decrease in the likelihood in response to globally warming temperature (PR<1). The proportion of regions showing a significant decrease in likelihoods is relatively lower by employing the %MAG metric than the PR.

Across the CFWIS indices, spatial patterns are generally similar, but certain regions show contrasting results. For instance, by choosing either BUI or FWI as the reference index for western Australia, we may find either a positive trend or no significant change in likelihoods (Figure 3.2). Similarly, in eastern Africa, increases in likelihood (PR>1) of ISI and FWI extremes are found, while for DC and BUI extremes decreases are found (PR<1) in DC and BUI extremes are found. Moreover, the largest discrepancies in both PR and %MAG between CFWIS indices are found in regions with large inter-index differences in recent trends (Figure 3.1a), and that are also poorly correlated with the fire-prone area (*i.e.*, eastern parts of South America for FWI, East Asia and Western Australia; Figure 3.1b). As these regions are also data-scarce (Menne et al., 2012), the observed differences could be due to the low reliability of the reanalysis product there (Burton et al., 2018; Liu et al., 2018; Acharya et al., 2019; Gleixner et al., 2020). Alternatively, this could also highlight that, in hot and humid tropical regions, relative humidity and precipitation are more important than temperature in driving changes in fire weather indices.

To summarise the results of our empirical-statistical attribution analysis on the regional scale, PR results are amalgamated across the 14 GFED Basis Regions (identified according to annual emission estimates; van der Wiel et al., 2017). Figure 3.3 shows the proportion of grid points that exhibit significant increases and decreases in likelihood in the five CFWIS indices in each of the 14 fire regions. Notably, for four of the fire regions (TENA, SHSA, NHAF and CEAS; see Figure 3.3 for definitions of the regions), an increase in the likelihood of extremes in all indices is found in more than 50% of grid points; for a fifth region (BOAS), the same results are found for each index except for DC. Similarly, for CEAM, EURO, and SHAF, increasing likelihoods are dominant in general, while BONA and MIDE predominantly show non-significant changes in likelihoods. Conversely, the NHSA and EQAS region exhibit decreasing likelihoods in extremes of all indices in up to approximately 50% of grid points. Meanwhile, only the SEAS region shows a homogeneous and consistent decrease in likelihood at more than 50% of the grid points, with the highest proportions evident for DMC and BUI. Efforts to attribute extreme heat in this region have been inconclusive; van Oldenborgh et al. (2018) were unable to detect trends in the highest maximum temperatures in India since the 1970s, noting the counteracting effect on global warming of (i) increased irrigation and resultant evaporative cooling, and (ii) the blocking of sunlight by aerosols as a

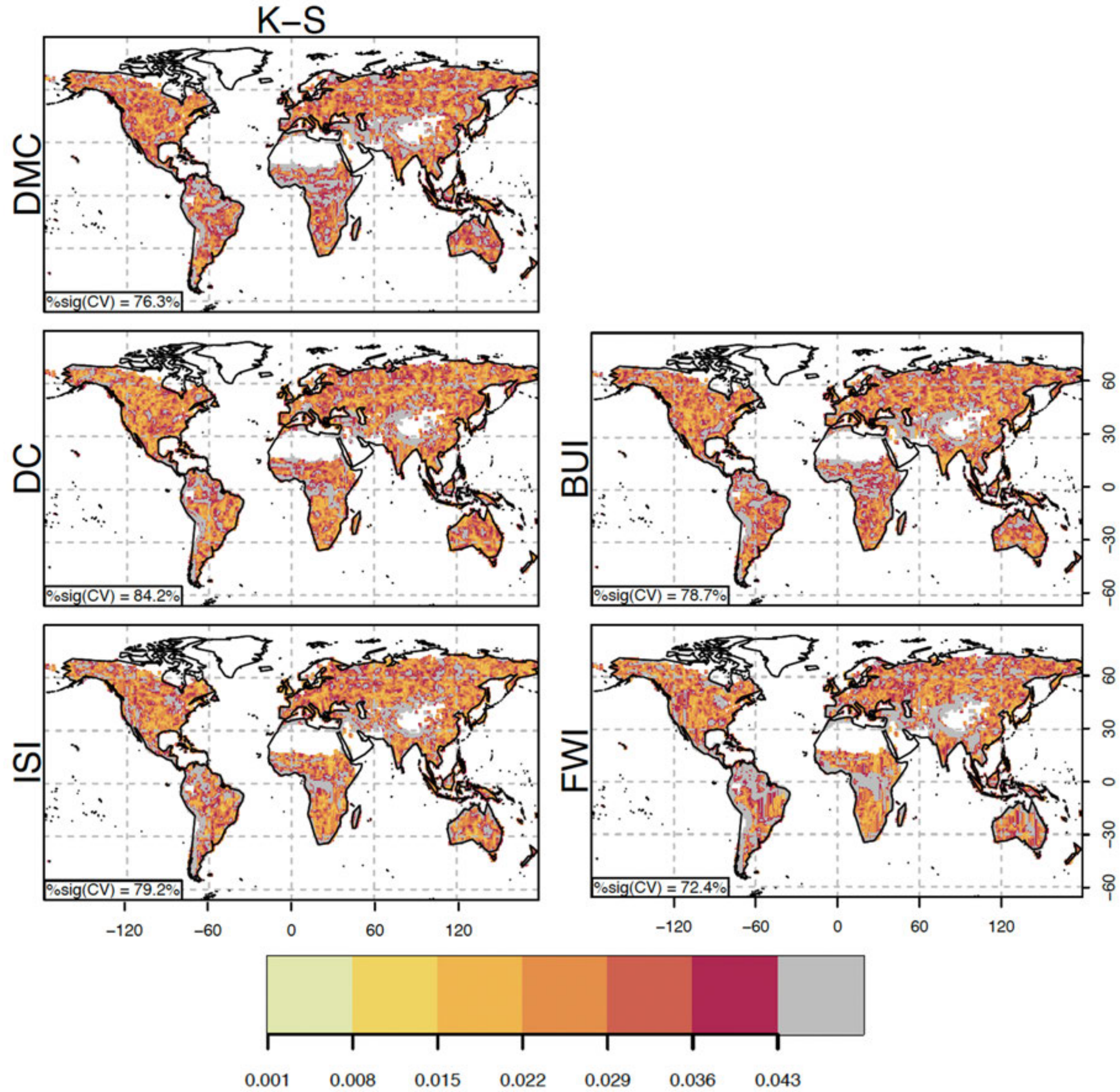
K–S
DMC
%sig(CV) = 76.3%
DC
%sig(CV) = 84.2%
BUI
%sig(CV) = 78.7%
ISI
%sig(CV) = 79.2%
FWI
%sig(CV) = 72.4%
−120 −60 0 60 120
60 30 0 −30 −60
0.001 0.008 0.015 0.022 0.029 0.036 0.043

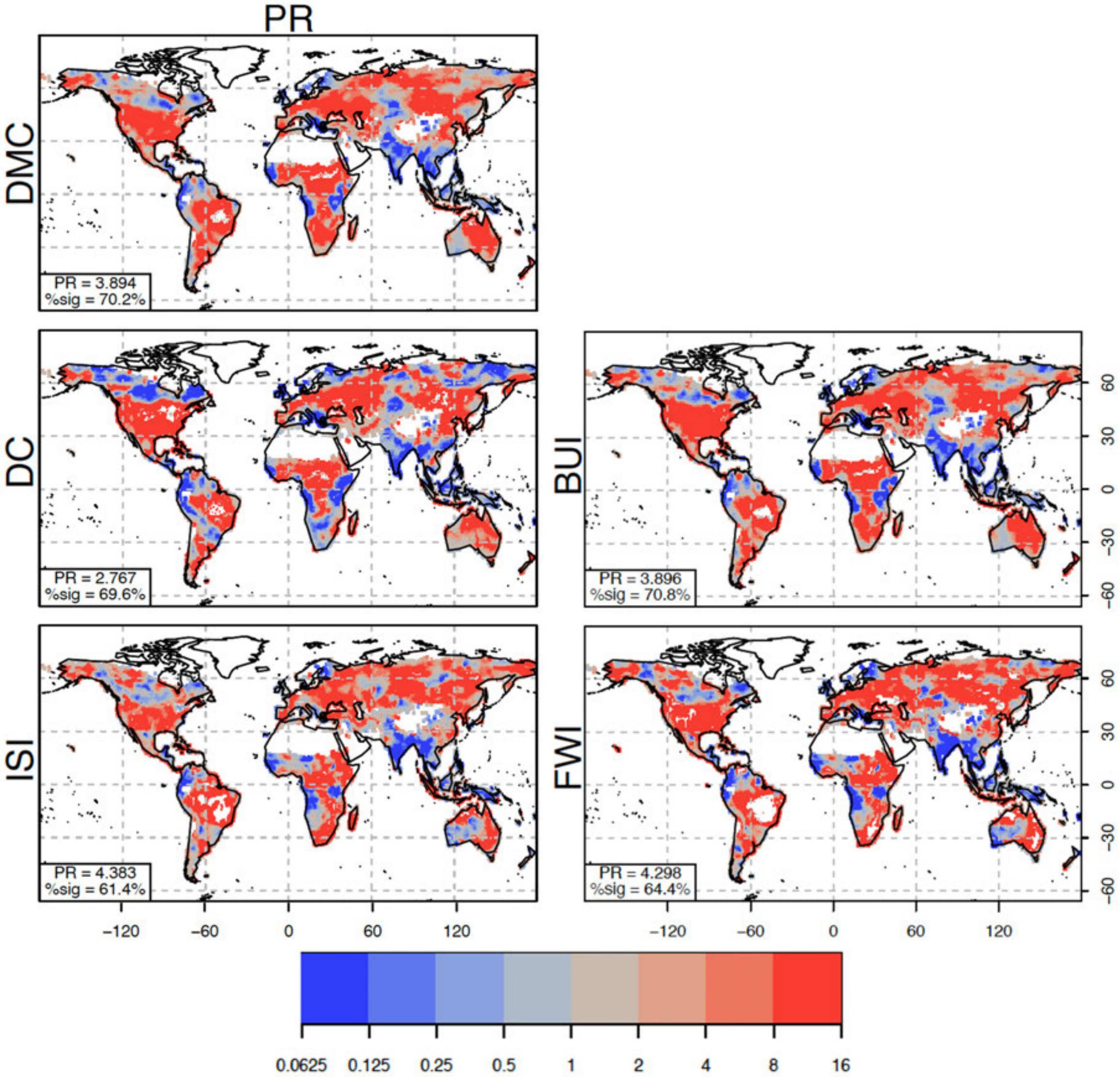
PR
DMC
DC
BUI
ISI
FWI
PR = 3.894
%sig = 70.2%
PR = 2.767
%sig = 69.6%
PR = 3.896
%sig = 70.8%
PR = 4.383
%sig = 61.4%
PR = 4.298
%sig = 64.4%
−120 −60 0 60 120
60 30 0 −30 −60
0.0625 0.125 0.25 0.5 1 2 4 8 16

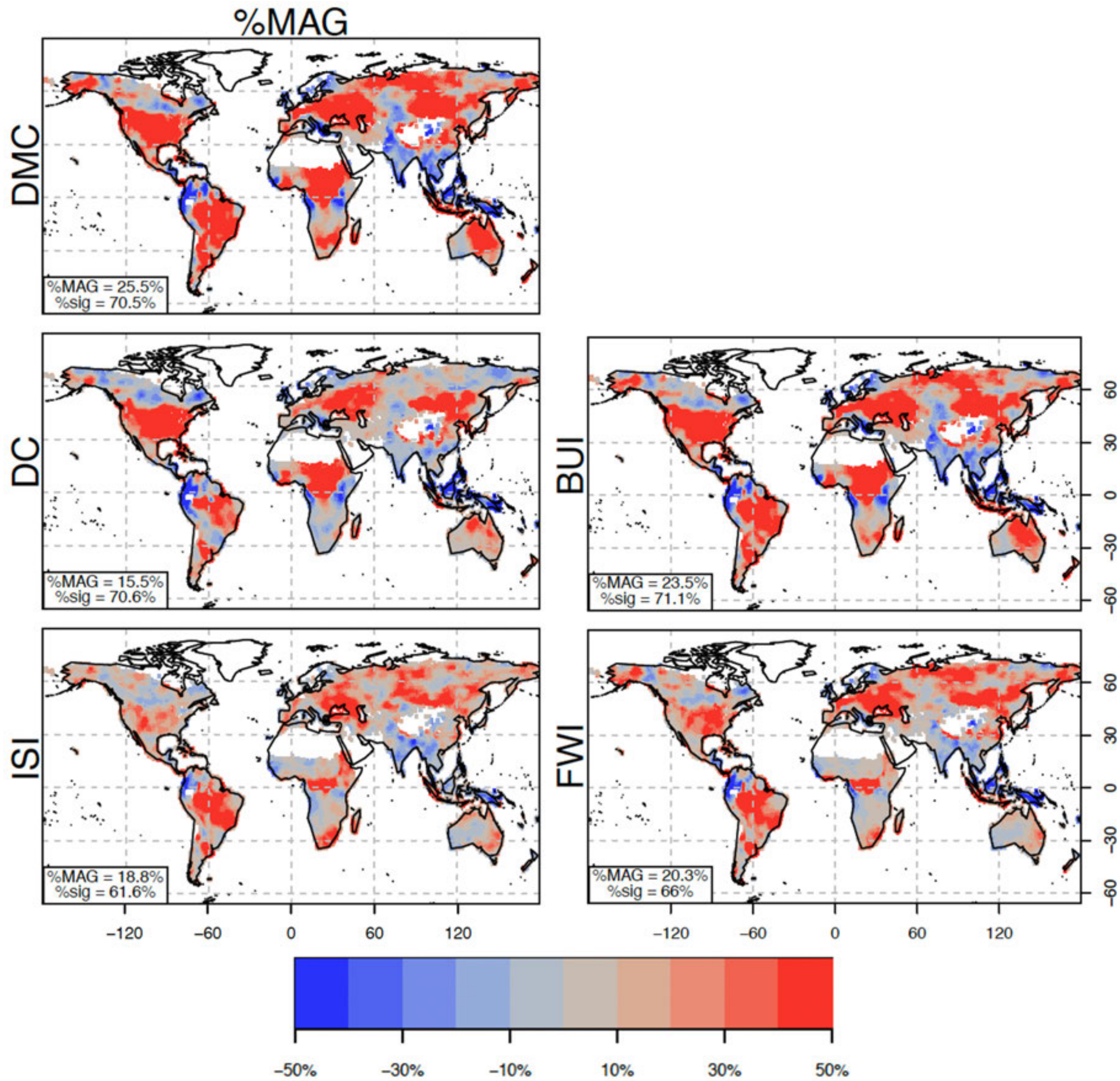

Figure 3.2: Goodness of GEV fit by using Kolmogorov Smirnov test (left), global view of probability ratio (PR; centre) and percentage change (%MAG; right), concerning the target event at each grid point for five CFWIS indices. Numbers in the bottom-left corner represent: (left) the percentage of significant results with a 95% confidence level (%sig(CV)), for which is lower than the critical value (here is 0.043; the calculation is based on the formula of K-S test of critical value = $1.36/\sqrt{N}$, when α=0.05 and N=39*5*5); (centre and right) globally averaged PR and %MAG, and the percentage of the grid points (%sig) for which PR and %MAG results are significant. The white areas for globally averaged PR (for instance, in Amazon) represent the regions where the extreme fire weather conditions are unlikely to occur in the past climate.

result of increased air pollution. Though most fire regions present similar proportions of grid

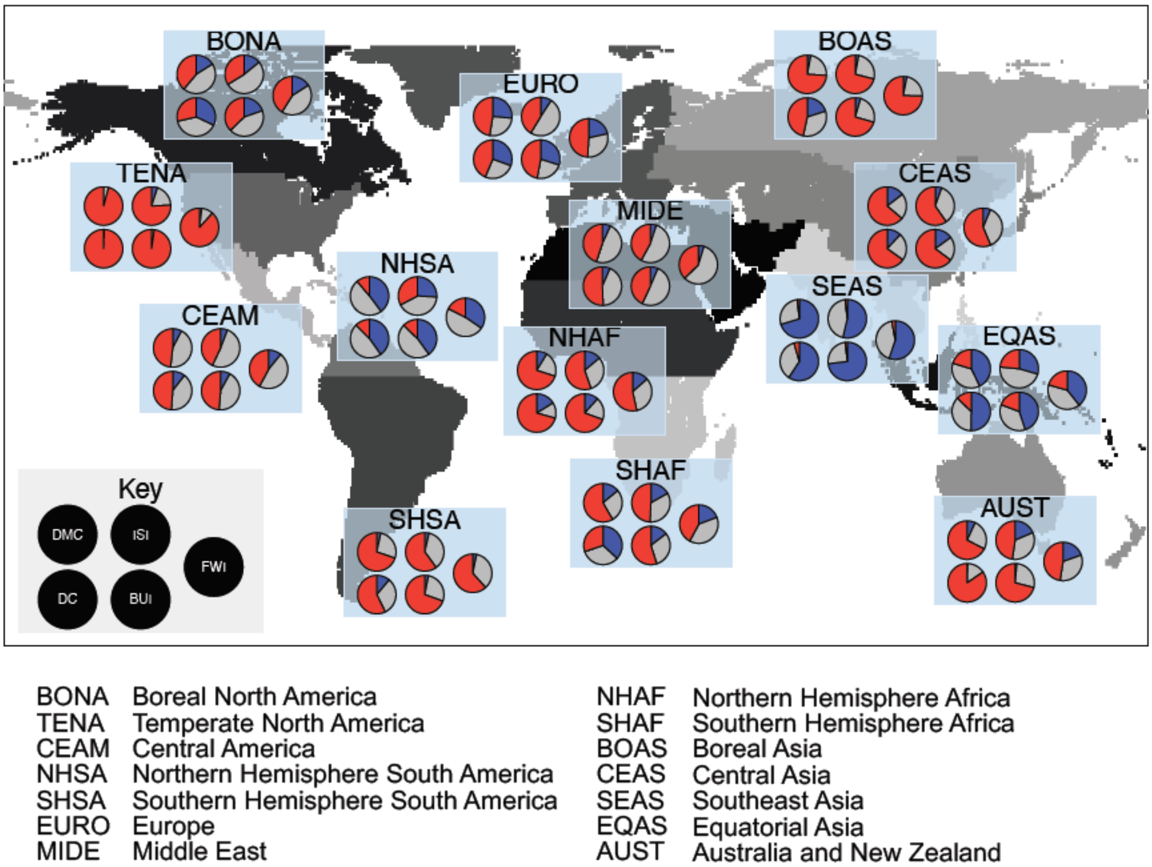

Figure 3.3: Regional summaries of PR results across the 14 GFED fire regions. Pie charts for each CFWIS index show the proportion of fire-prone grid points associated with positive (red; PR>1), negative (blue; PR<1) and no change (grey) at the 95% confidence level.

points with significant increase and decrease among all CFWIS indices, that in AUST present inter-index differences in PR. In AUST, among the five indices, DC, DMC and BUI present increasing likelihoods over 70%, ISI and FWI display the increasing likelihoods around 50% with decreasing likelihoods around 20%.

In summary, fire weather events have become more likely and greater in magnitude in most regions of the world. In some regions, particularly within the tropics and the high latitudes of the northern hemisphere, there is evidence that the likelihood of extremes has decreased as global temperatures have risen. In addition, we note that sensitivities in the choice between the different sub-indicies on FWI are particularly strong in Australia, while they are relatively small in other regions of wildfire prominence, such as North and Central America and much of Asia.

3.3.3 Attribution of recent exceptional fire weather events

As highlighted in section 3.3.1, the last decade has witnessed a sharp increase in efforts to attribute individual events. Studies related to wildfire or, alternatively, extreme fire weather are relatively rare. Here, we extend the application of our approach to a set of recent extreme fire weather episodes in the observational record that would have been considered as ‘exceptional’ and, in principle, would have been an appropriate focus of an event attribution study. We demonstrate that classifying extreme fire weather events according to the same strict event definition allows for collective conclusions to be drawn from the attribution of multiple events.

Our analysis defines events as ‘exceptional’ where the index value of an annual maximum, occurring between 2014 and 2018, exceeds the previous maxima (recorded since 1980) by more than 20%. The geographical distribution, comparative magnitude and PR tendency (at the 95% confidence level) of those exceptional events are shown in Figure 3.4. Exceptional fire weather events occurred prevalently in multiple locations around the world between 2014 and 2018. Four of the five CFWIS indices show that more than 50% of events were associated with an increase in likelihoods; the exception is DC, which is the only index that is, in principle, constrained by a maximum probable value (de Groot, 1987) with an upper limit. DMC and BUI were associated with the largest number of exceptional events, which were mostly associated with positive changes in PR. On the contrary, DC, ISI and FWI show relatively fewer exceptional events, but those are still strongly related to an increase in likelihood. Specifically, the largest exceptional fire weather events (*i.e.*, those exceeding the previous maxima by 50%) are detected in coastal North America, central and southeast South America, central and southern Africa, and boreal Asia, in addition to parts of Europe and Australia. Almost all of these occurrences are linked to an increase in likelihood (PR>1). Nevertheless, some exceptional events are associated with a decrease in likelihood (PR<1), particularly extremes in DMC in the Pacific Northwest of North America and central Europe, extremes in DMC and BUI in northern parts of South America, and extremes in BMC, DC and BUI in equatorial Asia.

The fact that different indices present disparate distributions of exceptional events highlights the sensitivity of a fire weather event study to the index used to define the event in question. There are several instances in which such sensitivity is strongly evident. In Alaska,

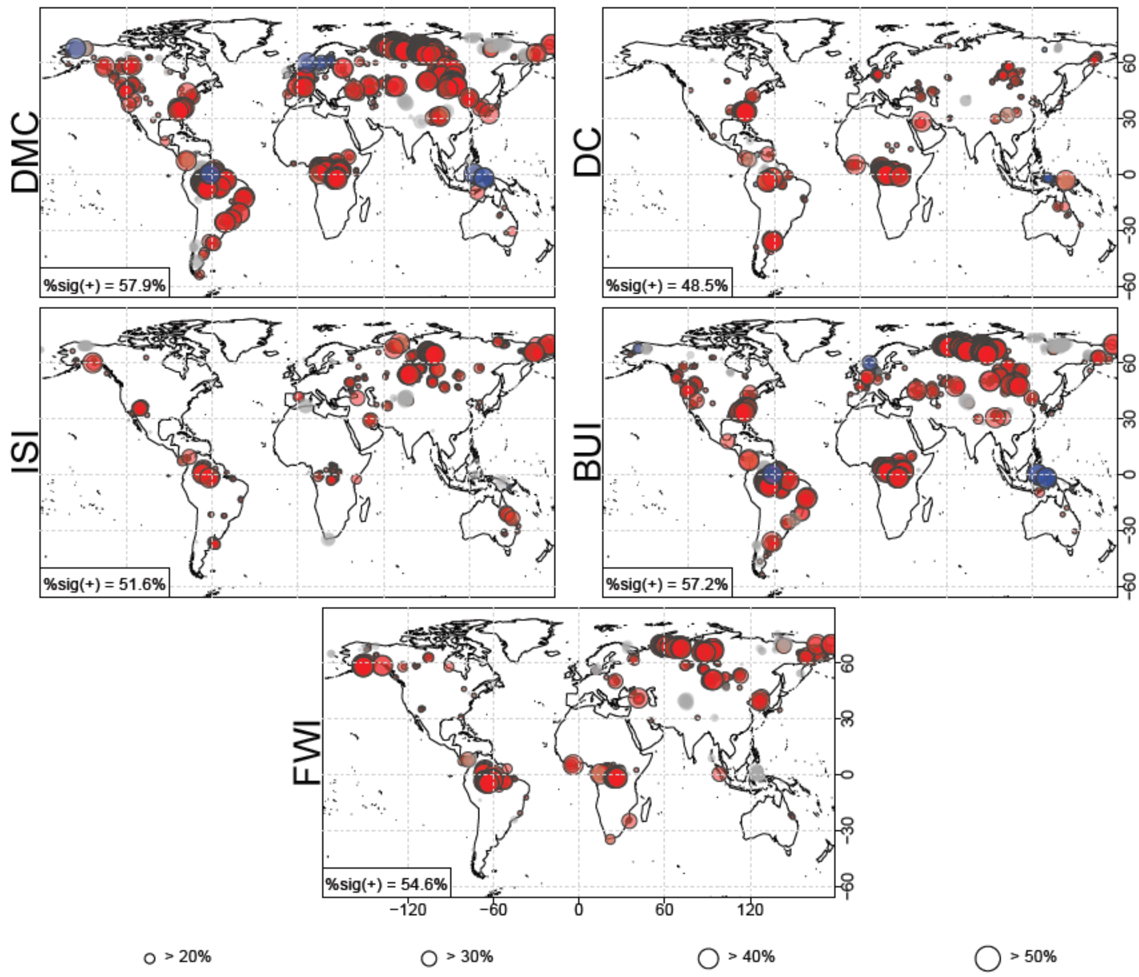

Figure 3.4: Global distribution of recent fire weather events (2014-2018), defined by each CFWIS index, for which the magnitude exceeds any previous annual maxima by more than 20%. Point size is representative of the exceptionality of each event. Point colour is representative of the corresponding PR: events associated with an increase (PR>1) and decrease (PR<1) in likelihood are shown in red and blue respectively; events associated with no significant change are shown in grey. Numbers in the bottom-left corner of each panel shows the percentage of events associated with an increase in likelihoods.

several ISI and FWI events are observed that exceed the magnitude of the previous maxima by more than 50% and are associated with a significant increase in likelihood. However, exceptional events in other indices are either not evident or, in the case of DMC extremes, associated with a significant decrease in likelihood. In South America, there is a large number of exceptional DMC and BUI events spanning the entire continent, but relatively few exceptional DC, FWI and ISI events are found outside of the northern region. In central Africa, extreme ISI events of lesser exceptionality (no more than 30% greater than the previous maxima) compared to other indices, but in all cases, those events are associated with increasing PR. Europe is associated with particularly exceptional events, but those events are linked with the decrease in PR in the Scandinavian region and the increase in PR over the rest of Europe. In Northern and East Asia, there are numerous exceptional DMC and BUI events (>50%), but far fewer for other indices.

The use of a consistent spatiotemporal event definition presents the possibility to attribute multiple events collectively, which we do by averaging the PR of all exceptional fire weather events across the 14 GFED fire regions.

Figure 3.5 summarises the PR averaged across each region for each CFWIS index. Exceptional fire weather events recorded in six regions (BOAS, TENA, CEAS, SHAF, NHAF and AUST) exhibit the largest collective increase in likelihood (average PR>8) irrespective of the index used to define them. For TENA and NHAF specifically, the increase in likelihood is exhibited for more than 95% of events used to construct the averages. By contrast, there are examples where the average PR differs substantially between indices. The recent exceptional BUI, ISI and FWI events occurring in SEAS collectively exhibit an averaged decrease in likelihood (PR<0.5), whereas an increase is found for DMC and DC events. There are also some notable inter-index differences among the exceptional events occurring in EQAS. This finding further illustrates the sensitivity of fire weather attribution studies to the choice of index. It is also important to highlight that the outcome may be influenced by the varying extents of different geographical areas.

3.4 Discussion and conclusions

This study has identified trends in fire weather extremes and quantified to what extent climate change has altered their likelihood and magnitude. Following a probabilistic approach, an established empirical-statistical method was used to construct a globally applicable framework to attribute worldwide extreme fire weather events. The results provide clarification

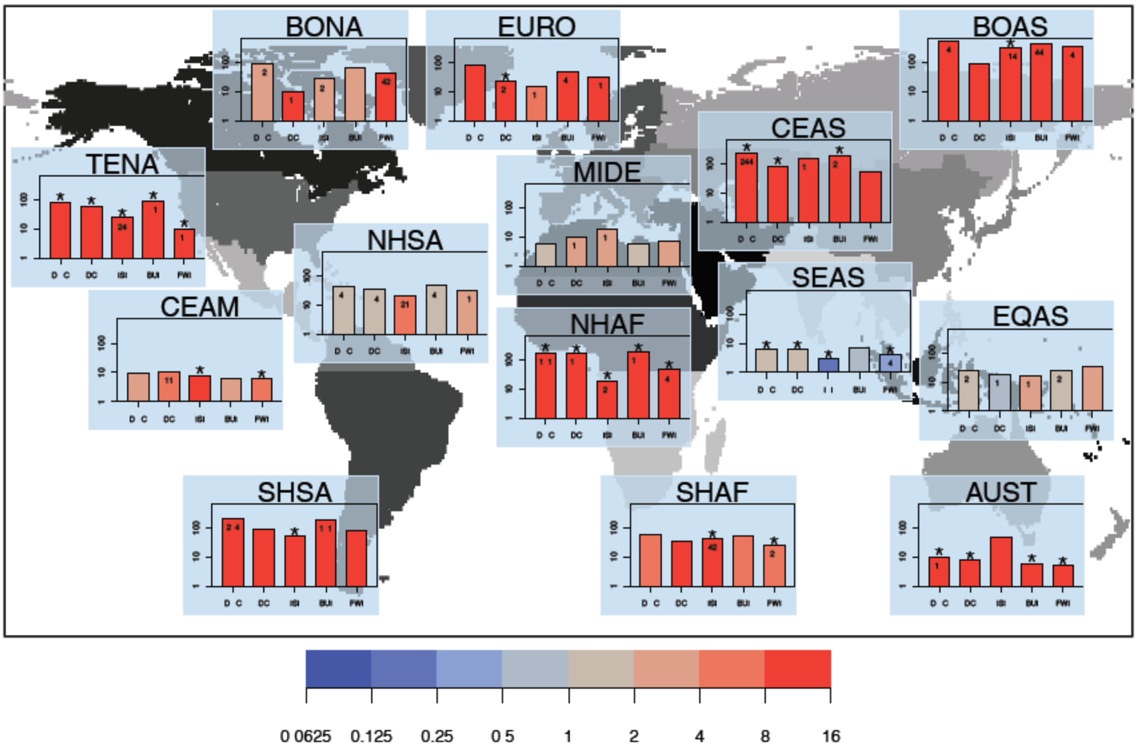

BONA	Boreal North America	NHAF	Northern Hemisphere Africa
TENA	Temperate North America	SHAF	Southern Hemisphere Africa
CEAM	Central America	BOAS	Boreal Asia
NHSA	Northern Hemisphere South America	CEAS	Central Asia
SHSA	Southern Hemisphere South America	SEAS	Southeast Asia
EURO	Europe	EQAS	Equatorial Asia
MIDE	Middle East	AUST	Australia and New Zealand

Figure 3.5: Regional summaries of exceptional event attribution across the 14 GFED fire regions. Bar charts for each CFWIS index show PR averaged across all the exceptional fire weather events identified for each CFWIS index. The size of each bar represents the number of exceptional events; the colours of each bar represent average PR; bars shown in bold and with an asterisk indicate where over 95% of exceptional events agree on either an increase (PR>1) or decrease (PR<1) in likelihood.

on uncertainties and sensitivities associated with the choice of an index for fire weather representation, particularly in the context of extreme event attribution.

The first part of the analysis of fire weather trends and correlation analysis presents preliminary knowledge about the performance of fire weather indicators in the form of the CFWIS indices across the world's fire-prone regions. A positive trend was found in the seasonal mean of each index in most fire-prone regions of the world, and broadly in line with the present understanding of global fire weather and its relationship with climate change (Jain et al., 2022). Reflecting on correlation with the occurrence of fire activity (in the form of burned area data), while inter-index differences are modest, there are several examples of substantial differences at the regional scale. Notably, we found that FWI is not systematically the closest match to fire activity, suggesting that other indices could potentially be more appropriate proxies for fire risk in specific regions.

The probability of extreme climate-related wildfire risk has increased substantially as a response to globally warming temperatures in large parts of the world. This is, however, not the case in some regions, such as southeast Asia. While our results are based on a relatively short record (39 years from 1980 to 2018), it is possible to conclude that the greater maximum daily temperature may not be the major driver of fires in these areas, which means other factors (*i.e.*, precipitation, humidity and surface wind) should play an important role in attribution methodologies. Since climate change effects at the regional scale are associated not only with warming temperatures but also with changes to precipitation and atmospheric moisture content, this does not imply that such extreme fire weather events are unrelated to anthropogenic climate change. Generally, these results are consistent irrespective of the index used to define extreme fire weather. However, there are some notable exceptions (*e.g.*, Australia and sub-Saharan Africa), where attribution results show a strong sensitivity to the choice of index.

It is evident that, while the CFWIS indices used here form part of a common wildfire information system, different indices can lead to disparate results with respect to changes in the nature of fire weather extremes in various regions of the world. Therefore, as highlighted in recent work (Philip et al., 2020; van Oldenborgh et al., 2021b), it is crucial to explore the availability and merits of indices or metrics that may be used to represent fire weather, and to fully justify their application in the context of event attribution. As illustrated through our analysis of recent exceptional events, attribution of changes in the likelihood of events in response to warming global temperature can be significantly different depending on the choice of index. With respect to future efforts to attribute fire weather extremes, we recommend the consideration of a full variety of indices or metrics to: (i) understand and communicate the sensitivity of the results to the chosen index or metric; (ii) better understand the effect of climate change on different combinations of the meteorological components of fire weather (temperature, precipitation, wind speed and atmospheric moisture content).

Empirical attribution analysis provides important preliminary knowledge of changing extreme fire weather based on observations, but robust attribution of extreme events requires the complementary application of similar methods to the outputs of climate model ensembles (van der Werf et al., 2017). We anticipate that the results presented here will serve as a benchmark against which results from climate models can be compared, and ultimately serve to improve the accuracy of attribution findings generated from models (van Oldenborgh et al., 2021b). In future studies, it may also be beneficial to include more indices from other risk assessment systems in a similar framework, such as the Keetch-Byram drought index (KBDI) from the US Department of Agriculture's Forest Service (Keetch and Byram, 1968), the energy release component (ERC) calculated from the United States national fire danger rating system (NFDRS; Deeming et al., 1978), and the McArthur forest fire danger index (FFDI) from the Centre for Australia Weather and Climate Research (McArthur, 1967).

Chapter 4

Multi-model attribution of extremes in fire weather intensity and duration to externally forced changes in global temperature anomalies

Abstract - In response to the occurrence of a number of large wildfire events across the world in recent years, the question of the extent to which climate change may be altering the meteorological conditions conducive to wildfires has become a hot topic of debate. Despite the development of attribution methodologies for extreme events in the last decade, attribution studies dedicated explicitly to wildfire, or otherwise extreme 'fire weather', are still relatively few. In turn, there is a lack of consensus on how to define fire risk in a meteorological context, posing a challenge for research in this subfield. Recent work has offered clarification on uncertainties associated with the choice of meteorological indicator to represent fire weather in the context of extreme event attribution but there are additional sensitivities that are still not fully understood.

Here, for the first time, a global probabilistic attribution of fire weather extremes is conducted using an established statistical methodology applied to six large (>10 member) climate model ensembles from CMIP6. Trends in extremes in the Canadian Fire Weather Index (FWI) are quantified using extreme value distributions, fitted with annual maxima in both FWI intensity and duration, and scaled to global mean surface temperature. An initial evaluation of model performance shows that, while all models are able to reasonably reproduce observed global patterns in extreme distribution parameters, there are some notable differences at the regional scale. Global probability ratio maps are used to quantify the

influence of rising global temperatures on the changing frequency of FWI extremes. The findings highlight the sensitivity of probabilistic fire weather attribution to the choice of climate model ensemble, and the value added by a model evaluation and selection step in maximising the robustness of attribution analysis. In conclusion, a set of recommendations is made for future efforts to attribute episodes of extreme fire weather.

This chapter appears as the following submitted manuscript to *Weather and Climate Extremes*: **Liu, Z.**, Eden, J. M., Dieppois, B., Drobyshev, I., Krikken, F., & Blackett, M. (2022). Multi-model attribution of extremes in fire weather intensity and duration to externally forced changes in global temperature anomalies. *Weather and Climate Extremes, (In review).*

4.1 Introduction

The frequency and severity of large wildfire events has increased globally in recent years (World Meteorological Organization, 2021). Particularly destructive fires have fostered debate on how the role of climate change may have altered the weather conditions favourable to wildfires (Boer et al., 2020; Bowman et al., 2020; Ellis et al., 2022). Efforts to quantify the role of climate change in altering the frequency and magnitude of weather and climate phenomena, broadly termed climate change attribution, have developed extensively during the last decade. This development includes a dramatic increase in the capacity to attribute individual extreme weather and climate events. However, attribution studies focused on wildfires remain rare compared to those focused on other extreme events, such as heatwaves, meteorological floods, and droughts.

The scarcity of wildfire attribution studies is surprising given that the link between wildfires and climate is well-established and widely used in operational fire management, *e.g.*, through the reliance of forest management agencies on the Canadian Fire Weather Index System (CFWIS; Van Wagner, 1987) and the United States National Fire Danger Rating System (NFDRS; Deeming et al., 1978). The Atlas of Mortality and Economic Losses from Weather, Climate and Water Extremes (1970-2019) (World Meteorological Organization, 2021) categorises wildfires as part of the 'climatological' subgroup of hazards. Strictly speaking, however, wildfires are not meteorological events, as other factors (*i.e.*, human activities) play a role in their ignition and spread, making their mechanisms of occurrence and development considerably more complex, and their relationship to weather and climate more obscure. As the understanding of the occurrence mechanism of wildfires is even poorer than other extremes, the confidence and reliability of the corresponding attribution studies of wildfires are also lower (National Academies of Sciences, Engineering, and Medicine, 2016). The limited understanding of wildfire attribution is often associated with uncertainty, including the sensitivity of attribution results to many factors, such as the choice of fire weather indicators (Liu et al., 2022a), event definitions and the climate models used in the analysis (Philip et al., 2020).

Although research on the attribution of extreme wildfires, particularly on a global scale, remains scarce, there are several global studies that are already working on fire weather, the term given to the meteorological conditions conducive to such events. For instance, according to Abatzoglou et al. (2019), 22% of the world's burnable land area is experiencing anthropogenic increases in extreme fire weather indices by 2019, including much of the Mediterranean and Amazon. Jain et al. (2022) found trends in extreme fire weather across almost half of the global burnable area based on the reanalysis data from 1979 to 2020. Additionally, Liu et al. (2022a) showed that, across more than 40% of the world's fire-prone regions, extreme fire weather became at least four times more likely due to global temperature increases between 1980 and 2018. There is enormous potential for regional- and local-scale studies to support and test global-scale frameworks' findings. Recent case studies have been undertaken in regions of Australia (Tett et al., 2018; Lewis et al., 2020; van Oldenborgh et al., 2021a), Canada (Kirchmeier-Young et al., 2017b), Sweden (Krikken et al., 2021), Siberia (Liu et al., 2022b) and South Africa (Liu et al., 2023). Nevertheless, attribution studies of individual wildfires, or otherwise extreme fire weather events, are rare in comparison to other weather and climate extremes.

While individual studies are an important supplement to global analysis, the extent to which their results can be integrated is limited by a lack of homogeneity in spatiotemporal definition of the event, and the choice of methodology. In turn, this limits our ability to understand the extent to which such increasing risks of fire-prone weather conditions are affecting different environments and climatic zones in response to climate change. Liu et al. (2022a) provided clarity on the sensitivity of the findings of an empirical-statistical attribution methodology in the definition of extreme fire weather. The authors also demonstrated that analysis of multiple events can be combined as part of a collective attribution, but acknowledged that studies combining results generated by different data sources must consider additional uncertainties and sensitivities.

The role of climate models is indeed vital to provide robust attribution of changes in extreme fire weather. In the context of their utilisation in attribution, model ensembles can be split into two categories (Philip et al., 2020): (a) 'fixed forcing' runs, which usually consist of a pair of simulations representative of current conditions and a counterfactual reality without anthropogenic emissions, and (b) 'transient' runs, such as those that contribute to the sixth phase of Coupled Model Intercomparison Project (CMIP6; Eyring et al., 2016). Despite the widespread use of climate model ensembles in attribution analysis, many studies are based on a small number of models (Kirchmeier-Young et al., 2017b, 2019b; Liu et al., 2022b), or otherwise do not conduct a specific model evaluation step (Kirchmeier-Young et al., 2017b). All climate models, either fixed-forcing or transient, exhibit (potentially large) biases, particularly in the representation of extremes (*e.g.*, Vautard et al., 2020). The capability of climate models to simulate statistics of extreme events that are comparable to the observed one has not always been given due attention in attribution studies, leading to uncertainties in the findings drawn from the analysis of simulations from different climate models. This introduces new questions about the suitability of the chosen climate model for attribution to the target extreme event (Philip et al., 2020). As noted by Philip et al. (2020) in their documentation of recommended protocols for probabilistic extreme event attribution analysis, it is important to examine a series of climate models to understand the sensitivity and to include the model evaluation step to quantify the uncertainty for event attribution studies.

The fast-paced development of attribution science during the last decade has been driven by the increased capacity for climate models to simulate large ensembles. Large climate ensemble models provide: (a) an opportunity to study multiple realisations and thus longer time series than what is possible with observations alone, which means that the detection and quantification of extreme thresholds and distributions should be more robust, (b) a homogeneous representation of climate, independent of the spatial and temporal distribution of the observational monitoring network, and (c) a better understanding of the role of externally forced trends from internal variability (Deser et al., 2020). Notably, the use of large-ensembles (>10 realisations of the same model) of coupled general circulation models smooths the impact of internal variations and enables extraction of more robust externally forced signals, via means of simple ensembles (Milinski et al., 2020; Maher et al., 2021).

With a growing number of attribution studies dedicated to wildfire, or extreme fire weather, across the globe, there is a clear need to identify and understand all sources of sensitivities and uncertainties. Here, using established statistical methodologies applied to six large ensembles from the sixth phase of the Coupled Model Intercomparison Project (CMIP6), we conduct probabilistic attribution of fire weather extremes across the world's fire-prone regions. We assess trends in both the intensity and duration of extremes in the Canadian Fire Weather Index (FWI) using a Generalised Extreme Value (GEV) distribution, fitted with annual maxima and scaled to externally forced global mean surface temperature (GMST). In terms of the analysis of extremes in FWI intensity, the current analysis builds on the empirical-statistical approach presented by Liu et al. (2022a). For the first time, we apply this approach to the output of multiple large-ensembles from CMIP6 models. The extension of the same approach to quantify trends in the duration of extreme FWI events also constitutes a novel application.

The remainder of this paper is structured as follows. In section 4.2, details of the CMIP6 data and methodology are presented, including the selection of a definition for global fire weather extremes. In section 4.3, results of the changing likelihoods in extreme fire weather and a multi-model synthesis are presented. In section 4.4, we conclude and make a set of recommendations for future attribution of extreme fire weather episodes.

4.2 Methods and Data

4.2.1 Defining fire weather extremes

Choosing an appropriate set of spatiotemporal parameters by which to define weather or climate extremes is a crucial step in an attribution study since the findings and interpretation of the results both rely upon this definition. To this end, we use the potential impact of extremes as the pivotal element of their definition (Philip et al., 2020; Krikken et al., 2021; van Oldenborgh et al., 2021b). Specifically, fire weather extremes are defined in two ways: (i) Extremes in fire weather intensity are defined by the annual maxima in 7-day averaged FWI (FWIx7day). The choice of a 7-day period for averaging is consistent with previous efforts to attribute FWI extremes (*e.g.*, Krikken et al., 2021; Liu et al., 2022b; 2023). (ii) Extremes in fire weather duration are defined by the annual maxima in the number of consecutive days for which FWI is above the historical 90$^{\text{th}}$ percentile (FWIxCD90). In both cases, the spatial extent of an extreme is limited to a radius of 250 km to ensure that they represent the immediate vicinity of the most intense fires. The annual maxima at each target grid point are defined by the spatial maximum of all grid points within a 250 km radius in order to avoid the overlap between grid cells and therefore, to avoid the risk of double counting.

4.2.2 Data

Simulations of the historical FWI data were derived from six CMIP6 models, all of which have an ensemble size of at least 10 members, for the period 1850-2014. Details of all six models are given in Table 4.1.

Table 4.1: Details of the six CMIP6 models used in the analysis.

Model	**Institution**	**Ens**	**Resolution (lon × lat)**	**Reference**
the Canadian Earth System Model version 5 (**CanESM5**)	Canadian Centre for Climate Modelling and Analysis (CCCma)	50	128×64 (∼2.8× 2.8°)	(Swart et al., 2019)
the Atmosphere-Ocean General Circulation Model (**CNRM-CM6-1**)	Centre National de Recherches Météorologiques (CNRM)	30	256×128 (∼1.4× 1.4°)	(Voldoire et al., 2019)
the Earth system (ES) model of the second generation (**CNRM-ESM2-1**)	Centre National de Recherches Météorologiques (CNRM)	10	256×128 (∼1.4× 1.4°)	(Séférian et al., 2019)
the fifth generation of the INMCM climate model (**INM-CM-5-0**)	Institute for Numerical Mathematics (INM) of the Russian Academy of Sciences	10	180×120 (2.0× 1.5°)	(Volodin and Gritsun, 2018)
the latest version of the IPSL climate model (**IPSL-CM6A-LR**)	Institut Pierre-Simon Laplace Climate Modelling Centre (IPSL CMC)	32	144×143 (∼2.5× 1.3°)	(Boucher et al., 2020)
the Earth System Model version 1.2 (**MPI-ESM1-2-HR**)	Max Planck Institute for Meteorology (MPI-M)	10	384×192 (∼0.9× 0.9°)	(Müller et al., 2018)

Data from the Global ECMWF Fire Forecast model (hereafter GEFF-ERA5) (Vitolo et al., 2020) is used as an observational reference for the period 1979-2020. GEFF-ERA5 is produced by the European Forest Fire Information System of the Copernicus Emergency Management Service and provides daily FWI data driven by input fields from the ERA5 Reanalysis (ERA5; Hersbach et al., 2020). GEFF-ERA5 is taken as a realistic representation of real-world day-to-day conditions and a reference against which model outputs are compared (see section 4.2.4 in detail).

Monthly burned area data from the Global Fire Emissions Database Version 4 (GFED4; Global Fire Emissions Database, 2022) were used to isolate 'fire-prone' regions of the world (*i.e.*, where evidence of past fires has been recorded). A 9-point smoothing with a quadrilateral curvilinear grid of GFED4 data on all fields is employed in order to account for the spatial randomness of fire occurrence during the relatively short time period for which GFED4 data is available (1996-2016; van der Werf et al., 2017).

4.2.3 Methodology

A probabilistic framework based on extreme value theory is used to estimate changes in the probability of extreme fire weather. Annual maxima of both intensity (FWIx7day) and duration (FWIxCD90) across all 165 years and all ensemble members are pooled and fitted to the GEV distribution. To investigate the dependence of the fit on global warming, the distribution is scaled with the corresponding 48-month running average in global mean surface temperature (GMST) from the ensemble means. In contrast to taking GMST for each ensemble member, this approach facilitates the estimation of responsiveness to externally forced temperature changes. The scaled (and thus non-stationary) distribution is constructed under the assumption that the location parameter μ and the scale parameter σ have the same exponential dependency on GMST, for which the 'dispersion' ratio σ/μ and the shape parameter δ remain constant (*e.g.*, van der Wiel et al., 2017; van Oldenborgh et al., 2018; Otto et al., 2018b; Eden et al., 2018; Krikken et al., 2021; Philip et al., 2020):

$$\mu = \mu_0 \cdot exp\frac{\alpha T}{\mu_0} \tag{4.1}$$

$$\sigma = \sigma_0 \cdot exp\frac{\alpha T}{\sigma_0} \tag{4.2}$$

where μ_0 and σ_0 are the fit parameters of the stationary GEV distribution; α, as a function of smoothed GMST anomaly T, represents the trend in fire indicator maxima. The three parameters μ, σ and δ indicate the mean, the variability in the tail and the bound of the tail of the distribution, separately. At each grid point, probabilities p0 and p1 of a given fire weather extreme occurring in periods of low and high anthropogenic forcing (1880-1884 and 2010-2014 respectively) are estimated. Therefore, changes in likelihood expressed as the 'probability ratio' (PR) p1/p0, are quantified across all fire-prone regions around the world. Additionally, changes in extremes in fire weather intensity are expressed as a percentage change in magnitude (%MAG) and changes in extremes in fire weather duration are expressed as a change in the number of consecutive days (durDays).

The scaled GEV approach is well-established and has been previously applied to extremes in heat (*e.g.*, van Oldenborgh et al., 2018; Otto et al., 2018b; Eden et al., 2018) and precipitation (*e.g.*, van der Wiel et al., 2017), in addition to extremes in fire weather intensity (Krikken et al., 2021). Here, for the first time, the approach is applied to the analysis of extremes defined by duration as well as by intensity on a global scale. The implementation of the approach here also marks its first global application to fire weather extremes from multiple large ensembles of the six CMIP6 models.

4.2.4 Model evaluation

According to Philip et al. (2020), the ability of climate models to represent a particular type of extreme event is critical for attribution studies and can influence the accuracy and uncertainty of attribution results. Here, we evaluate the capacity of each of the six CMIP6 models to represent realistic distributions of fire weather extremes. The basis of this evaluation is the comparison of a stationary GEV distribution (*i.e.*, not scaled by GMST) fitted with model-simulated annual maxima and a GEV distribution fitted with corresponding data from the fire danger reanalysis, GEFF-ERA5 (Vitolo et al., 2020). Assessment of the similarity of the distribution parameters, and particularly the dispersion ratio and shape parameter of each fit, reflects the suitability of each model at each target grid point. We conclude that, for a given grid point, a model can realistically represent the distribution of extremes when the dispersion ratio and shape parameter of the stationary GEV fit fall within the range of 95% confidence intervals determined for the dispersion ratio and shape parameter of a GEV fitted with GEFF-ERA5 data following a 1000-sample non-parametric bootstrapping method (Efron and Tibshirani, 1998; van der Wiel et al., 2017).

4.3 Results

In this section, results focus on model evaluation and attribution analysis of extreme fire weather intensity (section 4.3.1) and fire weather duration (section 4.3.2). This is followed by a multi-model synthesis (section 4.3.3) to complete the full story of the fire weather attribution. All the results are made throughout the world's fire-prone regions.

4.3.1 Extremes in fire weather intensity

4.3.1.1 Model performance in simulating the extremes in fire weather intensity

To obtain a preliminary insight into the performance of the six CMIP6 large ensembles, simulated global patterns of both the dispersion ratio ($\frac{\sigma}{\mu}$) and shape parameter (ξ) for GEV distribution fitted with FWIx7day, are compared with the GEFF-ERA5 reanalysis for the period from 1979 to 2014, with corresponding differences all shown in Figure 4.1.

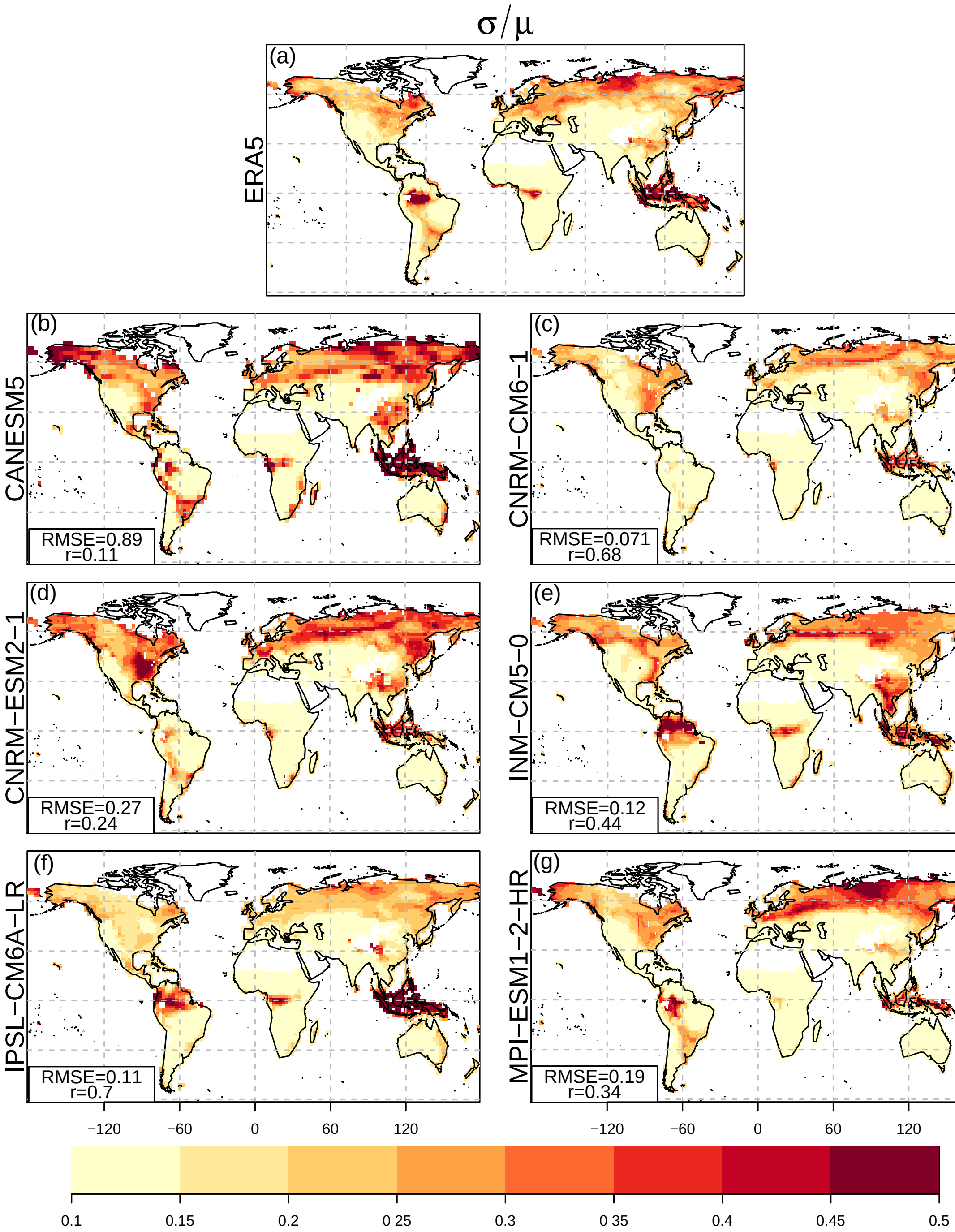
σ/μ
(a)
ERA5
(b)
CANESM5
RMSE=0.89
r=0.11
(c)
CNRM−CM6−1
RMSE=0.071
r=0.68
(d)
CNRM−ESM2−1
RMSE=0.27
r=0.24
(e)
INM−CM5−0
RMSE=0.12
r=0.44
(f)
IPSL−CM6A−LR
RMSE=0.11
r=0.7
(g)
MPI−ESM1−2−HR
RMSE=0.19
r=0.34
−120 −60 0 60 120
60 30 0 −30 −60
0.1 0.15 0.2 0.25 0.3 0.35 0.4 0.45 0.5

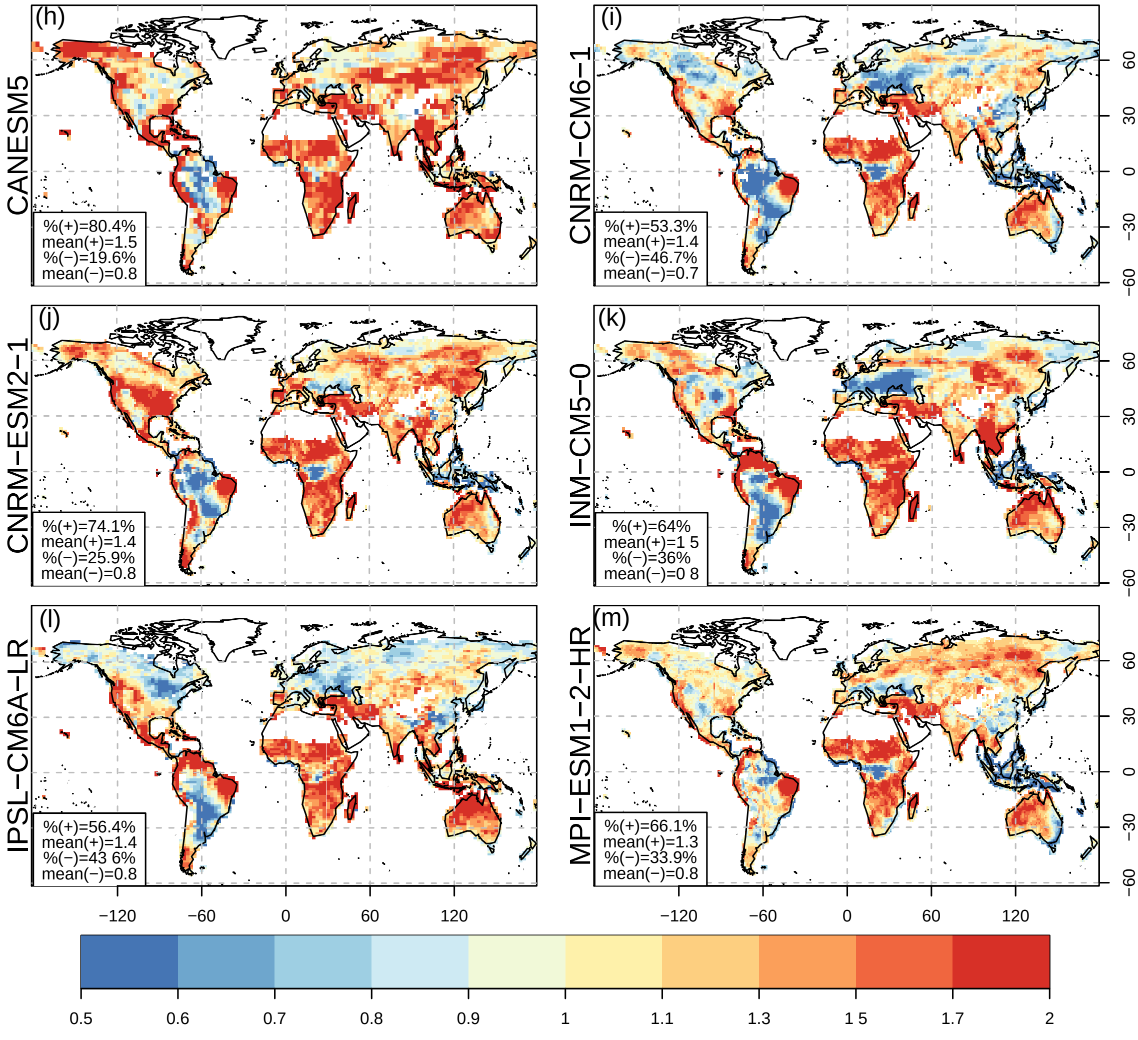
(h)
CANESM5
%(+)=80.4%
mean(+)=1.5
%(−)=19.6%
mean(−)=0.8
(i)
CNRM−CM6−1
%(+)=53.3%
mean(+)=1.4
%(−)=46.7%
mean(−)=0.7
(j)
CNRM−ESM2−1
%(+)=74.1%
mean(+)=1.4
%(−)=25.9%
mean(−)=0.8
(k)
INM−CM5−0
%(+)=64%
mean(+)=1 5
%(−)=36%
mean(−)=0 8
(l)
IPSL−CM6A−LR
%(+)=56.4%
mean(+)=1.4
%(−)=43 6%
mean(−)=0.8
(m)
MPI−ESM1−2−HR
%(+)=66.1%
mean(+)=1.3
%(−)=33.9%
mean(−)=0.8
−120 −60 0 60 120
60 30 0 −30 −60
0.5 0.6 0.7 0.8 0.9 1 1.1 1.3 1 5 1.7 2

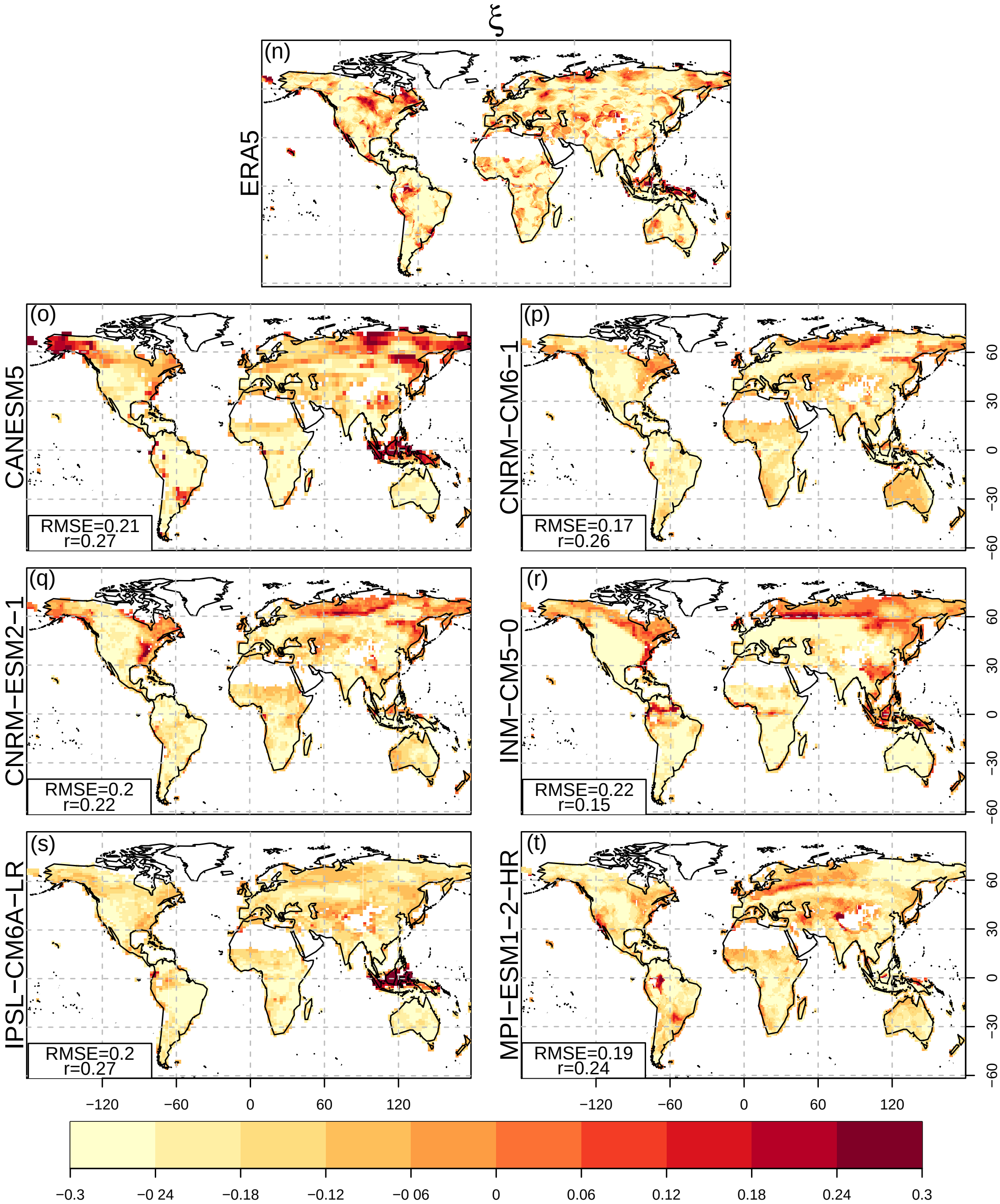

ξ
(n)
ERA5
(o)
CANESM5
RMSE=0.21
r=0.27
(p)
CNRM−CM6−1
RMSE=0.17
r=0.26
(q)
CNRM−ESM2−1
RMSE=0.2
r=0.22
(r)
INM−CM5−0
RMSE=0.22
r=0.15
(s)
IPSL−CM6A−LR
RMSE=0.2
r=0.27
(t)
MPI−ESM1−2−HR
RMSE=0.19
r=0.24
−120 −60 0 60 120
60 30 0 −30 −60
−0.3 −0.24 −0.18 −0.12 −0.06 0 0.06 0.12 0.18 0.24 0.3

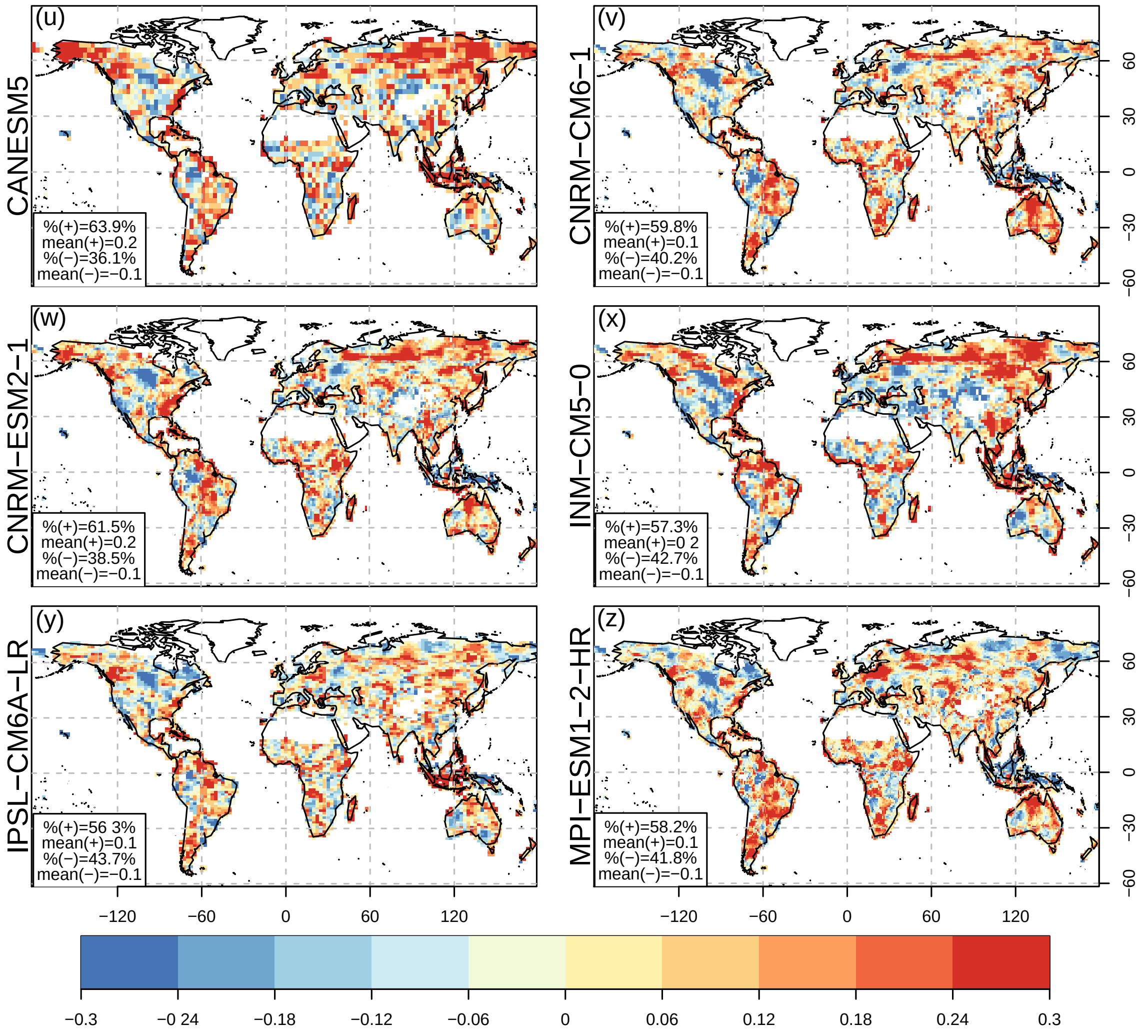

Figure 4.1: Dispersion ratio ($\frac{\sigma}{\mu}$) derived from the stationary GEV fitted with FWIx7day for the period 1979 to 2014 from the GEFF-ERA5 reanalysis (a) and six CMIP6 ensembles (b-g); corresponding differences between the reanalysis and the six CMIP6 models are shown from (h) to (m). Similarly, shape parameter (ξ) from the GEFF-ERA5 reanalysis (n) and six CMIP6 ensembles (o-t) with corresponding differences between the reanalysis and the six CMIP6 models from (u-z). Values in the bottom-left corner of each panel from (b-g) and (o-t) show the root mean square error (RMSE) and spatial correlation coefficient (r) of each six CMIP6 ensembles; while that from (h-m) and (u-z) show the percentage of overestimations (%(+)) and underestimations (%(-)) among all the grid cells.

With regard to the dispersion parameter, GEFF-ERA5 produces high values in northwestern and northeastern North America, some parts of equatorial South America, equatorial Africa and northern and southern Asia (Figure 4.1a). According to the differences (RMSE) and spatial correlation (r) between the reanalysis and models, CNRM-CM6-1 (Figure 4.1c) and IPSL-CM6A-LR (Figure 4.1f) show reasonable level of agreements ($r \sim 0.7$) with GEFF-ERA5 in many fire-prone regions of the world, in spite of the apparent inter-model differences in northern South America, equatorial Africa and northern Asia, while CanESM5 produces the lowest correlation (Figure 4.1b). CNRM-ESM2-1 (Figure 4.1d), INM-CM5-0 (Figure 4.1e) and MPI-ESM1-2-HR (Figure 4.1g) display a certain degree of similarity with GEFF-ERA5 ($0.2<r<0.5$), although they still overestimate (%(+)>50%) the results, particularly around equatorial and southern South Africa, Central Asia (Figure 4.1j, k & m). The highest overestimates (>80%; CanESM5) of the extent of the dispersion ratio are shown in northern and southern North America, central and southern Asia, northwest and southeast Australia (Figure 4.1h). It is worth noting that there are apparent underestimations across eastern Europe presented by CNRM-CM6-1 (Figure 4.1c), INM-CM5-0 and IPSL-CM6A-LR (Figure 4.1i, l & k).

Concerning the shape parameter (ξ) of the GEV fitted with GEFF-ERA5 maxima, the highest values appear in central and eastern North America, northern Europe, and some parts of northern and southern Asia (Figure 4.1n). CanESM5, CNRM-CM6-1 and IPSL-CM6A-LR are the most consistent models when compared with the GEFF-ERA5 data, exhibiting relatively small RMSE and a strong spatial correlation when compared with the other ensembles (Figure 4.1o, p & s), while INM-CM5-0 produced the largest RMSE values (0.22) and the weakest spatial correlations (0.15; Figure 4.1r). The other two models, CNRM-ESM2-1 and MPI-ESM1-2-HR, show similar results in terms of RMSE and spatial correlation, with inter-model differences especially apparent in northwestern and eastern North America, central Europe and northeastern Asia (Figure 4.1q & t). Figure 4.1u-z shows the spatial differences between GEFF-ERA5 and the models with the shape parameter overestimated in most of the world, indicating a heavier tail behaviour related to the extremes in the distribution. Again, CanESM5 (Figure 4.1u) and CNRM-ESM2-1 (Figure 4.1w) show the highest degree of overestimations (>60%), mainly in northern Asia. In general, the representation of the shape parameter in the models is generally less spatially consistent than that of the dispersion parameter.

In summary, the distribution of annual maxima taken from the CMIP6 ensembles is in reasonable agreement with that of GEFF-ERA5 annual maxima, although there are some notable differences at the regional scale. Compared to GEFF-ERA5, CNRM-CM6-1 and IPSL-CM6A-LR are the best-performing of the six climate models in terms of their representation of the dispersion and shape parameters, while CanESM5 and INM-CM5-0 are the most biased of the six 4.1.

4.3.1.2 Attribution of extremes in fire weather intensity

Based on the global probabilistic method introduced in section 4.2.3, the changes in the likelihood of extreme fire weather (FWIx7day) due to climate change are quantified using the GEV-scaling method for each climate model. For each grid box, the 95th percentile of the annual maxima in modelled extreme fire weather from 1850 to 2014 was chosen as a threshold defining extremes, from which we estimated the return level of events. Global maps showing the probability ratio (PR) and change in magnitude (%MAG) between periods of low and high anthropogenic forcing are presented in Figure 4.2.

Overall, there are several similarities in spatial patterns of both PR and %MAG across the six CMIP6 models. In response to externally forced global warming, a 2-fold increase in the probability (PR>2) of extreme fire weather is witnessed in many regions across the globe, such as central and southern North America, northern South America, and southern Africa (Figure 4.2a-f). This corresponds to an increase of at least 10% in the magnitude of extreme fire weather (Figure 4.2g-l). Regions with increasing likelihoods in %MAG are mainly similar to that identified in PR for each model. In contrast, in terms of the occurrence of extreme fire weather conditions, northern North America and central Africa reflect a decrease in likelihood (PR<1) across all six climate models (Figure 4.2a-f), and are generally in line with the results of observed global fire weather associated with climate change (Liu et al., 2022a).

There are some similarities in the spatial patterns across the six CMIP6 models, but many areas show sensitivity to the choice of model. For instance, CanESM5, INM-CM5-0 and, particularly, IPSL-CM6A-LR show a strong decrease in the likelihood (PR<1) of FWIx7day over northern North America (Figure 4.2a, d & e), while other models present a relatively small increase in the likelihood of such conditions (PR>1; Figure 4.2b, c & f). The CNRM-CM6-1 and INM-CM5-0 models are the only ones showing a decrease in the likelihood of extreme fire weather in central North America (Figure 4.2b) and in many parts of South America (Figure 4.2d), respectively. Such discrepancies between models are also found in northern and central Asia: i) decreasing PR over northern Asia and central Asia using CanESM5 (Figure 4.2a); ii) decreasing (increasing) PR over northern Asia (Central Asia) using CNRM-ESM2-1 and INM-CM5-0 (Figure 4.2c-d); iii) increasing (decreasing) PR are found over northern Asia (Central Asia) in CNRM-CM6-1 (Figure 4.2b); iv) IPSL-CM6A-LR

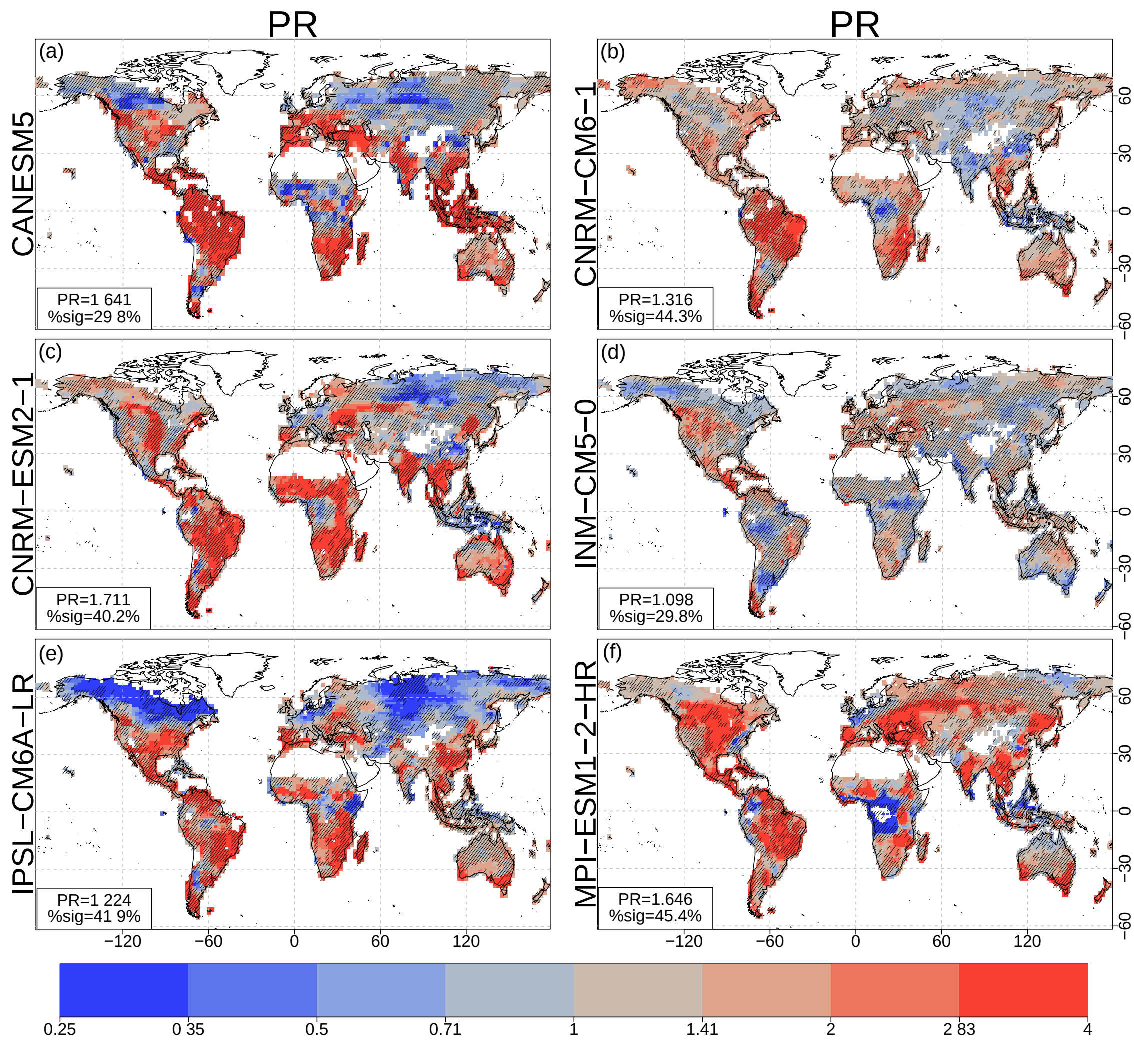
PR
PR
(a)
CANESM5
PR=1 641
%sig=29 8%
(b)
CNRM−CM6−1
PR=1.316
%sig=44.3%
(c)
CNRM−ESM2−1
PR=1.711
%sig=40.2%
(d)
INM−CM5−0
PR=1.098
%sig=29.8%
(e)
IPSL−CM6A−LR
PR=1 224
%sig=41 9%
(f)
MPI−ESM1−2−HR
PR=1.646
%sig=45.4%
−120 −60 0 60 120
60 30 0 −30 −60
0.25 0 35 0.5 0.71 1 1.41 2 2 83 4

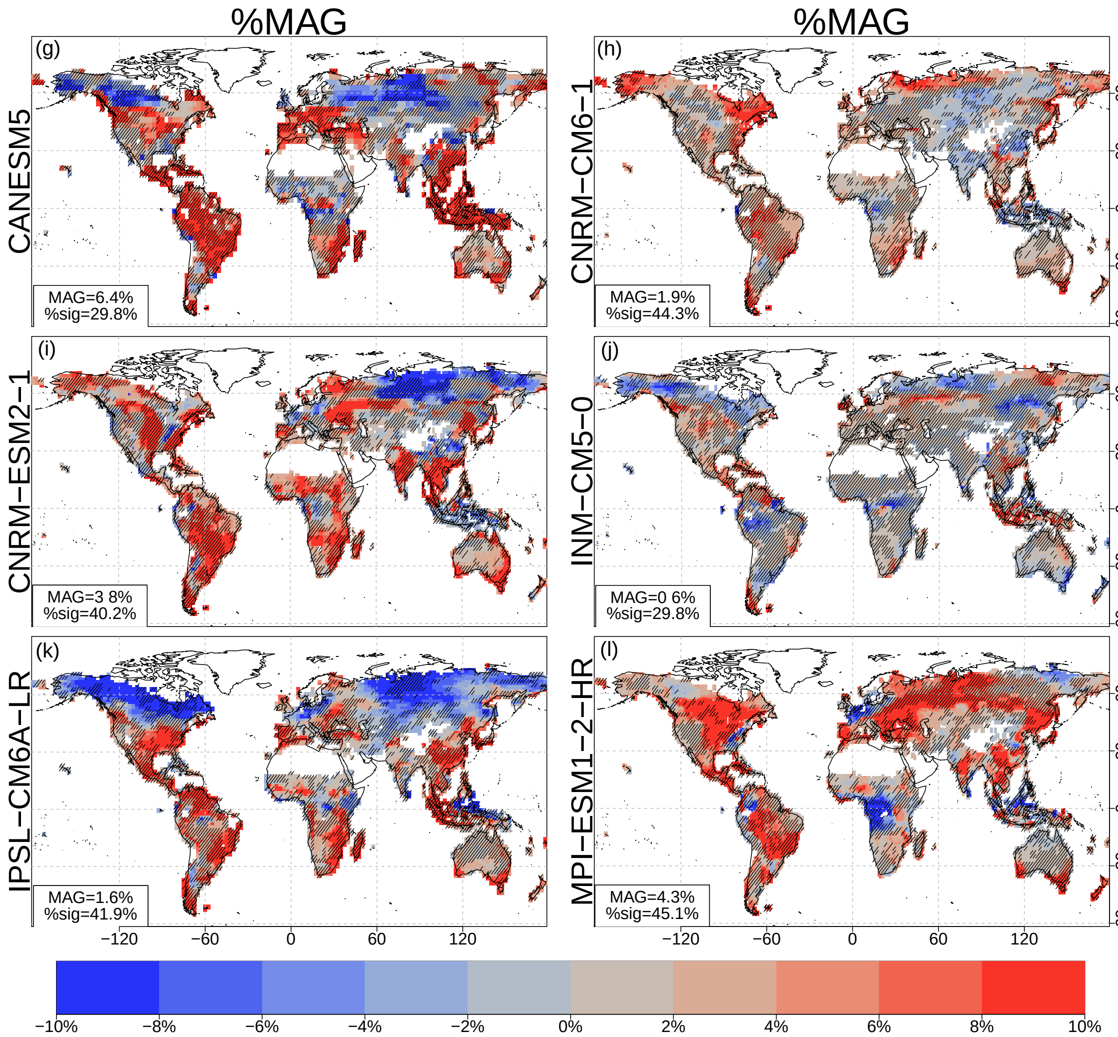

Figure 4.2: Global maps showing probability ratio (PR; left) and percentage change (%MAG; right) in extremes in FWIx7day for six CMIP6 models. The non-stippled areas indicate where the dispersion ratio and shape parameter of the GEV fitted with model-simulated FWIx7day falls within the 95% confidence interval range for the dispersion ratio of the GEV fitted with GEFF-ERA5 data. Numbers in the bottom-left corner represent the globally averaged PR (left) and %MAG (right), and the percentage of the burnable world (%sig) for which PR and %MAG results passed the evaluation.

(MPI-ESM1-2-HR) shows a decreasing (increasing) PR in almost the entirety of northern and central Asia (Figure 4.2e-f). In Australia, such discrepancies also exist: an increase in likelihood can be found in most areas in CanESM5, CNRM-ESM2-1 and IPSL-CM6A-LR (Figure 4.2a, c & e), while other models show a combination of increased and decreased change in likelihood (Figure 4.2b, d & f). Further section of model synthesis results can be found later in the chapter.

4.3.2 Extremes in fire weather duration

4.3.2.1 Model performance in simulating the extremes in fire weather duration

To assess the performance of the six CMIP6 large ensembles in representing the distribution of extremes in fire weather duration, simulated global patterns for individual parameters of a stationary GEV distribution fitted with FWIxCD90 were compared to distribution parameters from GEFF-ERA5 over the period 1979-2014 (Figure 4.3).

In terms of their capacity to realistically simulate the distribution of FWIxCD90, CMIP6 models produce GEV parameters that compare reasonably well with the GEFF-ERA5 reanalysis. Looking at the dispersion ratio, $\frac{\sigma}{\mu}$, correlation results show values between 0.3 and 0.7 across most of the world (Figure 4.3a-g). All models with the exception of IPSL-CM6A-LR reproduce spatial variability relatively well (r>0.5), with regional differences most apparent in northern North America and South America, northern and southern Asia (Figure 4.3a-g). Regions associated with high values of dispersion ratio (as identified in GEFF-ERA5), including central and southern North America, eastern Europe, northwestern Asia and equatorial Asia, are reproduced well by CNRM-CM6-1 (Figure 4.3c), CNRM-ESM2-1 (Figure 4.3d), INM-CM5-0 (Figure 4.3e) and MPI-ESM1-2-HR (Figure 4.3g). CanESM5 overestimates the dispersion ratio almost all over the fire-prone regions (>80%; Figure 4.3h), the only exception is central South America, while the rest five models are all underestimated (Figure 4.3i-m). Substantial overestimations are also found almost all over Australia shown by INM-CM5-0 (Figure 4.3k) and IPSL-CM6A-LR (Figure 4.3l), with underestimations reproduced by CNRM-CM6-1 (Figure 4.3i), CNRM-ESM2-1 (Figure 4.3j) and MPI-ESM1-2-HR (Figure 4.3m) in eastern Australia.

For the shape parameter, ξ, GEFF-ERA5 displays a substantial variation worldwide (Figure 4.3n). Corresponding spatial correlations between the observations and the six models show some level of agreement, with the highest correlation results around 0.3 reproduced by CanESM5 (Figure 4.3o) and MPI-ESM1-2-HR (Figure 4.3t). Five of the six models show more than half of the underestimations (%(-)>50%) over all grid cells, are

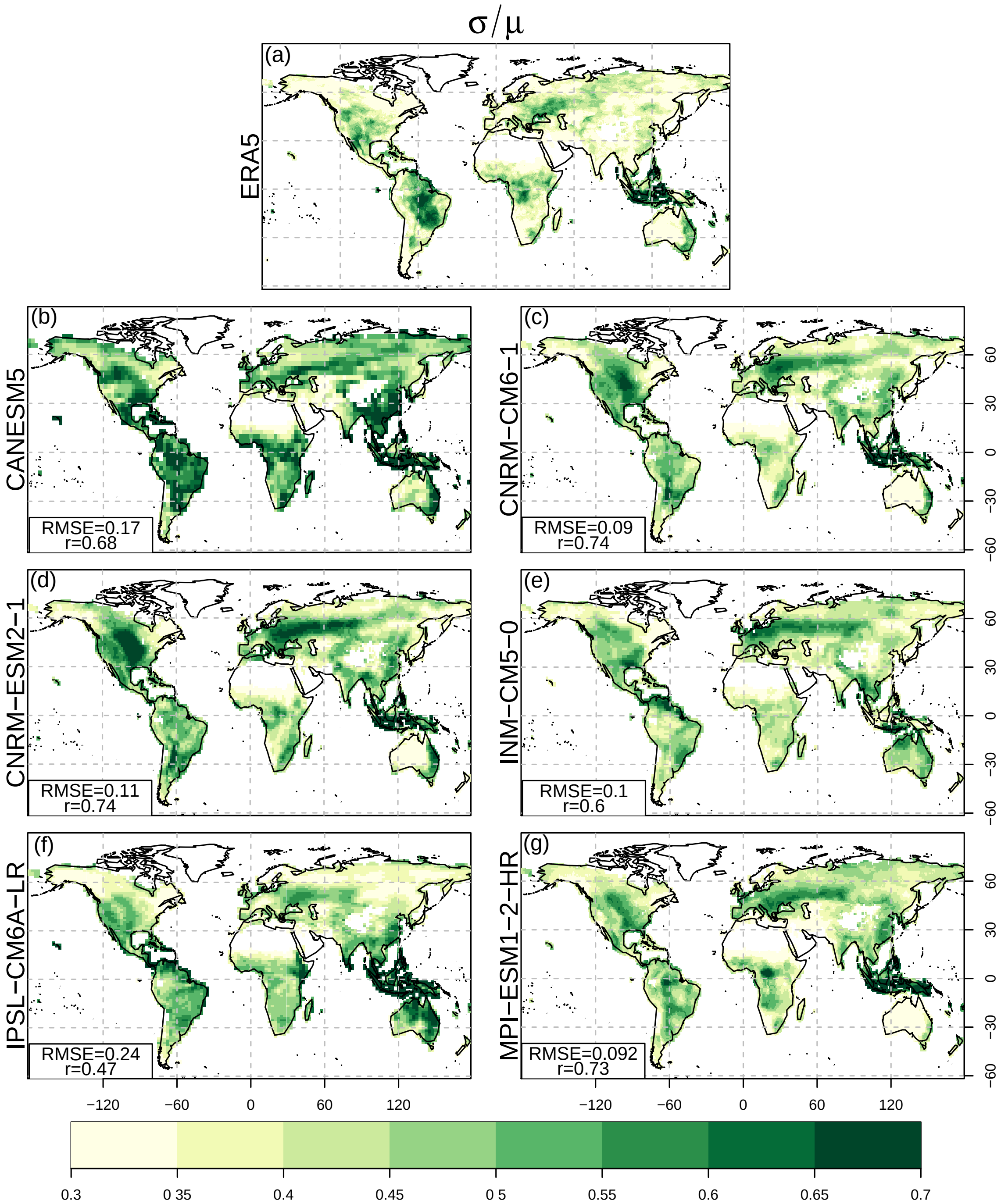
σ/μ
(a)
ERA5
(b)
CANESM5
RMSE=0.17
r=0.68
(c)
CNRM−CM6−1
RMSE=0.09
r=0.74
(d)
CNRM−ESM2−1
RMSE=0.11
r=0.74
(e)
INM−CM5−0
RMSE=0.1
r=0.6
(f)
IPSL−CM6A−LR
RMSE=0.24
r=0.47
(g)
MPI−ESM1−2−HR
RMSE=0.092
r=0.73
−120 −60 0 60 120
60 30 0 −30 −60
0.3 0 35 0.4 0.45 0 5 0.55 0.6 0.65 0.7

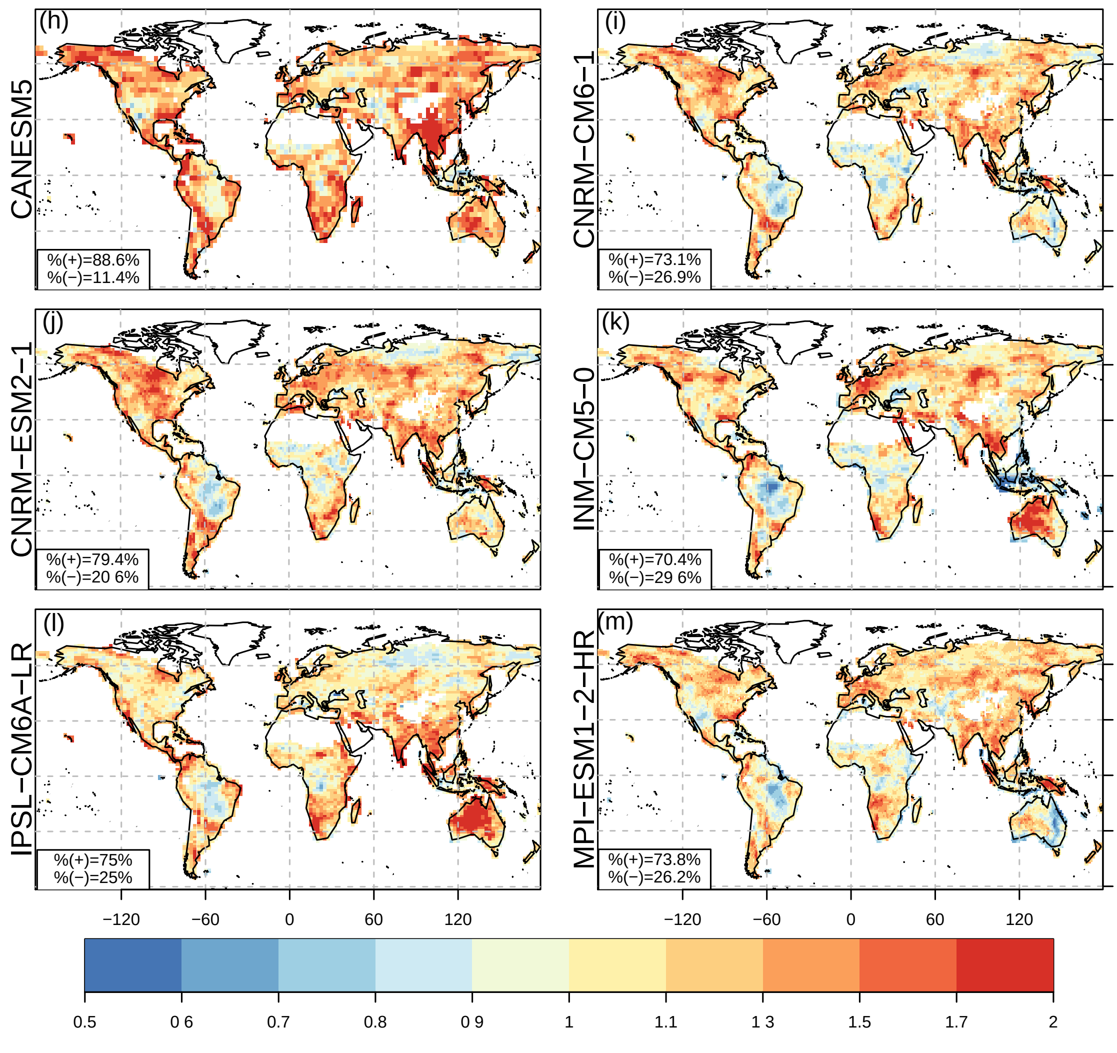

(h)
CANESM5
%(+)=88.6%
%(−)=11.4%
(i)
CNRM−CM6−1
%(+)=73.1%
%(−)=26.9%
(j)
CNRM−ESM2−1
%(+)=79.4%
%(−)=20 6%
(k)
INM−CM5−0
%(+)=70.4%
%(−)=29 6%
(l)
IPSL−CM6A−LR
%(+)=75%
%(−)=25%
(m)
MPI−ESM1−2−HR
%(+)=73.8%
%(−)=26.2%
−120
−60
0
60
120
60
30
0
−30
−60
0.5
0 6
0.7
0.8
0 9
1
1.1
1 3
1.5
1.7
2

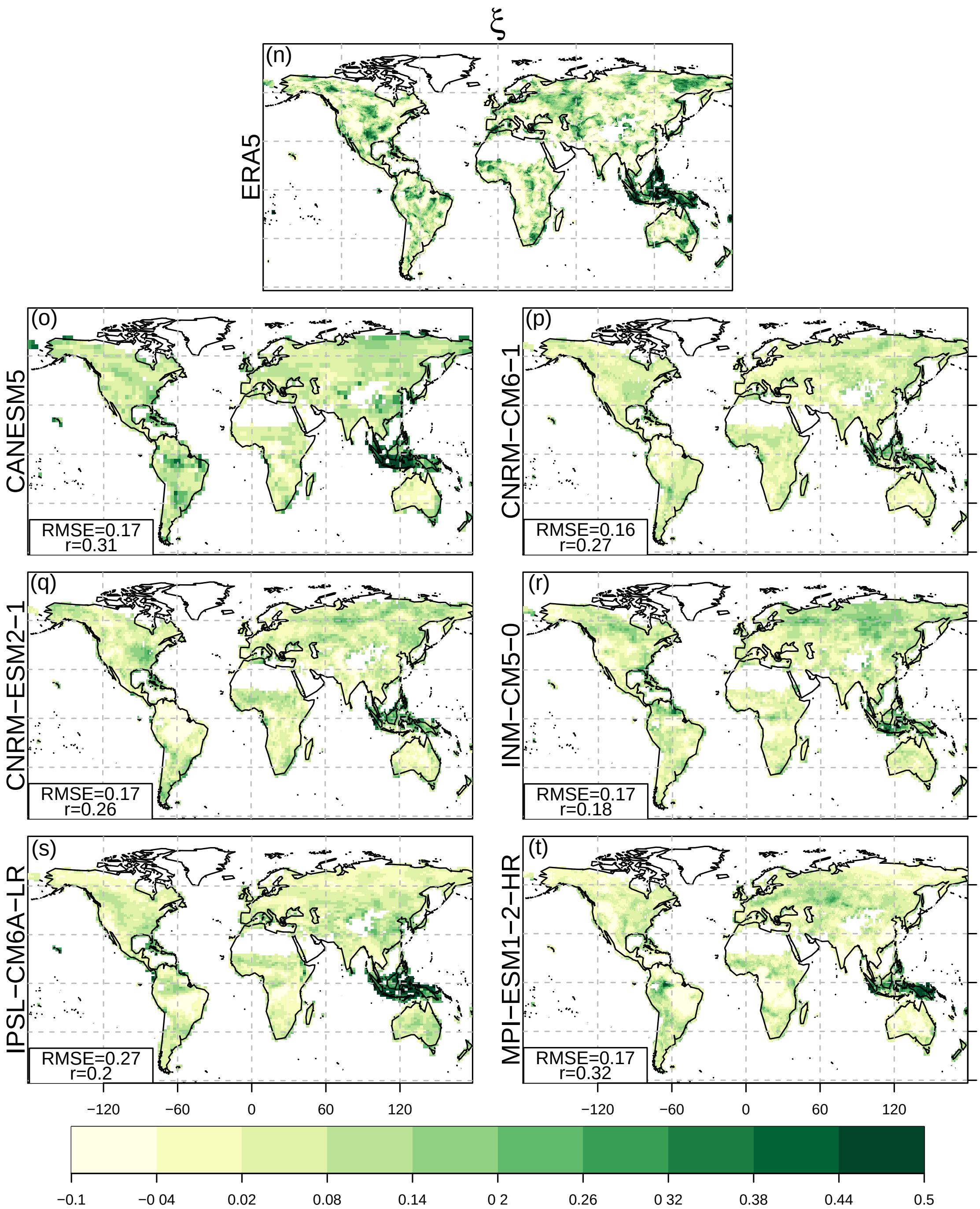
ξ
(n) ERA5
(o) CANESM5 RMSE=0.17 r=0.31
(p) CNRM−CM6−1 RMSE=0.16 r=0.27
(q) CNRM−ESM2−1 RMSE=0.17 r=0.26
(r) INM−CM5−0 RMSE=0.17 r=0.18
(s) IPSL−CM6A−LR RMSE=0.27 r=0.2
(t) MPI−ESM1−2−HR RMSE=0.17 r=0.32
−120 −60 0 60 120
60 30 0 −30 −60
−0.1 −0.04 0.02 0.08 0.14 0.2 0.26 0.32 0.38 0.44 0.5

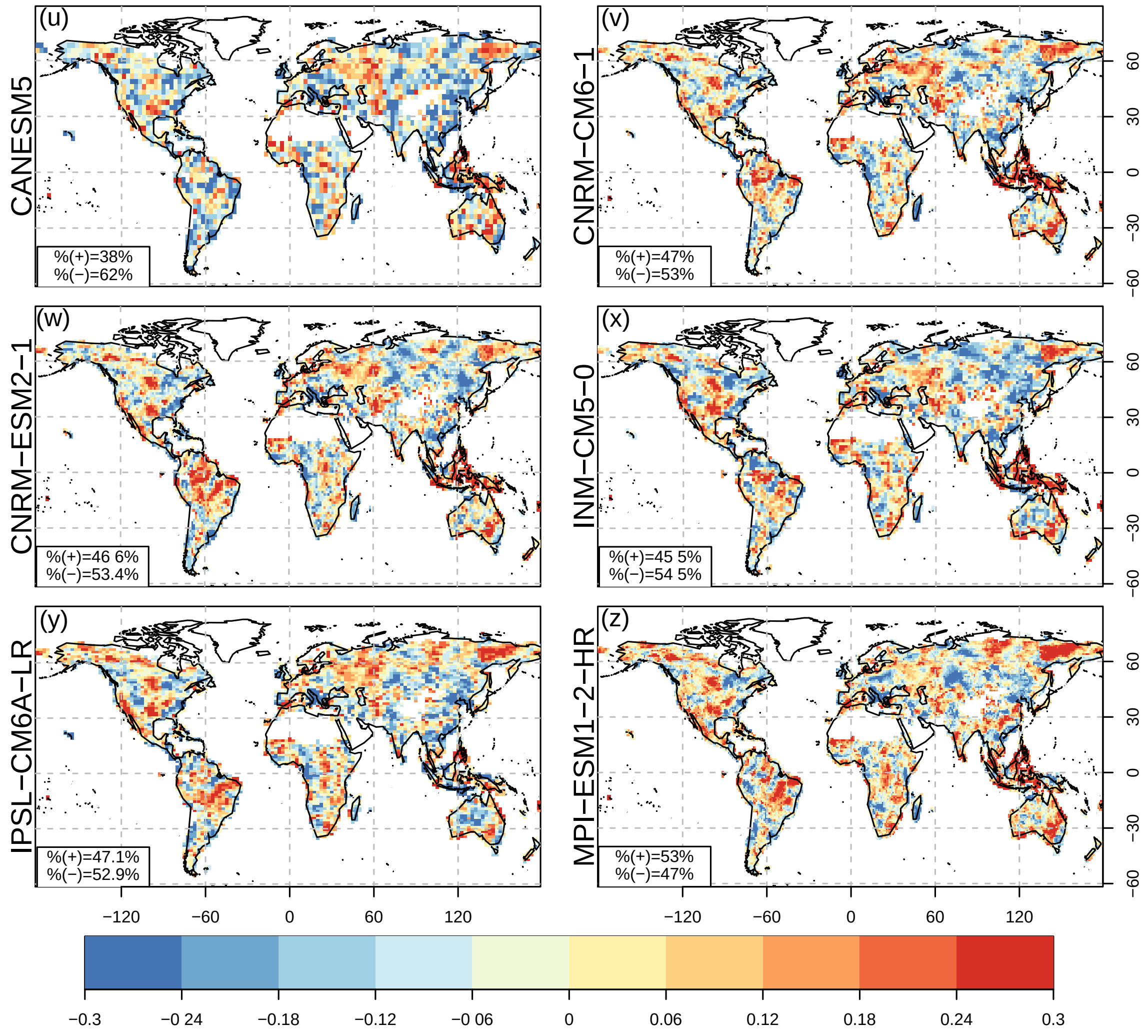

Figure 4.3: Dispersion ratio $\frac{\sigma}{\mu}$ and shape parameter (ξ) derived from the stationary GEV fitted with FWIxCD90 for the period 1979 to 2014 from the GEFF-ERA5 reanalysis (a) and six CMIP6 ensembles (b-g); corresponding differences between the reanalysis and the six CMIP6 models are shown from (h) to (m). Similarly, shape parameter (ξ) from the GEFF-ERA5 reanalysis (n) and six CMIP6 ensembles (o-t) with corresponding differences between the reanalysis and the six CMIP6 models from (u-z). Values in the bottom-left corner of each panel from (b-g) and (o-t) show the root mean square error (RMSE) and spatial correlation coefficient (r) of each six CMIP6 ensembles; while that from (h-m) and (u-z) show the percentage of overestimations (%(+)) and underestimations (%(-)) among all the grid cells.

mainly scattered around southern South Africa, North and Central Asia (Figure 4.3u-z). The only exception is MPI-ESM1-2-HR (Figure 4.3z), with strong overestimation in eastern South Africa and northeast Asia.

Again, concerning the dispersion and shape parameters in the distribution, MPI-ESM1-2-HR is the best-performing of the six climate models when compared to GEFF-ERA5, while IPSL-CM6A-LR is the most biased of the six.

4.3.2.2 Attribution of extremes in fire weather duration

Figure 4.4(a)-(l) shows a global map of the probability ratio (PR) and change in FWIxCD90 (durDays) at each grid point across the six CMIP6 models. Overall, for the period 2010-2014, the probability of more prolonged extreme fire weather conditions has markedly risen by a factor of two on a global scale compared to the 1880-1884 period (Figure 4.4a-f). This equates to an increase of at least 10 days in the maximum duration of extreme fire weather events in response to externally forced temperature rise (Figure 4.4g-l). In particular, the most pronounced increases in the likelihood of more prolonged extreme fire weather occur in southern North America, almost all over South America, southern Africa, Central and Southeast Asia and parts of Australia (Figure 4.4a-f). However, we note that northern North America (CanESM5 and IPSL-CM6A-LR; Figure 4.4a & e) and equatorial Africa (CNRM-CM6-1, CNRM-ESM2-1 and MPI-ESM1-2-HR; Figure 4.4b,c,f) are associated with a substantial (up to fourfold) decrease in the likelihood of FWIxCD90. This indicates that in these models the maximum duration of extreme fire weather tends to decrease in response to externally forced warming temperature.

The fact that different models produce different distributions of extremes highlights the sensitivity of studies on fire weather extremes to the models used in their analysis. In many regions, this sensitivity is especially evident. For central North America, western and southern Europe, the maximum duration of extreme fire weather simulated by CanESM5, INM-CM5-0, IPSL-CM6A-LR and MPI-ESM1-2-HR shows an upward trend in PR (Figure 4.4a, d, e & f), while a downward trend in PR is found using CNRM-CM6-1 and CNRM-ESM2-1 (Figure 4.4b & c). This regional divergence between climate models is more common in Asia. For example, in northern Asia, where wildfires occur more prevalently, CNRM-CM6-1, IPSL-CM6A-LR and MPI-ESM1-2-HR show a significant increase in the likelihood of maximum duration of extreme fire weather (Figure 4.4b, e & f), but the other three models show the opposite change in likelihood (Figure 4.4a, c & d). These patterns and deviations in regional distribution also appear in Australia, with most regions showing potential increase in the likelihood of more prolonged extreme fire weather conditions (Figure

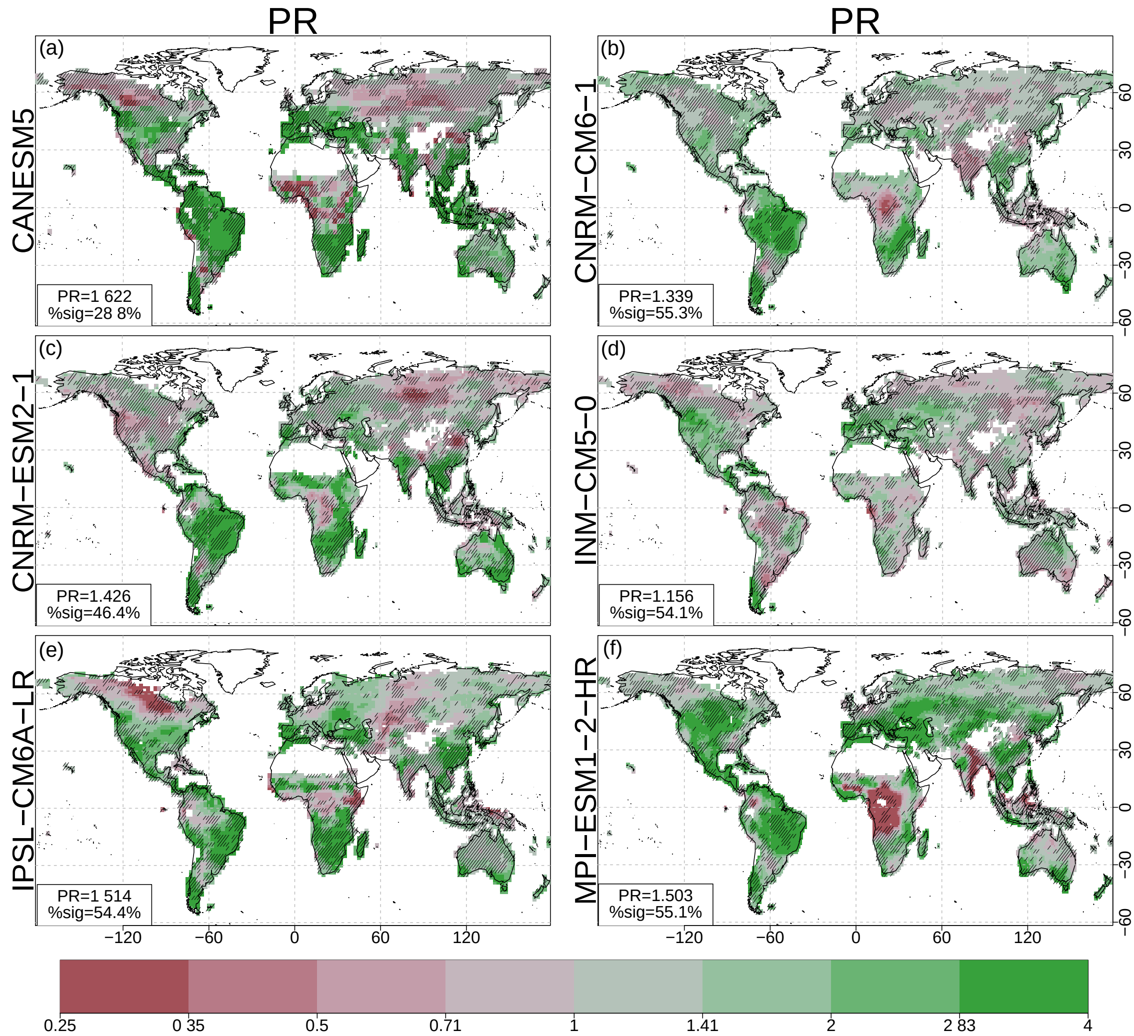

PR
PR
(a)
CANESM5
PR=1 622
%sig=28 8%
(b)
CNRM−CM6−1
PR=1.339
%sig=55.3%
(c)
CNRM−ESM2−1
PR=1.426
%sig=46.4%
(d)
INM−CM5−0
PR=1.156
%sig=54.1%
(e)
IPSL−CM6A−LR
PR=1 514
%sig=54.4%
(f)
MPI−ESM1−2−HR
PR=1.503
%sig=55.1%
−120 −60 0 60 120
60 30 0 −30 −60
0.25 0 35 0.5 0.71 1 1.41 2 2 83 4

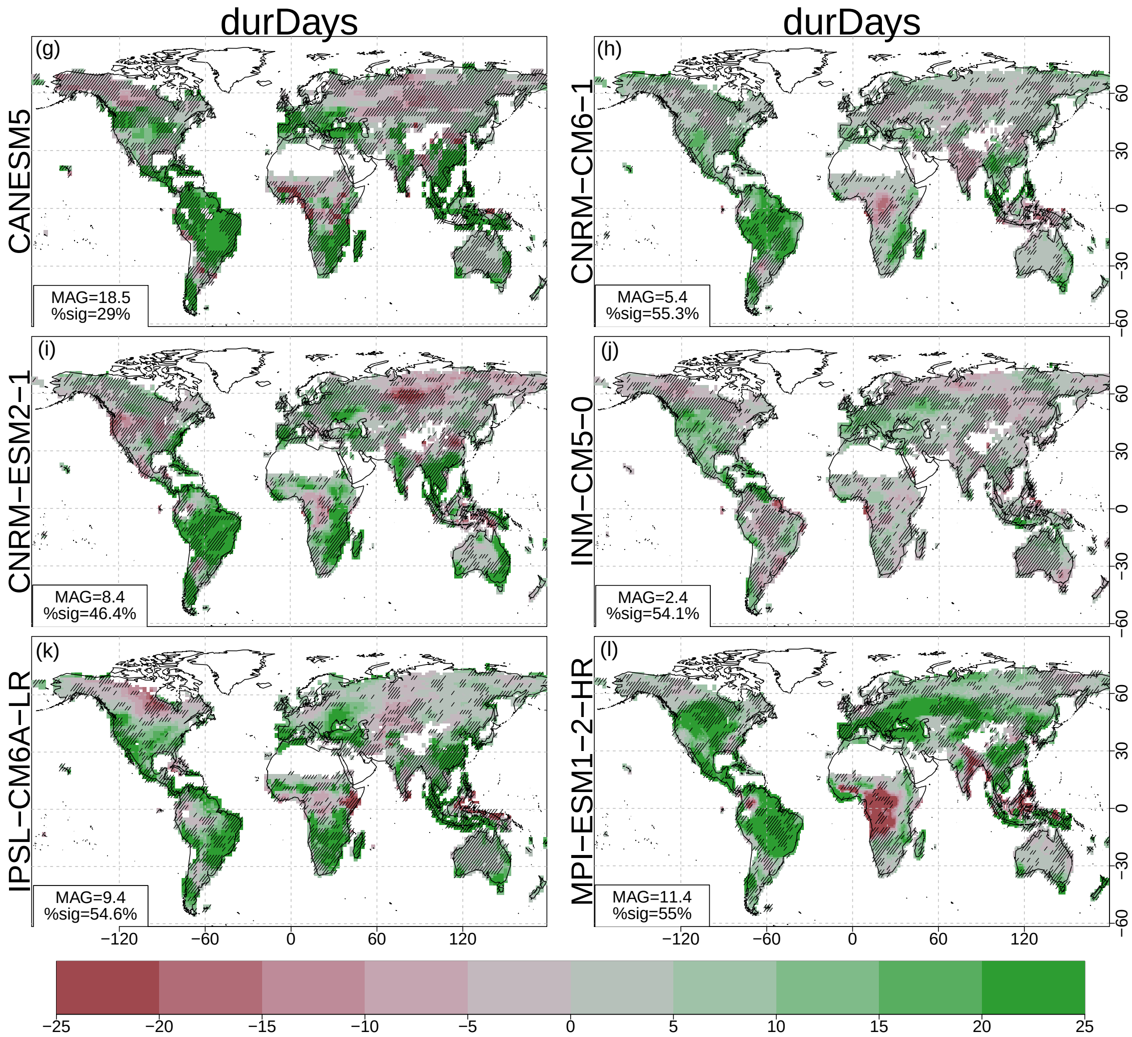

Figure 4.4: Global maps showing probability ratio (PR; left) and the absolute changes (durDays; right) in FWIxCD90 for the six CMIP6 models. The non-stippled areas indicate where the dispersion ratio and shape parameter of the GEV fitted with model-simulated FWIx7day falls within the 95% confidence interval range for the dispersion ratio of the GEV fitted with GEFF-ERA5 data. Numbers in the bottom-left corner represent the globally averaged PR (left) and durDays (right), and the percentage of the burnable world (%sig) for which PR and %MAG results passed the evaluation.

4.4a, b, c & e). Meanwhile, some models, such as INM-CM5-0 or MPI-ESM1-2-HR (Figure 4.4d, f), suggest a decreasing probability of prolonged extreme fire weather conditions in the southern or northern regions of Australia.

4.3.3 Attribution synthesis across multiple models

Combining results from different models often relies on simple multi-model averaging, without thorough consideration of the extent of inter-model spread or individual model performance. In this subsection, we firstly assess consensus among the six model ensembles, and secondly, explore the value of a model evaluation and selection step in synthesising multi-model attribution results.

Figure 4.5 summarises to what extent the six CMIP6 models agree on the tendency of the change in likelihood in extremes of fire weather intensity (Figure 4.5a) and duration (Figure 4.5b). The result suggests that, as a result of the externally forced warming temperature, 54.3% of the grid cells show an increased likelihood of both extreme fire weather intensity and duration when the number of model agreements is larger than three. All models simulate an increased likelihood of prolonged and high-intensity events in large parts of the world's fire-prone regions, including areas that have witnessed severe fire episodes in recent years (most notably southern Europe). An increase in likelihood in at least five of the six models is apparent across much of the Americas, southern Africa, Australia and eastern Asia. Models agree on an increased likelihood of the length of extreme fire weather episodes, but there is less consensus on the change in intensity. Regions of lower model agreement include large parts of the boreal forests and Canada and Eurasia, particularly with respect to intensity, in addition to central Africa and southeast Asia.

As discussed by Liu et al. (2022a), the use of a common method and event definition allows for the attribution of changes at various locations and from multiple data sources to be combined. However, combining attribution statistics from different climate models may prove troublesome if there are clear differences in model performance. Figure 4.5 clearly demonstrates a regional dependence in model agreement. It is important to understand the extent to which such discrepancies are due to model performance for the attribution analysis to be as robust as possible. Here, we apply a model evaluation and selection step to identify models that can realistically reproduce the dispersion and the shape of the distribution of fire weather extremes. All models that meet the evaluation criteria can therefore be combined to produce global attribution results that, in principle, are more robust and reliable than

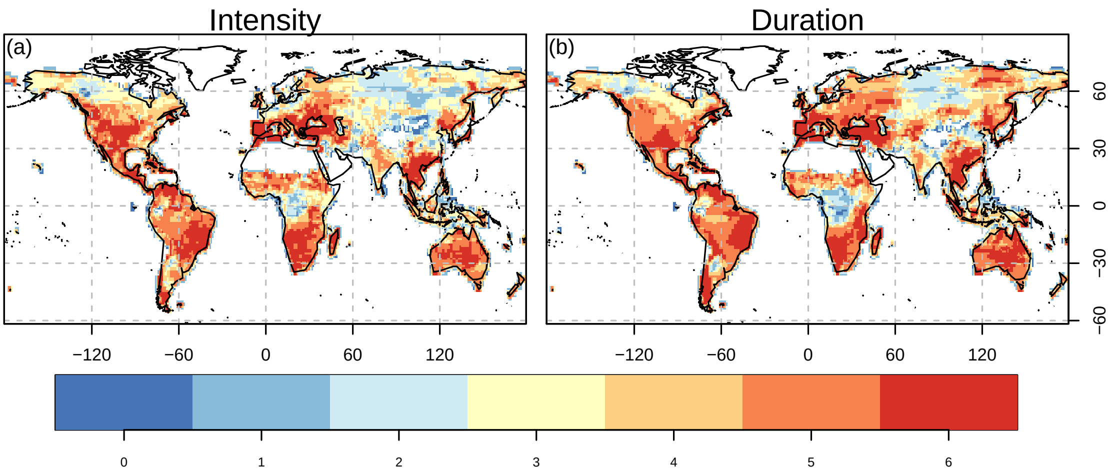

Figure 4.5: Maps showing the number of climate models that present an increased likelihood of extremes in (a) fire weather intensity and (b) fire weather duration across the six CMIP6 models. Results are presented on the resolution of MPI-ESM1-2-HR. Areas approaching red (blue) indicate that an increasing number of models show a positive (negative) change.

those that would be produced by combining the results of all models irrespective of their performance.

Figure 4.6 illustrates multi-model global probability ratio maps constructed, firstly, from a conventional averaging of the probability ratios simulated by all six CMIP6 models (Figure 4.6a-b) and, secondly, selective averaging only those models that pass an evaluation and selection step (Figure 4.6c-d) a model evaluation and selection step. The evaluation criterion is defined by a GEV dispersion ratio that falls within the range of the 95% confidence intervals for the dispersion ratio of the GEV fitted by GEFF-ERA5 data.

The global PR map in Figure 4.6a-b, based on the first, conventional synthesis, shows relatively small changes in the probability of extremes in both FWIx7day and FWIxCD90. Only a few regions such as northern South America, southern Africa and southern Asia, show an approximately two-fold increase in the probability of the fire weather extremes in both intensity and duration of days. There are no particularly strong or prominent trends, especially in the areas with decreasing probabilities, which is only present in a small part of the equatorial region of Africa. However, the conventional synthesis may underestimate the range of probabilities to some extent compared to the selective synthesis, which is shown in Figure 4.6c-d. In contrast to the conventional synthesis, the selective approach considers the individual performance of each model and combines the results of those that perform well. The outcomes show an even more remarkable degree of variability, with southern North America, south-eastern Europe and southwestern and south-eastern Australia exhibiting an

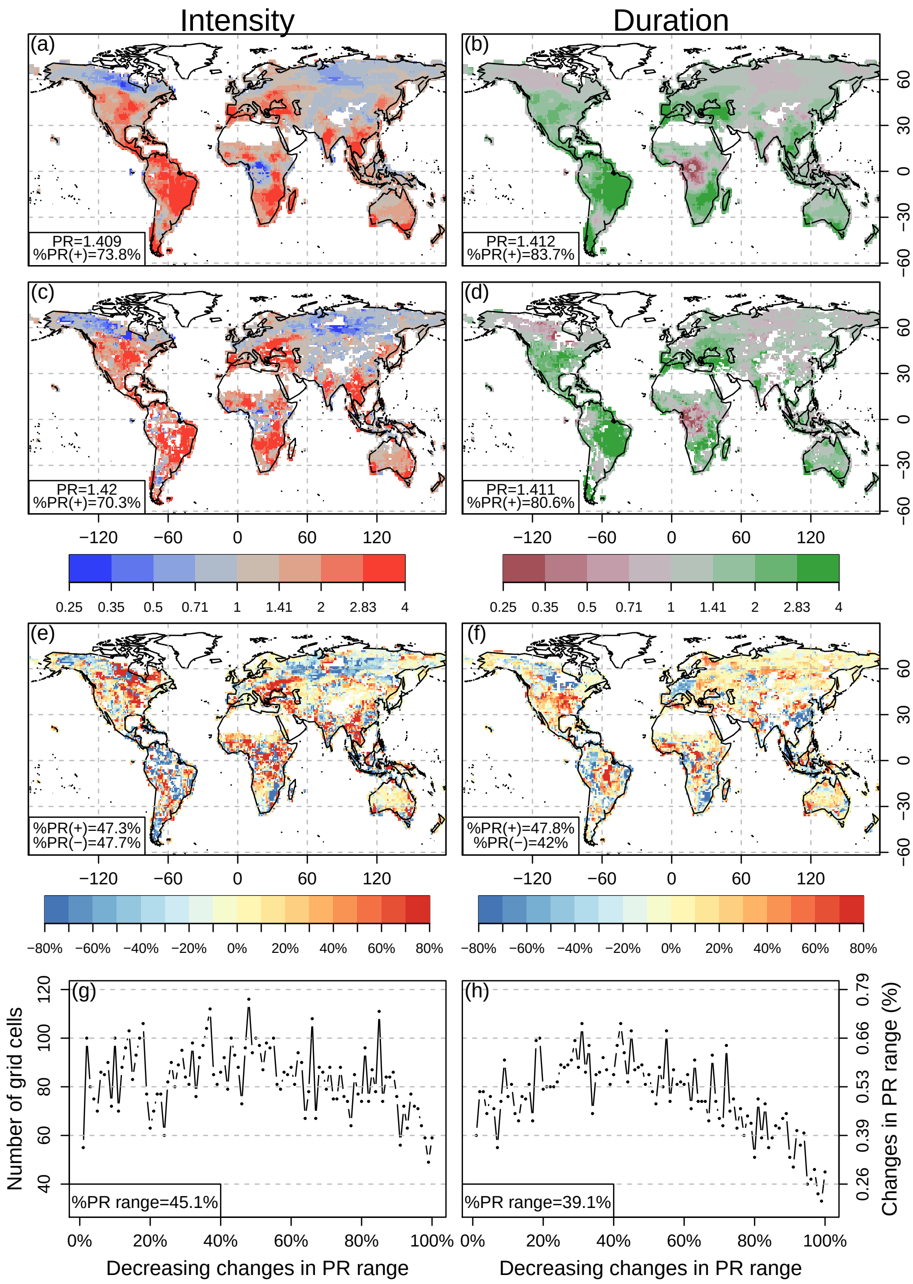

Figure 4.6: (a-d) Composite plots showing the average PR for trends across (a)-(b) all the six CMIP6 models in FWIx7day (a) and FWIxCD90 (b); (c)-(d) CMIP6 models that sufficiently well-reproduce the dispersion of the distribution and the parameter of the shape of extremes in FWIx7day (c) and FWIxCD90 (d). Additional white areas indicate the regions where no climate model met the evaluation criteria. Values in the bottom-left corner of each panel from (a-d) show the globally averaged PR and the percentage of the burnable world that shows an increase in PR (%PR(+)). (e) Changes in the average PR across all the six CMIP6 models (a) and the selected models (c) in FWIx7day. (f) as (e) but across all the six CMIP6 models (c) and the selected models (d) in FWIxCD90. Numbers in the bottom-left corner represent the percentage of the burnable world that shows an increase (%PR(+)) or decrease (%PR(-)) in PR. (g-h) Line charts for the number of grid cells (left axis) and the percentage (right axis) of uncertainty changes in PR range between the result across all the six CMIP6 models and evaluated results in FWIx7day (g) and FWIxCD90 (h). Values in the bottom-left corner of each panel show the percentage of the decreasing changes in the PR range across the burnable world.

apparent rise in PR of approximately four times to the fire weather extremes in intensity and duration of days (Figure 4.6c-d), in addition to northern South America, southern Africa and southern Asia regions mentioned in Figure 4.6a-b. Correspondingly, twofold decreases in likelihood of the fire weather extremes in both intensity and duration of days are not only encountered in the equatorial regions of Africa previously mentioned (Figure 4.6a-b), but are also apparent in northern North America and most parts of northern and central Asia. It is notable that changes in PR for both FWIx7day and FWIxCD90 tend to be spatially consistent, *i.e.*, the higher the probability of an increase in fire weather intensity, the longer the duration of the fire weather and, conversely, the lower the intensity the shorter the duration.

For each grid cell, Figure 4.6e-f displays the changes in PR of extreme fire weather intensity and duration of days between these two approaches. Results after the model evaluation and selection step manifest the variations of under- and over-estimations all around the world compared to the conventional synthesis, particularly the underestimations in eastern Europe and north-western Asia, overestimations in northern Asia in fire weather intensity (Figure 4.6e). Regarding the duration of extreme fire weather, we find underestimations in southern North America and the overestimations in northern North America in fire weather duration (Figure 4.6f).

Concerning each grid cell, the percentage of uncertainty changes in the range of PR (0-100%) is shown in Figure 4.6g-h. The range is provided by the lowest and highest PR among evaluated CMIP6 models, while the change of the range is according to the two synthesis approaches applied in Figure 4.6a-d. Overall, the global changes for both fire weather intensity (Figure 4.6g) and fire weather duration (Figure 4.6h) are 45.1% and 39.1%, as a decrease in the range of PR, separately. There is a positive trend in the number of grid cells reaching the averaged values (45.1% for fire weather intensity and 39.1% for fire weather duration) and a negative trend after that. This statistical analysis manifests the variation in PR ranges between the results of all the six climate model large ensembles. Subsequently, results of the model ensembles that passed the evaluation, clearly reveal the sensitivity of the application of large climate model ensembles and the importance of model evaluation and a selection step.

4.4 Discussion and conclusions

The occurrence and subsequent impact of severe wildfires in recent years has heightened scientific, public and media curiosity about how such events are linked to a changing climate. Attribution analysis of extreme wildfires requires a distinction to be made between the fire itself and the meteorological conditions that coincided with it. Studies seeking to attribute episodes of extreme fire weather are historically rare in comparison to flood- and drought-related studies, for instance. However, as the number of wildfire attribution studies begins to grow, there is a clear need to continue to build an understanding of the sensitivities and sources of uncertainty associated with the findings of such studies, particularly with respect to the latest generation of climate models.

Here, an established statistical methodology was used to conduct the first global probabilistic attribution of extreme fire weather intensity and duration based on six large ensembles from CMIP6. The approach taken and the findings drawn are important for several reasons. Firstly, established statistical methods are applied to six large CMIP6 model ensembles (*i.e.*, at least 10 members) to probabilistically attribute extreme fire weather in fire-prone areas throughout the world, thereby quantifying the extent to which climate change alters the likelihood and magnitude of extreme fire weather intensity and duration. The additional steps of model evaluation and selection add a layer of robustness to the findings that have often been absent in previous attribution analyses. Secondly, this work represents the first time that the scaled GEV approach has been used in the analysis of extremes in fire weather duration, in addition to fire weather intensity, simulated by multiple climate models. Thirdly, the results clarify the uncertainties and sensitivities associated with the selection of representative climate models for fire weather, particularly concerning the attribution of extreme events.

Using six large ensembles from CMIP6, attribution analysis of extremes in fire weather intensity was first presented to provide an understanding of the performance of the fire weather indicator FWI in fire-prone regions of the world, the risk-related assessment of fire weather hazards and trends in their probabilistic variability. In most fire-prone regions of the world, the majority of models show an increase in the likelihood of extreme fire weather occurrence since the pre-industrial era as a response to global warming, and this trend is broadly consistent with the current understanding of global fire weather activity and its relationship to climate change (Jain et al., 2022; Liu et al., 2022a). However, for some regions, the discrepancies between models are pronounced, demonstrating the non-negligible and large uncertainties associated with a single model, and the importance of integrating results from multiple climate models. It is also worth noting that in some regions, especially in equatorial rainforest regions, higher relative humidity due to warming temperatures may prevent extreme fire weather occurrence (Liu et al., 2022b).

Applying the same six large ensembles, we then analysed probabilistic changes in extremes in fire weather duration. We found an increasing trend in probabilities of fire weather extremes in duration of days across most of the globe, which appear consistent with the increasing probability of high-intensity extreme fire weather conditions. This is accompanied by a decreasing trend in probabilities of prolonged fire weather extremes for a small number of specific regions, such as northern North America and equatorial Africa. Notably, it was found that the upward trend in the probability of extreme fire weather intensity tends to be paired with an increase in its duration, *i.e.*, the occurrence of more intense fire weather also predicts a greater likelihood of a prolonged duration of the weather phenomenon.

Finally, a synthesis was generated from the results of the set of six climate models. Following a model evaluation and selection step, an averaging of results across multiple models was limited to those models that met performance criteria. A more reliable and specific global probability ratio plot reflects the changing likelihood of the fire weather extremes in intensity and duration of days. The results confirm an increasing trend in the probability and duration of extreme fire events corresponding to global warming as a feature of climate change, particularly in southern North America, south-eastern Europe and south-western and south-eastern Australia, where the probability of this increase is up to four times more likely compared to the pre-industrial era.

The results of this study also highlight the sensitivity of the probabilistic attribution of fire weather extremes to the choice of climate models. Single models suffer from unavoidable biases, while a simple combination of multiple models can lead to a significant underestimation of results under some circumstances. Therefore, the following recommendations are made for the attribution of future extreme fire weather events: (i) the use of ensembles of multiple models; (ii) comparison of results between models; (iii) a robust assessment of model capacity to represent extreme fire weather is required.

Chapter 5

Application of framework to case studies

Abstract - In recent years, the occurrence of a series of devastating wildfires events around the world has raised considerable public concern about how climate change is altering meteorological conditions conducive to such events. The relative scarcity of wildfire attribution studies, coupled with the limited observational record, has added to the difficulty of developing reliable collective conclusions for future forest management strategies. The preceding chapters have discussed the uncertainties and sensitivities associated with the choice of meteorological indicator to represent fire weather (cf. Chapter 3) and the validation of climate model ensemble in the context of extreme event attribution (cf. Chapter 4), but the value of linking the attribution of recent record-breaking and high-impact wildfire events with future risk assessment has not yet been fully explored.

This chapter consists of three independent case study analyses of recent high-impact wildfire episodes, namely those that occurred in Siberia in July and August 2020 (cf. section 5.1), in Cape Town, South Africa in April 2021 (cf. section 5.2) and across the Euro-Mediterranean region in June to August 2022 (cf. section 5.3). The scale, duration and impacts differ between each wildfire event, but all occur in regions that have, to date, been underrepresented in the event attribution literature (Fig. 1.7). Each case study follows the empirical-statistical framework and its application to one or more climate model ensembles, thereby drawing on the findings of Chapters 3 and 4. In addition to constituting robust attribution analyses of recent high-impact wildfire episodes, the case studies demonstrate the applicability of the framework to different event types with varying methodological emphases. The emphasis of each case study with respect to the framework is summarised in Figure 5.1.

The key differences in methodological emphasis stem from the spatiotemporal scale of each event, spanning the single-day wildfire with very localised impacts experienced in

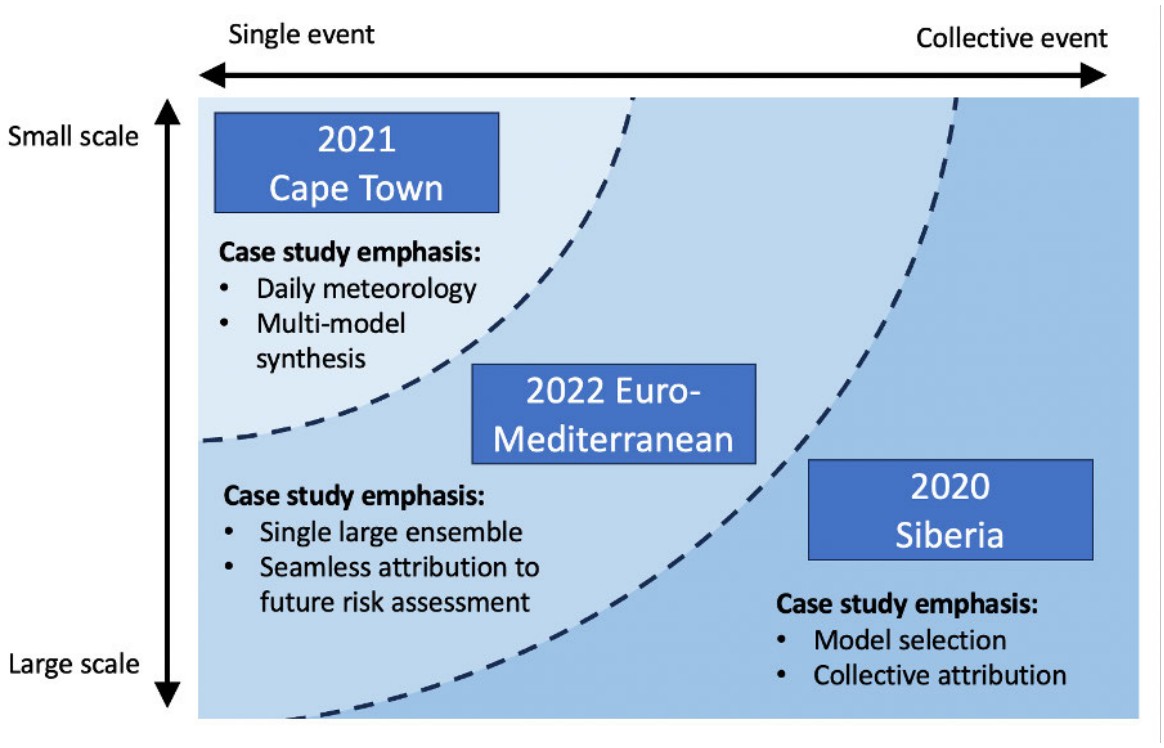

Figure 5.1: Schematic to show the nature and analytical emphasis of the three case studies.

Cape Town in April 2021 (section 5.2) to the regional-to-continental scale events that spread across Siberia (section 5.1) and the Euro-Mediterranean region (section 5.3) in 2020 and 2022 respectively. In the case of the latter event class, the use of a common spatiotemporal definition allows for multiple episodes of extreme fire weather to be attributed collectively. Climate model output is utilised in each case study, with the most appropriate model(s) selected on the basis of performance and/or ensemble size. Whereas the primary focus of each case study is to understand how the nature of a particular event type has changed in response to climate change, the analysis of the Euro-Mediterranean wildfires aims to seamlessly extend the framework toward future risk assessment by quantifying changes associated with projected global warming levels (section 5.3).

5.1 Case study 1: 2020 Siberia wildfires

Were Meteorological Conditions Related to the 2020 Siberia Wildfires Made More Likely by Anthropogenic Climate Change?

5.1.1 Introduction

The summer of 2020 saw Siberia hit by widespread wildfires for a second consecutive year. By September alone, 14 million hectares had been burnt by more than 18,000 individual fires (Witze, 2020). The 2020 fires were responsible for the emission of approximately 350 megatonnes of carbon, more than four times the annual average observed across Siberia during the preceding two decades (Ponomarev et al., 2021). While fire activity is common in Siberia, accounting for between 8.5% and 25% of the annual burned area worldwide (Kharuk et al., 2021), it was the dominance of fires at northerly latitudes that made the 2020 event truly exceptional. Fires beyond 65°N typically account for <10% of Siberia's annual total burned area – their contribution during 2020 exceeded 25%, the largest observed since 2001 (Conard and Ponomarev, 2020), promptly raising concerns about the growing influence of wildfires on permafrost thaw (Kim et al., 2020) and greenhouse gas emissions (Ponomarev et al., 2021).

During 2020, spring and summer temperatures were abnormally high across Siberia. At Verkhoyansk in Yakutia (67°33'N 133°23'E), a new record of 38°C was set for the highest daily maximum temperature ever recorded north of the Arctic Circle (WMO, 2020). A comprehensive study conducted by the World Weather Attribution consortium concluded that such intense temperature, spanning such a large area, would have been almost impossible during the first half of 2020 without the influence of human-induced climate change (Ciavarella et al., 2021).

While this period of extreme heat was undoubtedly an important factor driving wildfire activity, a specific assessment of the contribution of human-induced climate change should account for other meteorological factors that collectively present fire-conducive conditions. Such an assessment is made challenging by Siberia's vast geographical extent and varied climatology. Here, we isolate Siberia's most intense fire episodes during 2020 and quantify the influence of global warming on the meteorological conditions associated with each. The collective analysis of a series of individual events that formed part of a larger phenomenon constitutes a unique aspect of this study. In our analysis of individual fire hotspots, we maintain a consistent spatiotemporal event definition, allowing for comparisons of results at different hotspots.

5.1.2 Data and Methods

Throughout the study, fire-conducive meteorological conditions are defined by the Canadian Fire Weather Index (FWI; Van Wagner, 1987), a widely-used metric based on relative humidity, surface wind speed, precipitation, and temperature to quantify forest fire danger. It forms the basis of global fire weather datasets (Field et al., 2015; Vitolo et al., 2020) and the Global Wildfire Information System. Our study region is defined by the West, East, and Northeast Siberian taiga ecoregions (Olson et al., 2001), which collectively constitute an area of 6,700,000 km^2 and represent some of the most extensive areas of natural forests in the world. The location and intensity (defined by fire radiative power) of fire events during the April-September 2020 fire season were determined using satellite-derived data from the Visible Infrared Imaging Radiometer Suite (Schroeder et al., 2014), made available via the Fire Information for Resource Management System (FIRMS). Historical FWI data for the period 1979-2020 are taken from the global fire danger reanalysis (0.25° resolution; Vitolo et al., 2020) produced by the Copernicus Emergency Management Service for the European Forest Fire Information System. Simulations of historical FWI data for the period 1880-2014 ($\sim$0.7° resolution) are taken from the CNRM-CM6-1 general circulation model (Voldoire et al., 2019) developed for the sixth phase of the Coupled Model Intercomparison Project (CMIP6; Eyring et al., 2016). This model is chosen due to (a) the availability of a relatively large (30-member) ensemble, and (b) its capacity to realistically represent extreme FWI statistics across Siberia (Gallo Granizo et al., 2021).

We conduct independent attribution analysis at a series of 13 'hotspots' associated with the most intense 2020 fires (see section 5.1.5 for details). The '2020-type event' is defined at each hotspot as the April-September maximum value of 7-day mean FWI (hereafter FWIx7day) occurring within the hotspot's spatial domain. A statistical method based on a time-dependent Generalised Extreme Value (GEV) distribution, frequently applied to both observational and climate model data in previous work (*e.g.*, Schaller et al., 2014; Eden et al., 2016; van der Wiel et al., 2017; Eden et al., 2018; Otto et al., 2018b; Krikken et al., 2021), is used to estimate the change in probability of a 2020-type event as a result of global warming. For each hotspot, a pool of spatial maxima in FWIx7day from all 135 years and all 30 ensemble members are fitted to a GEV distribution in which the location μ and scale σ parameters are assumed to scale linearly with 4-year smoothed global mean surface temperature (GMST; GISTEMP Team, 2022; Lenssen et al., 2019. Both the shape ξ parameter and the $\frac{\sigma}{\mu}$ ratio remain constant (Philip et al., 2020).

At each hotspot, we evaluate the return time, and hence the probability, of a 2020-type event occurring in a 'past' climate of 1880 (p0) and a 'present' climate of 2020 (p1). Changes in the likelihood of 2020-type events are quantified using the probability ratio (PR) p0/p1. We also calculate the percentage change in FWI magnitude (%MAG) between a 2020-type event and an event of comparable likelihood occurring in 1880. Following the evaluation of the model's representation of extreme FWI statistics, a simple bias correction is used to account for systematic discrepancies between the reanalysis and CNRM-CM6-1 (see section 5.1.5 for details). Confidence intervals (CIs) for each GEV fit, and subsequently for both PR and %MAG, are estimated with a 1,000-sample non-parametric bootstrap.

5.1.3 Results

Fires were widespread throughout the study region during April-September 2020 (Figure 5.2a). The most intense fires occurred in several clusters and generally north of 60°N. The highest-intensity fires were detected throughout the fire season, with a large proportion occurring between mid-June and August (Figure 5.2b). The individual fire detections at the centre of each hotspot all reside in the upper tail of the fires' empirical cumulative distribution function (Figure 5.2c). The 2020 anomalies in FWIx7day were largest in central and northern Siberia, especially to the west of the Verkhoyansk mountains and across the Kolyma lowland (Figure 5.2d) where a large portion of 2020 FWIx7day values are among the highest 5% of annual maxima observed since 1979 (Figure 5.2e). At eight of the 13 hotspots, both the probability (PR > 1; Figure 5.3a-b) and magnitude (%MAG > 0; Figure 5.3c) of a 2020-type event increased between 1880 and 2020. The likelihood has increased by a factor of 1.1-1.8 corresponding to a change in magnitude of 2-6%; this is significant at the 95% confidence level at five hotspots (Figure 5.3e-i). Small decreases in both probability and magnitude are found at the remaining five hotspots (Figure 5.3b-c), of which only hotspot A at the western fringes of the fire-affected area is statistically significant (PR = 0.81; CI range 0.71-0.93; Figure 5.3d).

Positive changes in likelihood are found at the four hotspots (C, H, K and M) residing north of 65°N, where the exceptionality of 2020 fire weather is evidenced by large anomalies (>10 FWI units) amounting to some of the highest of FWIx7day values observed since 1979 (Figure 5.1d-e). At hotspot C, the likelihood of a 2020-type event is found to have increased by more than 30% (PR = 1.33; CI range of 1.10-1.55; Figure 5.3e). A change of almost 20% is found at hotspot H but is not significant at the 95% level. Further east, significant increases in likelihood are found at hotspots K, M and, further south, L (Figure 5.3g-i). At hotspot K, which represents an area of the Kolyma lowland that witnessed several extreme fires (FRP > 700MW; Figure 5.2a), a 2020-type event has become almost 80% more likely since 1880 (PR = 1.78; CI range of 1.22-2.58; Figure 5.3g). Significant, though smaller, increases are found at hotspots L (PR = 1.57; CI range of 1.29-1.1; Figure 5.3h) and M (PR = 1.15; CI range of 1.02-1.28; Figure 5.3i). FWI extremes across the eastern region are likely to be

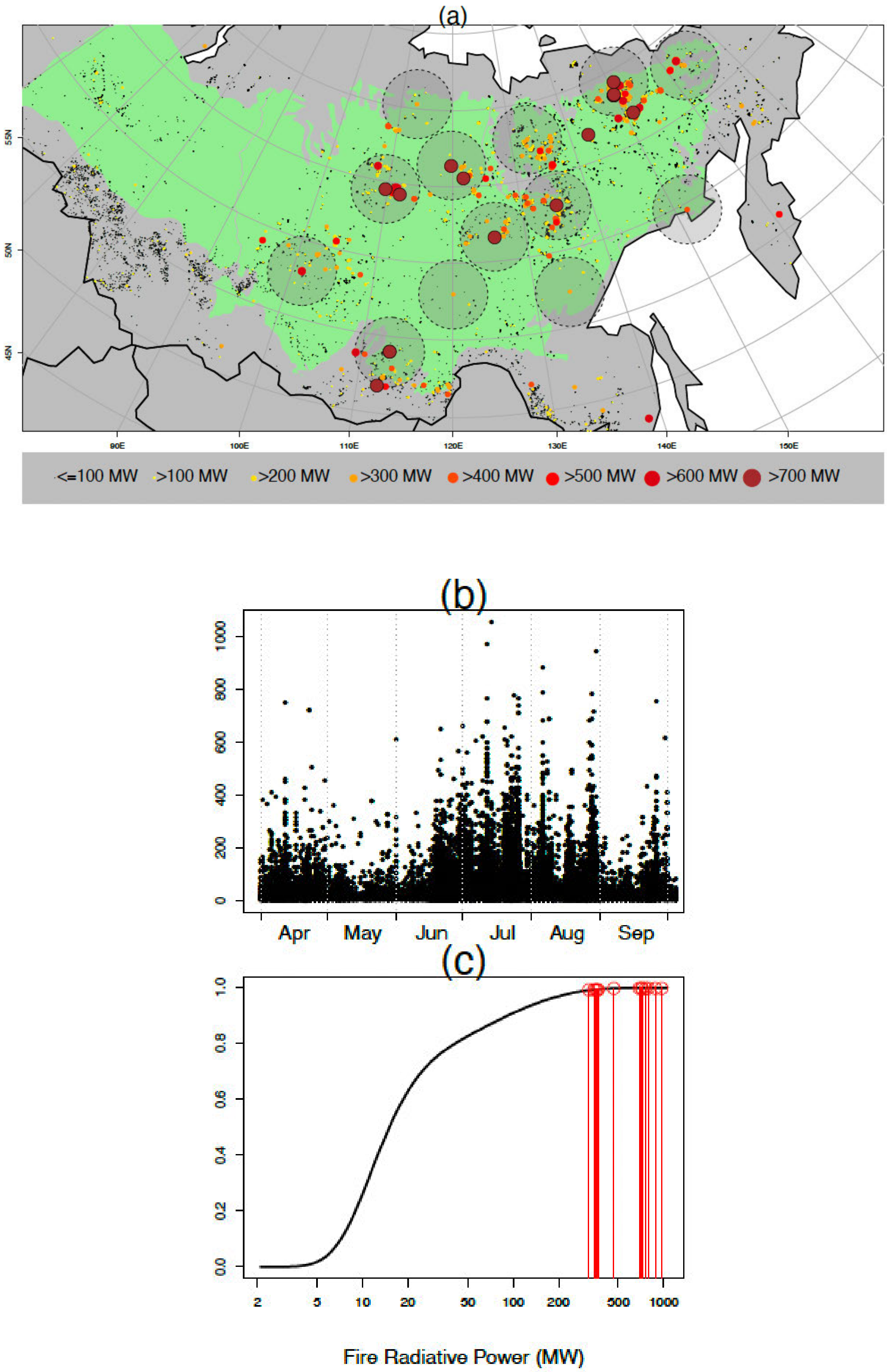
(a)
55N
50N
45N
90E
100E
110E
120E
130E
140E
150E
<=100 MW
>100 MW
>200 MW
>300 MW
>400 MW
>500 MW
>600 MW
>700 MW
(b)
0
200
400
600
800
1000
Apr
May
Jun
Jul
Aug
Sep
(c)
0.0
0.2
0.4
0.6
0.8
1.0
2
5
10
20
50
100
200
500
1000
Fire Radiative Power (MW)

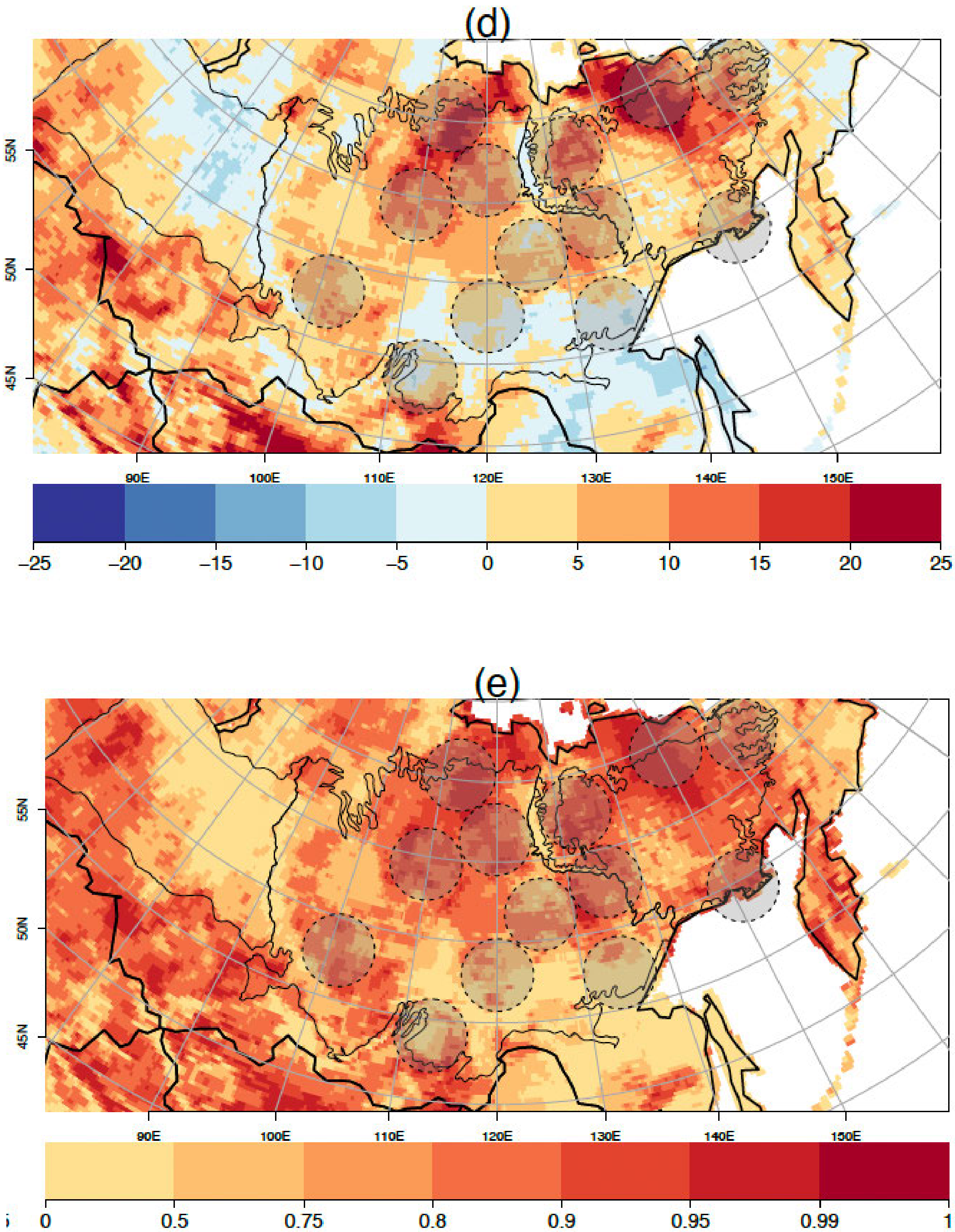

Figure 5.2: (a) Locations and intensity of April-September 2020 fires detected by FIRMS. Only detections that meet the FIRMS 'high-confidence' criteria are shown. Point size and colour show fire radiative power in megawatts (MW) as an indicator of fire intensity. Siberian ecoregions shown in green. (b) Maximum 7-day mean FWI during April to September 2020 expressed as an anomaly of the 1979-2019 mean annual maxima. In both (a) and (b), the shaded areas within the dashed circles show the location of the 13 hotspots.

linked to episodes of extreme heat across northern Siberia, but further analysis would be required to connect the attribution of FWI maxima at these hotspots to that of the distribution of extreme heat during the first half of 2020 (Ciavarella et al., 2021).

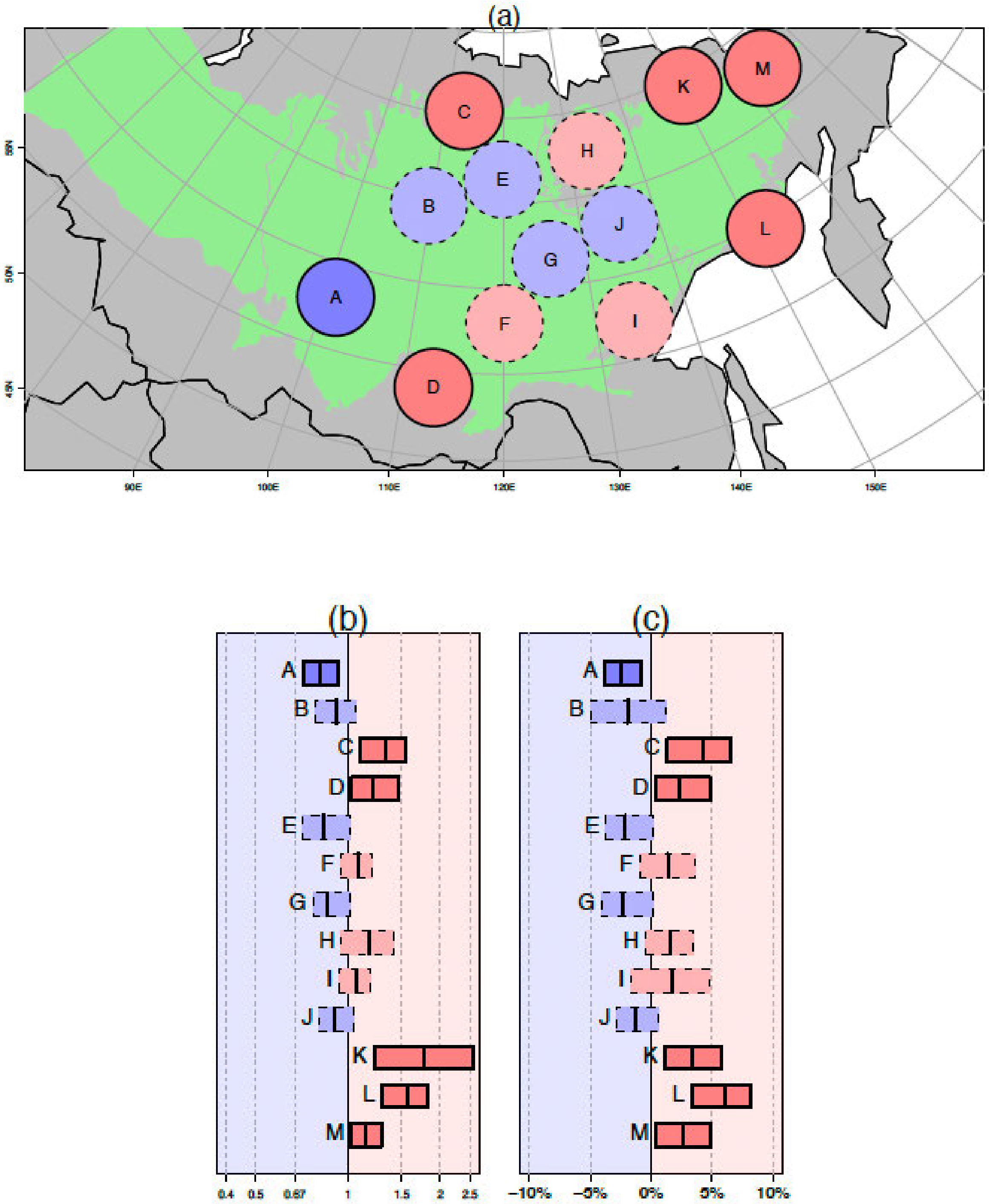

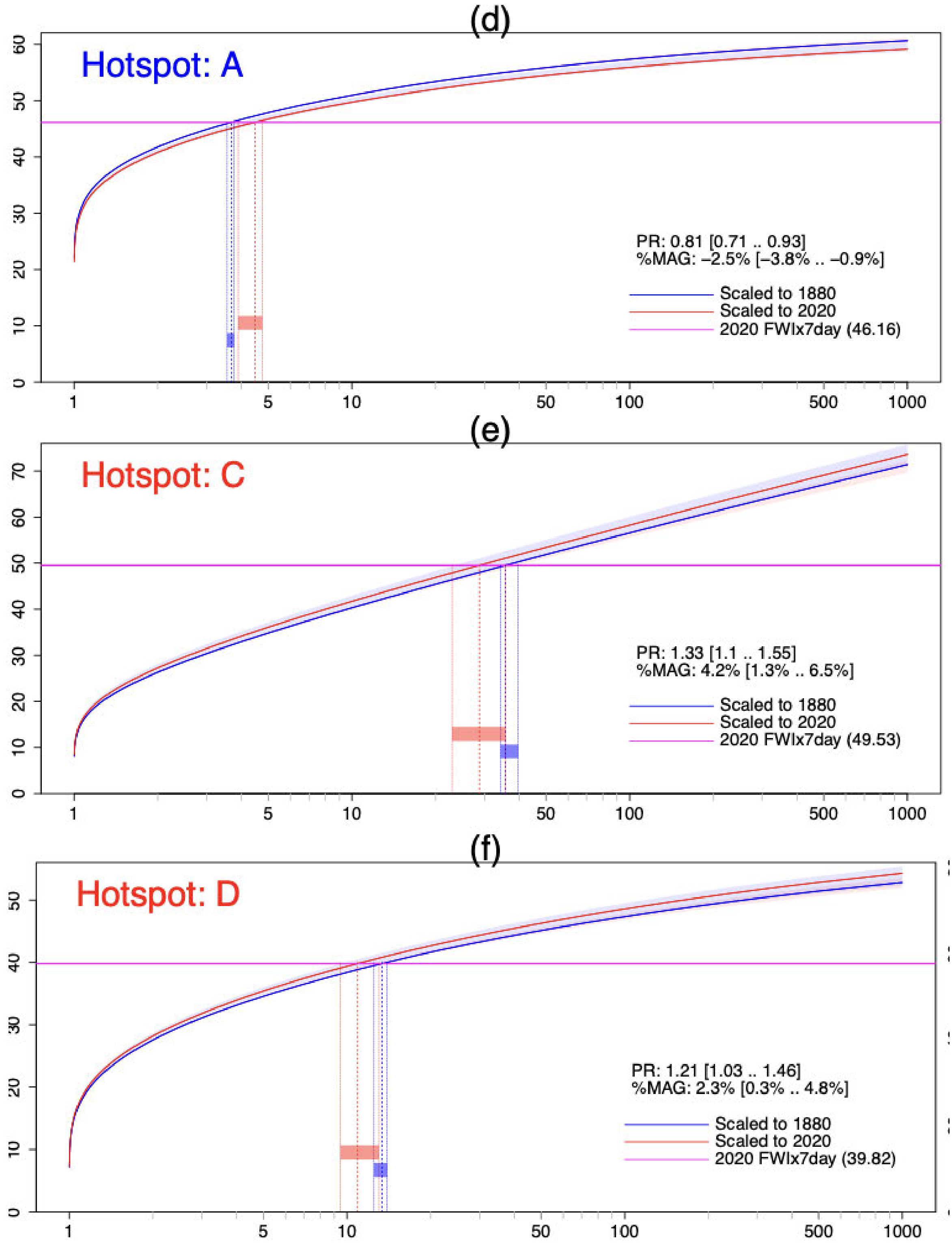
(d)
Hotspot: A
PR: 0.81 [0.71 .. 0.93]
%MAG: –2.5% [–3.8% .. –0.9%]
Scaled to 1880
Scaled to 2020
2020 FWIx7day (46.16)
(e)
Hotspot: C
PR: 1.33 [1.1 .. 1.55]
%MAG: 4.2% [1.3% .. 6.5%]
Scaled to 1880
Scaled to 2020
2020 FWIx7day (49.53)
(f)
Hotspot: D
PR: 1.21 [1.03 .. 1.46]
%MAG: 2.3% [0.3% .. 4.8%]
Scaled to 1880
Scaled to 2020
2020 FWIx7day (39.82)

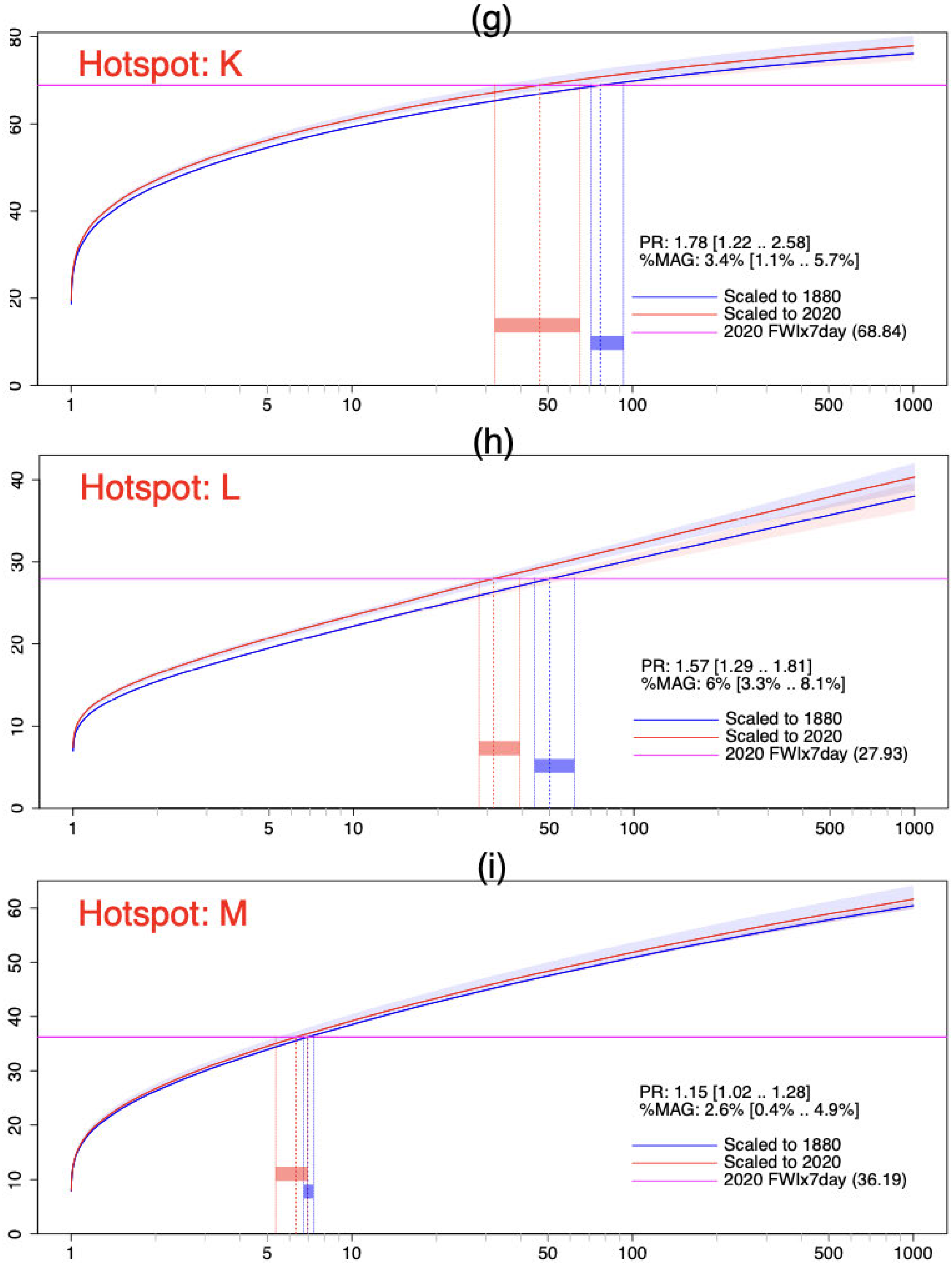

Figure 5.3: (a) Location of 13 fire hotspots and the overall sign change in likelihood of a 2020-type event between 1880 and 2020 (red: increase; blue: decrease; solid lines: significant; dashed lines: not significant). (b) PR calculated at each hotspot; bars show 95% CIs following non-parametric bootstrapping; central value shown in bold. (c) As (b) but for %MAG. (d)-(i) Gumbel plots for significant hotspots, showing the GEV model fit scaled to the smoothed GMST of 1880 (blue) and 2020 (red). Shading represents the 95% CIs. The magenta lines represent the 2020 FWIx7day events, scaled to the model distribution using bias correction. The blue (red) bars represent the 95% CIs for the return period of a 2020-type event in the climate of 1880 (2020).

5.1.4 Conclusions

Hotspots west of the Verkhoyansk range are not associated with significant increases in likelihood despite being representative of the most intense fire clusters across the central Siberian plateau. At hotspots B and E, which correspond to areas of particularly intense fires and large FWI anomalies during 2020, the likelihood of 2020-type conditions was found to have decreased by approximately 10-20% (not significant at the 95% level). The increase in likelihood of more than 20% (PR = 1.21; CI range 1.03-1.46) at the most southerly hotspot, D, is striking given that it is unlikely to be linked explicitly to the extreme heat in the north (Figure 5.3f).

Our analysis has sought to quantify the role of human-induced climate change on fire meteorological conditions associated with the most intense fire episodes, occurring in Siberia over the 2020 fire season. Previous work has identified the fingerprint of human influence on the extreme heat during the beginning of the year (Ciavarella et al., 2021). To complement such work, we considered the link between long-term global temperature and the meteorological parameters that collectively constitute extreme fire weather. We applied an established statistical method to output from CNRM-CM6-1 to quantify the long-term influence of global temperature trends on annual fire weather maxima separately at a series of regions experiencing the most intense fire activity. By averaging the results at different hotspots, we found that fire weather extremes are (a) around 10% more likely across the study region on average, and (b) up to 80% more likely in north-east Siberia, as a result of global warming.

The inter-hotspot differences are intriguing and merit further analysis to quantify the factors that contribute toward trends in extreme fire weather in this vast region. More generally, the results highlight the sensitivity of the findings of wildfire attribution analysis to the spatiotemporal characteristics used to define the event, either in terms of the impact (*i.e.*, the fire intensity) or the prevailing meteorology (*i.e.*, FWI). Results are also expected to be sensitive to the choice of general circulation model, which is an important additional source of uncertainty. While our analysis is based on a model that has been shown to realistically represent fire weather across Siberia (Gallo Granizo et al., 2021), further study would benefit from the inclusion of multiple models.

5.1.5 Supplementary material

The hotspots were defined by a 250-km radius and constructed using a stepwise approach to ensure that (a) they represent the immediate vicinity of the most intense fires, and (b) there is no overlap between them. All fires with fire radiative power (FRP) > 300 MW were selected and ranked by FRP. This set corresponds approximately to the highest 1% of FRP values among fires detected between April and September 2020. The first hotspot was centered on the location of the most intense fire; all smaller fires within two hotspot radii of this point were then removed from the ranked selection to ensure that none of the hotspots overlapped. The process was repeated for the fire with the next highest FRP, and so on until all fires had been assigned to a hotspot.

To assess the change in risk associated with a 2020-type event in the model, it is necessary to account for systematic discrepancy between the ERA5-driven global fire danger reanalysis (Vitolo et al., 2020) and CNRM-CM6-1. The mean (standard deviation) of FWIx7day maxima across the 13 hotspots was 38.7 (7.2) in the reanalysis and 42.5 (12.5) in CNRM-CM6-1. The $\frac{\sigma}{\mu}$ ratio of a GEV distribution fitted with CNRM-CM6-1 data (mean = 0.26; range = 0.18–0.35) compares favorably with that fitted with reanalysis data (mean = 0.25; range: 0.13–0.33), suggesting that the application of a simple additive bias correction to transform the reanalysis-derived maxima to match the distribution in CNRM-CM6-1 is appropriate (*e.g.*, Philip et al., 2020). Corrections were based on the difference in μ between the reanalysis- and model-fitted GEV distributions (mean = 3.8; standard deviation = 8.5).

5.2 Case study 2: 2021 Cape Town wildfire

The April 2021 Cape Town wildfire: has anthropogenic climate change altered the likelihood of extreme fire weather?

5.2.1 Introduction

In April 2021, a devastating wildfire tore through the iconic Table Mountain area of Cape Town, South Africa (Table Mountain National Park, 2021). Following a human-induced ignition on the morning of 18 April, worsening weather conditions led to increased fire spread that lasted until the afternoon of 20 April when the fire was eventually extinguished. The fire burned across more than 600 hectares of wildland (Palm, 2022), with its incursion into urban areas resulting in widespread evacuations and several hospitalisations (Davis, 2021). Up to 1 billion ZAR (approximately 60 million USD) worth of damage to buildings and infrastructure was incurred by the University of Cape Town campus alone3, and irreplaceable collections in its Jagger Library were destroyed. While summer wildfires are common in the Cape Town area, the rapid spread, spotting behaviour and unprecedented impacts of this fire so late in the fire season, which is usually considered to run from mid-November to mid-April (Forsyth and Bridgett, 2004; Christ et al., 2022), raise important questions about the challenges in responding to changing fire regimes at the wildland-urban interface.

The first three weeks of April 2021 were abnormally warm and dry along South Africa's west coast, at the southern tip of which Cape Town is situated. These conditions were highly conducive to wildfire ignition and spread. Previous work has demonstrated a link between extreme hydroclimatic events in the surroundings of Cape Town and anthropogenic climate change, most notably in an attribution study of the 2015-2017 drought (Otto et al., 2018b). While such droughts are likely to enhance fire risks, a quantification of how climate change has altered the likelihood of extreme weather conducive to late-season fires is worthy of dedicated analysis. Here, we analyse the exceptional nature of the meteorological conditions that coincided with the April 2021 event. Using an established probabilistic methodology applied to fire weather extremes simulated by multiple large ensembles from the latest generation of climate models, we quantify the influence of rising global temperatures on the likelihood of such conditions.

5.2.2 Data and methods

Firstly, to place the April 2021 event in the context of the regional fire regime, location and intensity data on historical fires (2001-2021) are taken from the Moderate Resolution Imaging Spectroradiometer (MODIS; Giglio et al., 2016) via the Fire Information for Resource Management System (FIRMS). Our analysis of fire-conducive meteorology is based on the Canadian Fire Weather Index (FWI; Van Wagner, 1987), which combines temperature, surface wind speed, relative humidity and precipitation. FWI has been widely used in related fire analysis across the world (*e.g.*, Krikken et al., 2021; Liu et al., 2022a; 2022b) and forms the basis of GEFF-ERA5, the fire danger reanalysis based on the Global ECMWF Fire Forecast model and the ERA5 reanalysis (Vitolo et al., 2020), from which we derive historical FWI data for the period 1979-2021. The FWI value of 67.77 on 18 April 2021 is the highest recorded during autumn (March to May) in GEFF-ERA5. Our attribution analysis questions to what extent rising global temperature associated with anthropogenic climate change has altered the likelihood of a "2021-type event", defined by the exceedance of the 18 April 2021 threshold by yearly maxima in autumn FWI. It is widely accepted that global mean temperature change since the late 19th century has been predominantly driven by anthropogenic forcings, with the influence of natural forcings very small by comparison (Hegerl et al., 2010; Bindoff et al., 2014; Philip et al., 2020; Ara Begum et al., 2022). Recent work has revealed positive trends in observed fire weather extremes (Jain et al., 2022) and fire weather maxima (Liu et al., 2022a) across much of southern Africa, although the extent of the observational record limits each analysis to just a few decades. Here, simulations of historical FWI are derived from six large ensembles (at least 10 members) from the 6th phase of the Coupled Model Intercomparison Project (CMIP6; Eyring et al., 2016) for the period 1850-2014 (see supplemental material for details). As the extent of the April 2021 fire was relatively small, model output is taken for a single grid point closest to the fire's approximate origin (33.92° S, 18.42° E). For all six models used, this point of origin sits close to the centre of the chosen grid cell. The meteorological and climatic diversity of the wider region (Conradie et al., 2022) means that including model output across a larger area is very likely to conflate spatially heterogeneous change signals not relevant to the event in question.

We apply a probabilistic statistical methodology based on a time-dependent generalized extreme value (GEV) distribution to each of the six CMIP6 model ensembles to quantify changes in the likelihood of extreme fire weather to rising global temperatures. This method has been widely used in the attribution of different extreme events (*e.g.*, Schaller et al., 2014; Eden et al., 2016; van der Wiel et al., 2017; Eden et al., 2018; Otto et al., 2018a), including episodes of extreme fire weather (*e.g.*, Krikken et al., 2021; Liu et al., 2022b). For each model, 165 yearly FWI maxima (1850-2014) across all corresponding ensemble members are fitted to a GEV distribution scaled with the 4-year smoothed global mean surface temperature (GMST), under the assumption that the location parameter μ and the scale parameter σ have the same exponential dependency on GMST, while the "dispersion ratio" $\frac{\sigma}{\mu}$ and the shape parameter ξ remain constant (Philip et al., 2020; van Oldenborgh et al., 2021b).

We evaluate the FWI threshold associated with the April 2021 event for each CMIP6 model following a bias correction based on the ratio between the μ parameters of the stationary GEV fit and that fitted with FWI maxima from GEFF-ERA5. The bias correction method matches that used in Case Study 1 (Section 5.1); further details are given in section 5.1.5). We then estimate the probability of this threshold being exceeded, firstly, in a "past" climate of 1880 (p_0) and, secondly, in a "present" climate of 2021 (p_1), both of which are defined by observed GMST (GISTEMP Team, 2022; Lenssen et al., 2019). The probability ratio (PR) $\frac{p_1}{p_0}$ is used to express the overall change in likelihood. A 1,000-sample non-parametric bootstrap is used to estimate confidence intervals (CIs) for each model. Following a model evaluation and selection step based on the dispersion ratio of each model's GEV fit, a final PR result is obtained by a multi-model weighted average (*e.g.*, Eden et al., 2016; Philip et al., 2018).

5.2.3 Results

Between 2001 and 2021, fires frequently occurred across the Cape Floristic Region along South Africa's southern and southwestern coastal margins. Fires during March-May occurred predominantly in the west of this region (Figure 5.4a) and regularly exceeded a fire radiative power (FRP) of 900MW (Figure 5.4b). The majority of fires observed within 50km of Cape Town occurred between December and March; far fewer fires are observed later than mid-March (Figure 5.4c). Synoptic conditions during the week leading up to the 18 April 2021 were characterised by a quasi-stationary mid-tropospheric ridge over South Africa and dry, downslope easterly or northerly drainage winds along the west coast, known locally as berg winds (Figure 5.4d), which contributed to the exceptional meteorological conditions. The approximate time of the fire's spread coincided with temperatures over 33°C and very low relative humidity (Figure 5.4e-f), in addition to the emergence of strong northwesterly winds (Figure 5.4g). While, during the 2020-21 summer months, the FWI was generally above average, the absence of prolonged periods of extreme conditions and isolated daily FWI values as anomalous as that recorded on 18 April 2021 further illustrates the exceptionality of the event (Figure 5.4h). FWI anomalies from the MAM climatology on 18 April 2021 were very positive (> 40) along the west and south coasts, yielding FWI values around Cape Town usually seen in the arid western interior (Figure 5.4i).

An overall increase in the likelihood of a 2021-type event between 1880 to 2021 was found for all six CMIP6 models, with PR ranging from 1.2 (INM-CM5-0) to 4.1 (MPI-ESM1-2-HR) (Figure 5.5a-f). The uncertainty ranges vary between models, and statistical significance is found only in CanESM5 (95% CI: 1.3-5.6; Figure 5.5a) and MPI-ESM1-2-HR (95% CI: 1.6-29.5; Figure 5.5f). These results complement the positive trends in observed extreme fire weather revealed in recent work (Jain et al., 2022; Liu et al., 2022a). In view of the inter-model differences, it is notable that the highest resolution model, MPI-ESM1-2-HR, is associated with the strongest trend but it is unclear whether results are sensitive to model resolution.

The small spatial extent of the April 2021 event, and the subsequent application of the method to a single model gridcell, results in a relatively large influence of internally driven natural variability on PR uncertainty (Kay et al., 2015). Combining results as part of a multi-model synthesis is a useful way to summarise and communicate overall findings when internal variability is large. Here, the synthesis is limited to those models that realistically represent FWI extremes, defined by the dispersion ratio of the GEV fit (see section 5.2.5). A weighted average is generated for the five models that meet the selection criteria, with weights for each model's PR given by the inverse of the squared uncertainty. The uncertainty of the

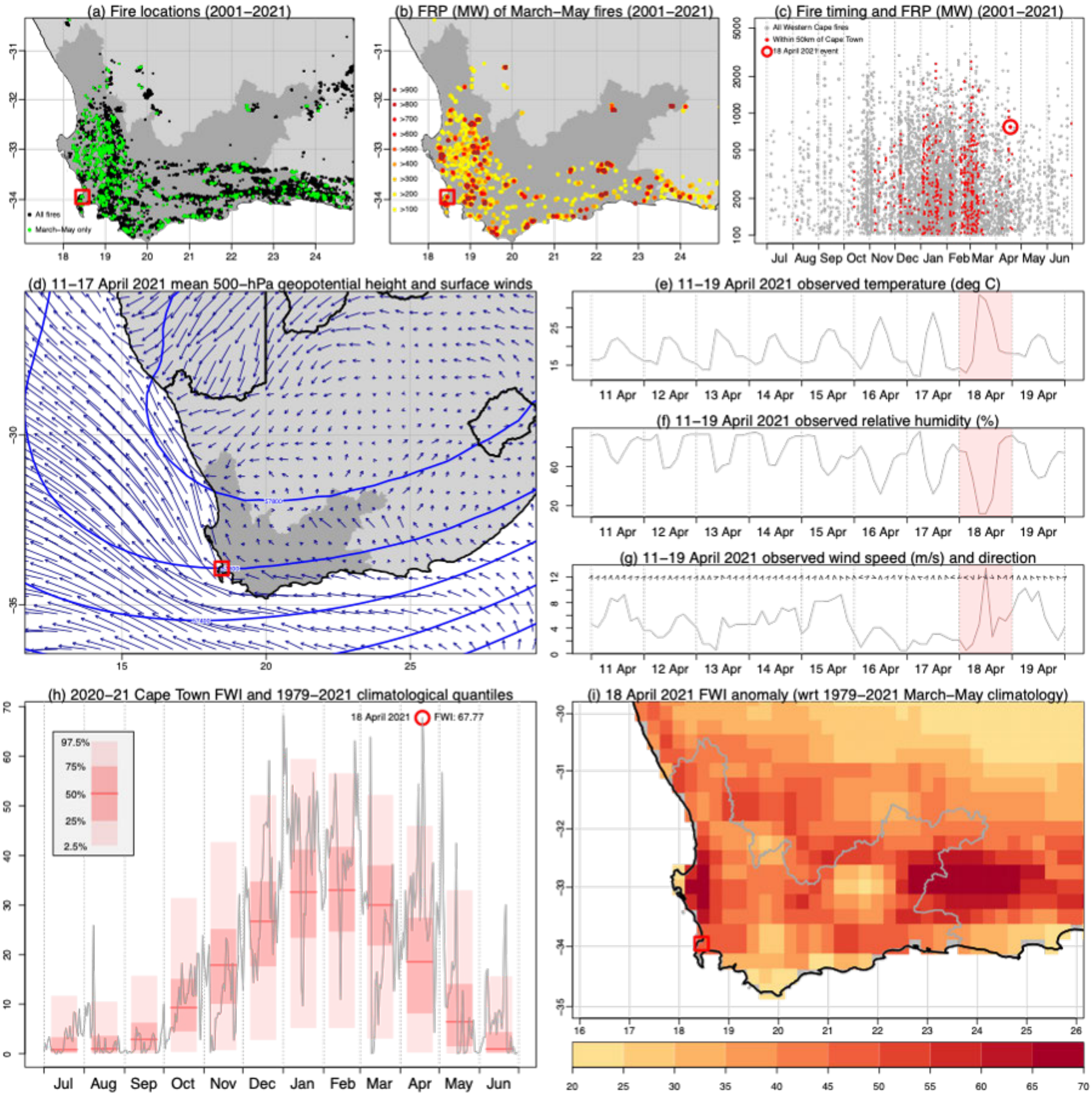

Figure 5.4: (a) Location and (b) intensity (FRP) of FIRMS-detected fires (2001-2021). (c) Intra-annual timing and FRP of FIRMS-detected fires within the Western Cape Province. Fires within 50km of Cape Town are shown in red. (d) ERA5 mean 500-hPa geopotential height (contours) and surface winds (arrows) for 11-17 April 2021. (e) Temperature (°C), (f) relative humidity (%) and (g) wind speed (m/s) and direction observed between 11 and 19 April 2021 at Cape Town WO. (h) Cape Town FWI between July 2020 and June 2021 from GEFF-ERA5 (line) and 1979-2021 monthly climatological quantiles (bars). (i) GEFF-ERA5 FWI anomalies on 18 April 2021 with respect to the 1979-2021 March-May climatology. Western Cape province is shaded in (a), (b) and (d), and outlined in (h).

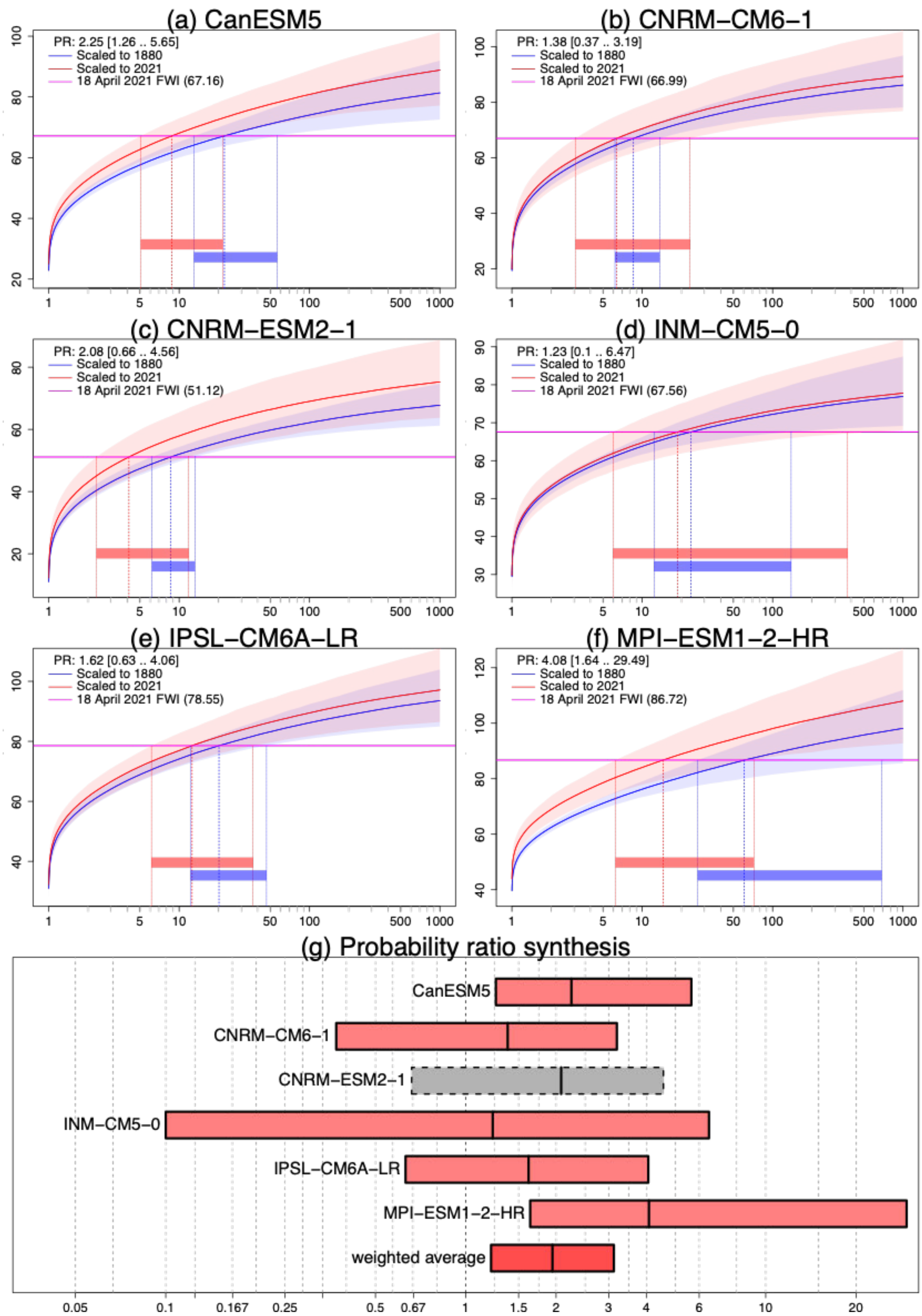

Figure 5.5: (a)-(f) Gumbel plots for the six CMIP6 models, showing the GEV model fit scaled to the smoothed observed GMST (GISTEMP Team, 2022; Lenssen et al., 2019) of 1880 (blue) and 2021 (red). Shaded areas represent the 95% CIs following non-parametric bootstrapping. The magenta lines represent the 2021-type event, scaled to the model distribution using bias correction. The blue (red) bars represent the 95% CIs for the return period of a 2021-type event in the climate of 1880 (2021). (g) PR estimates for the six CMIP6 models and the weighted average (for which CNRM-ESM2-1 is excluded). Bars show 95% CIs; central values are shown in bold.

weighted average is approximated by adding the errors for each PR estimate in quadrature (*e.g.*, Philip et al., 2018). The multi-model synthesis result suggests that the weighted average of the likelihood of the 2021-type event increased by a factor of 1.9 (95% CI: 1.2-3.1; Figure 5.5h) between 1880 and 2021 as a result of rising global temperatures.

5.2.4 Conclusions

Our analysis aimed to quantify the impact of a changing climate on the extreme fire weather that coincided with the Cape Town wildfire on 18 April 2021. We applied an established statistical method to the outputs of six large ensembles from CMIP6 to estimate how the likelihood of the 2021-type conditions has been altered by anthropogenic climate change, here expressed as the change in global mean temperature since the late 19th century. Averaging the results from multiple models revealed a mean probability ratio of 1.9, *i.e.*, an overall increase in likelihood of around 90%. Diagnosing discrepancies among different models of differing resolutions, particularly when the analysis is limited to a single model grid point, is challenging and a potential avenue for further study.

The results complement existing efforts to attribute hydroclimatological extremes around Cape Town, including droughts (*e.g.*, Otto et al., 2018b; Zscheischler and Lehner, 2022), and add to the growing set of attribution studies on wildfires and extreme fire weather in different parts of the world (*e.g.*, Krikken et al., 2021; van Oldenborgh et al., 2021a; Liu et al., 2022b). Our analysis also highlights the importance of drawing findings from multiple models in pursuit of the most robust statement possible for a singular wildfire episode. The model-derived evidence of trends in fire weather extremes add to that drawn from observational analysis (Jain et al., 2022; Liu et al., 2022a), and the application of alternative modelling approaches and statistical methodologies is a potential pathway toward further building this evidence base (Otto et al., 2020).

5.2.5 Supplemental Material

- **Observational data**

Observed weather data were taken from the Cape Town WO station (latitude: 33.9631°S, longitude: 18.6023°E; South African Weather Service SYNOP data). The data's sub-daily variability was cross-checked for consistency with observations from stations at Molteno Reservoir (latitude: 33.9377°S, longitude: 18.4109°E; South African Weather Service SYNOP data) and Elsenburg (latitude: 33.8424°S, longitude: 18.8394°E; obtained from the Elsenburg Western Cape Department of Agriculture Weather Data Portal: https://gis.elsenburg.com/apps/wsp/#).

- **CMIP6 model ensembles**

The application of the attribution approach to CMIP6 models (Eyring et al., 2016) was based on the availability of the required input variables for the FWI calculation. To reflect the value of a larger ensemble size in extreme event attribution (Hauser et al., 2017), a set of six large ensembles with at least 10 members was identified (detailed in Table 5.1). The use of a single grid cell represents the absolute lower limit of the scale that CMIP models could be used for conducting analysis of this nature.

Table 5.1: Details for the CMIP6 model ensembles used.

Model	**Ens**	**Resolution (lon $\times$ lat)**
CanESM5	50	128$\times$64 ($\sim$2.8$\times$ 2.8)
CNRM-CM6-1	30	256$\times$128 ($\sim$1.4$\times$ 1.4)
CNRM-ESM2-1	10	256$\times$128 ($\sim$1.4$\times$ 1.4)
INM-CM-5-0	10	180$\times$120 (2.0$\times$ 1.5)
IPSL-CM6A-LR	32	144$\times$143 ($\sim$2.5$\times$ 1.3)
MPI-ESM1-2-HR	10	384$\times$192 ($\sim$0.9$\times$ 0.9)

- **CMIP6 model ensembles**

A synthesis based on weighted averaging allows us to combine PR estimates from multiple models. The synthesis follows an initial model selection step in which the dispersion ratio of the GEV fit for each model is compared with that of GEFF-ERA5 (95% CI: 0.12-0.25; Figure 5.6). CNRM-ESM2-1 is the only model for which the dispersion ratio falls outside of the GEFF-ERA5 range, as indicated by the grey bar in Figure 5.6.

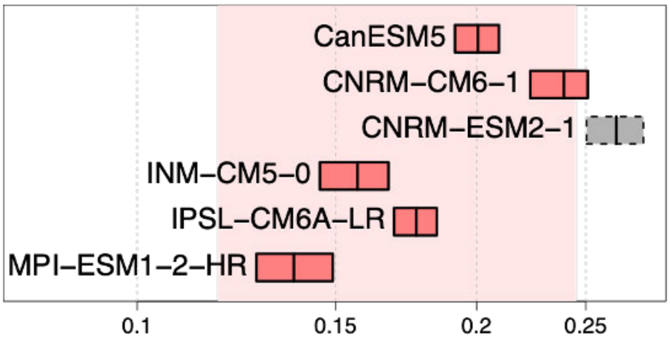

Figure 5.6: Dispersion ratio of the GEV fit for each six CMIP6 model ensemble. Bars show 95% CIs; central values are shown in bold. The shaded area shows the CIs for the dispersion ratio of the GEV fitted with yearly March-May maxima in daily FWI from GEFF-ERA5 (0.118-0.245).

5.3 Case Study 3: 2022 Euro-Mediterranean wildfires

How does climate change influence the past, present and future likelihood of the meteorological conditions associated with the 2022 Euro-Mediterranean wildfires?

5.3.1 Introduction

While wildfires are originally a natural phenomenon in Mediterranean countries, the increased intensity and severity of fires associated with climate change threaten the natural regime, the environment, and society (de Dios and Rinaudo, 2020; Cochrane and Bowman, 2021). In the summer of 2022, an unprecedented condition of wildfires across the Euro-Mediterranean region raised substantial public concerns about the changes to an earlier and longer wildfire season (Rodrigues et al., 2023). In particular, between late July and early August, an exceptionally high number of wildfire events (928; EFFIS, 2023) led to a record burned area of 508,260 hectares (compared to an average of 215,548 hectares between 2006 and 2021) and high levels of atmospheric emissions with 6.4 megatons of carbon associated with fires in summer 2022 (Sundström et al., 2022a; Copernicus Atmosphere Monitoring Service, 2022). The annual report in 2021 on Forest Fires in Europe, the Middle East, and North Africa published by the European Commission's Joint Research Centre (San-Miguel-Ayanz et al., 2022, 2023), concluded that the fire season in 2021 was the second worst in the EU territory in terms of burnt area, while acknowledging that 2022 was expected to be even worse.

Based on the Fire Information for Resource Management System (FIRMS), countries affected by the 2022 wildfires include, but are not limited to, France, Spain, Portugal, Morocco, Algeria, Italy, Slovenia, Croatia, Bosnia and Herzegovina, Montenegro, Albania, Greece, Bulgaria and Turkey. Spain alone accounted for 275,827 hectares of burned area, nearly 60% of the total burned area (468,793 hectares) of the entire European Union (EFFIS, 2023). According to information on natural disasters based on satellite imagery and geospatial data provided by Copernicus Emergency Management Services (CEMS), there were 47 rapid mapping activations on wildfires in EU member states between June and August 2022, 15 of which occurred in Spain, 11 in Greece and 6 in Portugal (CEMS, 2023).

Summer 2022 was associated with a series of heatwaves that appeared earlier and were more prolonged than usual, setting temperature records in both Spain and France and resulting in record-breaking wildfire events in the Euro-Mediterranean region (C3S, 2022; Sundström et al., 2022a). Additionally, across the Euro-Mediterranean region, such exceptional heatwaves could be considered as "average" by 2035, even if countries meet the climate commitments outlined in the 2015 Paris Agreement (CCAG, 2022). The 2022 season, therefore, has the potential to be a peephole into the 'new normal' to observe the increasing risks of extreme weather including fires, drought, and floods under climate change in the coming years (CCAG, 2022; Rodrigues et al., 2023).

Event attribution in wildfires, which aims to address to what extent anthropogenic climate change has altered the meteorological conditions conducive to wildfires, is an important mechanism to generate robust evidence of the changes in fire weather conditions. However, event attribution studies conducted over the Euro-Mediterranean region are relatively few compared to other fire-prone regions of the world (such as the US and Australia). Therefore, the aim of this study is to quantify the role of climate change on changes in present and future risk of the types of wildfire events witnessed across the Euro-Mediterranean region during Summer 2022. By applying a spatiotemporal definition over the study region, a series of high-intensity, high-impact events that are linked to extreme fire-conducive meteorological conditions are selected for attribution and future risk assessment. Given the current relevance, the focus is on estimating changes in future disaster risk under a global mean temperatures 1.5°C and 2.0°C warmer than the early 20th century. We also aim to combine probabilistic attribution of events and methods often applied in attribution studies with large ensembles of future simulations to provide information for future risk assessments. In the latter part of the section, subsequent to the methods section, we focus on the analysis of events. For each event, we present a brief background description and observational analysis, followed by a model attribution assessment. Additionally, a future risk analysis is conducted for all the events across different countries. This approach enables the synthesis of results for the entire region, offering a comprehensive summary. Finally, we conclude by highlighting the insights that can be drawn from this analysis, while reflecting on the benefits and limitations of our approach.

5.3.2 Data and methods

Data describing the location and intensity of fires detected between June and August 2022 are taken from the Moderate Resolution Imaging Spectroradiometer (MODIS; Giglio et al., 2016) via the Fire Information for Resource Management System (FIRMS). Canadian Fire Weather Index (FWI; Van Wagner, 1987) data for the period 1979-2022, taken from GEFF-ERA5, the fire danger reanalysis based on the Global ECMWF Fire Forecast model and the ERA5 reanalysis (0.25° resolution; Vitolo et al., 2020), are used to define the fire-conducive meteorological conditions. Simulations of historical FWI for the period 1850-2014 and future FWI under a high emission scenario (SSP585) are taken from the global coupled model, Canadian Earth System Model version 5 (CanESM5; 1.4° resolution; Swart et al., 2019), which is developed for the sixth phase of Coupled Model Intercomparison Project (CMIP6; Eyring et al., 2016). This model is chosen due to the availability of a large (50-member) ensemble for both the historical and future periods (*i.e.*, 1850-2100).

Independent attribution analysis is conducted at a series of hotspots associated with the most intense summer 2022 fires, using a selection approach developed by Liu et al. (2022b). The hotspots are based on a subset of fire episodes associated with (a) a minimum fire radiative power (FRP) of 1000 MW, and (b) a corresponding 7-day mean FWI value (hereafter FWIx7day) that is above the June-August historical (1979-2022) 95^{th} percentile. Once isolated, this subset of fires is ranked by FRP. Therefore, to quantify the high-impact fire weather risk over the Euro-Mediterranean region in June-August 2022, extreme fire weather conditions are linked to wildfires that occurred during the period 1979-2022. As outlined by Liu et al. (2022b), hotspots are spatially defined by a 250-km radius and subject to a stepwise selection to ensure that (a) each hotspot represents the immediate vicinity of the most intense fires, and (b) there is no overlap between hotspots. The first hotspot is centred on the location of the most intense fire according to FRP; all smaller fires within one hotspot diameter of this point are then removed from the ranked selection to ensure that none of the hotspots overlap. The process is repeated for the fire with the next highest FRP, and so on until all fires within the subset are assigned to a hotspot.

A total of ten hotspots are identified. For each hotspot, we use a statistical method based on a time-dependent Generalised Extreme Value (GEV) distribution, frequently applied to both observational and climate model data in previous work (*e.g.*, Schaller et al., 2014; Eden et al., 2016; van der Wiel et al., 2017; Eden et al., 2018; Otto et al., 2018a; Krikken et al., 2021; Liu et al., 2022a; 2022b; 2023), to estimate the change in probability of a '2022-type event' (defined at each hotspot by the maximum FWIx7day value recorded within a given hotspot's spatial domain) as a result of global warming. For each hotspot, a pool of annual FWIx7day maxima (hereafter FWIx7day) from all 50 ensemble members are fitted to a GEV distribution in which the location μ and scale σ parameters are assumed to scale linearly with a 4-year smoothed global mean surface temperature (GMST; GISTEMP Team, 2022; Lenssen et al., 2019) from the ensemble means. Both the shape ξ parameter and the $\frac{\sigma}{\mu}$ ratio remain constant (Philip et al., 2020). Two types of GEV fits are conducted according to the period: a) for the past and present climate 1850-2022, 173 years of simulations and (b) for the future change under 1.5°C and 2.0°C increase in GMST (with respect to the reference period 1900-1949), a total of all 251 years (1850-2100) of simulations are used.

For each wildfire hotspot, we evaluate the return time, and hence the probability, of the 2022-type event occurring in a 'past' climate of 1910-1919, a 'recent' climate of 2010-2019, a future climate under a 1.5°C and 2.0°C GMST increase. Using the probability ratio, we quantify the changes in the likelihood of 2022-type events between the past and recent climate (PR), and between the recent climate and the future climate associated with 1.5°C ($PR_{1.5}$) and 2.0°C ($PR_{2.0}$) GMST increases. An additive bias correction on the location parameter μ (van Oldenborgh et al., 2021a; Liu et al., 2022b), is applied to account for the systematic discrepancies between the reanalysis and CanESM5. Confidence intervals (CIs) for each GEV fit, and subsequently for PR results, are estimated with a 1,000-sample non-parametric bootstrap. The final synthesis is obtained by a weighted average of PR, $PR_{1.5}$ and $PR_{2.0}$ at all hotspots identified across the Euro-Mediterranean region, again following a similar approach outlined by Liu et al. (2022b).

5.3.3 Results

5.3.3.1 Detections in fire intensity and locations

We firstly explore the intensity and spatial extent of the 2022 wildfires in the context of previous fire seasons. Historically, fires occur across the Euro-Mediterranean region between June and August (Figure 5.7). However, when compared to the preceding two decades (2001-2021), the 2022 wildfires were especially intense in western parts than other areas of the Euro-Mediterranean region (Figure 5.7a). In particular, Portugal and Spain account for a very high number of fire occurrences in 2022. Fire clusters are also apparent along the Mediterranean coastlines of southern France, Morocco, Algeria, in addition to Sicily and southern Italy, the western Balkans, Greece, and western Turkey. We also note that the southwestern region of France, which experienced some fires between 2001 and 2021, has witnessed more frequent fire events in 2022 alone. Across the study region as a whole, the 2022 fire season was generally associated with high intensity fires. The 90th, 95th, and 99th FRP percentiles were the highest recorded since 2001, and only the 2007 and 2021 seasons have witnessed a larger number of fires with FRP that is above the long-term 90th percentile (Figure 5.7b).

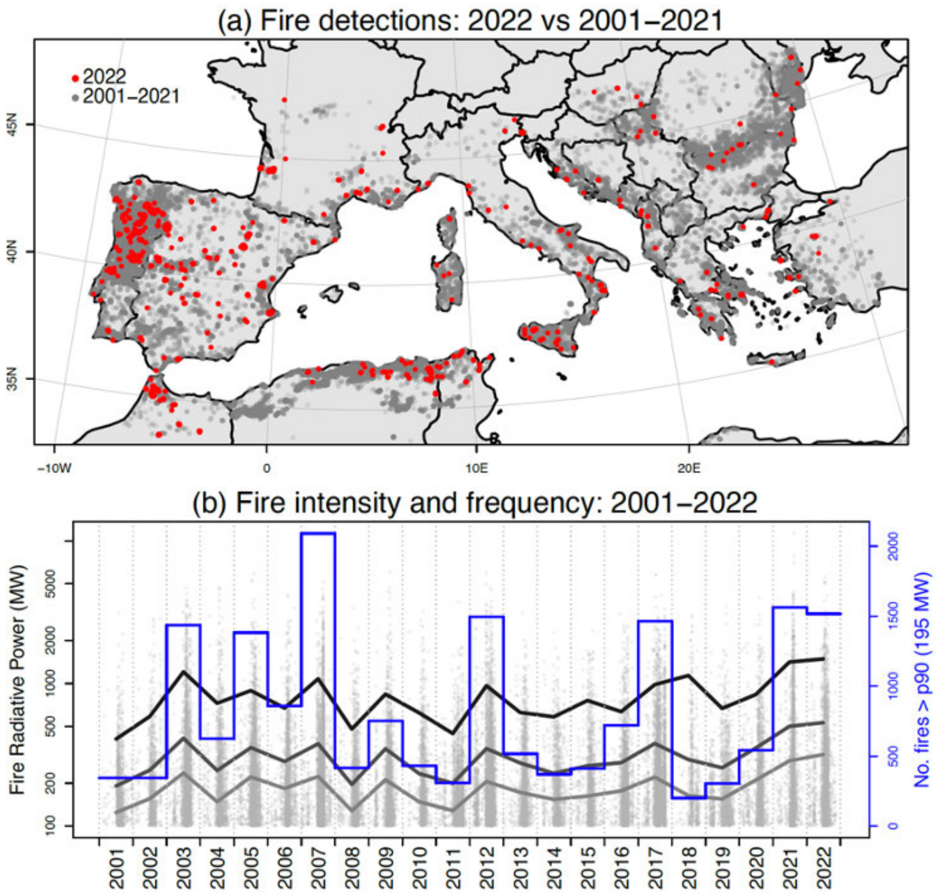

Figure 5.7: (a) Locations of fires detected by FIRMS in 2022 (red) compared to the period of 2001-2021 (grey). (b) The intensity (grey points) and frequency (blue line) of fires detected in the period of 2001-2021. The grey points show the date of detected fires with FRP>100 MW. The three grey lines (from light to dark) show the 90th, 95th and 99th percentile of the FRP values over JJA 2001-2022. The blue steps show the number of fires exceeding the 90th percentile (195 MW) of the period JJA 2001-2022.

Intra-annual data from 2001 to 2022 show that fire activity occurs primarily during the boreal summer and autumn months (*i.e.*, from June to November; Figure 5.8a, b). This was most evident in the summer of 2022, when many fire events exceeded the 95th and 99.9th

percentile FRP, especially during July and August, with the highest FRP even surpassing 5000 WM (Figure 5.8b). The intensity of fires occurring earlier in the year is generally much less than those occurring in summer (Figure 5.8b).

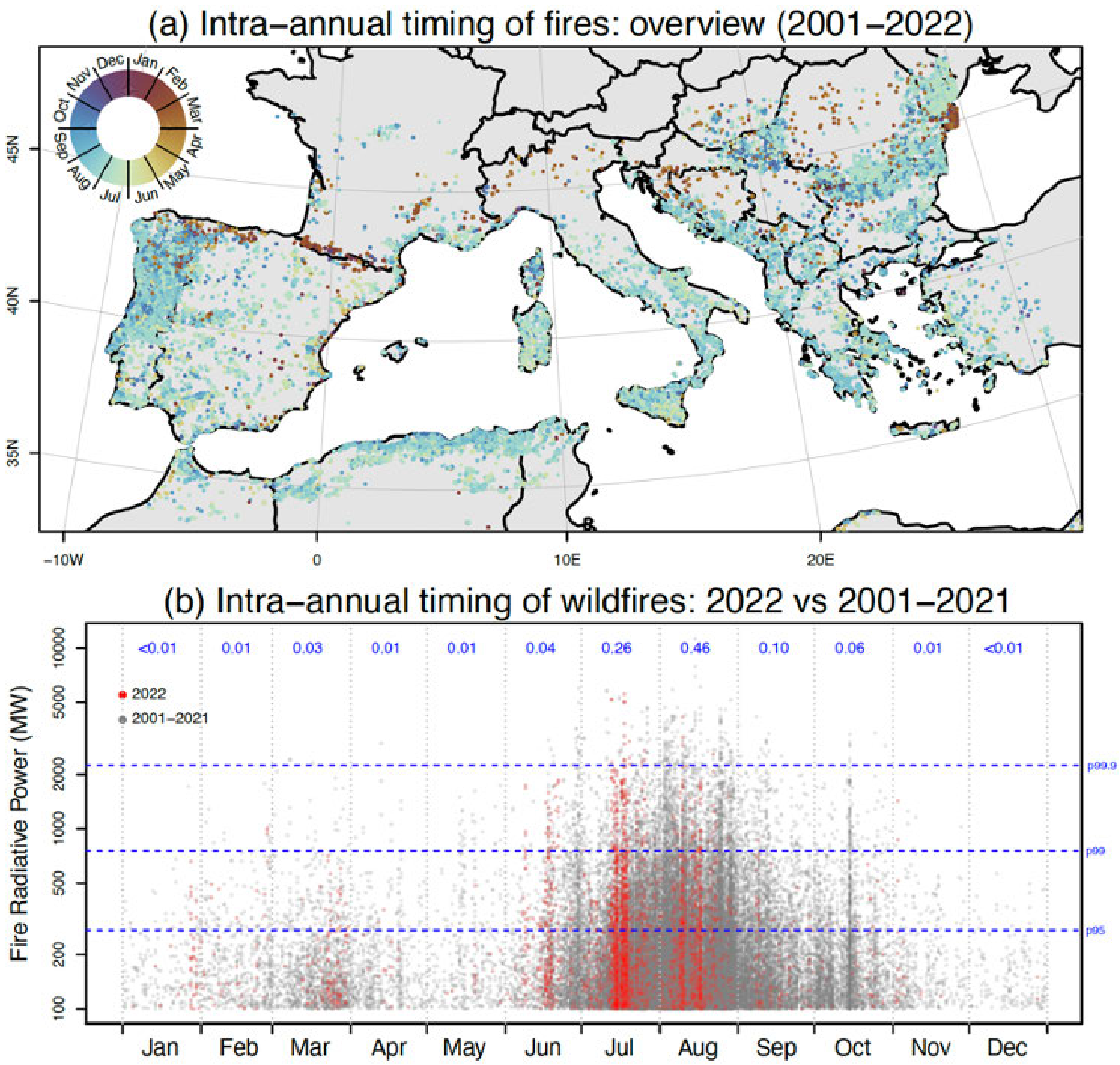

Figure 5.8: (a) Intra-annual timing for detected fires (2001-2022). (b) Distribution of intra-annual timing of the European wildfires from January to December in 2022 (red) compared to the period of 2001-2022 (grey), with corresponding FRP values presented on the left. Blue lines show the 99.9th, 99th and 95th percentile of the FRP values over 2001-2022. Numbers on the top represent the percentage of fire events detected for each month through all the fires during 2001-2022.

The spatial distribution of the most severe fires detected by FIRMS between June and August 2022 is shown in Figure 5.9a. The stepwise selection procedure outlined in section

5.3.2 was used to identify a total of ten hotspots that indicate where the most intense fires of summer 2022 coincided with episodes of extreme fire weather (Figure 5.9a-b). Note that fires observed in Greece, which were severe (FRP > 3000 MW), did not coincide with particularly extreme FWI, and, therefore, are not associated with a hotspot. Details of the individual fire event associated with each hotspot are given in the following section.

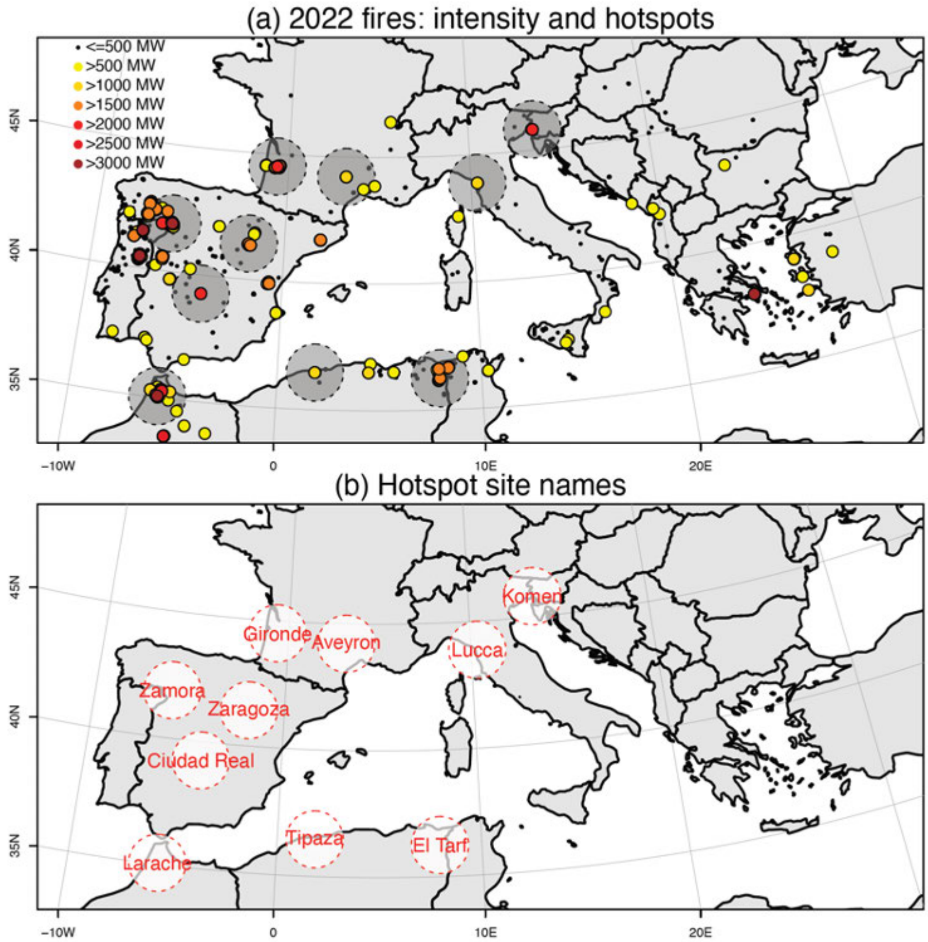

Figure 5.9: Locations with (a) intensity and (b) names only of the ten fire hotspots of June-August 2022 FIRMS-detected fires in Southwest Euro-Mediterranean regions. Detections in each site shown in the map meet 1) that corresponding daily FWI on the event day is higher than 95th percentile within the period of June-August 1979-2022 and 2) the FIRMS 'high-confidence' criteria. Point size and colour show fire radiative power in megawatts (MW) as an indicator of fire intensity. The study region is southwest Euro-Mediterranean regions.

5.3.3.2 Trends in observed fire weather conditions

The FWIx7day mean during JJA 2022 was the largest (> 50) in central and southern Portugal and Spain, as well as the north of Morocco, Algeria and Tunisia (Figure 5.10a). The highest anomalies of the JJA 2022 FWIx7day maxima values (> 25) were observed across France, southern Portugal and northern Spain, in addition to northern parts of Morocco, Algeria and Tunisia. Further east, high FWIx7day maxima were also observed in various parts of the western and eastern Balkans (Figure 5.10b). A large portion of the JJA 2022 FWIx7day values are among the highest 5% of annual maxima observed across southwest Euro-Mediterranean regions since 1979 (Figure 5.10c).

5.3.3.3 Events identified as wildfire hotspots

As described above, ten hotspots were identified (Figure 5.9a, b) and corresponding fire events are presented ranked by the degree of fire intensity (*i.e.*, FRP) with further detailed information about the event date, FWI values, area burned, and impacts summarized in Table 5.2.

Table 5.2: Hotspot information.

Hotspots	**Event date (yyyy-mm-dd)**	**FRP (MW)**	**FWI**	**Burned area (ha)**
(a) Zamora, Spain	2022-07-18	5563.7	73.4	>31,000
(b) Larache, Morocco	2022-07-13	5173.7	68.7	4,660
(c) Gironde, France	2022-07-18	2391.4	66.2	~20,000
(d) Komen, Slovenia	2022-07-20	2269.8	21.6	~3,705
(e) Ciudad Real, Spain	2022-07-25	2209.4	87.0	NA
(f) El Tarf, Algeria	2022-08-17	1775.6	109.6	~2,600
(g) Zaragoza, Spain	2022-07-19	1616.2	80.7	~14,000
(h) Aveyron, France	2022-08-13	1470.8	39.1	>500
(i) Lucca, Italy	2022-07-19	1447.1	19.0	>900
(j) Tipaza, Algeria	2022-08-14	1095.2	89.5	NA

Hotspot (a): Wildfires in Zamora, Spain on 18 July 2022 - The fire broke out on 17 July 2022 in Losacio, which is in northwestern Zamora province in Spain (Crisis24, 2022b). The intense fire reached its worst level on 18 July (Figure 5.11a), resulting in more than 31,000 hectares being burned (as of 21 July) with two deaths and three injuries, as well as the temporary evacuation of 6,000 people from the area (as of 18 July) (Crisis24, 2022b; Aljazeera, 2022b; Copernicus, 2022). Moreover, the fire was ignited in an adjacent area to

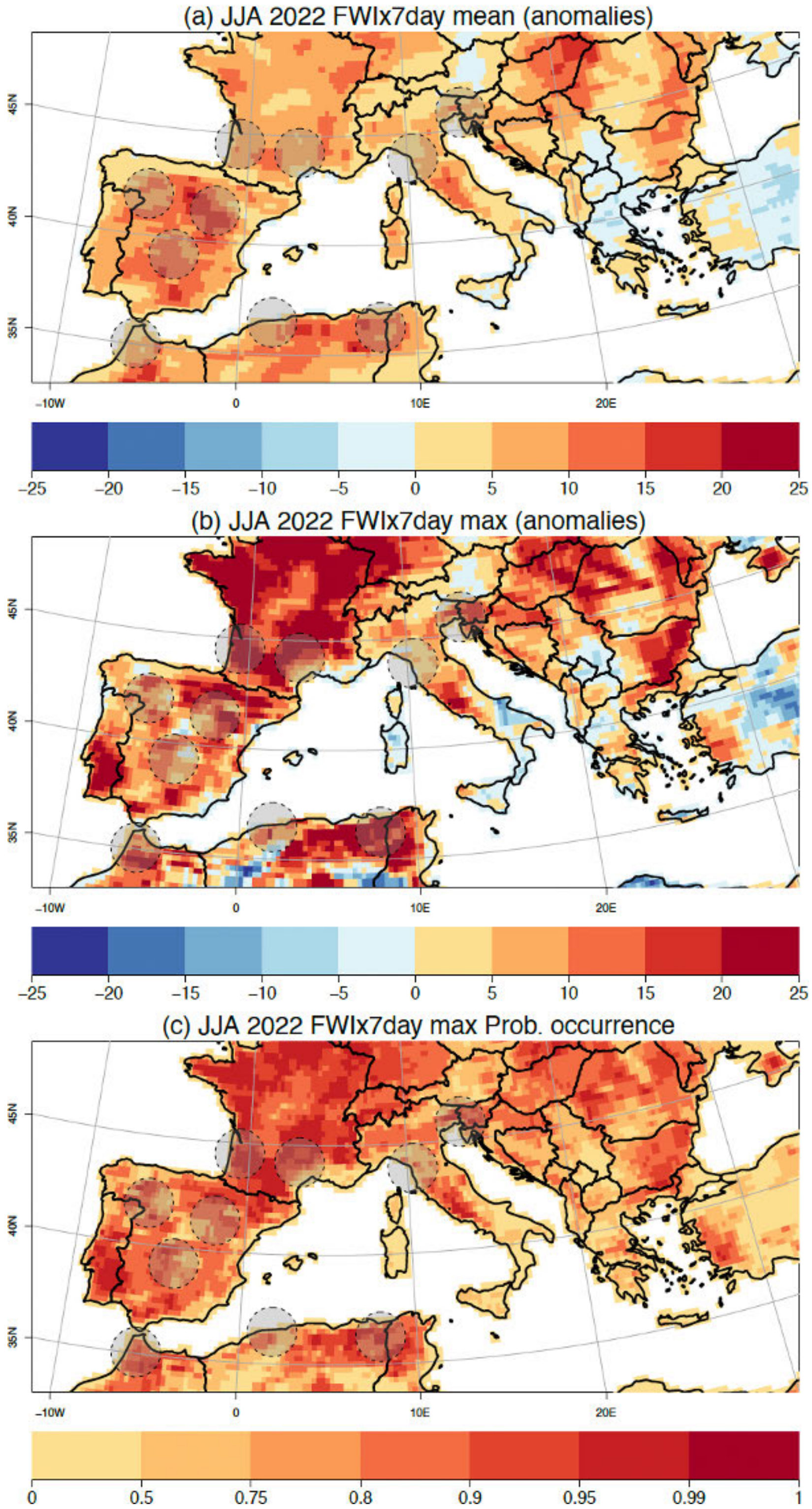

Figure 5.10: Anomalies of (a) the mean 7-day averaged FWI in June-August 2022 and (b) the maximum 7-day averaged FWI during June to August 2022 with respect to the 1979-2022 June-August climatology. (c) In terms of the probability of occurrence in maximum 7-day averaged FWI from June to August 2022 using 1979-2022 as climatological period.

the Sierra de la Culebra wildfire that burned 25,000 hectares of forest one month ago, in June 20223. Fire also affected some roads and trains, including the closure of the N-631 freeway between Moreruela de Tabara and Litos, and the suspension of train service on the AVE Madrid-Galicia highway line between Sanabria and Zamora (Crisis24, 2022b). The most intense fires detected in Zamora during the summer of 2022 occurred from mid- to late July (Figure 5.11a). This was preceded by a fire observed in mid-June, after which the FWI values dropped back to a lower level. The FWI values after this period climbed gradually until this fire occurred and reached the highest record in both FWI (73.4) and FRP (5563.7 MW) on July 18 (Table 5.2; Figure 5.11a). Additionally, the former record of FWI exceeds the 95th percentile ($\sim$60) of FWI during JJA 1979-2022 (Figure 5.11a), and the mean FRP and number of fires both reached the highest in 2022 (Figure 5.12a).

Hotspot (b): Wildfires in Larache, Morocco on 13 July 2022 - The fire that broke out on Wednesday 13 July 2022, driven by strong winds, destroyed 4,660 hectares of forestland in many provinces in Morocco, while half of them are located in Larache (Aljazeera, 2022a; Alarabiya News, 2022). The largest fire in Larache caused one death with more than 5,200 families being affected in 35 nearby villages (Latrech, 2022). To respond to and mitigate the impact of the recent fires on agricultural activities and forests across the burned area, the Moroccan government announced a MAD 290 million ($28.3 million) plan in the following week (Kasraoui, 2022). Several fires were detected in Larache (Morocco) in mid- and late July as well as late August in 2022 (Fig5.11b). The extreme fire event that occurred on 13 July shows the record-breaking values both in FWI (68.9) and FRP (5173.7 MW) over the period of JJA 2022 (Table 5.2; Figure 5.11b). An upward trend in FWI can be seen in the weeks leading up to the event, with a peak in FWI occurring on the day of the event and being nearly two-fold of the 95th percentile level (Fig5.11b), again, the mean FRP and number of fires both peaked in 2022 (Figure 5.12b).

Hotspot (c): Wildfires in Gironde, France on 18 July 2022 - Since 12 July 2022, wildfires had been raging in the south and southwest of France (Crisis24, 2022a). The most intense fire activity in the French Gironde region began on July 17 (Sundström et al., 2022b) and reached a record high intensity (2391.4 MW; Table 5.2) on the following day, which is very similar to the timing and evolution of the fire in Zamora, Spain (Hotspot a). Fires in the Gironde area lasted two weeks, causing nearly 20,000 hectares destroyed (as of 18 July) with around 37,000 people being temporarily evacuated from this area (Connexion, 2022). Severe weather conditions, such as the record-breaking temperatures over 40 °C combined with the wind and the dry vegetation, had led to the progress of fires in different directions, making the fires difficult to get under control (Crisis24, 2022a). From the beginning of July 2022,

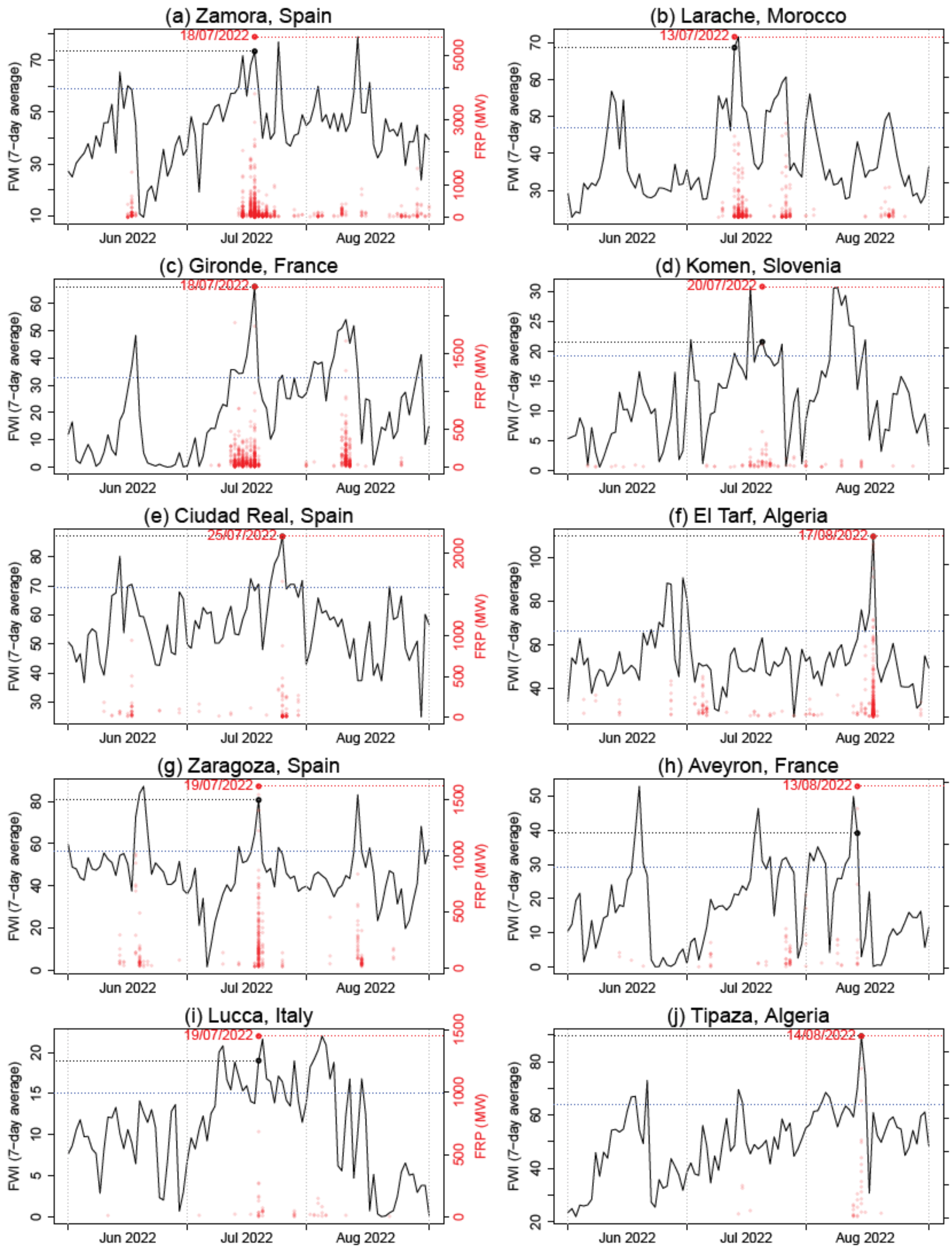

Figure 5.11: (a)-(j) Daily FWI (black lines) and fire radiative power (MW; red dots) of the fires occurred during the period June-August 2022 at selected ten sites. In each case, blue dashed line represents the 95th percentile in daily FWI over June-August 2022, the black dot with dashed line and the red dot with dashed line represent the FWI and FRP values with the date of the event shown alongside in red.

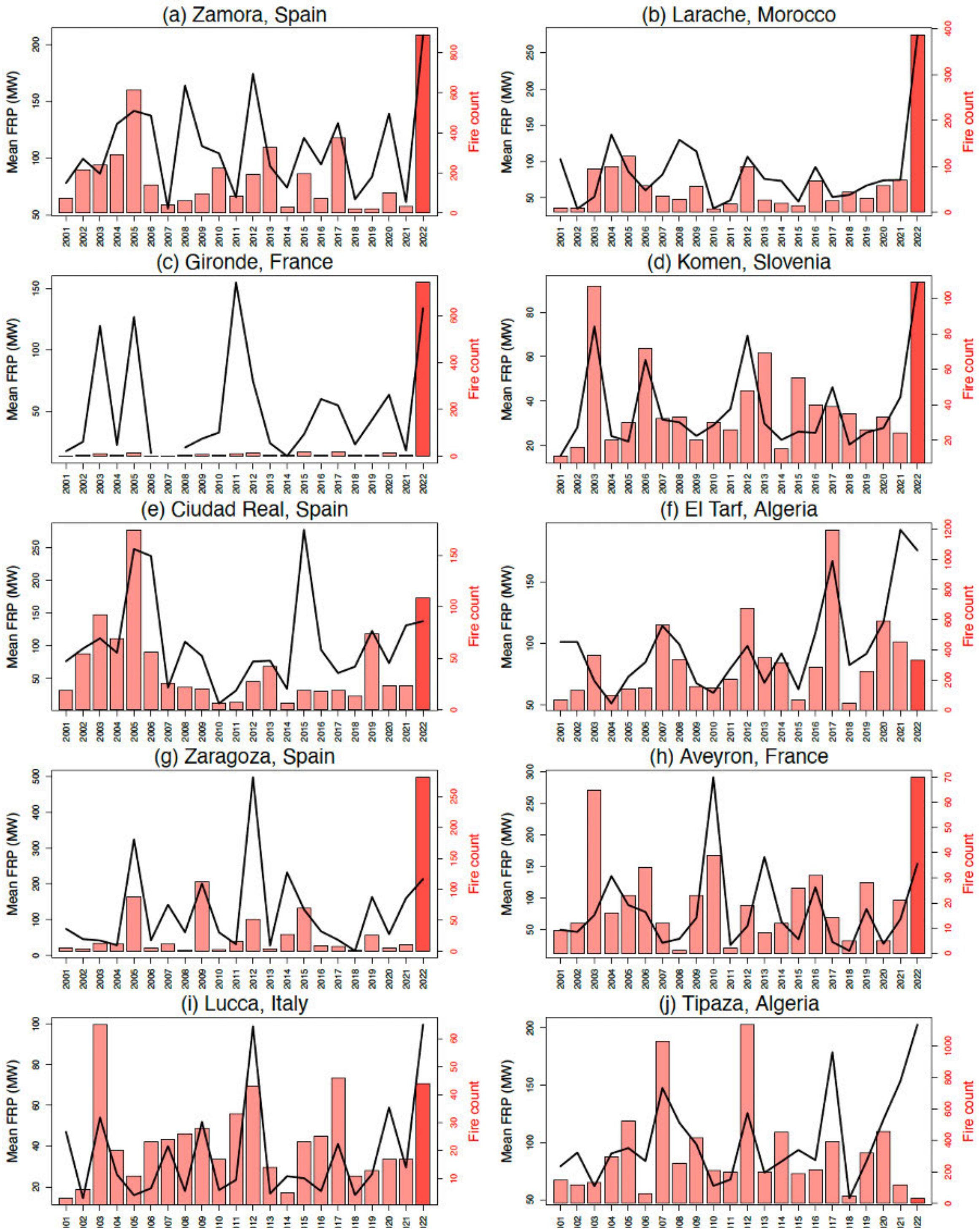

Figure 5.12: (a)-(j) Annual mean FWI (black lines) and the number of the fires (red bars) occurred during the period June-August from 2001 to 2022 at selected ten sites. In each case, fires are counted when the FRP value is above 500 WM.

FWI values in Gironde show an obvious increase until the event date of 18 July, with the highest value of 66.2, which is about doubled the 95th percentile of FWI during JJA 2022 (Table 5.2; Figure 5.11c). A large number of extreme fires occurred during the event date in mid-July, where similar intense fires associated with a similar trend in FWI emerged again around 10 August 2022. The number of fires reached an extremely high value of over 600, compared with the previous years of no more than 50 since 2001 (Figure 5.12c).

Hotspot (d): Wildfires in Komen, Slovenia on 20 July 2022 - The first wildfire in the Karst region in Komen (Slovenia) started on 15 July 2022, spreading by extreme heatwaves with strong winds and covering burning land as much as 3,705 hectares in 17 days (Korosec, 2022; Žarkovič, 2023). In total, approximately 15,000 firefighters battled the uncontrolled blaze to save the numerous villages and towns in the area, in addition to local volunteers and support from neighbouring countries (**?**). The highest fire radiative power (2269.8 MW) observed in the Korman region of Slovenia occurred on 20 July 2022, with a corresponding FWI value above the 95th percentile at around 21.6 (Table 5.2; Figure 5.11d). It is noteworthy that the fire started spreading around 15 July, and the corresponding FWI which reflects the weather conditions that are conducive to fires also reached its peak during this period in the summer of 2022. Additionally, the mean FRP and the fire counts both reached the highest in the year 2022 (Figure 5.11d).

Hotspot (e): Wildfires in Ciudad Real, Spain on 25 July 2022 - During summer 2022, extreme weather conditions that were conducive to wildfires (FWI > 95th percentile) occurred several times in the region of Ciudad Real in Spain (Figure 5.11e). Comparatively high FWI values were observed throughout the period in this area, differing from other wildfire events (Figure 5.11e). The most intensive fire (2209.4 MW) occurred on 25 July, when the FWI also reached its highest value of 87.0 (Table 5.2; Figure 5.11e). With regards to the mean FRP values and the number of fires, 2005 saw the highest record since 2001, while 2022 has the second largest fire count in this region (Figure 5.12e).

Hotspot (f): Wildfires in El Tarf, Algeria on 17 August 2022 - Since the commencement of August, Algeria has witnessed a staggering total of 106 fires, resulting in the devastation of over 2,500 hectares (6,200 acres) of woodland. Tragically, at least 26 people have lost their lives, and dozens more have sustained injuries due to the fires (The Guardian, 2022). Of particular concern were the fires in El Tarff (Reliefweb, 2022) in northern Algeria, near the Tunisian border, in which nearly 2,600 hectares were burned (Alkhaldi, 2022) and 24 people died with hundreds forced to leave their homes (The Guardian, 2022). Despite being the largest country in Africa, Algeria has only 4.1 million hectares (10.1 million acres) of forest and the north of the country is affected by forest fires every year, a problem that has worsened especially in recent years due to the climate crisis (The Guardian, 2022; Aljazeera, 2022c). Whilst there were some wildfires in the El Tard area of Algeria in June and July 2022, the most intensive fire occurred on 17 August, with a series of fires occurring on the same day (Figure 5.11f). The observed FWI value nearly doubled the 95th percentile during the summer from 1979 to 2022, at 109.6, with a corresponding FRP at 1775.6 MW (Table 5.2; Figure 5.11f). The mean FRP value in 2022 is the second-highest record since 2001, although the fire count is not that significant compared to the other years (Figure 5.11f). The mean FRP of this hotspot in 2022 reached the highest while the number of fires observed is around average-level (Figure 5.12f).

Hotspot (g): Wildfires in Zaragoza, Spain on 19 July 2022 - Wildfires in Zaragoza, Spain started on Tuesday 19 July 2022 and had been stabilized in three days on 21 July (Yahoo, 2022). The fire occurred in Ateca (Zaragoza province of Spain) and led to the closure of all train services with Madrid, Aragon and Catalonia as well as causing the burning of approximately 14,000 hectares on Wednesday (Yahoo, 2022; Aljazeera, 2022d). Weather conditions during summer 2022 in Zaragoza, Spain show a significant upward trend since early July and peaked at 80.7 on the event date of 19 July (Table 5.2; Figure 5.11g). Major fires are observed mainly in mid-June, July, and August while the fire weather indicator, FWI, also appears to have relative peak values at the same time (Figure 5.11g). The mid-July fires were the fiercest in terms of the frequency and intensity of fires, with the most dramatic lift in fire weather conditions in this region for this period (Figure 5.11g). Differring from Hotspot (f), the record of 2022 shows the highest fire counts of Hotspot (g) with the mean FRP not that exceptional (Figure 5.12g).

Hotspot (h): Wildfires in Aveyron, France on 13 August 2022 - On August 10 2022, wildfires engulfed the area around Mostuéjouls in the southern department of Aveyron, France (Reuters, 2022). The impact has been substantial, with over 750 hectares of vegetation reported burned as of August 12. In response to the escalating threat, approximately 3,500 people have been evacuated from the affected region (Brent, 2022). A few days later on Saturday 13 August, a reignited extreme fire broke out in the same area which forced the evacuation of over 1,000 people and burned more than 500 hectares, with a total of 1,260 hectares within a week (The Local, 2022; Science X, 2022). Fire weather conditions in Aveyron (France) during the summer of 2022 saw great fluctuations, particularly from late July to mid-August (Figure 5.11h). A series of fires alongside relatively high FWI values were witnessed in late July, but FWI values dropped rapidly after the events. Then, similar situations occurred twice until the most intensive fire (1470.8 MW) emerged on 13 August, with the fire weather indicator at around 39.1 (Table 5.2; Figure 5.11h). Similar to Hotspot (g), the fire count reached the highest to show the exceptionality of the fire activities that occurred in this hotspot (Figure 5.12h).

Hotspot (i): Wildfires in Lucca, Italy on 19 July 2022 - Wildfires erupted in Massarosa of Lucca, Italy, on the evening of Monday July 18 2022 (Cater, 2022). The situation persisted through Wednesday, leading to the evacuation of 500 people (Bressan and Agency, 2022). A helicopter intervention was initiated to control the fire, which, as of July 22, had ravaged over 900 hectares within a span of five days (Wikipedia, 2022). Although the fires observed in Lucca in the summer of 2022 were limited compared to other hotspots, wildfires that occurred on 19 July were still intense with FRP around 1500 WM (Table 5.2; Figure 5.11i). Corresponding FWI values around the event date were not as high as the other sites, they exceeded the 95^{th} percentile of the summer FWI in the period of 1979-2022 in this area, which are also very extreme and rare to experience. In Hotspot (i), the fire intensity presented by the fire radiative power is the highest since 2011, with a relatively higher number of fires observed in 2022 (Figure 5.12i).

Hotspot (j): Wildfires in Tipaza, Algeria on 14 August 2022 - In the forests of Mount Chenoua in Tipaza (Algeria) wildfires broke out on 14 August 2022 (Saada, 2022). As the event was located in the 1^{st} Military Region, helicopters that belonged to the Air Force participated to control the fire event, helping to reduce the losses (Saada, 2022). Major fires can be witnessed in mid-August in Tipaza (Algeria) with the most intensive one occurring on 14 August 2022 (Figure 5.11j). From late June to mid-August, FWI showed an increasing trend at 89.5 on the event date, while the highest FRP value occurred at 1095.2 MW at the same time (Table 5.2; Figure 5.11j). During the period of 2001-2022, the 2022 event shows the highest fire radiative power and the lowest fire count in Hotspot (j), potentially revealing the extreme intensity of this wildfire event (Figure 5.12j).

5.3.3.4 Attribution and projection of changing risks in extreme fire weather

Overall, the probabilities of the 2022-type events occurring across the Euro-Mediterranean region show statistically significant increasing trends either between the past and present climate or from recent to future scenarios, by using CanESM5 externally forced warming temperatures (Figure 5.13a-j). In the past climate during the period 1910-1919, seven of the ten events have a return period of around 20 years, while five of those events were likely to occur approximately every 50 years or more (Figure 5.13a-j). $PR_{1.5}$ and $PR_{2.0}$ in the future scenarios vary, with eight of the ten events likely to occur within every ten years, and three of these becoming less than five years in return period when the global warming level reaches 1.5 °C (Figure 5.13a-j). In a warmer world with a 2.0 °C rise in GMST, six of the ten events are likely to happen again within or around five years, with three of them having a return period of around three years (Figure 5.13a-j). The three most intensive wildfires that occurred in Zamora, Spain (Hotspot a), Larache, Morocco (Hotspot b), and Gironde, France (Hotspot c) all show return periods of around or over 50 years in the past climate of 1910-1919, and all the hotspots of the events become more frequent in the present climate of 2010-2019 and future scenarios (Figure 5.13a-c).

In Spain alone, three major wildfires were witnessed in Zamora, Ciudad Real and Zaragoza during 18-25 July 2022, ranked the first, fifth, and seventh in terms of the FRP across the study hotspots. PR results in Zamora, Spain illustrate one of the largest increases in likelihood over all the ten sites between the past climate (1910-1919) and the present climate (2010-2019), as well as the future climate for the 1.5 °C and 2.0 °C scenarios, with PR ranging from 2.9 to 7.5 $PR_{1.5}$ ranging from 2.1 to 2.8 and $PR_{2.0}$ ranging from 2.6 to 3.5, separately (Figure 5.13a). Events occurred in Ciudad Real and Zaragoza present similar results in PR, $PR_{1.5}$, and $PR_{2.0}$, with ranges from 3.0 to 5.0, 1.9 to 2.1, and 2.2 to 2.5 for the former, and 3.4 to 6.0, 2.0 to 2.3, and 2.4 to 2.8 for the latter, separately (Figure 5.13e, g).

Wildfires that occurred in mid-July 2022 in Gironde (France) are associated with the highest PR results among all the ten hotspots, while the current fire weather condition has become five times more likely (95% CI range: 4.0-7.2) to occur compared to the past, and is estimated to increase by a factor of 2.6 (95% CI range: 2.4-2.8) and 3.2 (95% CI range: 3.0-3.6) under 1.5 °C and 2.0 °C global warming levels respectively (Figure 5.13c). Later in mid-August 2022, another wildfire raged in Aveyron. Although the return period of this event ($\sim$ 14 years) in the past is not as rare as others, it is still 2.2 (95% CI range: 2.0-2.3) times more likely to occur in the present climate, with $PR_{1.5}$ of 1.7 (95% CI range: 1.7-1.8) and $PR_{2.0}$ of 2.0 (95% CI range: 2.0-2.1) in a warmer future (Figure 5.13h).

During the same period, there were two wildfires in El Tarf and Tipaza (Algeria), for which the PR values show an approximate doubling likelihood (El Tarf: 2.0, 95% CI range: 1.8-2.2; Tipaza: 1.7, 95% CI range: 1.5-1.9) under recent climate conditions (Figure 5.13f, j). In the past, such events had a 45-year and 30-year return period, respectively, in contrast to the current return period of approximately 20 years. Changes in likelihood are more than 70% (El Tarf: 98%; Tipaza: 80%) when an increase in GMST reaches 1.5 °C and over 100% (El Tarf: 143%; Tipaza: 114%) when GMST reaches 2.0 °C in the future (Figure 5.13f, j).

Weather conditions conducive to wildfires in the Larache region of Morocco, again, show significant increases from the past to present, as well as from the present to the warmer future (Figure 5.13b). The change in probability between the past (1910-1919) and present (2010-2019) climate is a factor of 2.0 (95% CI range: 1.7-2.4), while that between the present

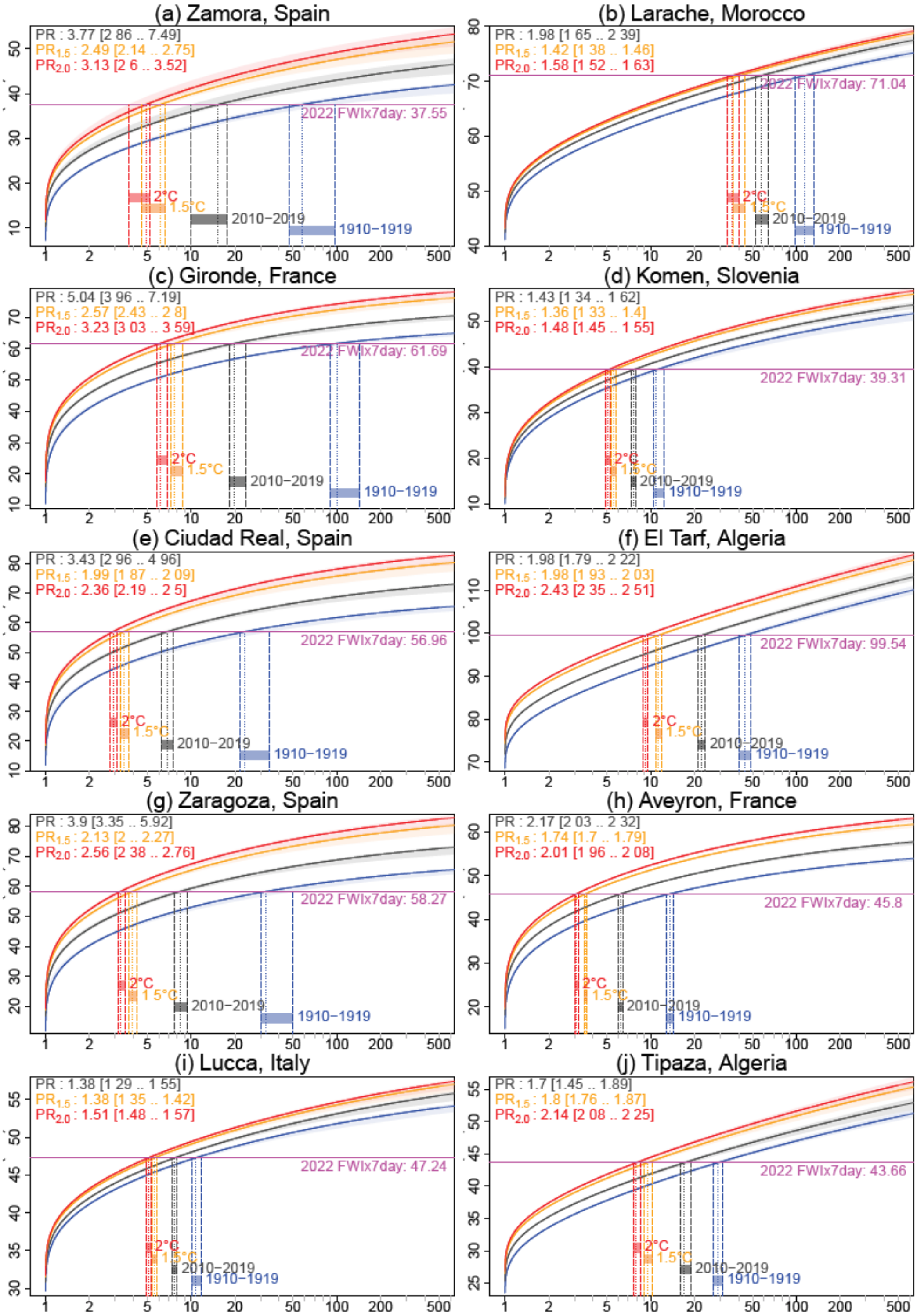

Figure 5.13: (a)-(j) Gumbel plots for the ten sites of wildfires, showing the GEV model fit scaled to the ensemble mean of GMST for the period 1910-1919 (blue), 2010-2019 (black), the period that GMST reached by 1.5°C (orange) and the period that GMST reached by 2.0 °C (red). Dashed lines represent the 95% CIs following a 1000-sample non-parametric bootstrapping. The magenta lines represent the 2022-type wildfire event in each case, scaled to the model distribution using bias correction. The blue, black, orange and red bars represent the 95% CIs for the return period of these 2022-type events in the climate from 1910 to 1910, 2010 to 2019, the period that GMST reached by 1.5 °C and the period that GMST reached by 2.0 °C.

climate and future scenarios of 1.5 °C and 2.0 °C warming levels are 1.4 (95% CI range: 1.4-1.7) and 1.6 (95% CI range: 1.5-1.6), separately (Figure 5.13b).

The return period for the wildfire events that occurred in the Komen region of Slovenia in the past climate has a value of around 10 years, while the return value of the same type of events is around 7.5 years in the present climate, and around 5-5.5 years in future scenarios (Figure 5.13d). This indicates the statistically significant increases in PR with a factor of 1.4 (95% CI range: 1.3-1.6), $PR_{1.5}$ of approximately 1.4 (95% CI range: 1.3-1.4) and $PR_{2.0}$ of 1.5 (95% CI range: 1.5-1.6), the lowest central value and smallest range of PR results of all ten hotspots (Figure 5.13d). Like the wildfires that occurred in Slovenia, the present fire weather conditions occurred in Lucca, Italy, had an increase in PR by approximately 40% compared to the past (Figure 5.13i). In addition to the future scenarios, the positive changes in likelihood compared to the current weather conditions are about a factor of 1.4 ($PR_{1.5}$) and 1.5 ($PR_{2.0}$) respectively (Figure 5.13i).

5.3.3.5 Attribution and projection synthesis across the region

The synthesis results across the ten hotspots in the Euro-Mediterranean region suggests that the weighted average of the likelihood of the 2022-type events increased by a factor of 1.8 (95% CI: 1.7-1.9; Figure 5.14a) over the last century as a result of rising global temperatures. The calculation of the weighted average across the ten hotspots matches the method introduced in Case Study 2 (section 5.2.3); the weights for each event's PR are given by the inverse of the squared uncertainty, with the uncertainty of the weighted average approximated by adding the errors for each PR estimate in quadrature (*e.g.*, Philip et al., 2018). The likelihood of such events is estimated to increase further by factors of 1.6 and 1.8 in the future risks under 1.5 °C and 2.0 °C global warming levels respectively (Figure 5.14b, c).

For the estimated change in likelihood during the last century, PR results range from 1.4 (Lucca, Italy) to 5.0 (Gironde, France), with large discrepancies witnessed between different hotspots, and up to 7.2 times more likely to occur across the study region (Figure 5.14a). Apart from France, which has the highest increase in PR, the three most substantial positive changes in PR over ten hotspots are all in Spain, where the fire weather conditions have become at least 3.2 times more likely to occur according to the central values (Figure 5.14a). The other six sites all have increasing trends in PR, ranging from 1.4 (Lucca, Italy) to 2.2 (Aveyron, France) (Figure 5.14a). By averaging the results over the study region, it suggests that fire weather extremes are around 80% more likely to occur as a result of externally forced warming temperatures (Figure 5.14a).

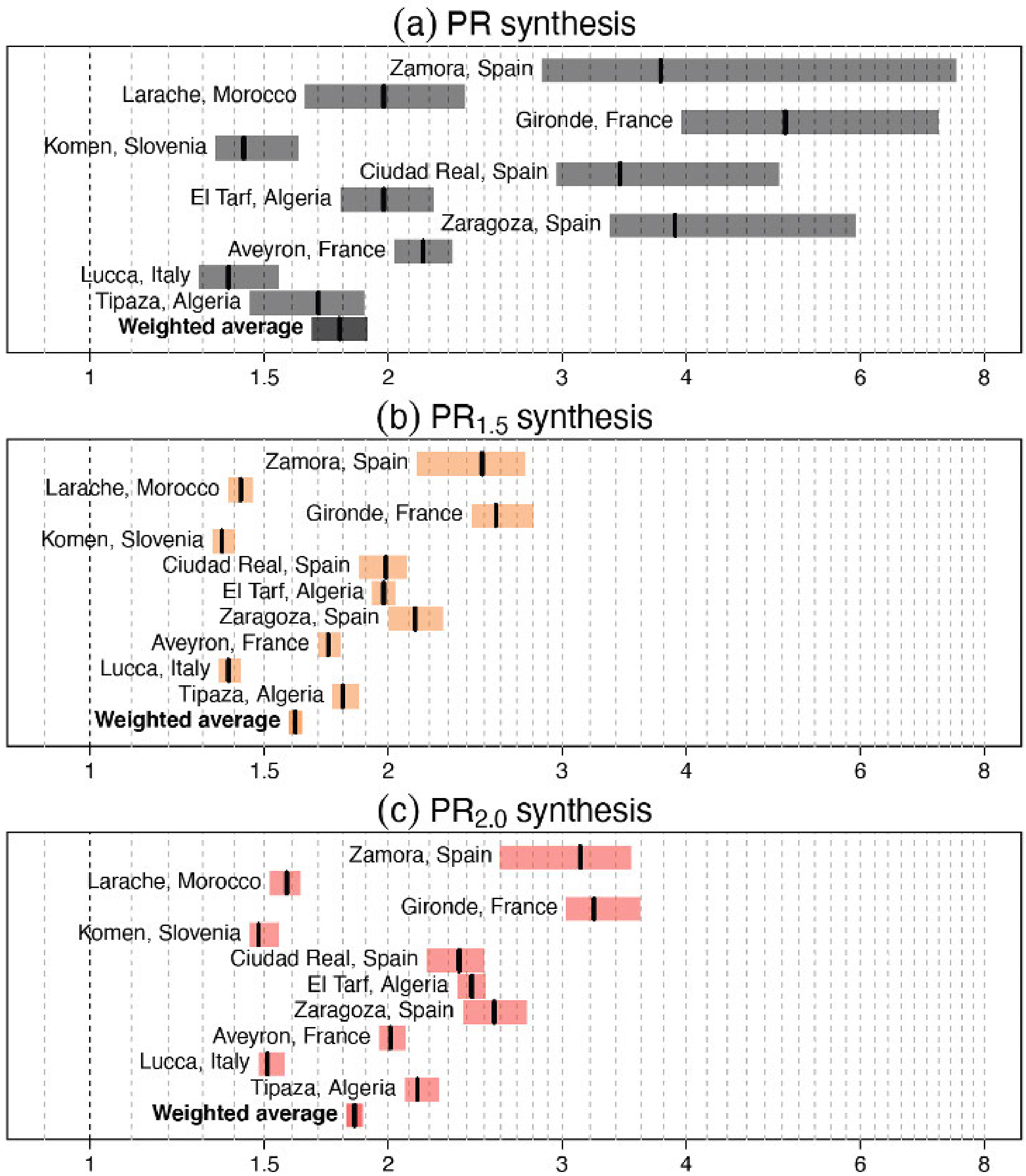

Figure 5.14: PR estimates based on the comparison between (a) the past climate of 1910-1919 and the present climate of 2010-2019, (b) the present climate of 2010-2019 and the period that GMST reached by 1.5°C and (c) the present climate of 2010-2019 and the period that GMST reached by 2°C for the ten sites of wildfire events in Southwest Euro-Mediterranean regions in summer 2022 by using CanESM5 and the corresponding weighted averages. Bars show 95% CIs; central values are shown in bold.

In terms of future scenarios, results in $PR_{1.5}$ present a great consistency of the events across ten hotspots, averaged as around 60% more likely to occur compared to the present climate conditions, with increasing likelihoods ranging from 1.3 (Komen, Slovenia) to 2.6 (Gironde, France) accordingly (Figure 5.14b). Like the results between the past and present climates, the 2022-type events that occurred in four sites in both Spain and France show the highest positive changes in likelihood as a factor between 2 and 2.6, while the other six sites present the relatively small but still significant increases from 1.3 to 2, separately (Figure 5.14b). In a warmer world with 2.0 °C warming level, results in $PR_{2.0}$ show a slightly higher risk in fire weather conditions compared to the 1.5 °C warming level, with extreme fire weather becoming 80% more likely to occur (Figure 5.14c). Wildfires occurred in Zamora, Zaragoza and Ciudad Real in Spain and Gironde in France still rank one of the highest risks in fire weather conditions with a factor from 2.4 to 3.1, while the two wildfires occurred in El Tarf and Tipaza in Algeria also present the changes in likelihood that is 2.4, and 2.1 times more likely to occur respectively, as a result of global warming (Figure 5.14c).

5.3.4 Conclusions

Analyses in this study aim to summarize and quantify the influence of the changing climate on extreme fire weather occurring across the Euro-Mediterranean region in the summer of 2022. An established statistical approach was applied by using the output from the CanESM5 large ensemble to estimate how the likelihood of the 2022-type fire weather conditions have been and will be altered by anthropogenic climate change, expressed here as the change in global mean surface temperature since 1850. The results were collectively averaged across multiple selected locations where fire events occurred and an average probability ratio of 1.8 was found, *i.e.*, an overall increase in likelihood, approximately 80%, during the last century, and a further increase of 60% and 80% under 1.5°C and 2.0° global warming levels respectively. Diagnosing variations in the extremes of occurrence of different wildfire events in the same region, further across different timescales spanning past, present, and future, is challenging and a potential avenue for research.

These results complement the positive trends in observed extreme fire weather revealed in recent works (Jain et al., 2022; Liu et al., 2022a) and clearly underline the importance of assessing present-day risk assessment and attribution studies further with future risks. For all events selected over the study area, the attribution results and the assessment of future risks are showing a positive trend in the probability of extreme fire weather. Nevertheless, the PR, $PR_{1.5}$ and $PR_{2.0}$ of such extreme fire-prone weather are relatively higher in Spain and southern France. In addition, we note that the range for PR is relatively larger compared to the range for $PR_{1.5}$ and $PR_{2.0}$ present relatively the highest values. The range for PR, in particular, is relatively larger compared to the range for $PR_{1.5}$ and $PR_{2.0}$ based on model simulations under future scenarios, due to the larger scale of data for longer years in the future scenarios, resulting in less uncertainty in the changes.

Attribution research has emerged to answer public questions about to what extent has anthropogenic climate change altered the occurrence of extreme events, such as extreme fire weather. This development has led to the quantification and estimation of extreme weather events with complex causes, such as wildfires and droughts, to help different stakeholders to respond. In addition, the inter-temporal information spanning from past, present, and future in this research analysis would make the findings more accessible to different stakeholders and provide relevant recommendations.

Chapter 6

Conclusions and outlook

6.1 Summary and Conclusions

In the context of climate change, wildfires have occurred more frequently and intensively across the globe in recent decades, posing enormous risk to natural and built environments and human livelihoods. This has led to significant public concern about the prevalence, spread, and impact of wildfires, and ultimately questions about the extent to which climate change is altering the meteorological conditions conducive to wildfires. Over the last decade, the emergence of attribution studies of high-impact weather and climate has sought to answer such questions. However, to date, attribution studies of wildfires have been far less common than those of other heat-related extremes (such as heatwaves and drought) due to the limited record from observational datasets, and the lack of consensus on the most appropriate and effective methodological approach for wildfire attribution.

The aim of this PhD project has been to develop a globally applicable empirical-statistical framework to better understand and quantify the changing nature of wildfire risk in the face of a changing climate. The research was motivated by three key themes, originally outlined in Chapter 1 (section 1.6): (a) the increasing prevalence and impact of severe wildfires in many parts of the world; (b) the relative paucity of wildfire, or otherwise fire weather, attribution studies and, consequently, the uncertainties associated with conducting such studies; (c) the potential of empirical-statistical methods to provide robust conclusions when applied to data from both observations and the latest generation of climate models. The development of the framework has shed considerable light on the implications of attributing fire weather extremes across the world and several methodological considerations, including the spatiotemporal event definition, the choice of an appropriate fire weather indicator and the selection, evaluation, and bias correction of climate models.

This chapter draws together the key findings of this research and details considerations for further study. In the remainder of section 6.1, the three research questions and related objectives outlined in Chapter 1 (section 1.6) are reasserted and discussed in terms of how each has been addressed and answered. In section 6.2, the limitations and scope for further research are identified and discussed.

6.1.1 Research Question 1: *To what extent can observed worldwide changes in extreme fire weather during recent decades be linked to warming global temperatures?*

Objective 1.1: To develop and apply a global approach for extreme fire weather attribution upon which future studies can build. Despite the growth of attribution science in recent years, there are still relatively few studies for certain types of extreme events, such as wildfires, due to the complexity of understanding their physical mechanisms (for wildfires, in the ignition and spread particularly) and the difficulties posed by the lack of data. In Chapter 3, a probabilistic framework based on extreme value distributions was proposed, bridging the gap in this subfield by applying protocols to other well-understood extreme event types. Based on this framework, an established empirical-statistical method was used to construct a global approach for attributing extreme fire weather events (cf. Chapter 3).

Objective 1.2: To evaluate the uncertainty concerning the choice of fire weather indicators and metrics in linking regional trends in observed fire weather extremes to global warming temperatures. In Chapter 3, a set of fire weather indicators from the CFWIS were assessed in all fire-prone areas of the world. On the global scale, a positive trend was found in the seasonal averages of each index, and this is in line with the observed global fire weather and its relationship with climate change (Jain et al., 2022). Differences between indicators and their link to burned area were generally marginal, there are several examples of significant discrepancies at the regional scale. Notably, FWI is not systematically the best match for fire activity, suggesting that other indices have the potential to be more appropriate proxies for fire risk in specific areas. With respect to attribution analysis, different indicators lead to different results, depending on the variability and nature of extreme fire weather in different regions of the world. Therefore, it is vital to explore the availability and merits of indices or indicators that can be used to represent fire weather and to fully demonstrate their application in event attribution.

In addressing Research Question 1, the following conclusions can be made:

- Most of the world is associated with an increase in mean fire weather for all five CFWIS indices. More than 25% of fire-prone grid points for all indices, including the Americas, Australia, Europe, central Asia, and central and southern Africa, show a significant positive trend.

- In about 40% of the world's fire-prone grid points, particularly in temperate North America, Europe, Africa, Boreal and Central Asia, the likelihood of an extreme fire weather increases by a factor of four (PR>4) in response to global warming in temperature. On the other hand,

- A decrease in the likelihood (PR<1) in response to a rise in global temperature suggests that extreme fire weather appears to be less likely across all CFWIS indices in South Asia, Southeast Asia, Northern Hemisphere South America, Western West Africa, Southern and Eastern Africa.

- While spatial patterns in likelihood are relatively similar across the CFWIS indices, some areas, such as Australia, display markedly different results, highlighting the sensitivities to the choice of fire weather indicators.

- A set of recent exceptional extreme fire weather episodes are classified according to the observational record, demonstrating how collective conclusions can be drawn from the attribution of multiple events.

6.1.2 Research Question 2: *What do state-of-the-art global climate models reveal about the extent to which extreme fire weather across the world has been altered as a result of anthropogenic climate change?*

Objective 2.1: To evaluate the performance of climate model large ensembles in representing extreme fire weather. As the number of wildfire attribution studies grows, there is an obvious need to continue to develop an understanding of the sources of sensitivity and uncertainty associated with the results of these studies, particularly when it comes to the most recent generation of climate models. In Chapter 4, a set of six large ensembles (>10 members) from CMIP6 were evaluated. Generally, all models can reasonably represent the fire weather extremes although considerable regional differences are apparent. Best practice should include a model evaluation and/or selection step.

Objective 2.2: To estimate the changes in extreme fire weather conditions using multi-model large ensembles from the latest generation of climate models. In Chapter 4, following the empirical analysis (Objective 1.1), the same statistical methodology was applied to the six large ensembles from CMIP6 to conduct the first global probabilistic attribution of both the intensity and duration of extreme fire weather. Across much of the world's fire-prone regions, most models show a 2-fold increase in likelihood of extreme fire weather occurrence as a response to globally warming temperatures since the pre-industrial era, particularly in southern North America, south-eastern Europe, and southern Australia. This trend is broadly consistent with the current understanding of global fire weather activity and its relationship to climate change (*e.g.*, Jain et al., 2022).

Objective 2.3: To facilitate and simplify communications from climate change modelling studies, while dealing with large uncertainties. For some regions, differences between models are evident, manifesting the large non-negligible uncertainties associated with the application of a single model and fewer simulations. This demonstrates the importance of integrating the results of multiple climate models. In Chapter 4, synthesis plots were generated from the results of the six CMIP6 model ensembles. Following the model evaluation and selection to remove weaker-performing models, the results from the model subset were combined and averaged. The result was the generation of more reliable global maps of model-simulated changes the likelihood of fire weather extremes defined by both intensity and duration.

In addressing Research Question 2, the following conclusions can be made:

- All six large-ensemble CMIP6 models realistically simulate extremes in both fire weather intensity and duration. There are considerable regional differences among models.

- The probability ratio of extremes in fire weather intensity has increased at least twofold (PR>2) as a result of externally forced global warming in many parts of the world, including central and southern North America, northern South America, and southern Africa.

- The probability ratio of more prolonged extreme fire weather conditions has increased noticeably by at least a factor of two (PR>2), particularly so in southern North America, almost all over South America, southern Africa, Central and Southeast Asia, and parts of Australia.

- A model evaluation and selection step avoids the over- and under-estimation of the probability analysis, offering a more robust synthesis results.

6.1.3 Research Question 3: *How is climate change altering the risk associated with recent episodes of high-impact fire weather?*

Objective 3.1: To conduct attribution analysis on a series of extreme fire weather case studies in different parts of the world. Based on the established framework and the global results shown in Chapters 3 and 4, a set of attribution case studies are conducted in Chapter 5. Three wildfire events were selected in Siberia in 2020 (cf. Chapter 5.1), Cape Town in 2021 (cf. Chapter 5.2) and Euro-Mediterranean regions in 2022 (cf. Chapter 5.3).

- **2020 Siberian wildfires**. This event covered a relatively large area. By selecting one of the best performing CMIP6 models, CNRM-CM6-1, attribution results show 8 of the 13 study point (termed "hotspots") with an average of 10% increase in likelihood in light of global warming temperatures. This study provided an initial attempt to attribute simultaneously multiple extreme fire weather episodes.

- **2021 Cape Town wildfire**. The far smaller spatiotemporal scale of this event is a potential source of greater uncertainty, and an opportunity to emphasise the value of using multiple climate models. Averaging the results from multiple models revealed an overall increase in likelihood of 2021-type conditions of around 90%. This second case study demonstrates that even relatively coarse globals climate models can still deliver accurte and reliable results in studies on very limited spatiotemporal scales.

- **2022 Euro-Mediterranean wildfires**. In the third case study, the framework is extended for risk assessment of projected changes in risk in a future climate. The CanESM5 model was chosen on the basis of its large set of 50 realisations, available for both the past and the future. A collective averaging of results from multiple selected locations where fire events occurred found an average increase in probability by approximately 80% compared to 100 years ago, with a 60% increase in 1.5°C warming levels and an 80% increase in 2.0°C warming levels compared to today under a future scenario of continued global temperature increase. This study poses the inter-temporal information by combining the previous collective synthesis results to make the findings more accessible to meet the diverse needs of society and academia.

Objective 3.2: To explore the potential for collective attribution of multiple extreme fire weather events. Throughout the analysis of those three cases, the final objective is also highlighted. Examples of how the fire danger of a specific wildfire event should be defined in a meteorological context are conducted, with attempts at model selection and synthesis in three disparate case studies. These provide the opportunity to give the most robust statements and recommendations to the public and stakeholders.

In addressing Research Question 3, the following conclusions can be made:

- As a result of global warming, the meteorological conditions that coincided with extreme wildfires in Siberia during 2020 were up to 80% more likely compared to a century ago, with a 10% increase in average across the study region.
- According to the six large-ensemble CMIP6 models, the likelihood of the extreme fire weather associated with the April 2021 wildfire in Cape Town has increased by 90% due to the external forced warming temperatures.
- Across the Euro-Mediterranean regions, an overall increase in likelihood of approximately 80% compared to one hundred years ago, and an increase of 60% at 1.5 °C warming level and 80% at 2.0 °C warming level compared to the present climate condition can be found for the 2022-type events in the context of continued global temperature increases in the future.

The results presented in this thesis shed light on attributing global fire weather extremes and typical wildfire cases spanning the changes from the past to the present, as well as from the present to the future. It is hoped that the results of the research presented here will contribute to the development of attribution study in fire weather extremes, offering robust recommendations to reduce and address the hazards posed by wildfires and to improve post-disaster resilience.

6.2 Limitations and scope for further research

The results generated by this research have shed light on the sensitivities and uncertainties associated with attribution of fire weather extremes. These include the choice of an appropriate spatiotemporal definition for the extreme event, the choice of fire weather indicator(s), and the selection, evaluation and, potentially, bias correction of the climate models(s). In the pursuit of accurate and reliable overall findings, it is crucial for further study give full consideration to these uncertainties and sensitivities, in addition to other limitations, which are hereby discussed with respect to potential avenues for future research.

6.2.1 Recent developments in representing fire danger

This work has focused exclusively on the set of fire weather indicators derived from the CFWIS. These indicators, particularly FWI, have been widely applied in many parts of the world. However, it is important to consider other fire risk indices that have also been proposed for different applications. These include the energy release component (ERC) from the United States (US) national fire danger rating system and the Keetch-Byram drought index (KBDI) from the US Department of Agriculture's Forest Service. These indices are included within National Fire Danger Rating System (NFDRS), and estimate, respectively, how hot a fire could burn, the effects of intermediate to long-term drying, and the net effect of evapotranspiration/precipitation in producing cumulative moisture deficiency in deep duff (Keetch and Byram, 1968; Hall et al., 2003). Like the FWI, the NFDRS system is based on environmental factors to understand the influence of ignition, spread, and behaviour of wildland fires, but with slight differences in input requirements and sensitivities to alterations in individual weather variables, such as temperature, precipitation, relative humidity and wind speed. Similarly, the McArthur Forest Fire Danger Index (FFDI) from the Centre for Australia Weather and Climate Research is widely used by Australian fire authorities to provide daily forecasts of the impact of weather on fire activity (Dowdy et al., 2009).

Furthermore, an index that only includes weather inputs without the state of wildland fuels or topography was introduced as the Lower Atmospheric Severity Index, known as the Haines Index (HI; Haines, 1988). The Hot-Dry-Windy Index (HDW) conducted by Srock et al. (2018) considers the potential for the atmosphere to affect a wildland fire by using meteorological variables such as temperature, moisture, and wind. In addition, the extreme-fire behavior index (EFBI; Artés et al., 2022) which considers the deep moisture convection is conducted to focus on how easily the fire behavior can change. These indices are particularly beneficial for investigating specific weather conditions such as wind shifts, thunderstorm outflows, and other complicated phenomena during a wildfire, illustrating the potential for wildland fire predictions and the forecast of extreme fire behavior (Srock et al., 2018; Artés et al., 2022).

While studies on specific indices can indicate the detailed alterations caused by climate change directly, intercomparison of multiple fire risk indices may help further understand weather and climatic driving mechanisms, better provide robust information on attributing extreme events and potentially inform forecasting systems for the future.

6.2.2 Advanced postprocessing methodologies for climate models

While GCMs are acknowledged as the major source of knowledge about future climate, they cannot provide entirely unbiased outputs (Maraun, 2016). Extreme events sometimes occur on a local scale, which is below the typical model resolution (50-200km); therefore, higher resolution for simulations, statistical postprocessing such as hybrid statistical-dynamical downscaling, ensemble bias-correction, or stochastic modelling are necessary to solve the problem (Kirchmeier-Young et al., 2019b). A good example from Hoerling et al. (2014) provided strong evidence in the importance of simulating resolutions, which was beneficial for the further step of statistical analysis. Additionally, to bridge the gap in regional-scale information and govern regional- to local-scale extreme events, regional climate models (RCMs) are becoming popular in the field (Maraun, 2016), such as convection-permitting regional climate models which provide more robust climate projections and better identification of their associated uncertainties (Lucas-Picher et al., 2021). Except for the bias from the aspect of poor understanding of physical algorithms, it is also helpful to reduce the the impact of internal climate variability by using a large ensemble mean of climate models with different forcing and scenarios (Otto et al., 2016; Stott et al., 2016). Then, the approach of bias correction, for correcting the systematic difference between a climatic statistical simulation and the corresponding real-world climate (Maraun, 2016), offers further possibilities to reduce uncertainty.

Most bias corrections, such as quantile mapping, are applied to univariate time series. The neglection of the connections between different variables often affect the accuracy of simulations (Cannon, 2018; Vrac, 2018). The recent advanced bias correction method, so-called multivariable bias correction algorithm, is advised by Cannon (2018), and offers an inspiring way to improve the accuracy of relative models. This approach has been applied by Kirchmeier-Young et al. (2017b) for the attribution research of fires in western Canada, obtaining four variables (air temperature, relative humidity, wind speed, and precipitation) with a multivariate dependence structure. Advanced bias correction and downscaling within the post-processing methodologies also offer a good point for improving the accuracy of simulation outputs and strengthen the robustness of wildfire attribution studies, especially for the regions of complex topography (Shepherd et al., 2018).

Additionally, as climate models are further developed, there is likely to be more emphasis on available and reliable modelling of extreme values, which will potentially allow more models to be included in the synthesis step to discretize uncertainty in the communication process (van Oldenborgh et al., 2021b). Therefore, while the individual GCM and RCM remain biased, the choice of the weighted scheme may be crucial to provide a more robust synthesis result. Except for the simple weighted average from multiple model results (*i.e.*, reliability ensemble averaging; Giorgi and Mearns, 2002, 2003), weighting schemes, considering both model performance and interdependence (Knutti et al., 2017), have been developed for a better understanding of the uncertainty and sensitivity in climate models and may prove beneficial in the pursuit of the most realistic simulation of fire weather extremes.

6.2.3 Novel techniques for attributing extreme events

Essentially, attribution studies are a kind of estimation problem tightly associated with statistics (Stott et al., 2017). Based on this relation, some efforts have been inspired by the possibility of applying Bayesian approaches, as an alternative way to solve this problem (Coles, 2001). As early as 1996, Coles and Powell published a paper about the Bayesian methods in extreme value modelling. Based on the prior experience, posterior distribution can be obtained by the potential likelihood of the prior events (Coles and Powell, 1996). However, a criticism of Bayesian approaches is that the result is strongly affected by the prior distribution, which can subjectively be selected by humans (Stott et al., 2017). In this case, the application of non-conditional probabilities that consider the risk irrespective of the meteorological cause is desirable for a more generalized attribution (Otto et al., 2016).

Aside from the distinction between slight differences in probabilistic attribution studies, the “storylines” approach originally proposed by Clark et al. (2016), to bypass the uncertainty in physical aspects of climate change, has recently been applied in the context of attribution (Shepherd et al., 2018). This approach concentrates on describing the extreme event rather than seeking to calculate probabilities of the risks, namely aims at qualitative analyses instead of quantitative estimations. In a particular extreme of the rain-on-snow event in the Swiss Alps in October 2011, which led to severe flooding and mudflows, the warming climate associated with the transport of a large amount of moisture to the Alps resulted in the snowmelt and the heavy rainfall in the western Alps (Shepherd et al., 2018). As Shepherd et al. (2018) stated, the governments eventually established a mudflow dyke and restructured the river morphology to prevent the potential risks caused by the warming event. In general, this storyline method focuses on the actions taken for the further future as a probable precautionary measure from the climate change aspect by considering and understanding past historical events.

In summary, the selections of framing, statistical paradigms, and modelling are open and creative. Attribution studies have no doubt given significant contributions in the field of extreme events, improving the relative developments in the field. That said, viewing existing approaches through a critical lens is an important part of innovation and the construction of new methods. More than anything, it is hoped that the work presented here provides a platform for further analysis, methodological comparison and the development of novel approaches to further quantify and communicate wildfire risk in a changing climate. This not only benefits the end users of such information but also guides them in transforming this knowledge into actionable insights.

Bibliography

Abatzoglou, J. T. and Kolden, C. A. (2011). Relative importance of weather and climate on wildfire growth in interior Alaska. *International Journal of Wildland Fire*, 20(4):479–486.

Abatzoglou, J. T. and Williams, A. P. (2016). Impact of anthropogenic climate change on wildfire across western US forests. *Proceedings of the National Academy of Sciences*, 113(42):11770–11775.

Abatzoglou, J. T., Williams, A. P., and Barbero, R. (2019). Global emergence of anthropogenic climate change in fire weather indices. *Geophysical Research Letters*, 46(1):326–336.

Acharya, S. C., Nathan, R., Wang, Q. J., Su, C.-H., and Eizenberg, N. (2019). An evaluation of daily precipitation from a regional atmospheric reanalysis over Australia. *Hydrology and Earth System Sciences*, 23(8):3387–3403.

Ager, A. A., Preisler, H. K., Arca, B., Spano, D., and Salis, M. (2014). Wildfire risk estimation in the Mediterranean area. *Environmetrics*, 25(6):384–396.

Alarabiya News (2022). Forest fires rage in Morocco, one dead. https://english.alarabiya.net/News/africa/2022/07/15/Forest-fires-rage-Morocco-one-dead. [Online; accessed 15-June-2023].

Aljazeera (2022a). Photos: Firefighters, soldiers battle Morocco's forest blazes. https://www.aljazeera.com/gallery/2022/7/18/photos-firefighters-soldiers-battle-moroccos-forest-blazes. [Online; accessed 15-June-2023].

Aljazeera (2022b). Spain, Germany battle wildfires amid unusual heatwave in Europe. https://www.aljazeera.com/news/2022/6/19/spain-germany-battle-wildfires-amid-unusual-heatwave-in-europe. [Online; accessed 15-June-2023].

Aljazeera (2022c). Wildfires across Algeria kill at least 37 people. https://www.aljazeera.com/news/2022/8/18/dead-in-wildfires-across-algeria. [Online; accessed 15-June-2023].

Aljazeera (2022d). Wildfires raging in Europe: What, where and why? https://www.aljazeera.com/news/2022/7/21/wildfires-rage-in-europe-what-where-and-why. [Online; accessed 15-June-2023].

Alkhaldi, C. (2022). Algerian forest fires kill at least 37 people and destroy nearly 2,600 hectares. https://edition.cnn.com/2022/08/18/africa/algeria-forest-fire-intl/index.html. [Online; accessed 15-June-2023].

Allen, M. (2003). Liability for climate change. *Nature*, 421(6926):891–892.

Andrews, T., Gregory, J. M., Paynter, D., Silvers, L. G., Zhou, C., Mauritsen, T., Webb, M. J., Armour, K. C., Forster, P. M., and Titchner, H. (2018). Accounting for changing temperature patterns increases historical estimates of climate sensitivity. *Geophysical Research Letters*, 45(16):8490–8499.

Ara Begum, R., Lempert, R., Elham, A., Benjaminsen, T. A., Bernauer, T., Cramer, W., Cui, X., Mach, K., Nagy, G., Stenseth, N. C., Sukumar, R., and Wester, P. (2022). Point of departure and key concepts. in: Climate change 2022: Impacts, Adaptation and Vulnerability. contribution of working group ii to the sixth assessment report of the intergovernmental panel on climate change [h.-o. pörtner, d.c. roberts, m. tignor, e.s. poloczanska, k. mintenbeck, a. alegría, m. craig, s. langsdorf, s. löschke, v. möller, a. okem, b. rama (eds.)]. Cambridge University Press, Cambridge, UK and New York, NY, USA:121–196.

Artés, T., Castellnou, M., Houston Durrant, T., and San-Miguel, J. (2022). Wildfire–atmosphere interaction index for extreme-fire behaviour. *Natural Hazards and Earth System Sciences*, 22(2):509–522.

Barbero, R., Abatzoglou, J. T., Pimont, F., Ruffault, J., and Curt, T. (2020). Attributing increases in fire weather to anthropogenic climate change over France. *Frontiers in Earth Science*, 8:104.

Bhatt, U. S., Lader, R. T., Walsh, J. E., Bieniek, P. A., Thoman, R., Berman, M., Borries-Strigle, C., Bulock, K., Chriest, J., Hahn, M., Hendricks, A. S., Jandt, R., Little, J., McEvoy, D., Moore, C., Rupp, T. S., Schmidt, J., Stevens, E., Strader, H., Waigl, C., White, J., York, A., and Ziel, R. (2021). Emerging anthropogenic influences on the Southcentral Alaska temperature and precipitation extremes and related fires in 2019. *Land*, 10(1):82.

Bindoff, N. L., Stott, P. A., AchutaRao, K. M., Allen, M. R., Gillett, N., Gutzler, D., Hansingo, K., Hegerl, G., Hu, Y., Jain, S., Sebbari, R., Zhang, X., Aldrin, M., Sarojini, B. B., Beer, J., Boucher, O., Braconnot, P., Browne, O., Chang, P., Christidis, N., Delsole, T., Domingues, C. M., Durack, P. J., Eliseev, A., Emanuel, K., Feingold, G., Forest, C., González Rouco, J. F., Goosse, H., Gray, L., Gregory, J., Held, I., Holland, G., Quintana, J. I., Ingram, W., Jungclaus, J., Kaser, G., Kerminen, V.-M., Knutson, T., Knutti, R., Kossin, J., Lockwood, M., Lohmann, U., Lott, F., Lu, J., Mahlstein, I., Masson-Delmotte, V., Matthews, D., Meehl, G., Mendoza, B., De Menezes, V. V., Min, S.-K., Mitchell, D., Mölg, T., Morak, S., Osborn, T., Otto, A., Otto, F., Pierce, D., Polson, D., Ribes, A., Rogelj, J., Schurer, A., Semenov, V., Shindell, D., Smirnov, D., Thorne, P. W., Wang, M., Wild, M., and Zhang, R. (2014). Detection and attribution of climate change: from global to regional. Climate Change 2013: The Physical Science Basis:867–952, Cambridge University Press.

Boer, M. M., Resco de Dios, V., and Bradstock, R. A. (2020). Unprecedented burn area of Australian mega forest fires. *Nature Climate Change*, 10(3):171–172.

Boucher, O., Servonnat, J., Albright, A. L., Aumont, O., Balkanski, Y., Bastrikov, V., Bekki, S., Bonnet, R., Bony, S., Bopp, L., Braconnot, P., Brockmann, P., Cadule, P., Caubel, A., Cheruy, F., Codron, F., Cozic, A., Cugnet, D., D'Andrea, F., Davini, P., de Lavergne, C., Denvil, S., Deshayes, J., Devilliers, M., Ducharne, A., Dufresne, J.-L., Dupont, E., Éthé, C., Fairhead, L., Falletti, L., Flavoni, S., Foujols, M.-A., Gardoll, S., Gastineau, G., Ghattas, J., Grandpeix, J.-Y., Guenet, B., Guez, Lionel, E., Guilyardi, E., Guimberteau, M., Hauglustaine, D., Hourdin, F., Idelkadi, A., Joussaume, S., Kageyama, M., Khodri, M., Krinner, G., Lebas, N., Levavasseur, G., Lévy, C., Li, L., Lott, F., Lurton, T., Sebastiaan, L., Madec, G., Madeleine, J.-B., Maignan, F., Marchand, M., Marti, O., Mellul, L., Meurdesoif, Y., Mignot, J., Musat, I., Ottlé, C., Peylin, P., Planton, Y., Polcher, J., Rio, C., Rochetin, N., Rousset, C., Sepulchre, P., Sima, A., Swingedouw, D., Thiéblemont, R., Traore, A. K., Vancoppenolle, M., Vial, J., Vialard, J., Viovy, N., and Vuichard, N. (2020). Presentation and evaluation of the IPSL-CM6A-LR climate model. *Journal of Advances in Modeling Earth Systems*, 12(7):e2019MS002010.

Bourdeau-Goulet, S.-C. and Hassanzadeh, E. (2021). Comparisons between CMIP5 and CMIP6 models: Simulations of climate indices influencing food security, infrastructure resilience, and human health in Canada. *Earth's Future*, 9(5):e2021EF001995.

Bowman, D. M., Kolden, C. A., Abatzoglou, J. T., Johnston, F. H., van der Werf, G. R., and Flannigan, M. (2020). Vegetation fires in the Anthropocene. *Nature Reviews Earth & Environment*, 1(10):500–515.

Brent, T. (2022). France's wildfires rage on as minister warns of more to come. https://www.connexionfrance.com/article/French-news/France-s-wildfires-rage-on-as-minister-warns-of-more-to-come. [Online; accessed 15-June-2023].

Bressan, C. and Agency, A. (2022). Wildfire in Massarosa and Bozzano. https://www.gettyimages.co.uk/detail/news-photo/helicopter-intervenes-in-wildfire-which-broke-out-in-the-news-photo/1242015521. [Online; accessed 15-June-2023].

Brown, T., Leach, S., Wachter, B., and Gardunio, B. (2020). The extreme 2018 northern California fire season. *Bulletin of the American Meteorological Society*, 101(1):S1–S4.

Burton, C., Rifai, S., and Malhi, Y. (2018). Inter-comparison and assessment of gridded climate products over tropical forests during the 2015/2016 El Niño. *Philosophical Transactions of the Royal Society B: Biological Sciences*, 373(1760):20170406.

C3S (2022). OBSERVER: A wrap-up of Europe's summer 2022 heatwave. https://www.copernicus.eu/en/news/news/observer-wrap-europes-summer-2022-heatwave. [Online; accessed 29-March-2023].

CAL Fire (2022). Top 20 Largest California Wildfires. https://34c031f8-c9fd-4018-8c5a-4159cdff6b0d-cdn-endpoint.azureedge.net/-/media/calfire-website/our-impact/fire-statistics/featured-items/top20_acres.pdf?rev=be2a6ff85932475e99d70fa9458dca79&hash=A355A978818640DFACE7993C432ABF81. [Online; accessed 12-June-2023].

Campos-Ruiz, R., Parisien, M.-A., and Flannigan, M. D. (2018). Temporal patterns of wildfire activity in areas of contrasting human influence in the Canadian boreal forest. *Forests*, 9(4):159.

Cannon, A. J. (2018). Multivariate quantile mapping bias correction: an N-dimensional probability density function transform for climate model simulations of multiple variables. *Climate dynamics*, 50(1):31–49.

Carbon Brief (2023). Attributing extreme weather to climate change. https://www.carbonbrief.org/mapped-how-climate-change-affects-extreme-weather-around-the-world/. [Online; accessed 08-June-2023].

Cater, D. (2022). Huge Fire Rages In Massarosa, Lucca – Evacuations Take Place. https://italynews.online/news-from-italy-in-english/fire-in-lucca-500-evacuated/. [Online; accessed 15-June-2023].

CCAG (2022). Record-breaking heatwave will be an average summer by 2035, latest Met Office Hadley Centre data shows. https://www.ccag.earth/newsroom/record-breaking-heatwave-will-be-an-average-summer-by-2035-latest-met-office-hadley-centre-data-shows. [Online; accessed 29-March-2023].

CEMS (2023). Rapid Mapping service provided by the Copernicus Emergency Management Service (CEMS). https://emergency.copernicus.eu/mapping/list-of-activations-rapid. [Online; accessed 30-March-2023].

Chen, H., Sun, J., Lin, W., and Xu, H. (2020). Comparison of CMIP6 and CMIP5 models in simulating climate extremes. *Science Bulletin*, 65(17):1415–1418.

Christ, S., Schwarz, N., and Sliuzas, R. (2022). Wildland urban interface of the City of Cape Town 1990–2019. *Geographical Research*, 60(3):395–413.

Ciavarella, A., Cotterill, D., Stott, P., Kew, S., Philip, S., van Oldenborgh, G. J., Skålevåg, A., Lorenz, P., Robin, Y., Otto, F., et al. (2021). Prolonged Siberian heat of 2020 almost impossible without human influence. *Climatic Change*, 166:1–18.

Clark, M. P., Wilby, R. L., Gutmann, E. D., Vano, J. A., Gangopadhyay, S., Wood, A. W., Fowler, H. J., Prudhomme, C., Arnold, J. R., and Brekke, L. D. (2016). Characterizing uncertainty of the hydrologic impacts of climate change. *Current Climate Change Reports*, 2(2):55–64.

Clarke, B., Otto, F., Stuart-Smith, R., and Harrington, L. (2022). Extreme weather impacts of climate change: an attribution perspective. *Environmental Research: Climate*, 1(1):012001.

Cochrane, M. A. and Bowman, D. M. (2021). Manage fire regimes, not fires. *Nature Geoscience*, 14(7):455–457.

Cohen, J. D. and Deeming, J. E. (1985). The national fire-danger rating system: basic equations. PSW-82:16. USFS, Pacific Southwest Forest and Range Experiment Station, Berkeley, CA.

Coles, S. (2001). An introduction to statistical modeling of extreme values. London, UK: Springer.

Coles, S. G. and Powell, E. A. (1996). Bayesian methods in extreme value modelling: a review and new developments. *International Statistical Review/Revue Internationale de Statistique*, pages 119–136.

Conard, S. G. and Ponomarev, E. (2020). Fire in the North. *Wildfire*, 29:26–32.

Connexion (2022). France wildfires rage on: 20,000 hectares burnt, one arrest made. https://www.connexionfrance.com/article/French-news/France-wildfires-rage-on-20-000-hectares-burnt-one-arrest-made. [Online; accessed 15-June-2023].

Conradie, W. S., Wolski, P., and Hewitson, B. C. (2022). Spatial heterogeneity in rain-bearing winds, seasonality and rainfall variability in southern Africa's winter rainfall zone. *Advances in Statistical Climatology, Meteorology and Oceanography*, 8(1):31–62.

Copernicus (2022). Spanish Province of Zamora, in Castilla y León, ravaged by wildfires. https://www.copernicus.eu/en/media/image-day-gallery/spanish-province-zamora-castilla-y-leon-ravaged-wildfires. [Online; accessed 15-June-2023].

Copernicus Atmosphere Monitoring Service (2022). Europe's summer wildfire emissions highest in 15 years. https://atmosphere.copernicus.eu/europes-summer-wildfire-emissions-highest-15-years. [Online; accessed 29-March-2023].

Cortez, P. and Morais, A. d. J. R. (2007). A data mining approach to predict forest fires using meteorological data. in Neves j, Santos MF, Machado J (eds) New trends in artificial intelligence, Proceedings of the 13th EPIA- Portuguese conference on artificial intelligence. appia, pp 512–523.

Crisis24 (2022a). France: Emergency crews continue to respond to wildfires in Gironde Department as of July 17. https://crisis24.garda.com/alerts/2022/07/. [Online; accessed 15-June-2023].

Crisis24 (2022b). Spain: Emergency crews working to contain wildfire in Zamora Province, Castile and Leon Autonomous Community, as of July 18. https://crisis24.garda.com/alerts/2022/07/spain. [Online; accessed 15-June-2023].

Davis, R. (2021). Calculating the losses of Cape Town's three days of Hell. https://www.dailymaverick.co.za/article/2021-04-20-calculating-the-losses-of-cape-towns-three-days-of-hell/. [Online; accessed 20-October-2022].

de Dios, R. and Rinaudo (2020). Plant-fire interactions: Applying ecophysiology to wildfire management. Vol.36. Springer Nature.

de Groot, W. (1987). Interpreting the Canadian forest fire weather index (FWI) system. In *Proceedings of the Fourth Central Region Fire Weather Committee Scientific and Technical Seminars*.

de Groot, W. J., Field, R. D., Brady, M. A., Roswintiarti, O., and Mohamad, M. (2007). Development of the Indonesian and Malaysian fire danger rating systems. *Mitigation and Adaptation Strategies for Global Change*, 12(1):165–180.

de Groot, W. J., Goldammer, J. G., Keenan, T., Brady, M. A., Lynham, T. J., Justice, C. O., Csiszar, I. A., O'Loughlin, K., et al. (2006). Developing a global early warning system for wildland fire. *Forest Ecology and Management*, 234(1):S10.

Dee, D. P., Uppala, S. M., Simmons, A. J., Berrisford, P., Poli, P., Kobayashi, S., Andrae, U., Balmaseda, M., Balsamo, G., Bauer, P., Bechtold, P., Beljaars, A.C.M.and Van de Berg, L., Bidlot, J., Bormann, N., Delsol, C., Dragani, R., Fuentes, M., Geer, A., Haimberger, L., Healy, S., Hersbach, H., Hólm, E., Isaksen, L., Kållberg, P., Köhler, M., Matricardi, M., McNally, A., Monge-Sanz, B., Morcrette, J.-J., Park, B.-K., Peubey, C., De Rosnay, P., Tavolato, C., Thépaut, J.-N., and Vitart, F. (2011). The ERA-Interim reanalysis: Configuration and performance of the data assimilation system. *Quarterly Journal of the royal meteorological society*, 137(656):553–597.

Deeming, J. E., Burgan, R. E., and Cohen, J. D. (1978). The national fire-danger rating system, 1978. *General technical report INT-39*, Intermountain Forest and Range Experiment Station, Ogden, Utah: USDA Forest Service (63 pp.).

Deser, C., Knutti, R., Solomon, S., and Phillips, A. S. (2012a). Communication of the role of natural variability in future North American climate. *Nature Climate Change*, 2(11):775–779.

Deser, C., Lehner, F., Rodgers, K. B., Ault, T., Delworth, T. L., DiNezio, P. N., Fiore, A., Frankignoul, C., Fyfe, J. C., Horton, D. E., Kay, J. E., Knutti, R., Lovenduski, N. S., Marotzke, J., McKinnon, K. A., Minobe, S., Randerson, J., Screen, J. A., Simpson, I. R., and Ting, M. (2020). Insights from Earth system model initial-condition large ensembles and future prospects. *Nature Climate Change*, 10(4):277–286.

Deser, C., Phillips, A., Bourdette, V., and Teng, H. (2012b). Uncertainty in climate change projections: the role of internal variability. *Climate dynamics*, 38(3):527–546.

Deser, C. and Phillips, A. S. (2023). A range of outcomes: the combined effects of internal variability and anthropogenic forcing on regional climate trends over Europe. *Nonlinear Processes in Geophysics*, 30(1):63–84.

Deser, C., Phillips, A. S., Alexander, M. A., and Smoliak, B. V. (2014). Projecting North American climate over the next 50 years: Uncertainty due to internal variability. *Journal of Climate*, 27(6):2271–2296.

Di Luca, A., Pitman, A. J., and de Elía, R. (2020). Decomposing temperature extremes errors in CMIP5 and CMIP6 models. *Geophysical Research Letters*, 47(14):e2020GL088031.

Dieppois, B., Pohl, B., Crétat, J., Eden, J., Sidibe, M., New, M., Rouault, M., and Lawler, D. (2019). Southern African summer-rainfall variability, and its teleconnections, on interannual to interdecadal timescales in CMIP5 models. *Climate Dynamics*, 53:3505–3527.

Dimitrakopoulos, A., Bemmerzouk, A., and Mitsopoulos, I. (2011). Evaluation of the Canadian fire weather index system in an eastern Mediterranean environment. *Meteorological Applications*, 18(1):83–93.

Dowdy, A. J. and Mills, G. A. (2012). Atmospheric and fuel moisture characteristics associated with lightning-attributed fires. *Journal of Applied Meteorology and Climatology*, 51(11):2025 – 2037.

Dowdy, A. J., Mills, G. A., Finkele, K., and De Groot, W. (2009). Australian fire weather as represented by the McArthur forest fire danger index and the Canadian forest fire weather index. *Technical Report 10*, the Centre for Australian Weather and Climate Research, Melbourne, Australia.

Du, J., Wang, K., and Cui, B. (2021). Attribution of the extreme drought-related risk of wildfires in spring 2019 over Southwest China. *Bulletin of the American Meteorological Society*, 102(1):S83–S90.

Dudfield, M. (2004). Art and science of forest and rural fire management. *Understanding the Variables that Affect Australian Hardwood Woodchip Export Performance–Perceptions and Lessons from the International Business Management*, page 79.

Eden, J. M., Kew, S. F., Bellprat, O., Lenderink, G., Manola, I., Omrani, H., and van Oldenborgh, G. J. (2018). Extreme precipitation in the netherlands: An event attribution case study. *Weather and climate extremes*, 21:90–101.

Eden, J. M., Wolter, K., Otto, F. E., and Van Oldenborgh, G. J. (2016). Multi-method attribution analysis of extreme precipitation in Boulder, Colorado. *Environmental Research Letters*, 11(12):124009.

EFFIS (2023). European Forest Fire Information System (EFFIS). https://effis.jrc.ec.europa.eu/apps/effis.statistics/seasonaltrend. [Online; accessed 20-March-2023].

Efron, B. and Tibshirani, R. (1998). The problem of regions. *The Annals of Statistics*, 26(5):1687–1718.

Ellis, T. M., Bowman, D. M., Jain, P., Flannigan, M. D., and Williamson, G. J. (2022). Global increase in wildfire risk due to climate-driven declines in fuel moisture. *Global change biology*, 28(4):1544–1559.

Exbrayat, J.-F., Viney, N., Seibert, J., Wrede, S., Frede, H.-G., and Breuer, L. (2010). Ensemble modelling of nitrogen fluxes: data fusion for a Swedish meso-scale catchment. *Hydrology and Earth System Sciences*, 14(12):2383–2397.

Eyring, V., Bony, S., Meehl, G. A., Senior, C. A., Stevens, B., Stouffer, R. J., and Taylor, K. E. (2016). Overview of the coupled model intercomparison project phase 6 (CMIP6) experimental design and organization. *Geoscientific Model Development*, 9(5):1937–1958.

Field, C. B., Barros, V., Stocker, T. F., and Dahe, Q. (2012). Managing the risks of extreme events and disasters to advance climate change adaptation: special report of the intergovernmental panel on climate change. Cambridge University Press.

Field, R., Spessa, A., Aziz, N., Camia, A., Cantin, A., Carr, R., De Groot, W., Dowdy, A., Flannigan, M., Manomaiphiboon, K., Pappenberger, F., Tanpipat, V., and Wang, X. (2015). Development of a global fire weather database. *Natural Hazards and Earth System Sciences*, 15(6):1407–1423.

Flannigan, M. D., Krawchuk, M. A., de Groot, W. J., Wotton, B. M., and Gowman, L. M. (2009). Implications of changing climate for global wildland fire. *International journal of wildland fire*, 18(5):483–507.

Forsyth, G. and Bridgett, J. (2004). Table Mountain National Park Fire Management Plan. Technical report, Report ENV-SC-2004-043, CSIR, Stellenbosch.

Frieler, K., Lange, S., Piontek, F., Reyer, C. P., Schewe, J., Warszawski, L., Zhao, F., Chini, L., Denvil, S., Emanuel, K., et al. (2017). Assessing the impacts of 1.5 C global warming–simulation protocol of the Inter-Sectoral Impact Model Intercomparison project (ISIMIP2b). *Geoscientific Model Development*, 10(12):4321–4345.

Funk, C., Peterson, P., Landsfeld, M., Pedreros, D., Verdin, J., Shukla, S., Husak, G., Rowland, J., Harrison, L., Hoell, A., et al. (2015). The climate hazards infrared precipitation with stations—a new environmental record for monitoring extremes. *Scientific data*, 2(1):1–21.

Gallo Granizo, C., Eden, J., Dieppois, B., and Blackett, M. (2021). Assessing the capacity of Earth system models to simulate spatiotemporal variability in fire weather indicators. In *EGU General Assembly Conference Abstracts*, pages EGU21–12208.

Gauthier, S., Bernier, P., Kuuluvainen, T., Shvidenko, A. Z., and Schepaschenko, D. G. (2015). Boreal forest health and global change. *Science*, 349(6250):819–822.

Gelaro, R., McCarty, W., Suárez, M. J., Todling, R., Molod, A., Takacs, L., Randles, C. A., Darmenov, A., Bosilovich, M. G., Reichle, R., et al. (2017). The modern-era retrospective analysis for research and applications, version 2 (MERRA-2). *Journal of climate*, 30(14):5419–5454.

Georgakakos, K. P., Seo, D.-J., Gupta, H., Schaake, J., and Butts, M. B. (2004). Towards the characterization of streamflow simulation uncertainty through multimodel ensembles. *Journal of hydrology*, 298(1-4):222–241.

Giglio, L., Schroeder, W., and Justice, C. O. (2016). The collection 6 MODIS active fire detection algorithm and fire products. *Remote sensing of environment*, 178:31–41.

Gill, A. M., Stephens, S. L., and Cary, G. J. (2013). The worldwide "wildfire" problem. *Ecological applications*, 23(2):438–454.

Gillett, N., Weaver, A., Zwiers, F., and Flannigan, M. (2004). Detecting the effect of climate change on Canadian forest fires. *Geophysical Research Letters*, 31(18).

Giorgi, F. and Mearns, L. O. (2002). Calculation of average, uncertainty range, and reliability of regional climate changes from AOGCM simulations via the "reliability ensemble averaging"(REA) method. *Journal of climate*, 15(10):1141–1158.

Giorgi, F. and Mearns, L. O. (2003). Probability of regional climate change based on the Reliability Ensemble Averaging (REA) method. *Geophysical research letters*, 30(12).

GISTEMP Team (2022). GISS Surface Temperature Analysis (GISTEMP), version 4.

Gleixner, S., Demissie, T., and Diro, G. T. (2020). Did ERA5 improve temperature and precipitation reanalysis over East Africa? *Atmosphere*, 11(9):996.

Global Fire Emissions Database (2022). Wildfires. https://www.globalfiredata.org/data.html/. [Online; accessed 07-June-2022].

Haines, D. (1988). A lower-atmospheric severity index for wildland fires. *National Weather Digest*, 13(3):23–27.

Hall, B. L., Brown, T. J., Bradshaw, L. S., Jolly, W. M., and Nemani, R. (2003). National standardized energy release component (ERC) forecasts. In *5th Symposium on Fire and Forest Meteorology*.

Hannart, A., Pearl, J., Otto, F., Naveau, P., and Ghil, M. (2016). Causal counterfactual theory for the attribution of weather and climate-related events. *Bulletin of the American Meteorological Society*, 97(1):99–110.

Hardy, C. C. (2005). Wildland fire hazard and risk: Problems, definitions, and context. *Forest ecology and management*, 211(1-2):73–82.

Hauser, M., Gudmundsson, L., Orth, R., Jézéquel, A., Haustein, K., Vautard, R., Van Oldenborgh, G. J., Wilcox, L., and Seneviratne, S. I. (2017). Methods and model dependency of extreme event attribution: The 2015 european drought. *Earth's Future*, 5:1034–1043.

Haustein, K., Otto, F. E., Venema, V., Jacobs, P., Cowtan, K., Hausfather, Z., Way, R. G., White, B., Subramanian, A., and Schurer, A. P. (2019). A limited role for unforced internal variability in Twentieth-Century warming. *Journal of Climate*, 32(16):4893–4917.

Hawkins, E. and Sutton, R. (2011). The potential to narrow uncertainty in projections of regional precipitation change. *Climate dynamics*, 37(1):407–418.

Hegerl, G. C., Hoegh-Guldberg, O., Casassa, G., Hoerling, M. P., Kovats, R., Parmesan, C., Pierce, D. W., Stott, P. A., et al. (2010). Good practice guidance paper on detection and attribution related to anthropogenic climate change. In *Meeting report of the intergovernmental panel on climate change expert meeting on detection and attribution of anthropogenic climate change*, volume 9. IPCC Working Group I Technical Support Unit, University of Bern, Bern.

Hegerl, G. C., Zwiers, F. W., Braconnot, P., Gillett, N. P., Luo, Y., Orsini, J. A. M., Nicholls, N., Penner, J. E., and Stott, P. A. (2007). Understanding and attributing climate change. In S. D. Solomon, et al. (Eds.). Climate change 2007: The physical science basis. Contribution of Working Group I to the Fourth Assessment Report of the Intergovernmental Panel on Climate. Cambridge, UK and New York, USA: Cambridge University Press.

Her, Y., Yoo, S.-H., Seong, C., Jeong, J., Cho, J., and Hwang, S. (2016). Comparison of uncertainty in multi-parameter and multi-model ensemble hydrologic analysis of climate change. *Hydrology and Earth System Sciences Discussions*, pages 1–44.

Herring, S. C., Christidis, N., Hoell, A., Hoerling, M. P., and Stott, P. A. (2021). Explaining extreme events of 2019 from a climate perspective. *Bulletin of the American Meteorological Society*, 102(1):S1–S115.

Herring, S. C., Christidis, N., Hoell, A., and Stott, P. A. (2022). Explaining extreme events of 2020 from a climate perspective. *Bulletin of the American Meteorological Society*, 103(3):S1 – S129.

Hersbach, H., Bell, B., Berrisford, P., Hirahara, S., Horányi, A., Muñoz-Sabater, J., Nicolas, J., Peubey, C., Radu, R., Schepers, D., et al. (2020). The ERA5 global reanalysis. *Quarterly Journal of the Royal Meteorological Society*, 146(730):1999–2049.

Hoerling, M., Wolter, K., Perlwitz, J., Quan, X., Eischeid, J., Wang, H., Schubert, S., Diaz, H., and Dole, R. (2014). Northeast Colorado extreme rains interpreted in a climate change context. *Bulletin of the American Meteorological Society*, 95:S15–8.

Hope, P., Black, M. T., Lim, E.-P., Dowdy, A., Wang, G., Fawcett, R. J., and Pepler, A. S. (2019). On determining the impact of increasing atmospheric CO2 on the record fire weather in eastern Australia in February 2017. *Bulletin of the American Meteorological Society*, 100(1):S111–S117.

Hope, P., Wang, G., Lim, E., Hendon, H., and Arblaster, J. (2016). What caused the record-breaking heat across australia in october 2015? *Bulletin of the American Meteorological Society*, 97:122–126.

Howe, P. D., Boudet, H., Leiserowitz, A., and Maibach, E. W. (2014). Mapping the shadow of experience of extreme weather events. *Climatic change*, 127(2):381–389.

IPCC (1995). IPCC Second Assessment: Climate change 1995. A Report of the Intergovernmental Panel on Climate Change, WMO-UNEP.

IPCC (2001). IPCC Third Assessment Report. The Scientific Basis: Geneva, Switzerland.

IPCC (2007). IPCC fourth assessment report (AR4). Climate change 2007.

IPCC (2014). *Climate Change 2014: Synthesis Report. Contribution of Working Groups I, II and III to the Fifth Assessment Report of the Intergovernmental Panel on Climate Change [Core Writing Team, R.K. Pachauri and L.A. Meyer (eds.)]*. IPCC, Geneva, Switzerland, 151 pp.

IPCC (2021). *Climate Change 2021: The Physical Science Basis. Contribution of Working Group I to the Sixth Assessment Report of the Intergovernmental Panel on Climate Change*, volume In Press. Cambridge University Press, Cambridge, United Kingdom and New York, NY, USA.

IPCC (2022a). *Climate Change 2022: Impacts, Adaptation and Vulnerability*. Summary for Policymakers. Cambridge University Press, Cambridge, UK and New York, USA.

IPCC (2022b). *Mitigation of Climate Change. Contribution of Working Group III to the Sixth Assessment Report of the Intergovernmental Panel on Climate Change*. Cambridge University Press, Cambridge, UK and New York, USA.

IPCC (2023). *Climate Change 2023: Synthesis Report. Contribution of Working Group III to the Sixth Assessment Report of the Intergovernmental Panel on Climate Change [P. Arias, M. Bustamante, I. Elgizouli, G. Flato, M. Howden, C. Méndez, J. Pereira, R. Pichs-Madruga, S. K. Rose, Y. Saheb, R. Sánchez, D. Ürge-Vorsatz, C. Xiao, N. Yassaa (eds.)].*, volume In Press. Cambridge University Press, Cambridge, UK and New York, USA.

Jackson, P. (2007). From Stockholm to Kyoto: A Brief History of Climate Change. https://www.un.org/en/chronicle/article/stockholm-kyoto-brief-history-climate-change. [Online; accessed 12-June-2023].

Jain, P., Castellanos-Acuna, D., Coogan, S. C., Abatzoglou, J. T., and Flannigan, M. D. (2022). Observed increases in extreme fire weather driven by atmospheric humidity and temperature. *Nature Climate Change*, 12(1):63–70.

Jolly, W. M., Cochrane, M. A., Freeborn, P. H., Holden, Z. A., Brown, T. J., Williamson, G. J., and Bowman, D. M. (2015). Climate-induced variations in global wildfire danger from 1979 to 2013. *Nature communications*, 6(1):1–11.

Kasraoui, S. (2022). Morocco Adopts $28 Million Plan to Mitigate Wildfire Damage. https://www.moroccoworldnews.com/2022/07/350405/morocco-adopts-28-million-plan-to-mitigate-wildfire-damage. [Online; accessed 15-June-2023].

Kay, J. E., Deser, C., Phillips, A., Mai, A., Hannay, C., Strand, G., Arblaster, J. M., Bates, S., Danabasoglu, G., Edwards, J., et al. (2015). The Community Earth System Model (CESM) large ensemble project: A community resource for studying climate change in the presence of internal climate variability. *Bulletin of the American Meteorological Society*, 96(8):1333–1349.

Keetch, J. J. and Byram, G. M. (1968). A drought index for forest fire control. research paper se-38. *US Department of Agriculture, Forest Service, Southeastern Forest Experiment Station, Asheville, NC*, page 35.

Kharuk, V. I., Ponomarev, E. I., Ivanova, G. A., Dvinskaya, M. L., Coogan, S. C., and Flannigan, M. D. (2021). Wildfires in the Siberian taiga. *Ambio*, pages 1–22.

Kim, J.-S., Kug, J.-S., Jeong, S.-J., Park, H., and Schaepman-Strub, G. (2020). Extensive fires in southeastern Siberian permafrost linked to preceding Arctic Oscillation. *Science advances*, 6(2):eaax3308.

Kim, Y.-H., Min, S.-K., Cha, D.-H., Byun, Y.-H., Lott, F. C., and Stott, P. A. (2022). Attribution of the unprecedented 2021 October heatwave in South Korea. *Bulletin of the American Meteorological Society*, 103(12):E2923–E2929.

Kim, Y.-H., Min, S.-K., Zhang, X., Zwiers, F., Alexander, L. V., Donat, M. G., and Tung, Y.-S. (2016). Attribution of extreme temperature changes during 1951–2010. *Climate dynamics*, 46(5):1769–1782.

King, A. D., van Oldenborgh, G. J., Karoly, D. J., Lewis, S. C., and Cullen, H. (2015). Attribution of the record high central England temperature of 2014 to anthropogenic influences. *Environmental Research Letters*, 10(5):054002.

Kirchmeier-Young, M., Wan, H., Zhang, X., and Seneviratne, S. I. (2019a). Importance of framing for extreme event attribution: The role of spatial and temporal scales. *Earth's Future*, 7(10):1192–1204.

Kirchmeier-Young, M. C., Gillett, N. P., Zwiers, F. W., Cannon, A. J., and Anslow, F. (2019b). Attribution of the influence of human-induced climate change on an extreme fire season. *Earth's Future*, 7(1):2–10.

Kirchmeier-Young, M. C., Zwiers, F. W., and Gillett, N. P. (2017a). Attribution of extreme events in Arctic sea ice extent. *Journal of Climate*, 30(2):553–571.

Kirchmeier-Young, M. C., Zwiers, F. W., Gillett, N. P., and Cannon, A. J. (2017b). Attributing extreme fire risk in Western Canada to human emissions. *Climatic Change*, 144(2):365–379.

Knutson, T., Camargo, S. J., Chan, J. C., Emanuel, K., Ho, C.-H., Kossin, J., Mohapatra, M., Satoh, M., Sugi, M., Walsh, K., et al. (2019). Tropical cyclones and climate change assessment: Part I: Detection and attribution. *Bulletin of the American Meteorological Society*, 100(10):1987–2007.

Knutson, T., Kossin, J., Mears, C., Perlwitz, J., and Wehner, M. (2017). Detection and attribution of climate change. In D. J. Wuebbles, D. W. Fahey, K. A. Hibbard, D. J. Dokken, B. C. Stewart, T. K. Maycock (Eds.). *Climate science special report: Fourth national climate assessment*, Volume I:114–132.

Knutson, T. R., McBride, J. L., Chan, J., Emanuel, K., Holland, G., Landsea, C., Held, I., Kossin, J. P., Srivastava, A., and Sugi, M. (2010). Tropical cyclones and climate change. *Nature geoscience*, 3(3):157–163.

Knutti, R. (2010). The end of model democracy? An editorial comment. *Climatic change*, 102(3-4):395–404.

Knutti, R., Sedláček, J., Sanderson, B. M., Lorenz, R., Fischer, E. M., and Eyring, V. (2017). A climate model projection weighting scheme accounting for performance and interdependence. *Geophysical Research Letters*, 44(4):1909–1918.

Korosec, M. (2022). Karst Region on Fire – The Largest, Historic Wildfire on Record in Slovenia spreads fast under the new extreme heat dome Heatwave event over Europe. https://www.severe-weather.eu/global-weather/. [Online; accessed 15-June-2023].

Krawchuk, M. A., Moritz, M. A., Parisien, M.-A., Van Dorn, J., and Hayhoe, K. (2009). Global pyrogeography: the current and future distribution of wildfire. *PloS one*, 4(4):e5102.

Krikken, F., Lehner, F., Haustein, K., Drobyshev, I., and Van Oldenborgh, G. J. (2021). Attribution of the role of climate change in the forest fires in Sweden 2018. *Natural Hazards and Earth System Sciences*, 21(7):2169–2179.

Kunkel, K. E., Karl, T. R., Brooks, H., Kossin, J., Lawrimore, J. H., Arndt, D., Bosart, L., Changnon, D., Cutter, S. L., Doesken, N., et al. (2013). Monitoring and understanding trends in extreme storms: State of knowledge. *Bulletin of the American Meteorological Society*, 94(4):499–514.

Latrech, O. (2022). One Dead, 33 Hectares Charred in Wildfires in Northern Morocco. https://www.moroccoworldnews.com/2022/07/350465/. [Online; accessed 15-June-2023].

Lavell, A., Oppenheimer, M., Diop, C., Hess, J., Lempert, R., Li, J., Muir-Wood, R., Myeong, S., Moser, S., Takeuchi, K., et al. (2012). Climate change: new dimensions in disaster risk, exposure, vulnerability, and resilience. In *Managing the risks of extreme events and disasters to advance climate change adaptation: Special report of the intergovernmental panel on climate change*, pages 25–64. Cambridge University Press.

Lawson, B. D. and Armitage, O. (2008). Weather guide for the Canadian Forest Fire Danger Rating System. Natural Resources Canada, Canadian Forest Services, Northern Forestry Centre, Edmonton, AB.

Le Treut, H., Somerville, R., Cubasch, U., Ding, Y., Mauritzen, C., Mokssit, A., Peterson, T., and Prather, M. (2007). Historical overview of climate change. In: Climate Change 2007: The Physical Science Basis. Contribution of Working Group I to the Fourth Assessment Report of the Intergovernmental Panel on Climate Change [Solomon, S., D. Qin, M. Manning, Z. Chen, M. Marquis, K.B. Averyt, M. Tignor and H.L. Miller (eds.)].

Lenssen, N. J., Schmidt, G. A., Hansen, J. E., Menne, M. J., Persin, A., Ruedy, R., and Zyss, D. (2019). Improvements in the GISTEMP uncertainty model. *Journal of Geophysical Research: Atmospheres*, 124(12):6307–6326.

Lewis, S. C., Blake, S. A., Trewin, B., Black, M. T., Dowdy, A. J., Perkins-Kirkpatrick, S. E., King, A. D., and Sharples, J. J. (2020). Deconstructing factors contributing to the 2018 fire weather in Queensland, Australia. *Bulletin of the American Meteorological Society*, 101(1):S115–S122.

Li, S., Sparrow, S. N., Otto, F. E., Rifai, S. W., Oliveras, I., Krikken, F., Anderson, L. O., Malhi, Y., and Wallom, D. (2021). Anthropogenic climate change contribution to wildfire-prone weather conditions in the cerrado and arc of deforestation. *Environmental Research Letters*, 16(9):094051.

Lin, H.-W., McCarty, J. L., Wang, D., Rogers, B. M., Morton, D. C., Collatz, G. J., Jin, Y., and Randerson, J. T. (2014). Management and climate contributions to satellite-derived active fire trends in the contiguous United States. *Journal of Geophysical Research: Biogeosciences*, 119(4):645–660.

Liu, Z., Eden, J. M., Dieppois, B., and Blackett, M. (2022a). A global view of observed changes in fire weather extremes: uncertainties and attribution to climate change. *Climatic Change*, 173(1):1–20.

Liu, Z., Eden, J. M., Dieppois, B., Conradie, W. S., and Blackett, M. (2023). The april 2021 Cape Town wildfire: Has anthropogenic climate change altered the likelihood of extreme fire weather? *Bulletin of the American Meteorological Society*, 104(1):E298–E304.

Liu, Z., Eden, J. M., Dieppois, B., Drobyshev, I., Gallo, C., and Blackett, M. (2022b). Were meteorological conditions related to the 2020 Siberia wildfires made more likely by anthropogenic climate change? *Bulletin of the American Meteorological Society*, 103(3):S44–S49.

Liu, Z., Liu, Y., Wang, S., Yang, X., Wang, L., Baig, M. H. A., Chi, W., and Wang, Z. (2018). Evaluation of spatial and temporal performances of ERA-Interim precipitation and temperature in mainland China. *Journal of Climate*, 31(11):4347–4365.

Lucas-Picher, P., Argüeso, D., Brisson, E., Tramblay, Y., Berg, P., Lemonsu, A., Kotlarski, S., and Caillaud, C. (2021). Convection-permitting modeling with regional climate models: Latest developments and next steps. *Wiley Interdisciplinary Reviews: Climate Change*, 12(6):e731.

Maher, N., Power, S. B., and Marotzke, J. (2021). More accurate quantification of model-to-model agreement in externally forced climatic responses over the coming century. *Nature communications*, 12(1):788.

Maraun, D. (2016). Bias correcting climate change simulations-a critical review. *Current Climate Change Reports*, 2(4):211–220.

Masson, D. and Knutti, R. (2011). Climate model genealogy. *Geophysical Research Letters*, 38(8).

McArthur, A. (1967). Fire behaviour in Eucalypt forests. Department of National Development Forestry and Timber Bureau. *Canberra*, Leaflet 107.

McElhinny, M., Beckers, J. F., Hanes, C., Flannigan, M., and Jain, P. (2020). A high-resolution reanalysis of global fire weather from 1979 to 2018–overwintering the Drought Code. *Earth System Science Data*, 12(3):1823–1833.

Meehl, G. A., Washington, W. M., Ammann, C. M., Arblaster, J. M., Wigley, T. M. L., and Tebaldi, C. (2004). Combinations of natural and anthropogenic forcings in Twentieth-Century climate. *Journal of Climate*, 17(19):3721 – 3727.

Menne, M. J., Durre, I., Vose, R. S., Gleason, B. E., and Houston, T. G. (2012). An overview of the global historical climatology network-daily database. *Journal of atmospheric and oceanic technology*, 29(7):897–910.

Mera, R., Massey, N., Rupp, D. E., Mote, P., Allen, M., and Frumhoff, P. C. (2015). Climate change, climate justice and the application of probabilistic event attribution to summer heat extremes in the California Central Valley. *Climatic Change*, 133(3):427–438.

Milinski, S., Maher, N., and Olonscheck, D. (2020). How large does a large ensemble need to be? *Earth System Dynamics*, 11(4):885–901.

Müller, W. A., Jungclaus, J. H., Mauritsen, T., Baehr, J., Bittner, M., Budich, R., Bunzel, F., Esch, M., Ghosh, R., Haak, H., et al. (2018). A higher-resolution version of the max planck institute earth system model (MPI-ESM1. 2-HR). *Journal of Advances in Modeling Earth Systems*, 10(7):1383–1413.

National Academies of Sciences, Engineering, and Medicine (2016). *Attribution of extreme weather events in the context of climate change*. National Academies Press.

National Geographic Society (2022). Wildfires. https://education.nationalgeographic.org/resource/wildfires/. [Online; accessed 12-June-2023].

National Wildfire Coordinating Group (2022). Fire Weather Index (FWI) System | NWCG. https://www.nwcg.gov/publications/pms437/cffdrs/fire-weather-index-system. [Online; accessed 06-Dec-2022].

National Wildfire Coordinating Group (2023). Fire Weather Index (FWI) System. https://www.nwcg.gov/publications/pms437/cffdrs/fire-weather-index-system#:~:text=The%20Fire%20Weather%20Index%20(FWI,Again%2C%20unitless%20and%20open%20ended. [Online; accessed 12-June-2023].

NOAA National Centers for Environmental Information (2023). Billion-Dollar Weather and Climate Disasters. https://www.ncei.noaa.gov/access/billions/. [Online; accessed 12-June-2023].

Olson, D. M., Dinerstein, E., Wikramanayake, E. D., Burgess, N. D., Powell, G. V., Underwood, E. C., D'amico, J. A., Itoua, I., Strand, H. E., Morrison, J. C., et al. (2001). Terrestrial ecoregions of the world: A new map of life on Earth: A new global map of terrestrial ecoregions provides an innovative tool for conserving biodiversity. *BioScience*, 51(11):933–938.

Otto, F. E., Harrington, L. J., Frame, D., Boyd, E., Lauta, K. C., Wehner, M., Clarke, B., Raju, E., Boda, C., Hauser, M., et al. (2020). Toward an inventory of the impacts of human-induced climate change. *Bulletin of the American Meteorological Society*, 101(11):E1972–E1979.

Otto, F. E., van der Wiel, K., van Oldenborgh, G. J., Philip, S., Kew, S. F., Uhe, P., and Cullen, H. (2018a). Climate change increases the probability of heavy rains in Northern England/Southern Scotland like those of storm Desmond—a real-time event attribution revisited. *Environmental Research Letters*, 13(2):024006.

Otto, F. E., Van Oldenborgh, G. J., Eden, J., Stott, P. A., Karoly, D. J., and Allen, M. R. (2016). The attribution question. *Nature Climate Change*, 6(9):813–816.

Otto, F. E., Wolski, P., Lehner, F., Tebaldi, C., Van Oldenborgh, G. J., Hogesteeger, S., Singh, R., Holden, P., Fučkar, N. S., Odoulami, R. C., et al. (2018b). Anthropogenic influence on the drivers of the Western Cape drought 2015–2017. *Environmental Research Letters*, 13(12):124010.

Pall, P., Aina, T., Stone, D. A., Stott, P. A., Nozawa, T., Hilberts, A. G., Lohmann, D., and Allen, M. R. (2011). Anthropogenic greenhouse gas contribution to flood risk in England and Wales in autumn 2000. *Nature*, 470(7334):382–385.

Palm, K. (2022). A year after devastating Table Mountain fire, recovery expected to take years. https://ewn.co.za/2022/04/18/. [Online; accessed 20-October-2022].

Partain, J. L., Alden, S., Strader, H., Bhatt, U. S., Bieniek, P. A., Brettschneider, B. R., Walsh, J. E., Lader, R. T., Olsson, P. Q., Rupp, T. S., et al. (2016). An assessment of the role of anthropogenic climate change in the Alaska fire season of 2015. *Bulletin of the American Meteorological Society*, 97(12):S14–S18.

Philip, S., Kew, S., van Oldenborgh, G. J., Otto, F., Vautard, R., van der Wiel, K., King, A., Lott, F., Arrighi, J., Singh, R., et al. (2020). A protocol for probabilistic extreme event attribution analyses. *Advances in Statistical Climatology, Meteorology and Oceanography*, 6(2):177–203.

Philip, S., Kew, S. F., Jan van Oldenborgh, G., Aalbers, E., Vautard, R., Otto, F., Haustein, K., Habets, F., and Singh, R. (2018). Validation of a rapid attribution of the May/June 2016 flood-inducing precipitation in France to climate change. *Journal of Hydrometeorology*, 19(11):1881–1898.

Pinto, M. M., DaCamara, C. C., Hurduc, A., Trigo, R. M., and Trigo, I. F. (2020). Enhancing the fire weather index with atmospheric instability information. *Environmental Research Letters*, 15(9):0940b7.

Ponomarev, E., Yakimov, N., Ponomareva, T., Yakubailik, O., and Conard, S. G. (2021). Current trend of carbon emissions from wildfires in Siberia. *Atmosphere*, 12(5):559.

Randerson, J., Chen, Y., Van Der Werf, G., Rogers, B., and Morton, D. (2012). Global burned area and biomass burning emissions from small fires. *Journal of Geophysical Research: Biogeosciences*, 117(G4).

Randerson, J. T., Chen, Y., Wiggins, E. B., Hantson, S., Andela, N., Morton, D. C., Hall, J., Giglio, L., and van der Werf, G. (2018). Development of the Global Fire Emissions Database (GFED): toward reconciliation of top-down and bottom-up constraints on fire contributions to variability and trends in carbonaceous aerosol. In *AGU Fall Meeting Abstracts*, volume 2018, pages A41E–01.

Reliefweb (2022). Algeria: Wild Fires - Aug 2022. https://reliefweb.int/disaster/. [Online; accessed 15-June-2023].

Reuters (2022). Wildfires rage in southwestern France amid new heatwave. https://www.tbsnews.net/worldbiz/europe/wildfires-rage-southwestern-france-amid-new-heatwave-474710. [Online; accessed 15-June-2023].

Rodrigues, M., Camprubí, À. C., Balaguer-Romano, R., Megía, C. J. C., Castañares, F., Ruffault, J., Fernandes, P. M., and de Dios, V. R. (2023). Drivers and implications of the extreme 2022 wildfire season in southwest Europe. *Science of the total environment*, 859:160320.

Saada, H. (2022). Firefighting in Tipaza: Algerian Army takes part in extinction operations. https://www.dzbreaking.com/2022/08/15/. [Online; accessed 15-June-2023].

San-Miguel-Ayanz, J., Durrant, T., Boca, R., Maianti, P., Liberta‘, G., Artes Vivancos, T., Jacome Felix Oom, D., Branco, A., De Rigo, D., Ferrari, D., Pfeiffer, H., Grecchi, R., Onida, M., and Loffler, P. (2022). Forest fires in Europe, Middle East and North Africa 2021. pages EUR 31269 EN, Publications Office of the European Union, Luxembourg, 2022, ISBN 978–92–76–58616–6.

San-Miguel-Ayanz, J., Durrant, T., Boca, R., Maianti, P., Liberta‘, G., Oom, D., B. A., De Rigo, D., Ferrari, D., Roglia, E., and Scionti, N. (2023). Advance report on forest fires in Europe, Middle East and North Africa 2022. pages EUR 31479 EN, Publications Office of the European Union, Luxembourg, 2023, ISBN 978–92–68–02143–9.

Sansom, P. G., Stephenson, D. B., Ferro, C. A., Zappa, G., and Shaffrey, L. (2013). Simple uncertainty frameworks for selecting weighting schemes and interpreting multimodel ensemble climate change experiments. *Journal of Climate*, 26(12):4017–4037.

Schaller, N., FRIEDERIKE, E. O., GEERT, J., OLDENBORGH, N. R., Sparrow, S., and MYLES, R. A. (2014). The heavy precipitation event of May-June 2013 in the upper Danube and Elbe basins. *Bulletin of the American Meteorological Society*, 95(9):S69–S72.

Schewe, J., Gosling, S. N., Reyer, C., Zhao, F., Ciais, P., Elliott, J., Francois, L., Huber, V., Lotze, H. K., Seneviratne, S. I., et al. (2019). State-of-the-art global models underestimate impacts from climate extremes. *Nature communications*, 10(1):1005.

Schroeder, W., Oliva, P., Giglio, L., and Csiszar, I. A. (2014). The new VIIRS 375 m active fire detection data product: Algorithm description and initial assessment. *Remote Sensing of Environment*, 143:85–96.

Science X (2022). Rain brings relief to France fires, but more evacuated in south. https://phys.org/news/2022-08-relief-france-evacuated-south.html. [Online; accessed 15-June-2023].

Séférian, R., Nabat, P., Michou, M., Saint-Martin, D., Voldoire, A., Colin, J., Decharme, B., Delire, C., Berthet, S., Chevallier, M., et al. (2019). Evaluation of CNRM earth system model, CNRM-ESM2-1: Role of earth system processes in present-day and future climate. *Journal of Advances in Modeling Earth Systems*, 11(12):4182–4227.

Seneviratne, S., Nicholls, N., Easterling, D., Goodess, C., Kanae, S., Kossin, J., Luo, Y., Marengo, J., McInnes, K., and Rahimi, M. (2012). Changes in Climate Extremes and their Impacts on the Natural Physical Environment. In: Managing the Risks of Extreme Events and Disasters to Advance Climate Change Adaptation. A Special Report of Working Groups I and II of IPCC Intergovernmental Panel on Climate Change [Field, C.B., V. Barros, T.F. Stocker, D. Qin, D.J. Dokken, K.L. Ebi, M.D. Mastrandrea, K.J. Mach, G.–K. Plattner, S.K. Allen, M. Tignor, and P.M. Midgley (eds.)]. Cambridge University Press, Cambridge, United Kingdom and New York, NY, USA, pp. 109-230.

Seneviratne, S., Zhang, X., Adnan, M., Badi, W., Dereczynski, C., Di Luca, A., Ghosh, S., Iskandar, I., Kossin, J., Lewis, S., Otto, F., Pinto, I., Satoh, M., Vicente-Serrano, S., Wehner, M., and Zhou, B. (2021). *Weather and Climate Extreme Events in a Changing Climate. In Climate Change 2021: The Physical Science Basis. Contribution of Working Group I to the Sixth Assessment Report of the Intergovernmental Panel on Climate Change [Masson-Delmotte, V., P. Zhai, A. Pirani, S.L. Connors, C. Péan, S. Berger, N. Caud, Y. Chen, L. Goldfarb, M.I. Gomis, M. Huang, K. Leitzell, E. Lonnoy, J.B.R. Matthews, T.K. Maycock, T. Waterfield, O. Yelekçi, R. Yu, and B. Zhou (eds.)]*. Cambridge University Press, Cambridge, United Kingdom and New York, NY, USA.

Sharples, J. J., McRae, R. H., Weber, R., and Gill, A. M. (2009). A simple index for assessing fire danger rating. *Environmental Modelling & Software*, 24(6):764–774.

Shepherd, T. G. (2016). A common framework for approaches to extreme event attribution. *Current Climate Change Reports*, 2(1):28–38.

Shepherd, T. G., Boyd, E., Calel, R. A., Chapman, S. C., Dessai, S., Dima-West, I. M., Fowler, H. J., James, R., Maraun, D., Martius, O., et al. (2018). Storylines: an alternative approach to representing uncertainty in physical aspects of climate change. *Climatic change*, 151(3):555–571.

Sippel, S., Walton, P., and Otto, F. E. (2015). Stakeholder perspectives on the attribution of extreme weather events: An explorative enquiry. *Weather, Climate, and Society*, 7(3):224–237.

Smith, J. B., Schellnhuber, H.-J., Mirza, M. M. Q., Fankhauser, S., Leemans, R., Erda, L., Ogallo, L., Pittock, B., Richels, R., Rosenzweig, C., et al. (2001). Vulnerability to climate change and reasons for concern: a synthesis. *Climate Change*, pages 913–967.

Spracklen, D. V., Mickley, L. J., Logan, J. A., Hudman, R. C., Yevich, R., Flannigan, M. D., and Westerling, A. L. (2009). Impacts of climate change from 2000 to 2050 on wildfire activity and carbonaceous aerosol concentrations in the western United States. *Journal of Geophysical Research: Atmospheres*, 114(D20).

Srock, A. F., Charney, J. J., Potter, B. E., and Goodrick, S. L. (2018). The hot-dry-windy index: A new fire weather index. *Atmosphere*, 9(7):279.

Stott, P. A., Allen, M., Christidis, N., Dole, R. M., Hoerling, M., Huntingford, C., Pall, P., Perlwitz, J., and Stone, D. (2013). Attribution of weather and climate-related events. *Climate Science for Serving Society: Research, Modeling and Prediction Priorities*, pages 307–337.

Stott, P. A., Christidis, N., Otto, F. E., Sun, Y., Vanderlinden, J.-P., van Oldenborgh, G. J., Vautard, R., von Storch, H., Walton, P., Yiou, P., et al. (2016). Attribution of extreme weather and climate-related events. *Wiley Interdisciplinary Reviews: Climate Change*, 7(1):23–41.

Stott, P. A., Karoly, D. J., and Zwiers, F. W. (2017). Is the choice of statistical paradigm critical in extreme event attribution studies? *Climatic change*, 144(2):143–150.

Stott, P. A., Stone, D. A., and Allen, M. R. (2004). Human contribution to the European heatwave of 2003. *Nature*, 432(7017):610–614.

Stouffer, R. J., Eyring, V., Meehl, G. A., Bony, S., Senior, C., Stevens, B., and Taylor, K. (2017). CMIP5 scientific gaps and recommendations for CMIP6. *Bulletin of the American Meteorological Society*, 98(1):95–105.

Sullivan, A., Baker, E., and Kurvits, T. (2022). Spreading like wildfire: The rising threat of extraordinary landscape fires. UNEP: United Nations Environment Programme.

Sundström, A., Szeto, S., Wagemann, J., and Fierli, F. (2022a). In July and August 2022 significant fire events took place across Europe, especially in France, Portugal and Spain. https://www.eumetsat.int/summer-2022-exceptional-wildfire-season-europe. [Online; accessed 29-March-2023].

Sundström, A.-M., Szeto, S., Wagemann, J., and Fierli, F. (2022b). Summer 2022: exceptional wildfire season in Europe. https://www.eumetsat.int/summer-2022/. [Online; accessed 15-June-2023].

Swart, N. C., Cole, J. N., Kharin, V. V., Lazare, M., Scinocca, J. F., Gillett, N. P., Anstey, J., Arora, V., Christian, J. R., Hanna, S., et al. (2019). The Canadian earth system model version 5 (CanESM5. 0.3). *Geoscientific Model Development*, 12(11):4823–4873.

Table Mountain National Park (2021). Table Mountain National Park Fire Investigation Report. https://www.sanparks.org/assets/docs/parks_table_mountain/tmnp-fire-investigation-report.pdf. [Online; accessed 20-October-2022].

Tanskanen, H. and Venäläinen, A. (2008). The relationship between fire activity and fire weather indices at different stages of the growing season in Finland. *Boreal Environment Research*, 13:285–302.

Taylor, K. E., Stouffer, R. J., and Meehl, G. A. (2012). An overview of CMIP5 and the experiment design. *Bulletin of the American meteorological Society*, 93(4):485–498.

Tedim, F., Leone, V., Amraoui, M., Bouillon, C., Coughlan, M. R., Delogu, G. M., Fernandes, P. M., Ferreira, C., McCaffrey, S., McGee, T. K., et al. (2018). Defining extreme wildfire events: Difficulties, challenges, and impacts. *Fire*, 1(1):9.

Tett, S. F., Falk, A., Rogers, M., Spuler, F., Turner, C., Wainwright, J., Dimdore-Miles, O., Knight, S., Freychet, N., Mineter, M. J., et al. (2018). Anthropogenic forcings and associated changes in fire risk in western North America and Australia during 2015/16. *Bulletin of the American Meteorological Society*, 99:S60–S64.

The Guardian (2022). At least 26 killed and dozens injured by forest fires in northern Algeria. https://www.theguardian.com/world/2022/aug/17/. [Online; accessed 15-June-2023].

The Local (2022). More evacuated as forest fire reignites in southern France. https://www.thelocal.fr/20220814/more-evacuated-as-forest-fire-reignites-in-southern-france. [Online; accessed 15-June-2023].

Thomas Ambadan, J., Oja, M., Gedalof, Z., and Berg, A. A. (2020). Satellite-observed soil moisture as an indicator of wildfire risk. *Remote Sensing*, 12(10):1543.

Tradowsky, J., Bodeker, G., Bird, L., Kremser, S., Kreft, P., Soltanzadeh, I., Rausch, J., Rana, S., Rye, G., Ziegler, A., et al. (2020). The Extreme Weather Event Real-time Attribution Machine (EWERAM)-An Overview. In *EGU General Assembly Conference Abstracts*, page 11715.

Trenberth, K. E., Fasullo, J. T., and Shepherd, T. G. (2015). Attribution of climate extreme events. *Nature Climate Change*, 5(8):725–730.

United Nations (1992). UNITED NATIONS FRAMEWORK CONVENTION ON CLIMATE CHANGE. https://unfccc.int/files/essential_background/background_publications_htmlpdf/application/pdf/conveng.pdf. [Online; accessed 12-June-2023].

van der Werf, G. R., Randerson, J. T., Giglio, L., Van Leeuwen, T. T., Chen, Y., Rogers, B. M., Mu, M., Van Marle, M. J., Morton, D. C., Collatz, G. J., et al. (2017). Global fire emissions estimates during 1997–2016. *Earth System Science Data*, 9(2):697–720.

van der Wiel, K., Kapnick, S. B., Van Oldenborgh, G. J., Whan, K., Philip, S., Vecchi, G. A., Singh, R. K., Arrighi, J., and Cullen, H. (2017). Rapid attribution of the August 2016 flood-inducing extreme precipitation in south Louisiana to climate change. *Hydrology and Earth System Sciences*, 21(2):897–921.

van Oldenborgh, G. J., Krikken, F., Lewis, S., Leach, N. J., Lehner, F., Saunders, K. R., Van Weele, M., Haustein, K., Li, S., Wallom, D., et al. (2021a). Attribution of the Australian bushfire risk to anthropogenic climate change. *Natural Hazards and Earth System Sciences*, 21(3):941–960.

van Oldenborgh, G. J., Philip, S., Kew, S., van Weele, M., Uhe, P., Otto, F., Singh, R., Pai, I., Cullen, H., and AchutaRao, K. (2018). Extreme heat in India and anthropogenic climate change. *Natural Hazards and Earth System Sciences*, 18(1):365–381.

van Oldenborgh, G. J., Stephenson, D. B., Sterl, A., Vautard, R., Yiou, P., Drijfhout, S. S., Von Storch, H., and Van Den Dool, H. (2015). Drivers of the 2013/14 winter floods in the UK. *Nature Climate Change*, 5(6):490–491.

van Oldenborgh, G. J., van der Wiel, K., Kew, S., Philip, S., Otto, F., Vautard, R., King, A., Lott, F., Arrighi, J., Singh, R., et al. (2021b). Pathways and pitfalls in extreme event attribution. *Climatic Change*, 166(1):1–27.

van Oldenborgh, G. J., van der Wiel, K., Sebastian, A., Singh, R., Arrighi, J., Otto, F., Haustein, K., Li, S., Vecchi, G., and Cullen, H. (2017). Attribution of extreme rainfall from Hurricane Harvey, August 2017. *Environmental Research Letters*, 12(12):124009.

van Oldenborgh, G. J., Van Urk, A., and Allen, M. (2012). The absence of a role of climate change in the 2011 Thailand floods. *Bulletin of the American Meteorological Society*, 93:1047–1049.

Van Wagner, C. (1987). Development and structure of the Canadian forest fireweather index system. In *Forestry Technical Report, Canadian Forestry Service Headquarters*, volume 35. Ottawa.

Vautard, R., van Aalst, M., Boucher, O., Drouin, A., Haustein, K., Kreienkamp, F., Van Oldenborgh, G. J., Otto, F. E., Ribes, A., Robin, Y., et al. (2020). Human contribution to the record-breaking June and July 2019 heatwaves in Western Europe. *Environmental Research Letters*, 15(9):094077.

Vidal, J.-P., Martin, E., Franchistéguy, L., Baillon, M., and Soubeyroux, J.-M. (2010). A 50-year high-resolution atmospheric reanalysis over France with the Safran system. *International Journal of Climatology*, 30(11):1627–1644.

Viegas, D. X., Bovio, G., Ferreira, A., Nosenzo, A., and Sol, B. (1999). Comparative study of various methods of fire danger evaluation in southern Europe. *International Journal of wildland fire*, 9(4):235–246.

Vitolo, C., Di Giuseppe, F., Barnard, C., Coughlan, R., San-Miguel-Ayanz, J., Libertá, G., and Krzeminski, B. (2020). ERA5-based global meteorological wildfire danger maps. *Scientific data*, 7(1):1–11.

Vitolo, C., Di Giuseppe, F., Krzeminski, B., and San-Miguel-Ayanz, J. (2019). A 1980–2018 global fire danger re-analysis dataset for the Canadian Fire Weather Indices. *Scientific data*, 6(1):1–10.

Voldoire, A., Saint-Martin, D., Sénési, S., Decharme, B., Alias, A., Chevallier, M., Colin, J., Guérémy, J.-F., Michou, M., Moine, M.-P., et al. (2019). Evaluation of CMIP6 deck experiments with CNRM-CM6-1. *Journal of Advances in Modeling Earth Systems*, 11(7):2177–2213.

Volodin, E. and Gritsun, A. (2018). Simulation of observed climate changes in 1850–2014 with climate model INM-CM5. *Earth System Dynamics*, 9(4):1235–1242.

Vrac, M. (2018). Multivariate bias adjustment of high-dimensional climate simulations: the Rank Resampling for Distributions and Dependences (R 2 D 2) bias correction. *Hydrology and Earth System Sciences*, 22(6):3175–3196.

Wallace, J. M. (2012). Weather-and climate-related extreme events: teachable moments. *Eos, Transactions American Geophysical Union*, 93(11):120–120.

Walters, D., Boutle, I., Brooks, M., Melvin, T., Stratton, R., Vosper, S., Wells, H., Williams, K., Wood, N., Allen, T., et al. (2017). The met office unified model global atmosphere 6.0/6.1 and JULES global land 6.0/6.1 configurations. *Geoscientific Model Development*, 10(4):1487–1520.

Wang, D., Guan, D., Zhu, S., Kinnon, M. M., Geng, G., Zhang, Q., Zheng, H., Lei, T., Shao, S., Gong, P., et al. (2021). Economic footprint of California wildfires in 2018. *Nature Sustainability*, 4(3):252–260.

Wikipedia (2022). 2022 European and Mediterranean wildfires. https://en.wikipedia.org/wiki/2022_European_and_Mediterranean_wildfires. [Online; accessed 15-June-2023].

Witze, A. (2020). The Arctic is burning like never before–and that's bad news for climate change. *Nature*, 585(7825):336–338.

WMO (2020). Reported new record temperature of 38°C north of Arctic Circle. https://public.wmo.int/en/media/news/reported-new-record-temperature/. [Online; accessed 12-June-2023].

World Health Organization (2023). Wildfires. https://www.who.int/health-topics/wildfires#tab=tab_1/. [Online; accessed 12-June-2023].

World Meteorological Organization (2021). *The Atlas of Mortality and Economic Losses from Weather, Climate and Water Extremes (1970-2019)*. World Meteorological Organization, Geneva, Switzerland.

World Weather Attribution (2023). World Weather Attribution initiative. https://www.worldweatherattribution.org/about/. [Online; accessed 12-June-2023].

Xie, J. (2022). Record high warm 2021 February temperature over East Asia. *Bulletin of the American Meteorological Society*, 103(12):E2917–E2922.

Xu, C., Kohler, T. A., Lenton, T. M., Svenning, J.-C., and Scheffer, M. (2020). Future of the human climate niche. *Proceedings of the National Academy of Sciences*, 117(21):11350–11355.

Yahoo (2022). Wildfires in Zaragoza. https://consent.yahoo.com/v2/collectConsent?sessionId=3_cc-session_5e09a461-2bf2-4197-bc29-4dce66b721db. [Online; accessed 15-June-2023].

Yoon, J.-H., Wang, S.-Y. S., Gillies, R. R., Hipps, L., Kravitz, B., and Rasch, P. J. (2015). 2. extreme fire season in California: A glimpse into the future? *Bulletin of the American Meteorological Society*, 96(12):S5–S9.

Yu, Y., Dunne, J. P., Shevliakova, E., Ginoux, P., Malyshev, S., John, J. G., and Krasting, J. P. (2021). Increased risk of the 2019 Alaskan July fires due to anthropogenic activity. *Bulletin of the American Meteorological Society*, 102:S1–S7.

Zelinka, M. D., Myers, T. A., McCoy, D. T., Po-Chedley, S., Caldwell, P. M., Ceppi, P., Klein, S. A., and Taylor, K. E. (2020). Causes of higher climate sensitivity in CMIP6 models. *Geophysical Research Letters*, 47(1):e2019GL085782.

Zhai, P., Zhou, B., and Chen, Y. (2018). A review of climate change attribution studies. *Journal of meteorological research*, 32(5):671–692.

Zhou, C., Wang, K., and Qi, D. (2018). Attribution of the July 2016 extreme precipitation event over China's Wuhan. *Bulletin of the American Meteorological Society*, 99:S107–S112.

Zhou, X., Josey, K., Kamareddine, L., Caine, M. C., Liu, T., Mickley, L. J., Cooper, M., and Dominici, F. (2021). Excess of COVID-19 cases and deaths due to fine particulate matter exposure during the 2020 wildfires in the United States. *Science advances*, 7(33):eabi8789.

Zscheischler, J. and Lehner, F. (2022). Attributing compound events to anthropogenic climate change. *Bulletin of the American Meteorological Society*, 103(3):E936–E953.

Žarkovič, V. (2023). Photo exhibition "The Karst wildfire 2022". https://slovenia.si/inside-view/photo-exhibition-the-karst-wildfire-2022/. [Online; accessed 15-June-2023].

Appendix A

Abbreviations & Acronyms

%MAG - a percentage change in magnitude

AGCMs - atmospheric-only general circulation models

AOGCMS/CGCMS - coupled ocean-atmosphere general circulation models

BAMS - the Bulletin of the American Meteorological Society

BUI - Buildup Index

CEMS - Copernicus Emergency Management Services

CFWIS - Canadian Fire Weather Index System

CI - confidence intervals

CMIP5 - the fifth phase of the Coupled Model Intercomparison Project

CMIP6 - the sixth phase of the Coupled Model Intercomparison Project

DC - Drought Code

DMC - Duff Moisture Code

EFBI - extreme-fire behavior index

ERA - ECMWF Re-Analysis

ERA-Interim - ECMWF Re-Analysis Interim

ERC - energy release component

FAR - fraction of attributable risk

FFDI - the McArthur forest fire danger index

FFMC - Fine Fuel Moisture Code

FIRMS - Fire Information for Resource Management System

FRP - fire radiative power

FWI - Fire Weather Index

FWIx7day - the annual maxima in 7-day averaged FWI

FWIxCD90 - the annual maxima in the number of consecutive days for which FWI is above the historical 90th percentile

GEV - generalized extreme value distribution

GEFF-ERA5 - Global ECMWF Fire Forecast model

GFED - Global Fire Emissions Database

GISTEMP - the Goddard Institute for Space Studies Surface Temperature Analysis

GMST - global mean surface temperature

HDW - Hot-Dry-Windy Index

IPCC - Intergovernmental Panel on Climate Change

ISI - Initial Spread Index

KBDI - Keetch-Byram drought index

MERRA2 - the second version of Modern-Era Retrospective analysis for Research and Applications

MODIS - Moderate Resolution Imaging Spectroradiometer

MW - Megawatt

NFDRS - National Fire Danger Rating System

PR - Probability Ratio

RR - Risk Ratio

SAFRAN - the French reanalysis Système d'Analyse Fournissant des Renseignements Atmosphèriques à la Neige

TRMM - Tropical Rainfall Measuring Mission

VIRS - Visible and Infrared Scanner

WMO - World Meteorological Organization

WRF - Weather Research and Forecasting Model

WWA - World Weather Attribution

Appendix B

Ethics documentation

The following pages contain the supporting documents for the ethics process, with the reference number P97345.

Appendix C

Co-authors declaration

The following page(s) contain the supporting document(s) for the co-authors' declaration of the journal articles included in this thesis.

Co-authors declaration

To whom it may concern,

We the undersigned are writing this letter to stipulate the role of Zhongwei Liu in the preparation and submission of the following journal article:

Liu, Z., Eden, J. M., Dieppois, B., Drobyshev, I., Gallo, C., & Blackett, M. (2022). Were Meteorological Conditions Related to the 2020 Siberia Wildfires Made More Likely by Anthropogenic Climate Change?, *Bulletin of the American Meteorological Society*, *103*(3), S44-S49. doi: https://doi.org/10.1175/BAMS-D-21-0168.1

Zhongwei Liu, during her PhD research, under the supervision of **Jonathan Eden, Bastien Dieppois and Matthew Blackett**, was the first author responsible for refining the research questions, conducting the different analyses, writing the draft manuscript, responding to reviewers' comments and submitting the original research paper.

Sincerely,

Co-authors declaration

To whom it may concern,

We the undersigned are writing this letter to stipulate the role of Zhongwei Liu in the preparation and submission of the following journal article:

Liu, Z., Eden, J. M., Dieppois, B., Conradie, W. S., & Blackett, M. (2023). The April 2021 Cape Town Wildfire: Has Anthropogenic Climate Change Altered the Likelihood of Extreme Fire Weather?, *Bulletin of the American Meteorological Society*, *104*(1), E298-E304. doi: https://doi.org/10.1175/BAMS-D-22-0204.1

Zhongwei Liu, during her PhD research, under the supervision of **Jonathan Eden, Bastien Dieppois and Matthew Blackett**, was the first author responsible for refining the research questions, conducting the different analyses, writing the draft manuscript, responding to reviewers' comments and submitting the original research paper.

Sincerely,

Co-authors declaration

To whom it may concern,

We the undersigned are writing this letter to stipulate the role of Zhongwei Liu in the preparation and submission of the following journal article:

Liu, Z., Eden, J. M., Dieppois, B., Drobyshev, I., Krikken, F., & Blackett, M. (2023). Multi-Model Attribution of Extremes in Fire Weather Intensity and Duration to Externally Forced Changes in Global Temperature Anomalies. *(In review)*. http://dx.doi.org/10.2139/ssrn.4470852

Zhongwei Liu, during her PhD research, under the supervision of **Jonathan Eden, Bastien Dieppois and Matthew Blackett**, was the first author responsible for refining the research questions, conducting the different analyses, writing the draft manuscript, responding to reviewers' comments and submitting the original research paper.

Sincerely,